NTNU – Trondheim
Norwegian University of
Science and Technology

Design and Analysis of Turning Frame for new Goliath Crane at Kværner Stord

A feasibility study and design of a turning frame intended to improve safety and efficiency at Kværner Stord shipyard

Eirik Aase
Kristian Farstad

Civil and Environmental Engineering
Submission date: June 2013
Supervisor: Kjell H. Holthe, KT
Co-supervisor: Kjell Håvard Belsvik, Kværner Stord

Norwegian University of Science and Technology
Department of Structural Engineering

PREFACE

This thesis is the result of a collaborative effort of two graduate students at the Department of Structural Engineering at NTNU, constituting 30 credits for each of the students. The students have had invaluable aid from the supervisor at Kværner Stord, Kjell Håvard Belsvik, who had the original idea of the turning frame. The students also wish to show their gratitude to Prof. Kjell H. Holthe, for supervising the project and for all the excellent lectures throughout the years at NTNU. The scope of the project has been customized throughout the process in order to suit the overall goal of the project. Thus, the resulting report diverges in part from the initial task description.

As Kværner faces ever tougher competition from foreign companies from countries with lower cost levels, it is necessary to increase efficiency at the shipyard in order to be able to win contracts. The idea of the turning frame is exactly to enable higher work efficiency as well as improved safety at the shipyard. The design of the turning frame has proven a challenging task, starting from scratch with a large structure weighing hundreds of tonnes supposed to be rotated 180°. Working on this thesis has given the students valuable experience in undertaking a large project, applying theory and knowledge obtained in the course of the years at NTNU.

The project may be considered as a feasibility study as well as a FEED (Front End Engineering and Design) project. Further work is required and necessary before the structure can be built. The report is divided into three parts. Part 1 includes initial assessments, concepts and ideas, and justification of the chosen design. Part 2 is includes structural analysis and calculations intended to document the capacity of the turning frame design. Part 3 concludes the work with a reflective evaluation of the result of the thesis, as well as suggestions to further work.

ABSTRACT

As the industrial company Kværner faces ever tougher competition from foreign companies, increasing productivity and reducing costs is essential in order to win contracts and be successful in the future. With regards to increasing productivity, the Kværner shipyard at Stord wishes to assemble the topside modules manufacture at the yard in an up-side-down position. It is expected by Kværner that this rationalizes the manufacturing process of the topside modules while also increasing personnel safety. Consequently, Kværner wants to assess the possibility of turning topside modules of up to 500 tonnes in mass up,-side-down at the shipyard.

This project aims to investigate the feasibility of this idea. Starting with a broad and open perspective, creation and evaluation of ideas, applying strategies from engineering design methods leads to detailed solutions. The result is a planar steel structure, hereby denoted turning frame, onto which the topside module is mounted in the horizontal position. The turning frame acts as an intermediary structure between the crane and the topside module. The frame has lifting points at the edges onto which the ropes of the crane are connected.

The lifting process is rather complicated compared with usual lifting operations. The rope forces have to stay within the capacity of the crane, all the while maintaining stability of the turning frame with the topside module. Stability is essential in order to limit unintended motion of the frame, which elicits large dynamic effects due to the mass inertia of the load.

A detailed design of the turning frame is obtained and analyzed with respect to capacity toward critical load combinations. The frame is analyzed in the horizontal and vertical positions, which are deemed the critical positions. MS Excel is applied to calculate support and internal forces, as well as check of cross section capacity and capacity toward column and plate buckling. Welds are also designed and documented. The calculations are used to verify finite element models. Peak stresses in the frame are investigated using 2D and 3D elements. Overall, the design of the frame is deemed acceptable, given that some stress concentrations are mitigated by rounding off sharp corners. The shortcomings of the analysis of the frame are explained, and suggestions to further work are presented.

With respect to the overall feasibility of the concept, there are major obstacles which must be overcome in order for the concept to be feasible. A major problem is overcoming instability of the system as the frame approaches the vertical position. As the topside module is mounted on top of the frame, the center of gravity of the module is eccentric from the plane of the frame. This eccentricity results in a moment which at the point the frame is at 90°, must be carried by horizontal components of the rope forces alone. An optimal scheme of rope forces is presented, which can be a guideline for the crane operator. The optimal scheme ensures that the stability of the frame is maintained, as well as "acceptable" rope forces. "Acceptable" means that the total rope force is within the capacity of the crane, but the direction of the rope force is however not acceptable. As the moment due to the eccentricity of the topside module is carried by horizontal forces alone in the vertical position, horizontal components of the rope forces must be the equivalent of up to 111 tonnes of mass to maintain stability of the frame in the vertical position. If stability is not maintained, the frame will tip over due to the moment caused by the eccentricity of the module. Given the assumptions about the module applied in this project, the frame reaches the tipping point at roughly 70° rotation. The horizontal forces are led to the trolleys of the crane, which are absolutely not able to carry this load. This problem must be solved in order for the concept to be feasible. Also, the topside modules must be examined thoroughly to determine whether they can withstand being lifted as proposed in this project, as there will also be internal moments in the vertical position which the modules are not designed for originally. Overall, the feasibility of the concept is considered to most likely be unacceptable, as long as the obstacles are not overcome.

The students have had a challenging task in this thesis. Creative thinking as well as ability to apply understanding of mechanics of moving objects and advanced load scenarios has been crucial to the progress of the work. The students are of the opinion that the work has been interesting and a valuable experience, highly relevant for future careers.

SAMMENDRAG

Industriselskapet Kværner møter stadig hardere konkurranse fra utenlandske selskaper. Det er avgjørende at produktiviten ved verftene forbedres og kostnader kuttes slik at Kværner er konkurransdyktige og kan vinne kontrakter også i framtiden. For å øke produktiviteten ved Kværners verft på Stord, ønsker man å kunne montere topside moduler opp-ned. Kværner antar at dette vil rasjonalisere produksjonen, blant annet ved at mer arbeid kan foregå på bakkenivå i stedet for i høyden, og at sikkerheten i produksjonshallen samtidig vil bli forbedret. Kværner ønsker dermed å undersøke gjennomførbarheten til dette, og få utarbeidet en løsning som muliggjør rotasjon av moduler med opptil 500 tonn masse ved verftet.
Målet med dette prosjektet er å undersøke hvorvidt det er mulig å snu moduler 180°, og utarbeide en detaljert løsning og design som Kværner eventuelt kan gå videre med. Arbeidet starter med en kreativ prosess hvor målet er å finne flest mulig idèer til hvordan modulene kan snus. Litteratur om produktdesign er benyttet som verktøy for å skape så mange idèer som mulig og finne de beste løsningene. Resultatet er en plan stålramme, heretter betegnet snuramme, hvorpå modulen som skal snus monteres oppå i horisontalposisjonen. Snurammen har løftepunkter på sidene, som tauene fra kranen festes til.

Løfteprosessen fra 0° til 180° er nokså komplisert sammenlignet med vanlige løfteoperasjoner. Kranføreren må kontinuerlig trekke inn eller slippe ut tau, samtidig som løpekattene til kranen skal bevege seg for å få rotert snurammen. Samtidig må kranføreren påse at taukreftene ikke overstiger kapasiteten til kranen og at snurammen med modulen holdes stabil gjennom hele rotasjonen. Rotasjonen må foregå rolig og kontrollert for å begrense dynamiske effekter på grunn av tregheten i systemet mest mulig.

Et detaljert design av snurammen er utarbeidet og kapasiteten er undersøkt for de kritiske lasttilfellene. Snurammen er analysert i horisontal posisjon og vertikal posisjon, som er antatt kritiske tilstander. MS Excel er brukt for å beregne lastvirkninger og opplagerkrefter i lasttilfellene, samt å utføre kontroll av tverrsnittskapasitet og kontroll mot søyleknekking og plateknekking ifølge gjeldende standarder. Resultatene fra Excel-beregninger er sammenlignet og verifisert med elementmetodeanalyser av bjelkeelementmodeller. Design og beregning av sveiser er også utført. Lokale spenninger er undersøkt ved hjelp av skall- og volumelementmodeller av rammen. Totalvurderingen av designet er at designet har akseptabel kapasitet, gitt at enkelte lokale spenningskonsentrasjoner dempes ved hjelp av forskjellige løsninger for å runde av skarpe hjørner. Svakheter og mangler i dokumentasjonen er påpekt og forslag til videre arbeid er presentert.

Med hensyn til gjennomførbarheten av konseptet, er det alvorlige hindringer som må løses for at konseptet skal være gjennomførbart. Først og fremst er det et stort problem å opprettholde stabilitet til rammen i vertikalposisjonen. Siden topside modulen monteres oppå rammen i horisontal posisjon, er tyngdepunktet til module eksentrisk med flere meter fra planet til rammen. Denne eksentrisiteten skaper et rotasjonsmoment som gjør at rammen vil ”tippe over” når den nærmer seg vertikal posisjon. For å hindre dette, må det være horisontale kraftkomponenter i tauene, som balanserer ut momentet. Det er foreslått en retningslinje for optimal tauføring som sikrer ”akseptable” laster i tauene, samtidig som at rammen holdes stabil. Med ”akseptabel” menes at totalkraften i tauene er innenfor begrensingen til kapasiteten til kranen. Derimot er den horisontale komponenten, som kommer opp i tilsvarende 111 tonn i det mest ideelle tilfellet, langt fra akseptabel. Denne horisontale kraften vil overføres til løpekattene, som ikke er laget for å tåle denne belastningen. Hvis denne horisontale kraften ikke er til stede, vil rammen tippe over ved omkring 70°, gitt antagelsene i dette prosjektet. Dette må unngås, men det er foreløpig ingen gode idéer til hvordan dette problemet skal løses. I tillegg er det nødvendig at det undersøkes om hvorvidt topside modulene tåler å bli rotert på denne måten. Totalvurderingen av gjennomførbarheten til konseptet er at det mest sannsynlig ikke er gjennomførbart å rotere topside modulene, så lenge hindringene ikke løses.

Studentene har hatt en utfordrende oppgave i dette prosjektet. Kreativitet har vært viktig for å kunne skape idèer ut fra et svært åpent utgangspunkt. Konstruksjonsforståelse har vært viktig for å kunne vurdere laster og lastvirkninger, og for å kunne gjennomføre troverdige beregninger av en avansert konstruksjon. Presentasjonen av arbeidet i denne rapporten har også vært utfordrende, da hele designprosessen er forsøkt belyst. Arbeidet har vært spennende og lærerikt, og er verdifull og relevant erfaring å ta med seg inn i arbeidslivet.

CONTENTS

LIST OF FIGURES

LIST OF TABLES

PART 1: DESIGN

1. INTRODUCTION

This project is in essence an engineering product design exercise. Internet research does not reveal any examples of structures resembling the turning frame. The design of the frame relies on a few requirements and boundaries, and the turning frame itself is a novel product. Thus, the design process started at the very beginning. The importance of a systematic and comprehensive design process is considered to be major. Theory of design methods may increase work efficiency and facilitate correct decision-making. Literature by Cross (2000) was applied to aid the design process, together with helpful advice from the supervisors.

The turning frame is a structure that enables a crane, more precisely the Goliath crane at Kværner Stord, to lift and rotate the topside modules that are built at the shipyard up-side-down. The immediate questions that arise as one understands the idea of the turning frame is: What is the purpose of the turning frame? Why is it necessary to build the topside modules up-side-down? The simple answer is work efficiency and safety. The topside of an oil platform constitutes the living quarters, the helideck, the drilling rig, the flare boom and an oil production plant, among other features. The shipyard at Kværner Stord manufactures topsides mainly for the North Sea oil fields. The topsides are vast structures, so they are built in modules of up to 500 tonnes of mass, although most of the modules built at Stord are considerably smaller.

The topside modules, hereinafter modules, are complex structures, housing an intricate web of tubes and wires. It is expected that mounting the tubes is significantly easier if the module is up-side-down. Many tubes are supported by a roof, which means that workers find themselves in an awkward position when they mount the tubes. Also, the tubes are heavy and need machinery to be lifted and kept in position while the workers mount it to the structure. By accident, the tubes may fall on top of the workers and cause physical harm to personnel. The process could be made much easier and without danger had the module been up-side-down. Then there is the consideration of whether it is really worth it to manufacture a turning frame, and whether it is safe to use and leaves the modules unharmed.

2. THEORY OF DESIGN METHODS

Cross (2000) presents a rather detailed procedure from start to finish of the design process, which has to some extent been incorporated into this project. Some parts of the procedure did not apply to this particular work, and were consequently let out.

There are various approaches to product design, and in this project both creative and rational methods were adopted. Creative methods typically include brainstorming sessions, in which the goal is to create large number of ideas. No ideas shall be discarded in this session, but the participants are encouraged to build upon each others ideas to create new ones. The need for a brainstorming session arose many times through the course of the project.(Cross, 2000)

While the creative brainstorming method should not be subject to too many constraints, rational methods provide a systematic approach to design by setting guidelines to the process. Systematic design is intended to improve the quality of design decisions. A hallmark of rational methods is quantified variables. A systematic and comprehensive approach to design may be achieved by applying rational and creative methods together. Intuitively, one will apply creative methods to come up with ideas, and rational methods to assess them. (Cross, 2000)

The design process may roughly be divided into stages like the simple scheme presented in (Cross, 2000), as shown in Figure 1.

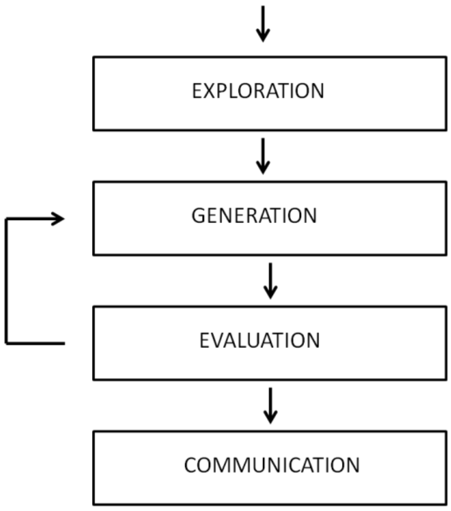

FIGURE 1: THE STAGES OF THE DESIGN PROCESS

EXPLORATION

In design situations, there is usually a customer who approaches a designer with a product need or a problem that needs a solution. The designer is left with a rather ill-defined problem. It is therefore necessary to clarify the problem by defining objectives. The customer may state vague objectives to the designer such as ‘The product must be safe and reliable’. This will then be a primary objective. In the process of clarifying the objectives, one should look more specifically at what (secondary) objectives must be fulfilled in order for the primary objective to be fulfilled. Then, the objectives are refined further into well-defined and specific objectives. Well-defined objectives are crucial for the designer’s ability to come up with good solutions (Cross, 2000). The result may then be visualized in an objective tree, as shown in Figure 2.

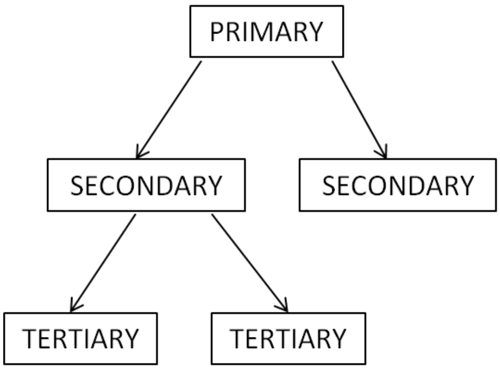

FIGURE 2: OUTLINE OF OBJECTIVE TREE

The objectives may be weighted with numerical factors depending on their importance for the success of the design. The factors may then be applied later on in deciding upon a design by comparing different alternative designs. This weighted factor objective tree was applied in this project to determine the geometry of the turning frame. Quantifying the importance of the objectives is trademark rational methods. (Cross, 2000)

The design shall fulfill the objectives satisfactorily within the requirements, or boundaries, of the design. Such boundaries may be the cost of the product, or the maximum acceptable size and weight. Design requirements narrow the range of possibilities, so they should not be set too tightly. Neither should they be set to loosely, so that the alternatives the designers come up with are ultimately useless. In this project, the requirements were discussed and stated in collaboration with the supervisor of Kværner Stord.

Generation

At this point, the goal is to generate a large number of alternative designs based on the input data from the exploration stage. Brainstorming sessions are useful tools in this respect. Drawings are a key feature of this process (Cross, 2000). It is desirable to come up with ideas that are highly diverse and novel. Unconventional ideas shall be appreciated, and not killed off by immediate criticism pointing out obvious flaws. Unconventional ideas may contain novel solutions that could not have been found otherwise. Ideas shall not be dismissed in this stage, but they shall be built upon and developed. In the design process of the turning frame, the students spent approximately a week doing brainstorming. Alternatives to the general geometry of the turning frame, as well as structural details, were generated. The alternatives were visualized by hand drawings, and the results of the brainstorming were documented continuously.

Evaluation

A range of alternatives have been generated. In the evaluation stage, one will set out to select the best one. The decision can be made by intuition, experience, or simply arbitrarily. However, a rational procedure in decision making will help validate the result and justify the decision. The evaluation of alternatives can only be carried out by considering to which degree each alternative fulfils each of the objectives stated in the exploration stage (Cross, 2000). The weighted objectives method assigns numerical weights to the objectives and numerical scores to the performance of each alternative. This exact method was applied in deciding upon the general geometry of the turning frame. The total score of each alternative is found by multiplying the performance scores with the weighted objective score.

The best solution is then the alternative with the highest total score, but it can still be improved. This is where the process enters an iterative scheme. One may go back to the generation stage, as shown in Figure 1, and iterate to come up with even better solutions. At one point, though, one has to make a final decision in order to move on to the final stage of the design process. (Cross, 2000)

COMMUNICATION

The general design of the product has been decided upon previously. At this point, the result of the design process must be communicated to the customer. The customer who approached the designer will request detailed descriptions of the final product. Usually, in engineering, the product will be described in high detail by technical drawings. In order to validate that the design fulfils the customer’s requests and standard regulations, structural analysis must also be performed. (Cross, 2000)

3. PRELIMINARY DESIGN

The objective of the preliminary design phase is to decide upon the geometrical and functional concepts of the frame. The process is based largely upon mechanical intuition, as well as a few simple hand calculations. The preliminary design enables the designers to create a model and start examining it closer by more detailed calculations. The calculations are likely to reveal weaknesses which are then taken care of by modifying the design. The calculations thus produce the final design.

3.1. EXPLORATION

The project work with the turning frame started December 20th, when the students visited the yard at Kværner Stord for a meeting with the supervisor and a tour of the yard. The students were briefed on the task at hand. In other words, the design process had started and the students were in the exploration stage. The information gathered was classified as objectives, functions and requirements, according to Cross (2000). The information is rendered below.

FUNCTIONS

The turning frame is to serve one function, namely to enable Kværner Stord to turn the topside modules up-side-down.

OBJECTIVES

The primary objectives of the turning frame are stated by the supervisor at Kværner Stord. The primary objectives are stated in the following list.

- HSE: The turning frame shall provide good safety against harm to personnel, and low risk of damage to facilities at the yard.
- Economy: The turning frame shall be a good economical investment to Kværner Stord.

From these primary objectives, an objective tree is developed, as shown in Figure 3.

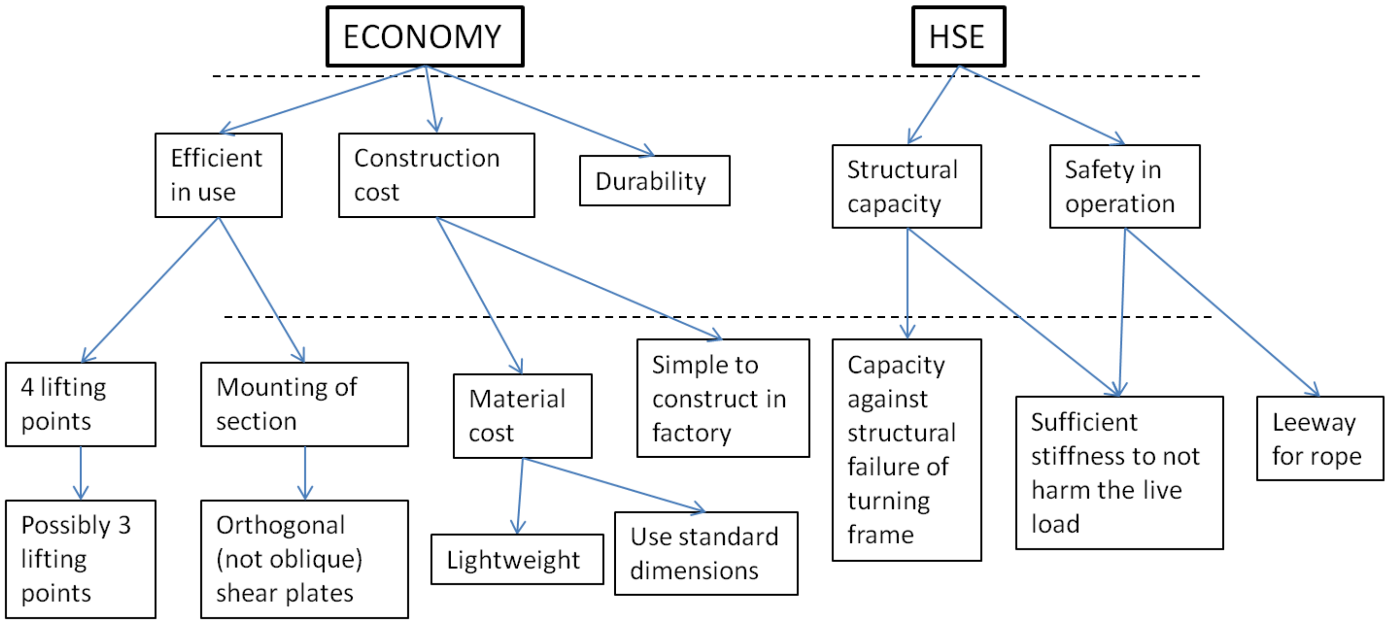

FIGURE 3: OBJECTIVE TREE

REQUIREMENTS

The requirements as to the design of the turning frame are related to the capacity of the gantry crane itself. The turning frame shall be designed to match the lifting capacity of the gantry crane, as well as match the geometry of the crane. The requirements were stated by the supervisor of Kværner Stord, and are rendered in the following list.

- The turning frame must be designed for a maximum live load of 500 tonnes. Hence, the topside modules are up to 500 tonnes in mass.
- The cranes WLL is 800 tonnes, hence the turning frame must be no more than 300 tonnes.
- The turning frame must be designed for topside modules of dimensions (L x W x H): 25m x 15m x 10m. The shape of the modules is prismatic.
- The lifting points of the turning frame must be no more than 17m apart. Consequently, the turning frame must be no more than 17m wide. This is because the upper trolley cannot tolerate a horizontal component of the rope force in the width direction of the frame.
- There shall be 4 lifting points on the turning frame, and it is desirable to have the possibility of 3 lifting points as well, to provide versatility for the lifting operation.

With this information at hand, the students went on from the exploration stage to the generation stage.

3.2. GENERATION

Through brainstorming in the exploration phase, several aspects of the design were treated. Many of the ideas are concerned with structural details, like joints and lifting points. The most fundamental ideas are concerned with the general design of the turning frame. There is more than one method of rotating the topside modules up-side-down. Which is the easiest and safest? Is a turning frame needed at all? Figure 4 depicts the progress in the session. The direction of the arrows indicates the order in which order the ideas were created.

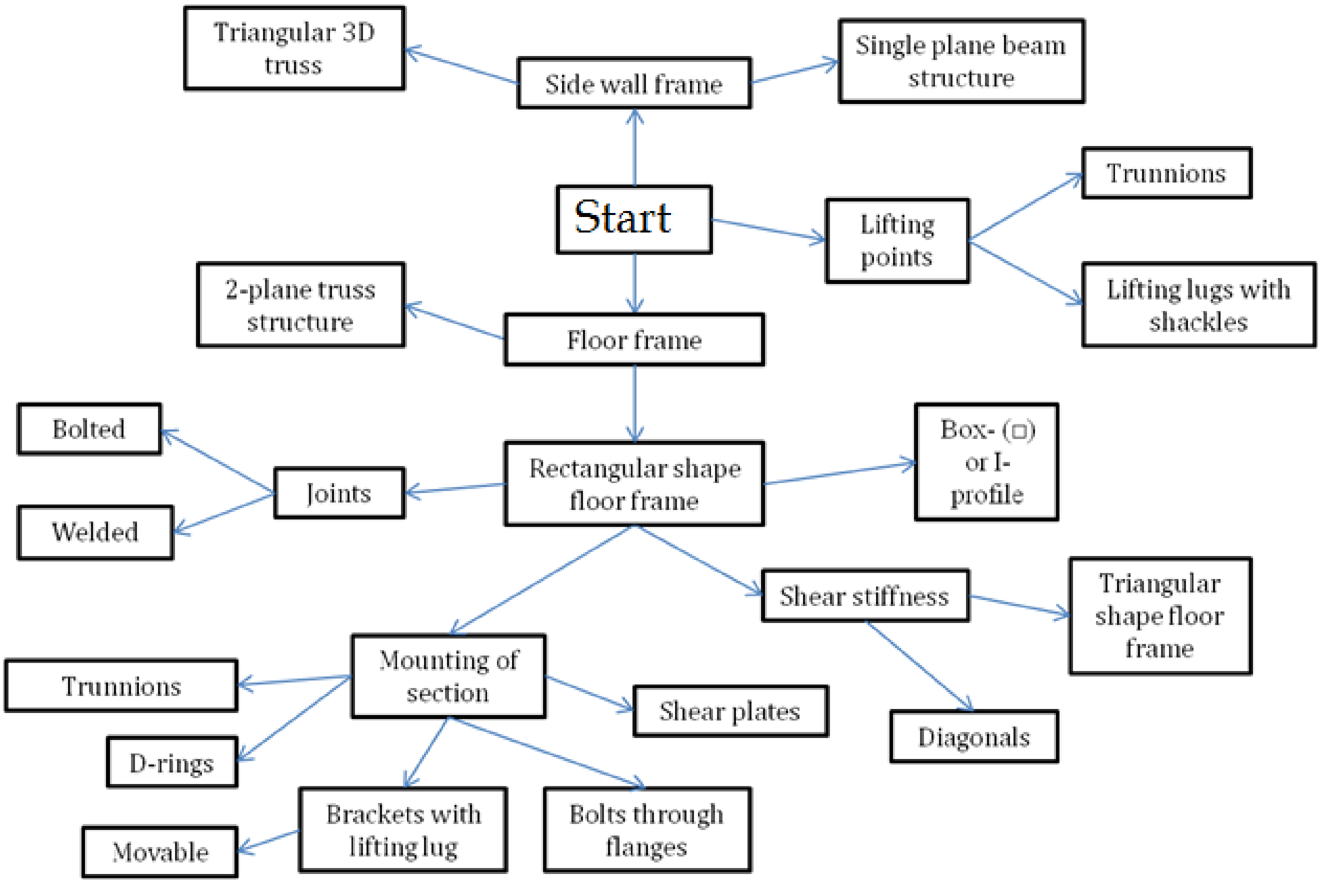

FIGURE 4: OVERVIEW OF BRAINSTORMING

As to whether a turning frame is needed at all, the answer is yes. The topside modules are not designed to be handled in such a way. The modules are usually rather fragile structures, and they vary in shapes and sizes. The design of the topside modules is complicated as it is.

3.3. CONCEPTS OF LIFTING PROCESS

In order to turn the modules up-side-down, the modules must necessarily be rotated 180° about any axis in the horizontal plane. The lifting operation will be carried out with a gantry crane, similar to the crane in Figure 5. At this point, it is appropriate to define a global coordinate system, as depicted in Figure 6. The crane has an upper trolley and a lower trolley. The trolleys move independently from each other in the x-direction. The topside modules could be rotated about both the x- and y-axes. However, if the module was to be rotated about the x-axis, one would need a second lifting device, e.g. a portable crane, to apply the force to rotate the module, while the gantry crane carries the weight. The second crane would have to position itself with the boom in the y-direction, under the gantry crane, connect with the module, and move in the y-direction to rotate the module.

FIGURE 5: GOLIATH GANTRY CRANE BY KONE CRANES (KONECRANES, 2013)

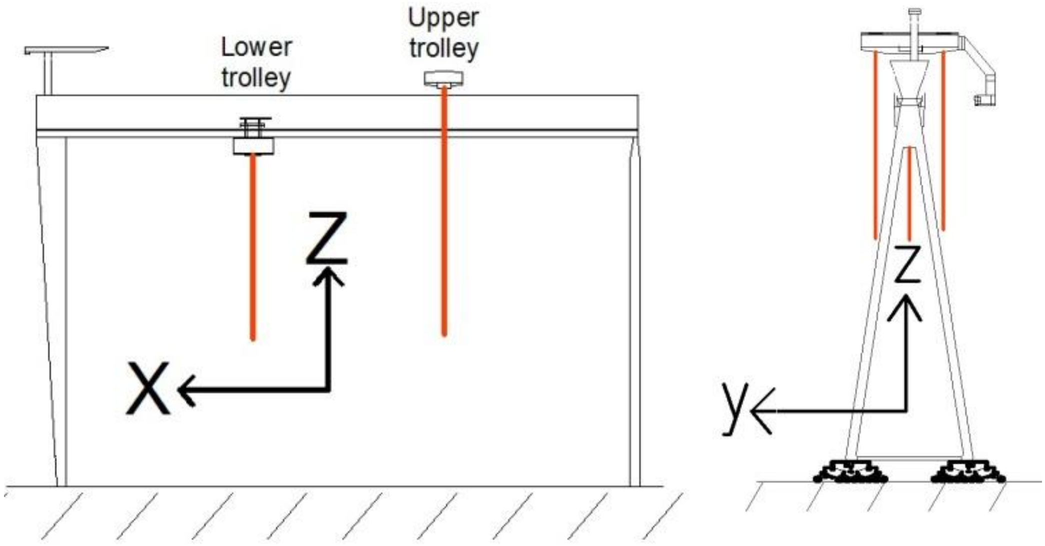

FIGURE 6: COORDINATE SYSTEM

Optionally, the module could be rotated about the y-axis. The upper trolley has two ropes extending from it, while the lower trolley has one rope. The distance between the ropes in the upper trolley can be adjusted by the crane operator. The maximum allowable distance between the ropes in the upper trolley is 17m. The gantry crane can carry out a rotation about the y-axis by itself. The upper and lower trolley will be connected with either side of the object. The lower trolley will withdraw rope while it moves in the x-direction towards the upper trolley. As the lower trolley is exactly below the upper trolley, the object will have been rotated 90°. Further, the lower trolley will continue to move in the same direction, while releasing rope until the module is turned 180°.

Though it is possible to do, there are no obvious reasons why it would be better to rotate the module about the x-axis instead of the y-axis. Rotating the module about the x-axis involves utilizing an external device, operating below the gantry crane. This might complicate the operation and be hazardous. For this reason, the concept of rotating the module about the x-axis was abandoned. With this decision made, two concepts as to the general design of the frame were created, as seen in Figure 7 and Figure 8.

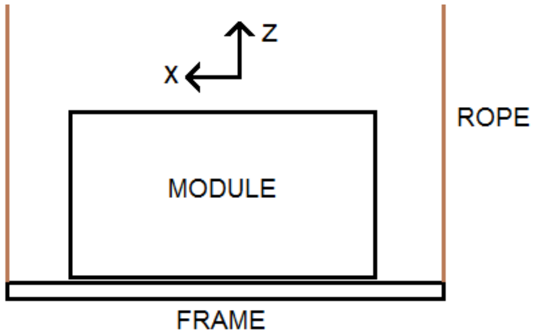

FIGURE 7: FLOOR FRAME

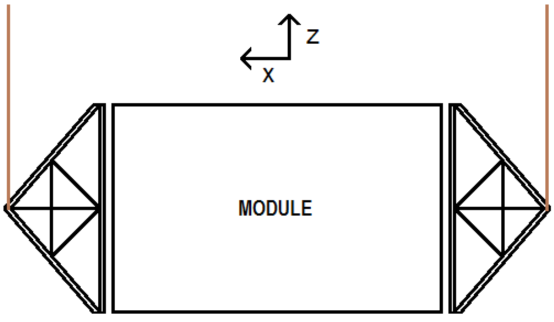

FIGURE 8: SIDE WALL FRAME

THE FLOOR FRAME

Before looking into structural details, it is necessary to have decided upon the general shape and design of the structure. However, a general design is useless if it is not possible to design adequate structural details given the general design. The floor frame may be laid to rest on the ground, before the module is mounted on top of it. Optionally, the floor frame may be placed on top of the module. The frame will have lifting points in the outer edges on the left and right side in the figure. The frame will need to be no shorter than the module, 25 m.

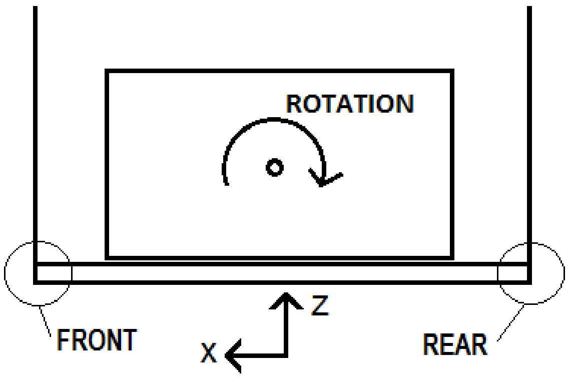

FIGURE 9: THE LIFTING OPERATION (1)

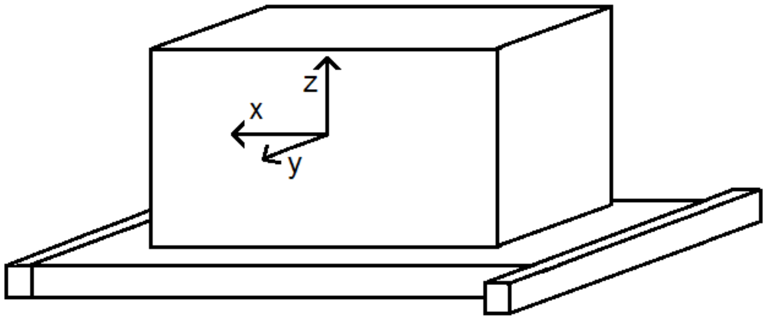

FIGURE 10: THE LIFTING OPERATION (2)

The objective of the lifting operation is to turn the module up-side-down. The module will be rotated about the y-axis, as indicated in Figure 10. In the following, the end of the frame that is lifted upwards in the lifting operation is denoted the front end. The side that is lowered down is denoted the rear, as illustrated in Figure 9. By necessity, in order for the rotation to be possible, the lifting points in the rear end must be wider apart than the width of the frame, so the ropes connected to the rear are allowed to pass freely along the sides of the frame.

The Side Wall Frame

The side frame may be attached to two opposite side of the topside module, and will consist of two separate parts. The parts must be slightly different from each other. Similarly as with the floor frame, the ropes will be connected to lifting points in the front and rear. The rear will be lowered down under the lifting operation. Consequently, the lifting points must be placed wide apart as with the floor frame, so the ropes can pass along the side of the frame and the module. The side wall frame could either be designed as a truss structure as shown in Figure 8, or a plane beam structure, as shown in Figure 11. Other methods of turning the module around have been considered.

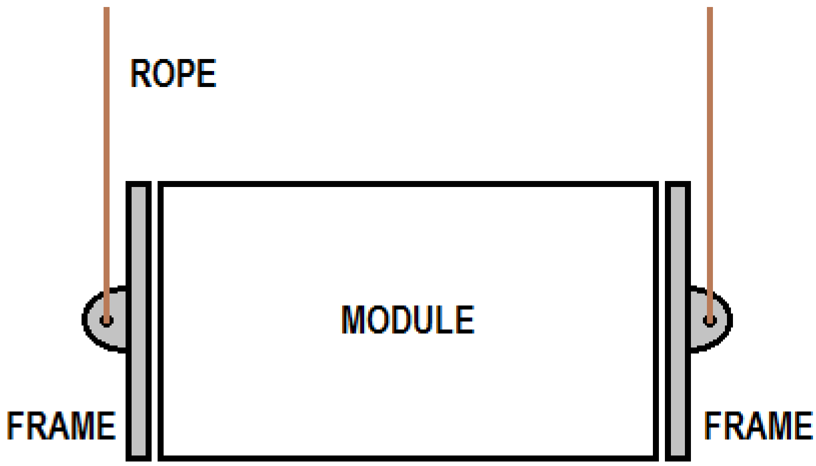

FIGURE 11: PLANE BEAM SIDE WALL FRAME

EVALUATION OF FLOOR FRAME AND SIDE WALL FRAME

The side wall frame has many virtues and advantages over the floor frame. Due to its light weight compared to the floor frame, it is likely to be cheaper, easier to use (does not need as heavy lifting devices to be handled) and needs less storage space. All the while these are good reasons to prefer the side wall frame; however, it comes with a major disadvantage. It needs the topside modules to be able to carry their own weight. This fact alone makes the side wall frame inappropriate. The topside modules are not designed to be lifted in this way. Generally, when the topside modules are lifted, they are placed on top of and connected to large beams carrying its weight, much like the floor frame.

The disadvantages of the side wall frame make the floor frame the only option going forward. The floor frame carries the weight, and thus moment, of the topside module. Obviously, to be able to carry 500 tonnes over a span of 25m, the floor frame needs a massive moment resistance, as shown in the simple calculation in Figure 12.

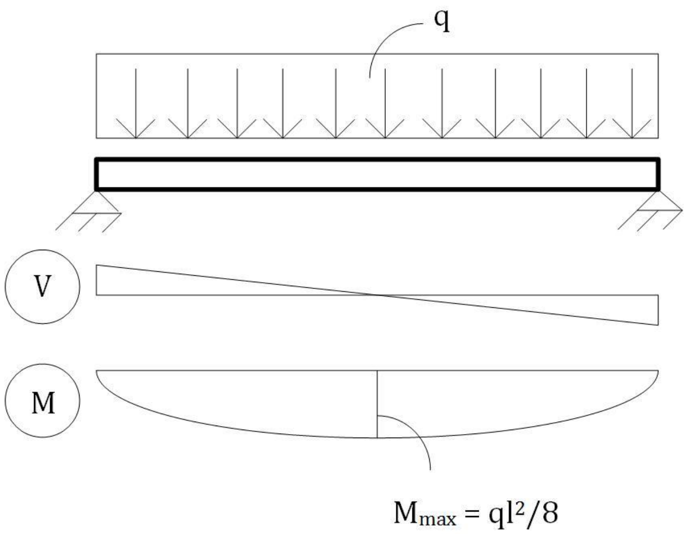

Mass of module, m	500	tonnes
Gravitational acceleration, g	9.81	m/s^2
Dynamic factor	1.6	
Live load factor	1.5	
Dynamic weight of live load, W_d	11 772	kN
Length of frame, L	26	m
Dynamic distributed load, q_d	453	kN/m
Max moment, M_{max}	38 259	kNm
Max allowed stress, σ_a	280	N/mm^2
Required moment resistance, W_{req}	136 639	$10^3 \cdot mm^3$
Moment resistance of HEB-1000	12 890	$10^3 \cdot mm^3$
Necessary no. of HEB-1000s	10.60	

FIGURE 12: SIMPLE CALCULATION OF MOMENT RESISTANCE

According to the calculation, the moment resistance of more than 10 HEB-1000 profiles is necessary to carry the dynamic live load alone. In addition, there is the self weight of the frame that needs to be taken into account. Having some sense of which size the frame needs to have is helpful in the early design phase. The simple calculation also shows that it will probably not be possible to employ standard beam cross sections in the design, as they are too small. The alternative is to make welded profiles of appropriate size. Welded profile beams may be more expensive, but offer versatility and adaptability. The designers can choose optimal profile dimensions, resulting in more efficient use of material and less weight. Both I/H profiles and box profiles may be appropriate. The profiles are illustrated with local axis system in Table 1.

TABLE 1: WELDED PROFILES

Welded profiles

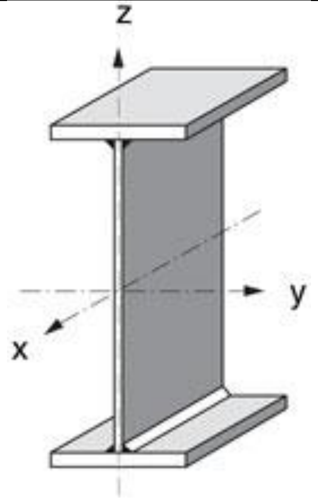

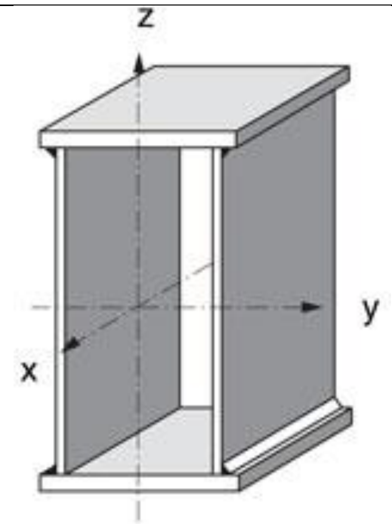

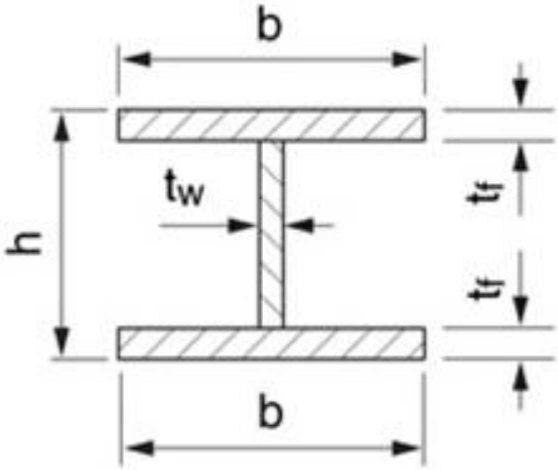

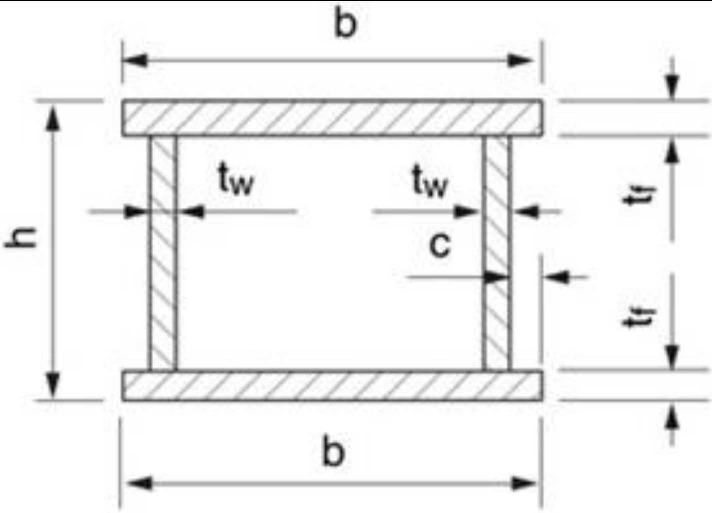

Source: (Rautaruukki Corporation, 2013)

3.4. Concepts of Design

In the following figures, the front end of the frame is always to the left side. Figure 13 shows the first idea of the floor frame that came to mind. The members of the frame are given names that are applied throughout the rest of this project.

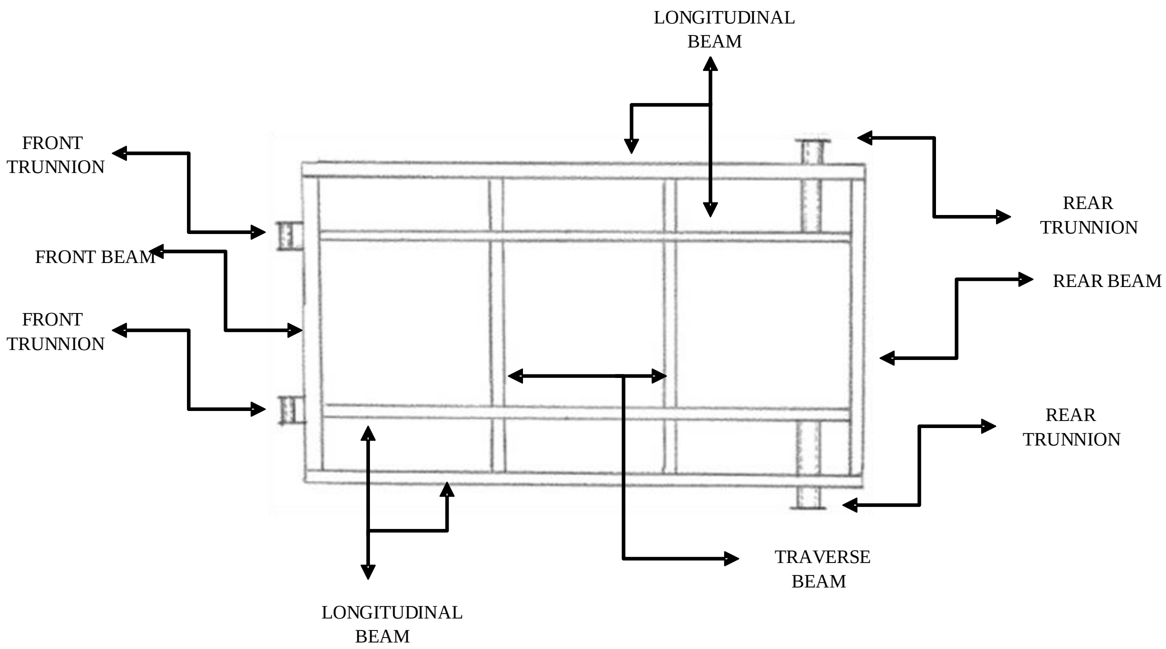

FIGURE 13: TERMINOLOGY

The frame in Figure 13 consists of four beams in the longitudinal direction. Hence, they are referred to as the longitudinals. There are beams in the traverse direction in the front and in the rear, denoted front beam and rear beam. In between, there are more beams in the traverse direction, denoted traverse beams. In the front and rear there are trunnions that make up the lifting points. This is where ropes will be attached to the frame. The frame in Figure 13 shares many similarities to the wealth of proposed geometries. However, to avoid difficulty in design of structural details, like joints and lifting points, it is helpful to know a little about how these details will be, and keep them in mind throughout the process.

Design of lifting points

The trunnion is a lifting point consisting of a steel tube which is intended for use with a rope. In this project, it is assumed that polyester rope is applied. Alternatively, steel wire rope can be applied. As an alternative solution to the trunnion, a plate with a lifting eye intended for use with shackle and a rope. The plate with lifting eye is hereby denoted the lifting lug.

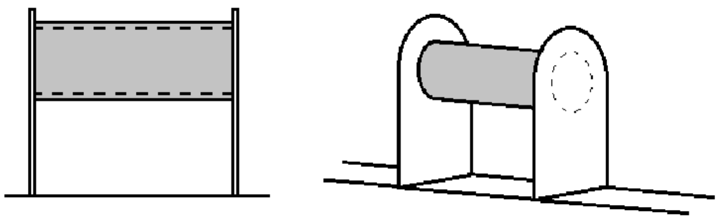

FIGURE 14: TRUNNION

The lifting points must transfer a very large shear force, so the design must be robust. The trunnion illustrated in Figure 14 consists of two plates, so the shear capacity of the design may be rather good. Polyester slings would simply be threaded round the tube. The friction between the tube and the polyester slings must be checked, in order to prevent damage to the slings as the frame rotates. Friction can probably be kept sufficiently low by cleaning, brushing and polishing the surface of the tube. The friction should be investigated in further work to establish whether it is acceptable or not. In this project, the friction is assumed to be acceptable.

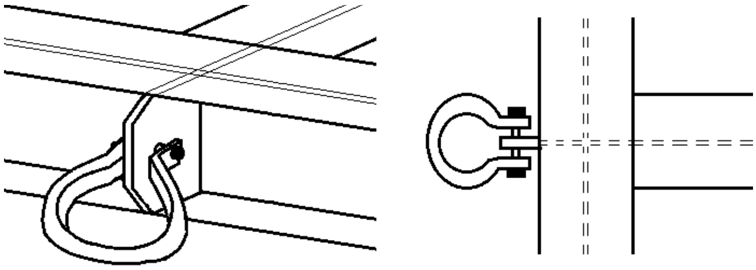

FIGURE 15: LIFTING LUG WITH SHACKLE

The lug design in Figure 15 means there is only one plate carrying the shear force. Resistance of the shackle bolt as well as bearing resistance of the lifting lug may pose a challenge in the design. One may have to use a rather thick plate as lifting lug. This solution fits well together with I/H profile beams, as the plate of the lifting lug will be parallel and in line with the web of the beam.

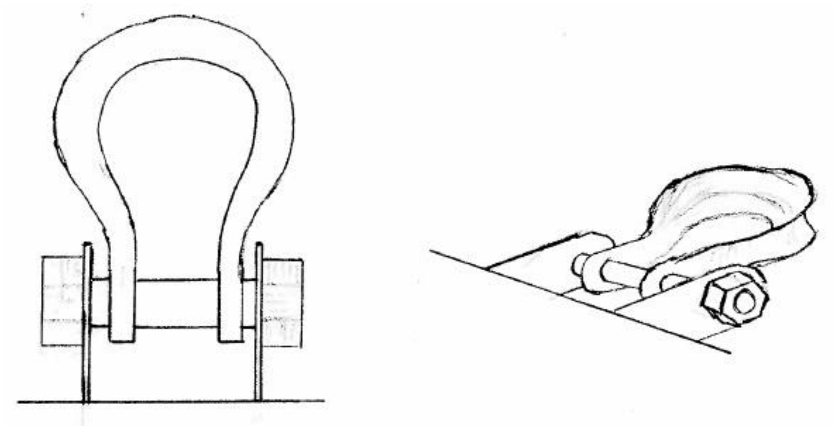

FIGURE 16: CUSTOM SHACKLE BOLT

Figure 16 involves a shackle bolt threaded through two parallel plates, similar looking to the trunnion in Figure 14. This is not a standard solution, and one would have to manufacture a custom shackle bolt to fit to the joint. However, there are two plates carrying the shear force, and two surfaces transmitting load to the shackle, so that shear failure of the bolt and bearing resistance of the lugs are less of a problem. The solutions involving two plates are best suited together with box profile beams, so the plane of the lugs coincides with the planes of the box profile.

At this point there is too much uncertainty to decide upon a design of the lifting points. The design is concluded upon later in the process, as the geometry of the frame and the magnitude of forces is known.

DESIGN OF BEAM JOINTS

Another structural detail that is important to keep in mind is the joints. A design like the one in Figure 13 involves several perpendicular joints of large steel beams, of both I/H profile and/or box profile. Joining I/H beams is straight forward, as shown in Figure 17. The joint may be welded or bolted, as illustrated in Figure 18. However, Kværner Stord does not have much experience with bolted joints. Therefore, welded joints are pursued in the design.

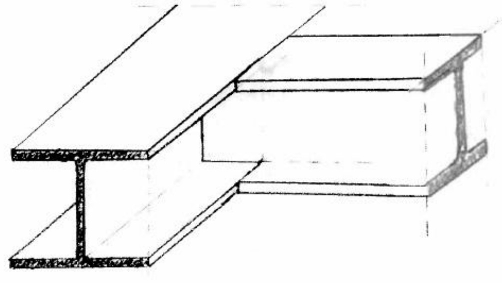

FIGURE 17: JOINT OF I/H BEAMS

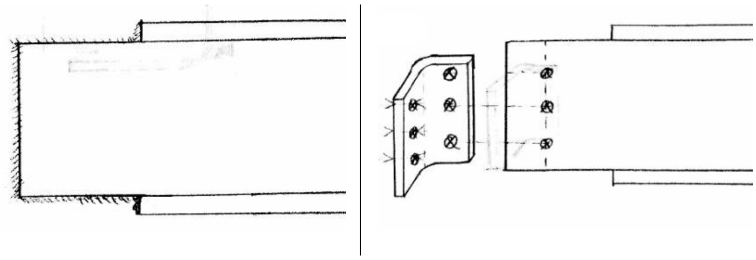

FIGURE 18: WELDED AND BOLTED JOINT OF I/H BEAMS

Joining perpendicular a box profile with either an I/H profile or another box profile is not as straight forward. As shown in Figure 19, plates should be welded inside the box profile to transmit shear forces effectively. A long box profile beam with several plates welded to the inside may prove difficult to achieve in practice, especially if the plates must be welded on both sides.

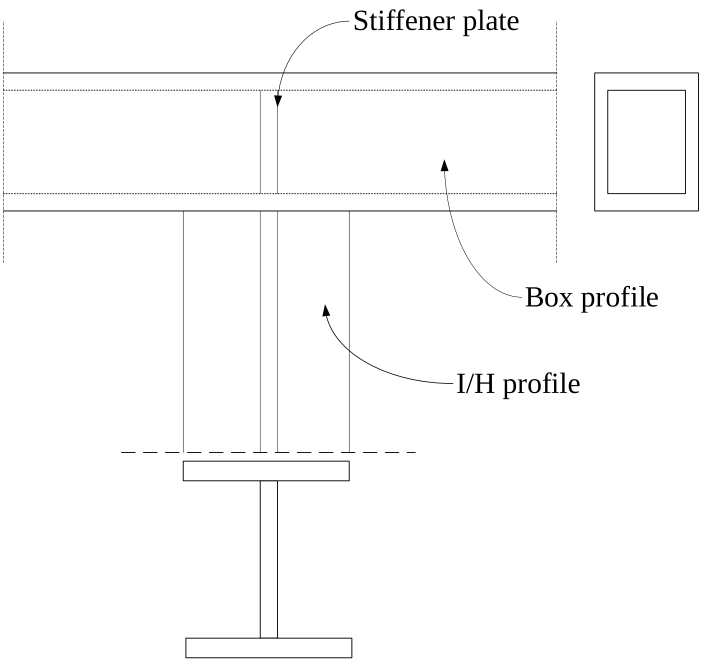

FIGURE 19: JOINTS OF BOX PROFILE TO I/H PROFILE

FIXING THE TOPSIDE MODULE TO THE FRAME

An important part of the structure is how the topside module is fixed to the frame. The module is fixed to the frame at specific points throughout the frame. The points where the module is fixed to the frame is hereby denoted load points. The load points must provide versatility, as the topside modules vary in size, shape and weight. To provide versatility, there should be a large number of load points throughout the frame. The load points must be robust, as they must carry normal forces, shear forces and moment, throughout the complete 180° rotation. In Table 2 are some of the ideas to the design of load points presented.

TABLE 2: DESIGN OF LOAD POINTS

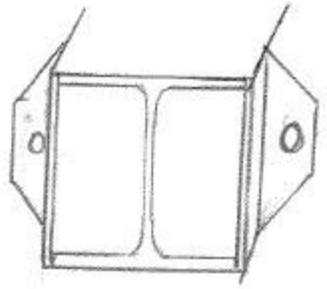	This load point consists of a lifting lug extending to the side of a beam. The beam may be either I/H profile or box profile. In an I/H beam, the bracket should extend all the way to the web of the beam, so as to transmit the shear force effectively to the web. To fix the topside module to the bracket, a rope and shackle may be used. This solution should provide decent versatility. However, it is somewhat uncertain if the topside module will be completely fixed, or if it may slide, especially when in the vertical position.
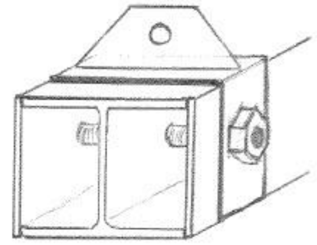	This load point provides versatility by being movable. A shackle and rope solution shall be employed to fix the topside module. I/H beams must probably be strengthened with additional plates on the sides, so that the beam becomes a hybrid of I/H and box profile.
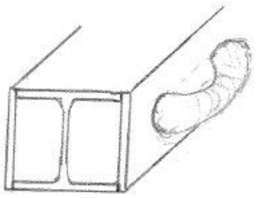	This load point resembles D-rings that are welded to the beam. If the beam is a I/H-profile, the beams must be enhanced with plates on the sides.
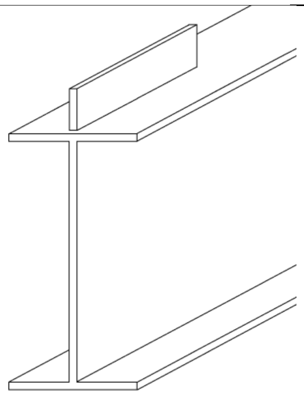	This fixing points consists simply of a plate welded to the top of the beams. The topside module is fixed to the frame by welding it to the plate. Kværner Stord has experience using this solution of fixing topside modules from standard lifting operations. This solution is most appropriate with I/H beams, as the plane of the plate coincides with the plane of the web of the beam. For box profile beams, there could be two plates, one on each side, coinciding with the planes of each web as well. It would then be important to use both plates together, not just one, as this would cause torsion. This solution is hereby referred to as the shear plate.

After a discussion of the load point designs, the shear plate solution was chosen as the preferred solution. Kværner Stord has experience with this method. It is very simple and very robust. The shear plates will be 1000mm long and 250mm wide. The plate thickness should be roughly the same as the thickness of the web of the beam. The shear plates should largely be oriented in the longitudinal direction of the frame. The reason for this is so that they are able to carry the weight of the topside module by shear force in the vertical position. It might be necessary to have some shear plates in the traverse direction of the frame as well, to restrict traverse motion of the module. Shear plates should either be oriented in the longitudinal or traverse direction, hence not in an oblique angle.

With the current knowledge about structural details in mind, one can effectively come up with and evaluate ideas to the geometry of the frame.

IDEAS TO THE GEOMETRY

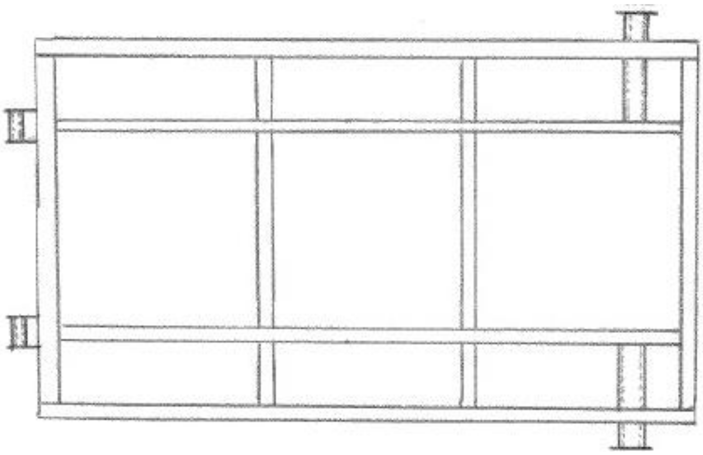

FIGURE 20: RECTANGULAR FRAME IDEA

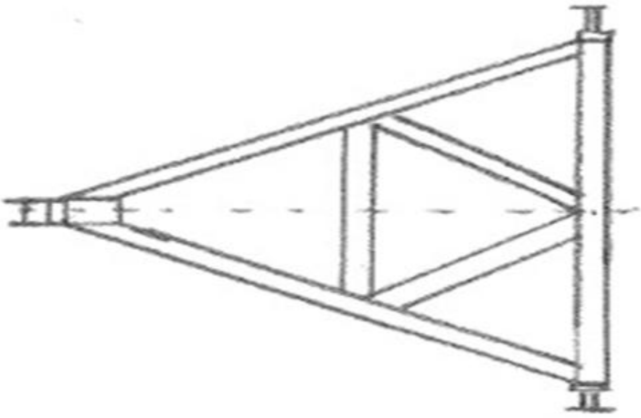

FIGURE 21: TRIANGULAR FRAME IDEA

Figure 20 and Figure 21 were the first ideas that came to mind. It is important that the frame is very stiff toward shear deformation in the plane of the frame. The reason for this is so as to prevent damage to the topside module, which is fragile for this deformation. The rectangular frame in Figure 20 does not have any stiffeners to shear deformation. Thus, the shear stiffness of this frame stems only from the shear stiffness of each beam individually. The triangular shape of the frame in Figure 21, however, resembles a truss structure, and is likely to be very stiff toward shear deformation. The members work together to create shear stiffness, using axial stiffness, which is very rigid.

To strengthen the rectangular shape of Figure 20, diagonal members are necessary. In Table 3 are drawings of the various geometries that were evaluated. The frames are rotated 90° clockwise so they illustrate better the vertical position.

TABLE 3: IDEAS TO THE GEOMETRY OF THE FRAME

A	B	C
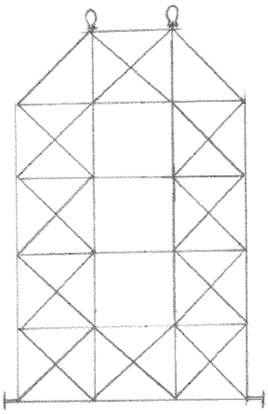	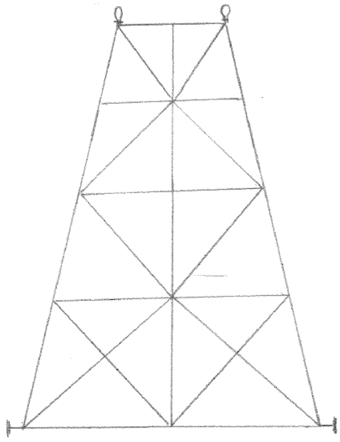	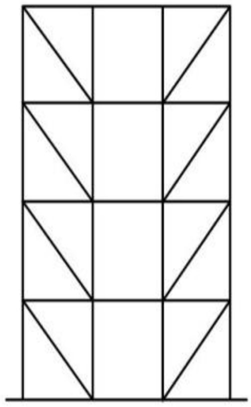
D	E	F
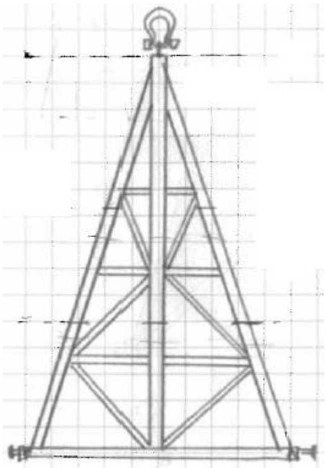	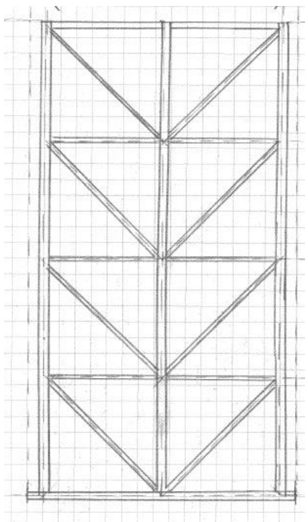	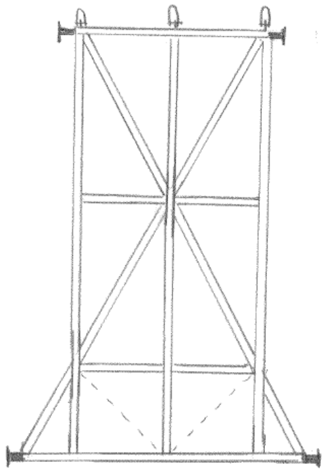
G	H	I
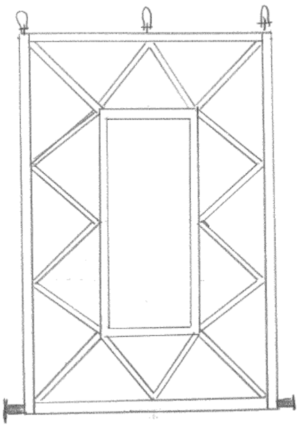	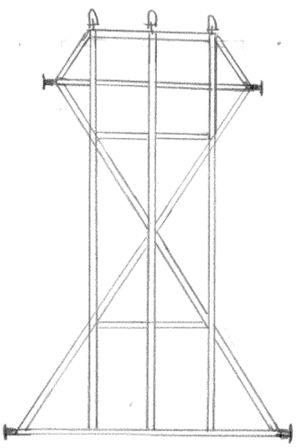	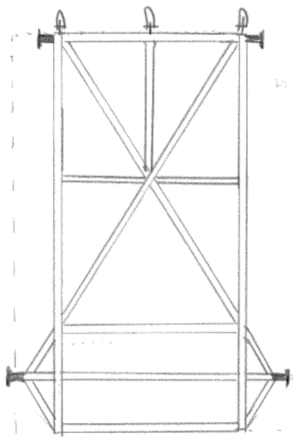

3.5. Evaluation

The ideas to the geometry were evaluated using the weighted objectives method, as described in Cross, 2000. A list of objectives was stipulated in an Excel spreadsheet. The importance of each objective was recognized by factors. Then each idea was given points to each objective reflecting the level to which the geometry fulfilled the objective. The points were then summed up to reveal the idea with the highest score as the best idea.

TABLE 4: EVALUATION OF GEOMETRIES

	Objectives	Longitudinal bending capacity	Traverse bending capacity	Shear stiffness	Shear plates	Sufficient width of frame	Leeway for rope	Complexity of construction	Complexity of calculation	Lifting points	
Idea	Weights	3	3	3	3	3	3	2	2	2	Sum
A	SCORES	15	18	18	18	18	12	6	10	6	121
B		18	18	18	9	12	18	12	12	6	123
C		18	18	18	18	18	18	18	18	12	144
D		18	18	18	6	9	18	8	12	4	111
E		15	18	18	15	18	18	12	12	8	134
F		18	18	18	12	18	18	4	8	12	126
G		9	12	18	15	18	9	12	10	12	115
H		18	18	15	18	15	18	10	8	12	132
I		15	18	12	15	15	12	10	10	12	119

TABLE 5: EXPLANATIONS TO THE OBJECTIVES

Objective	Criteria
Longitudinal bending capacity	Efficient transmission of weight through the longitudinal direction to the lifting points. Straight and continuous beams between the lifting points provide good bending capacity.
Traverse bending capacity	Efficient transmission of weight in the traverse direction.
Shear stiffness	The degree of truss-like behavior in preventing shear deformation in the plane of the frame.
Shear plates	The amount and distribution of area suitable for shear plates. Oblique angled members are not suitable, only members in longitudinal and traverse direction.
Sufficient width of frame	The width of the frame should be no less than 15m, but limited areas where the frame is narrower are tolerable.
Leeway for and angle of rope	Sufficient traverse distance from the lifting points in the rear to the sides of the frame so as to provide decent leeway for the rope. Also, the lifting points in the rear must not be placed more than 17m apart so as to avoid non-vertical alignment of the rope.
Complexity of construction	Complexity of joints is largely determined by the number of members and angles. Angles below 30° are intolerable. If the frame is complex, it gets a low score.
Complexity of calculation	Complexity of calculation is determined by several factors, including the number of unique joint designs, the number of unique members and design of lifting points.
Lifting points	Robustness and versatility of lifting points. The lifting points in the front should coincide with the joint of the front beam and a longitudinal beam. It is desirable to have the opportunity to lift the frame using either 4 or 3 lifting points.

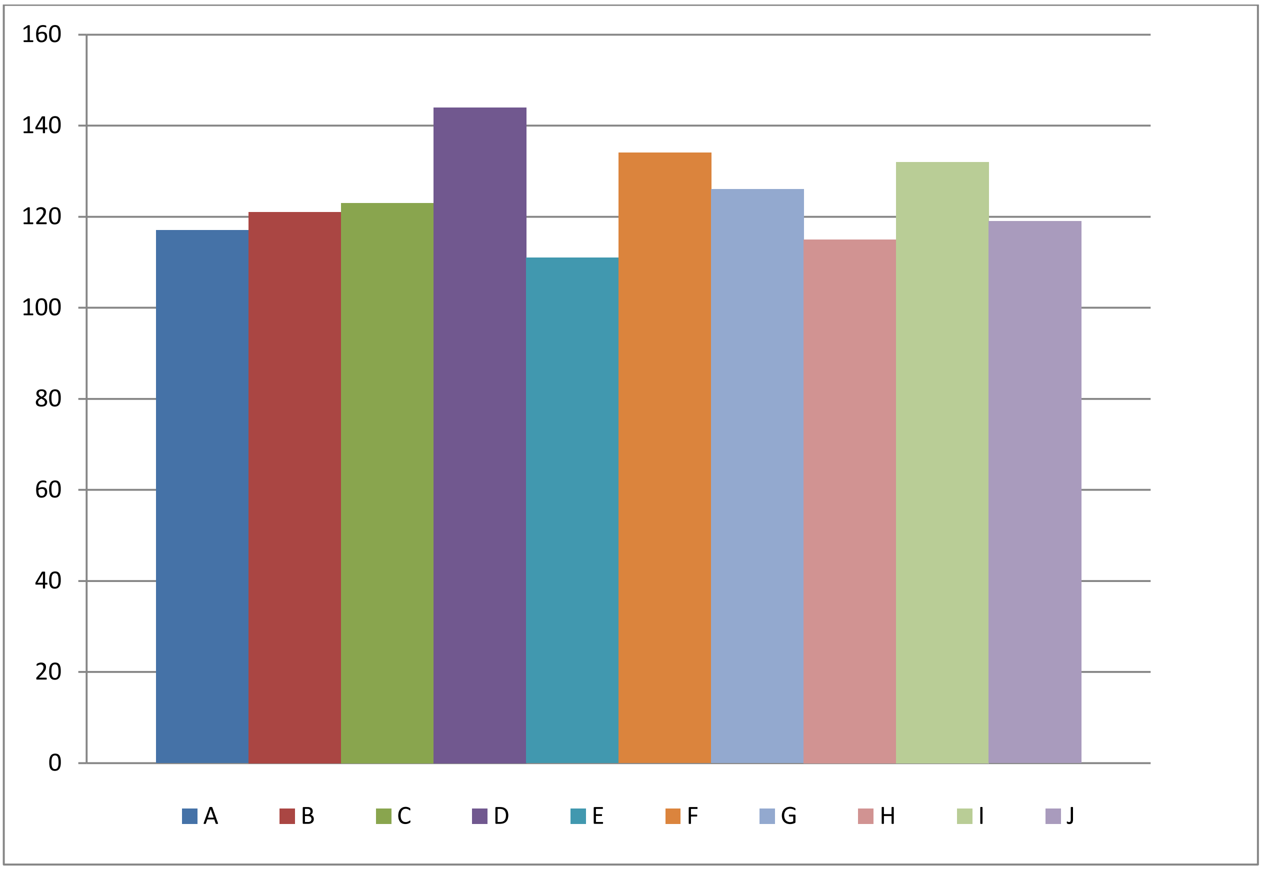

FIGURE 22: EVALUATION SCORES

The chart in Figure 22 illustrates the results of the evaluation. Geometry D was awarded top score in every objective, and consequently turned out to be the best choice. Many of the other structures are not feasible within the limitations, given that the frame must be 15m wide to have room for the module, but not more than 17m wide due to the maximum width in the upper trolley of 17m. Considering the size of the beam cross sections, the angled beam joints in geometries such as D, F, H and I are practically difficult or even impossible. Some if the ideas scored low on shear plates. This is because they have largely oblique angled members, which are unsuitable for shear plates.

3.6. CONCLUSION TO PRELIMINARY DESIGN

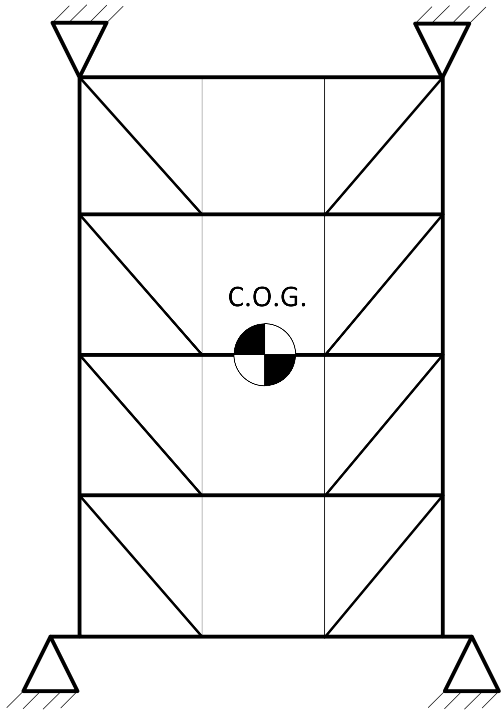

FIGURE 23: PREFERRED GEOMETRY AFTER EVALUATION

Geometry D, as depicted in Figure 23, turned out to be the preferred geometry after the evaluation. In the vertical position, the diagonals carry load. They help transfer weight from the center of the frame to the periphery, where the lifting points are. The lifting points are indicated by the support symbols. The center of gravity of the topside module is somewhere near the middle of the frame, indicated in the figure by the abbreviation C.O.G. The supports, i.e. the ropes, are to the sides. The diagonals included in the drawing act as trusses, and help the front and rear beam carry the moment from the weight of the module.

A distance of 26m from the centerlines of the rear and the front beam is chosen. The frame should be longer than the module, so that the whole module is supported by the frame. However, the frame should not be unnecessarily long, as bending moment grows as the length increases.

The lifting points in the rear must be wider apart than the width of the rest of the frame, so that ropes have the leeway necessary during the rotation. The distance between the lifting points in the rear is set to 17m, due to the limitation set by the upper trolley. This grants only 1m of space from the centerline of the outer longitudinal on each side. It may be uncomfortably little leeway for the rope but, given the limitations of this project, this is the only option. The resulting geometry is depicted Figure 24.

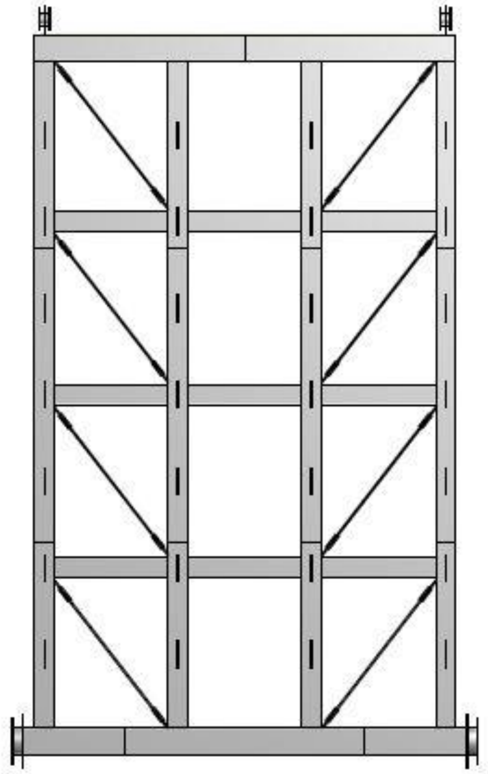

FIGURE 24: FRAME GEOMETRY

As seen in Figure 24, the frame has three rows of inner traverse beams. The longitudinal beams are roughly 25m long, and they benefit from lateral support over their length to prevent instability in compression (Euler buckling) and in bending (lateral torsional buckling). Two rows of traverse beams could suffice, but with respect to shear stiffness contributions by the diagonals, it is advantageous to avoid elongated rectangles in the grid. If the rectangles were rather elongated, it might be difficult to weld the joints, due to sharp angles. Three rows of traverse beams give rectangles that are L x W: 6500mm x 5000mm.

The geometry in Figure 24 is concluded upon as the preliminary design, and is subject to examination in the calculations. While the preliminary design is largely based upon intuition, the final design rests upon a foundation of calculations documenting the capacity of the design. Investigation of the preliminary design reveals new information about the behavior of the frame as well as the behavior of external loads and boundary conditions. This prompts modifications to improve the design, and is a continuous process throughout the calculations. Also, there are parts of the design that are not described by the preliminary design which are defined in the final design.

The parts of the design not described in preliminary design are:

- Design of the lifting points
- Joints with diagonals
- Welds

Concepts to the lifting points have been discussed, but not concluded upon. The diagonals are possibly an important part of the frame, but the design of the joints and the necessary size of the diagonals are not considered in the preliminary design. The frame shall be welded from steel plates, and the welds need to be described and documented. Welding is expensive, so it is important to limit the amount of welding as far as possible, and design welds with appropriate capacity.

4. Final design

During work on calculations, the structural details not described in the preliminary design were defined, and the position of the front trunnions and the alignment of diagonals were revised. The conclusions in the final design are elaborated in the following.

4.1. Lifting points

Suggestions to the design of lifting points are depicted in Figure 14, Figure 15 and Figure 16. The lifting points can either be a trunnion type of design, or a lifting lug type of design, which involves applying a shackle. The structural calculations prove that the shackle solution is unfeasible. It is not possible to design a lifting lug that is strong enough to carry the necessary load and at the same time not be in the way of the shackle. In order for the shackle to fit, a much heavier shackle than necessary is needed, i.e. a shackle able to carry much more load than it needs to.

As the shackle solution is proven unfeasible, a trunnion type of design is chosen for the lifting points. The chosen design for the trunnions are illustrated in the figures in Table 6. In this project, it is assumed that polyester ropes are applied. Alternatively, steel wire rope can be applied. This decision influences the design of the trunnions, as polyester ropes are larger in diameter than steel wire ropes. The ropes are led around the tubes of the trunnions. Contact between steel and rope is assumed frictionless. This provides a support that is free to rotate, and fixed toward displacement in the direction of the ropes. The validity of this assumption should be verified in further work.

TABLE 6: DESIGN OF TRUNNIONS

Front trunnion	Rear trunnion
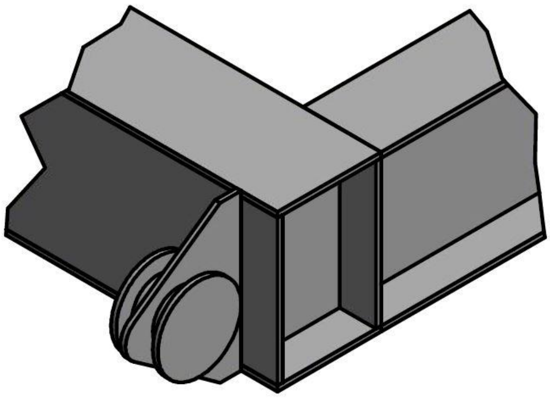 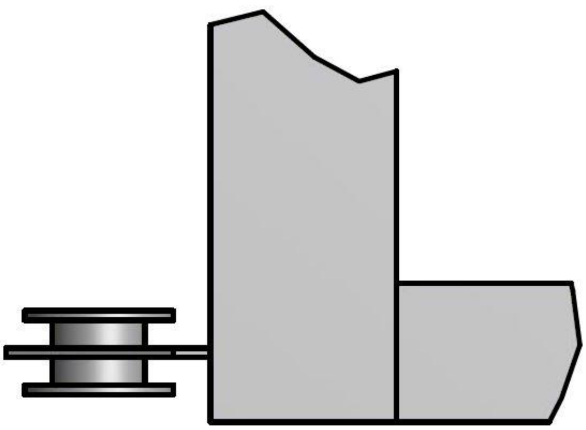	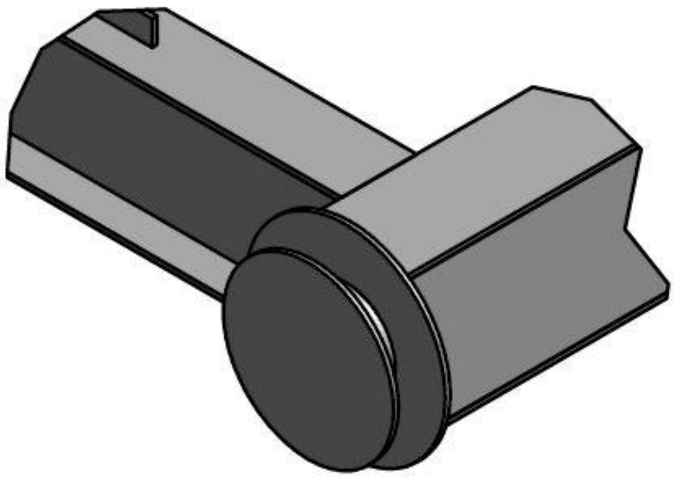 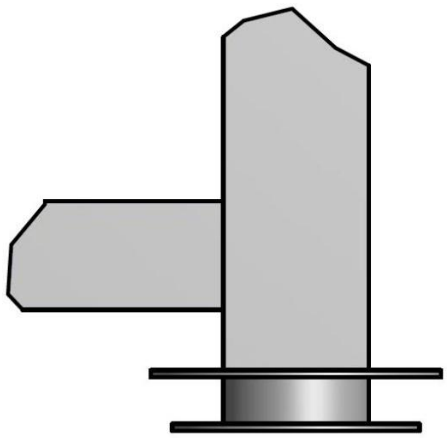

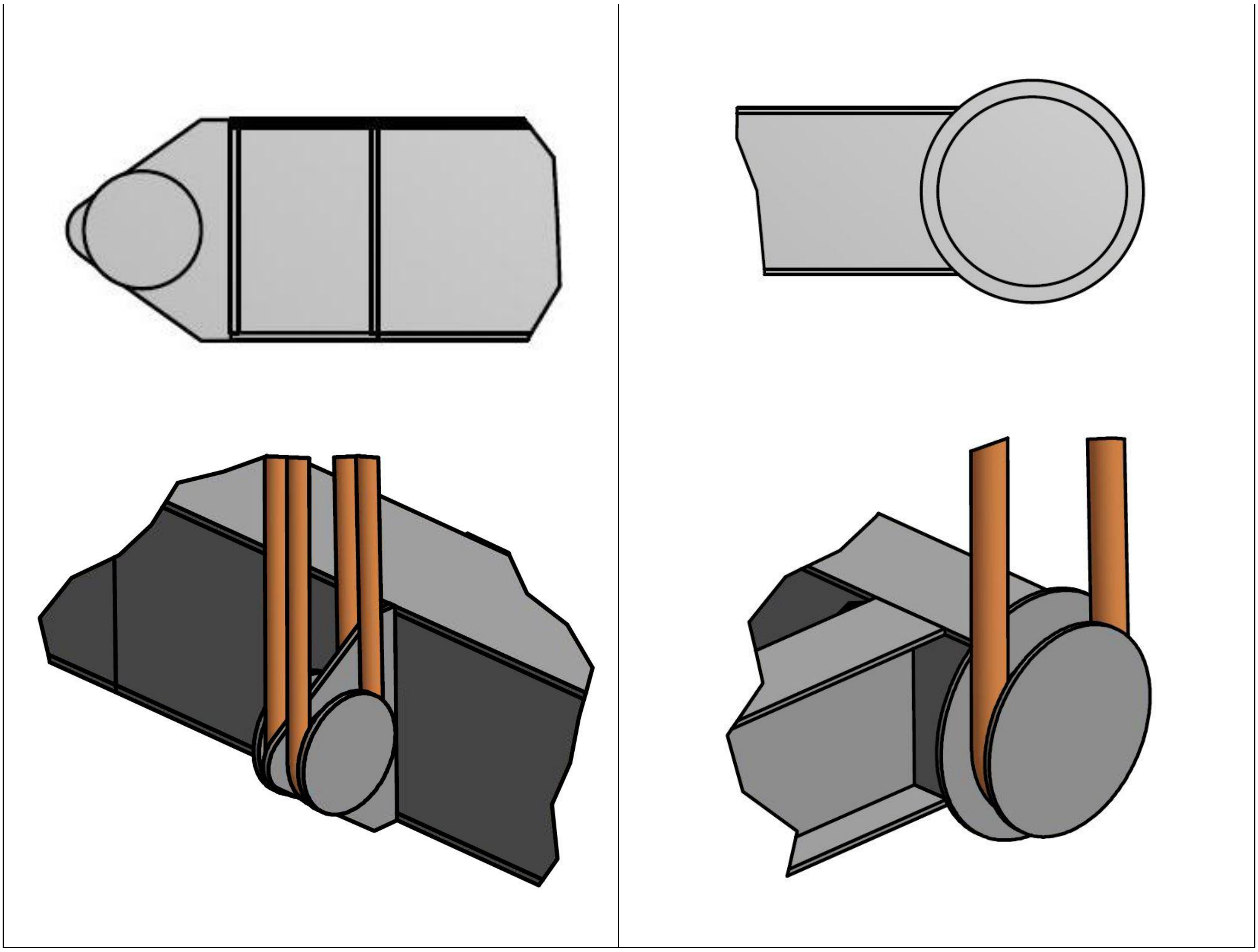

From the illustration of the front trunnion, it is visible that the ropes are eccentric from the center of the front beam. This eccentricity is 1100mm. The trunnion in the rear is eccentric 1000mm from the centerline of the nearby longitudinal, but coincides with the centerline of the rear beam.

4.2. DIAGONALS

The diagonals restrict shear deformation by axial forces. The axial forces in the diagonals must be distributed across the whole height of the beam cross sections. Simple designs that are connected merely to the flanges or to the web are deemed insufficient. The suggested design of the diagonals is shown in Figure 25. The design ensures decent transmission of the axial load to the whole height of the beams. The diagonal bar is connected to a plate by either a weld or a bolted connection. The plate is welded to the beam joint. The design may be "too" solid, but the stiffer the design is, the more efficient the diagonals are.

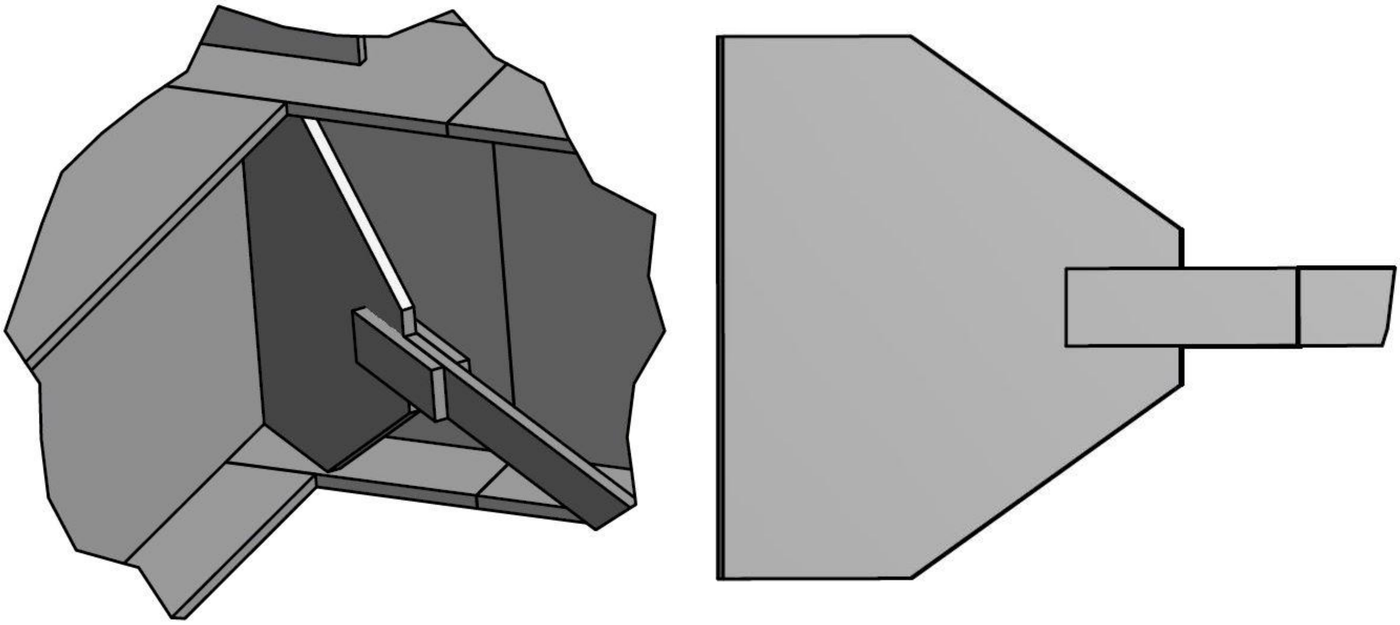

FIGURE 25: DESIGN OF DIAGONALS

4.3. FRAME GEOMETRY

As works on calculations were in process, the idea of moving the front trunnions from the peripheral longitudinal beams to the central longitudinal beams was considered. The deformation pattern of the frame is dependent on where the front trunnions are placed in both horizontal and vertical position. Figure 26 illustrates the deformation pattern of the vertical position when trunnions are placed either on the peripheral (a) and the central (b) longitudinal. The deformation pattern of the Figure 26 (b) seems more advantageous than the deformation pattern in (a). There is less need for transmission of shear forces between the central and peripheral longitudinals, as illustrated in Figure 27. Thus, the need for diagonals is reduced, which may open up the possibility of omitting the diagonals. This would be positive considering the design and manufacturing complexity of the diagonals. Positioning the front trunnions at the central longitudinal beams seems a more rational choice. Nonetheless, both cases are considered in the structural calculations.

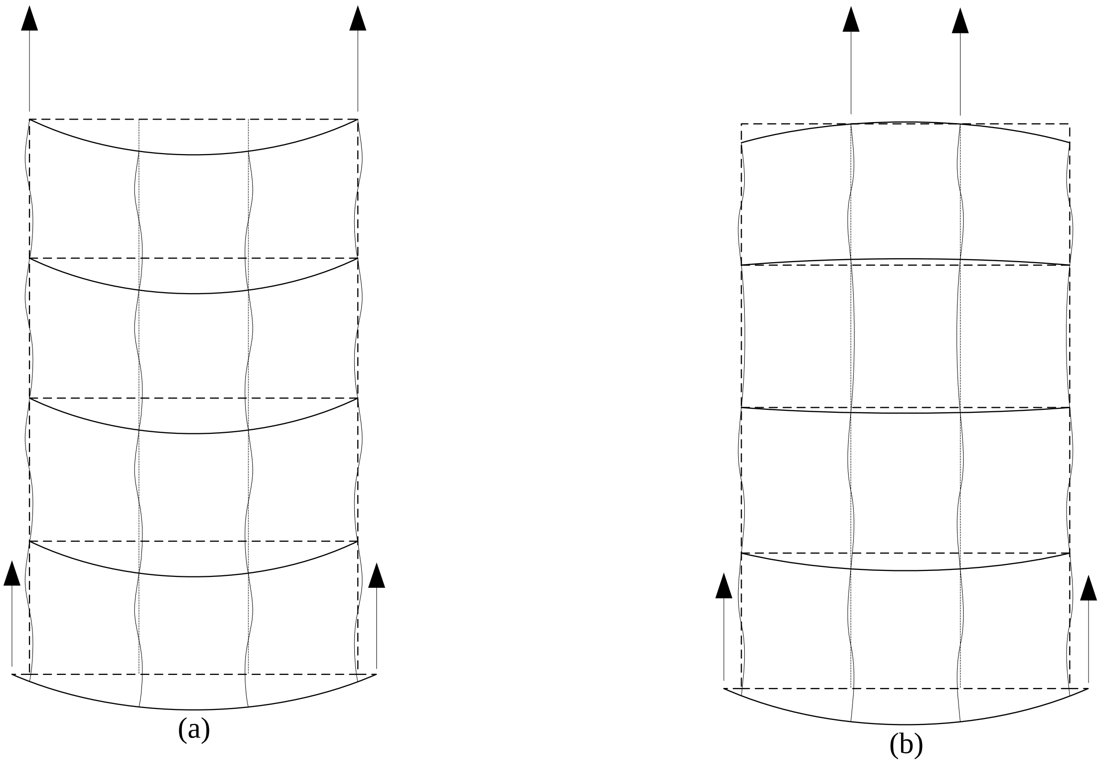

FIGURE 26: DEFORMATION PATTERNS OF VERTICAL POSITION

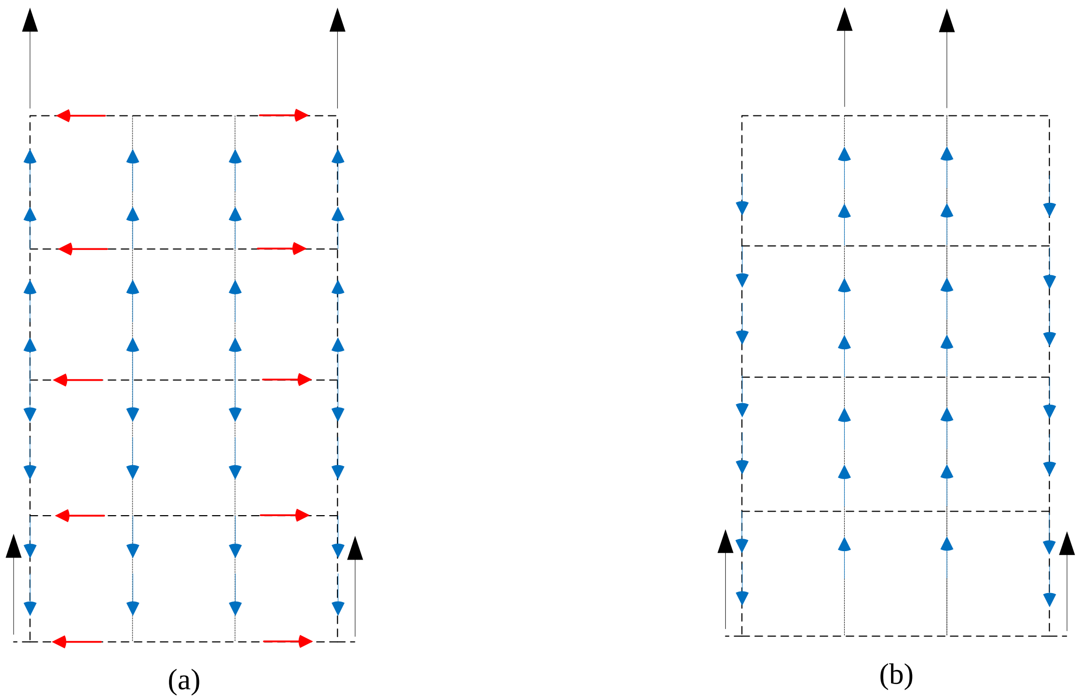

Blue arrows: Axial forces
Red arrows: Shear forces
FIGURE 27: WEIGHT TRANSMISSION IN VERTICAL POSITION

In order to distinguish between the two cases of position of front trunnions, the cases are referred to as Case A and Case B. Due to the deviation in deformation patterns, there is reason to modify the alignment of the diagonals in Case B compared to Case A, to maintain tension in the diagonals in stead of compression. The chosen alignment in the diagonals in Case B is shown together with Case A in Figure 28.

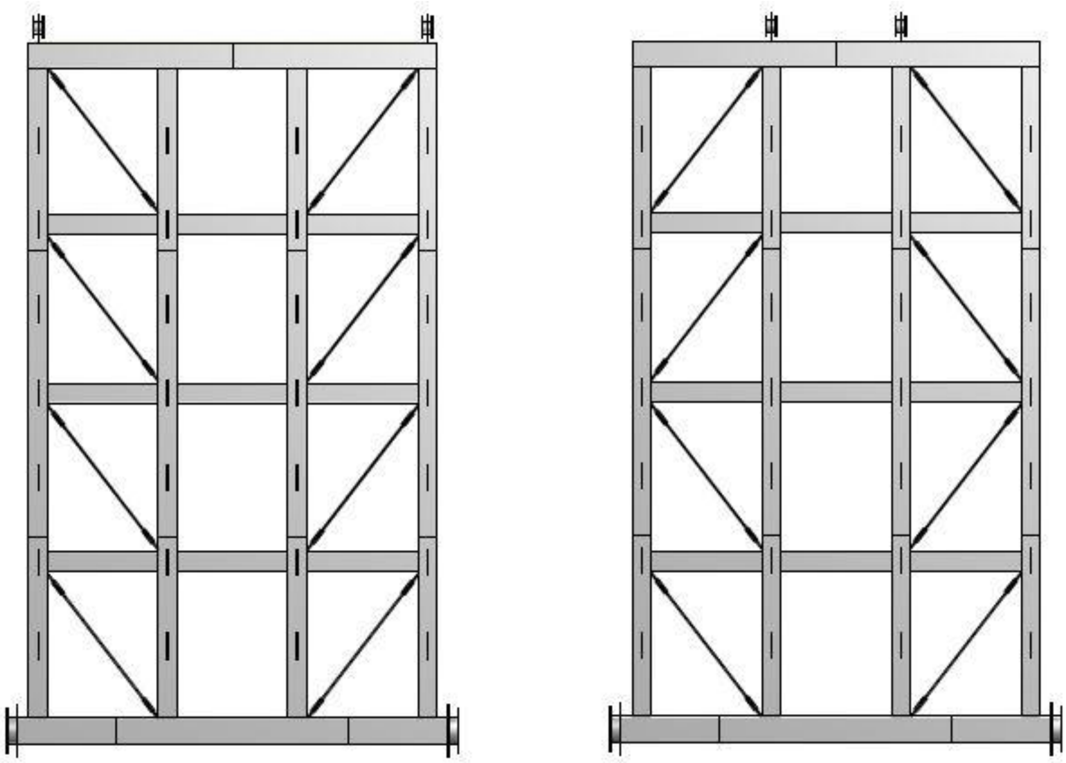

Case A Case B

FIGURE 28: CASE A AND CASE B DESIGNS

4.4. LIFTING EQUIPMENT

As stated previously, polyester rope is chosen in this project. The product data given by the supplier Dawson Group Ltd is applied in the design of the trunnions. The trunnions are designed with respect to the diameter of the ropes which are assumed to be used. There must be enough room for the rope to be led around the tube, but there should not be too much space so that the rope can slide sideways. Figure 29 is a section view of the trunnions with ropes, showing that the ropes fit decently into the trunnions.

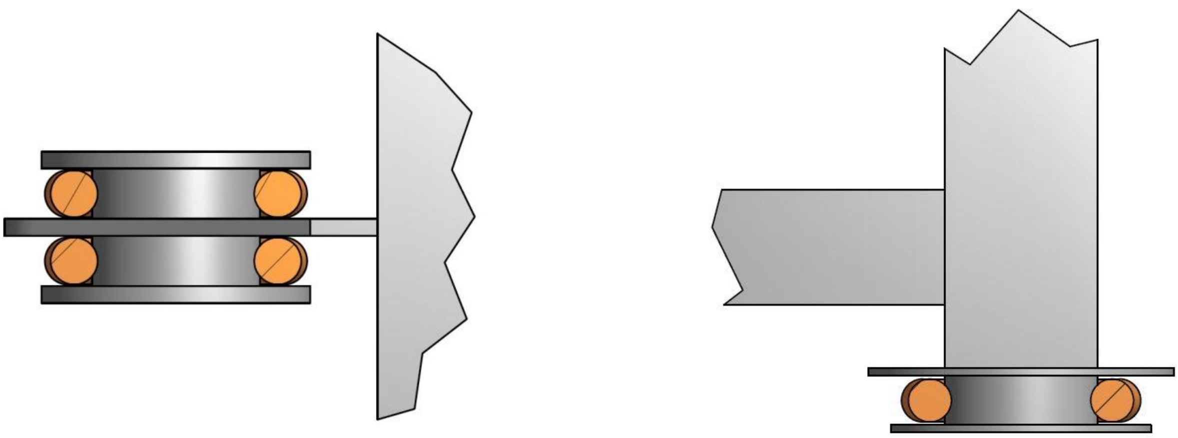

Front trunnion Rear trunnion

FIGURE 29: SECTION VIEW OF TRUNNIONS

Note that in the front trunnion, there are a total of four sections of rope. Consequently, the total capacity is that of four times the individual capacity of each rope cross section. The capacity of a rope's cross section is referred to as working load limit, or WLL. The chosen WLL for the front rope is 100 tonnes. Thus, the ropes in each trunnion are capable of carrying a total of 400 tonnes, and the two front trunnions are capable of carrying 800 tonnes. The rear trunnion has two rope cross sections. The chosen WLL of the rear rope is 300 tonnes. Consequently, the capacity of the rope in the rear trunnion is 600 tonnes, and the total capacity of the ropes is the two rear trunnions is 1200 tonnes. The WLL of the ropes is corrected with a safety factor of 7; hence the nominal capacity is 7 times the given WLL. Thus, the capacity of the chosen ropes is more than sufficient, and could possibly be reduced in order to reduce cost and weight. (Dawson Group Ltd, 2013)

As the front ropes are to be connected to the lower trolley which has but one rope, as discussed earlier, the ropes of the front trunnions must be joined together to a single rope. Suggestions to the arrangement of the front ropes are given in Figure 30. Arrangement (a) has the advantage of not inducing a large bending moment in the spreader beam, as arrangement (b) does. In stead, arrangement (a) induces axial compression force, but this force is expected to be not as severe as the bending moment in (b), given that the angle of the intermediary ropes is perhaps around 20° from vertical. The arrangement (b) might be a simpler arrangement, but the bending moment in the spreader beam means that the beam must probably be rather large. It is expected that the spreader beam in (a) can be smaller than the beam in (b). The design of the spreader beam and specific details regarding the lifting equipment is not considered any further in this project.

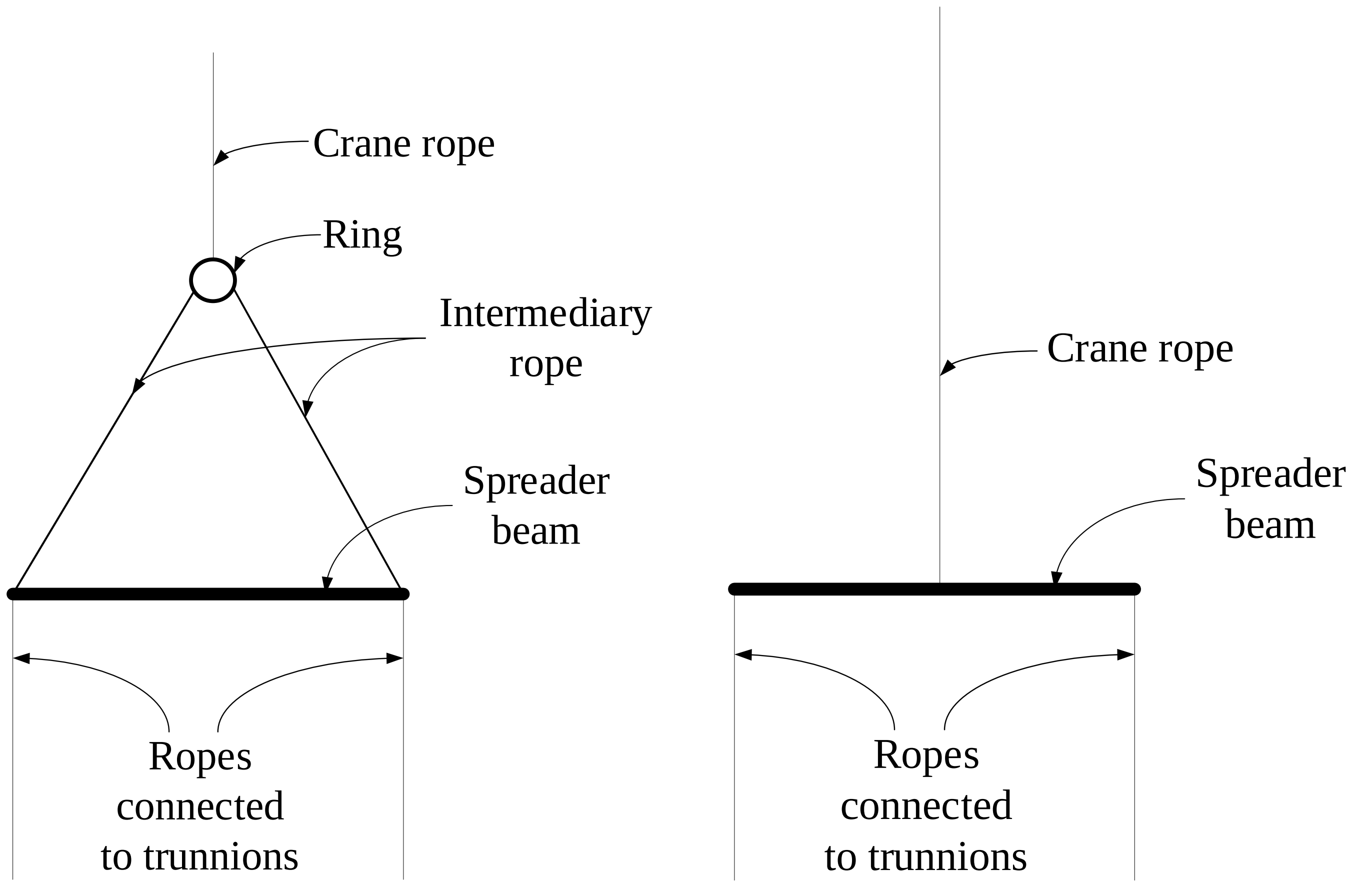

(a) (b)

FIGURE 30: SUGGESTIONS TO ARRANGEMENT OF LIFTING EQUIPMENT

The polyester ropes are fragile to contact with sharp surfaces, especially when there is tension in the rope. The slings provided by Dawson Group Ltd are covered with a protective layer of non load bearing polyester, to protect the load bearing rope fibers from contact. However, the polyester rope may be exposed to contact with the edges of the trunnion plates. The trunnion plates should thus be chamfered and treated such that there are no sharp corners.

As an alternative to polyester rope, steel wire rope may be used. The steel wire rope features a smaller diameter compared to a polyester rope with equivalent WLL. The design of the trunnions is dependent on the diameter of the chosen rope. There must be made a permanent decision as to which type of rope is to be used, so that the rope diameter is constant. Then the width of the trunnions can be altered to fit well with the chosen rope diameter.

PART 2: STRUCTURAL ANALYSIS

5. GENERAL

5.1. CODES AND STANDARDS

The selected design standards are:

- NS 5514: Cranes and lifting equipments/Steel structures/Calculations
- Eurocode 3 Part 1-1: Design of steel structures/General rules and rules for buildings
- Eurocode 3 Part 1-3: Design of steel structure/General rules/Supplementary rules for cold-formed members and sheeting
- Eurocode 3 Part 1-5: Design of steel structures/Plated structural elements
- Eurocode 3 Part 1-8: Design of steel structures/Design of joints

5.2. ENVIRONMENT

The turning frame lifting operation will be carried out outdoors at the shipyard. Thus, environmental loads may exert load on the system. The lifting operation will be carried out only a few times a year. It is assumed that the lifting operation will be carried out in calm wind conditions. Environmental load from snow and ice could appear in winter. It is assumed that the lifting operation is not carried out in snowy weather and that the crew ensures that there is no accumulation of ice on the turning frame or the topside module.
Following these assumptions all environmental loads are neglected.

5.3. LIMITATIONS OF THE STRUCTURAL ANALYSIS

The following aspects regarding structural analysis are considered:

- Estimation of internal load effects, i.e. forces and moments
- Check of cross section capacity
- Check of capacity against column buckling and local plate buckling
- Estimation of local peak stresses
- Design of welds

Fatigue is not considered in the structural analysis of this project, but should be assessed in further work. However, it is assumed that the frame is to be subject to a rather small number of load cycles within a realistic time span, such that fatigue failure is not a problem.

5.4. COORDINATE SYSTEMS

The global coordinate system is referred to the geometry of the crane. The x-axis is parallel to the bridge beam of the crane. The z-axis is in the vertical direction. The global coordinate system is illustrated in Figure 31.

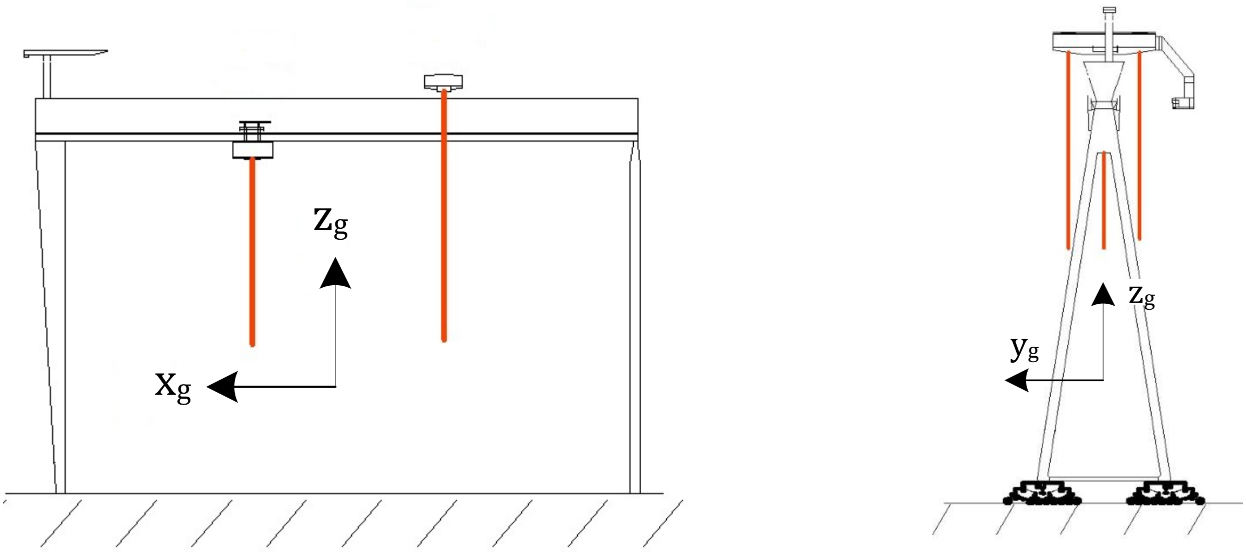

FIGURE 31: GLOBAL COORDINATE SYSTEM

For practical reasons, the turning frame is given a local coordinate system. The x-axis is in the length direction of the frame. The y-direction is in the width direction of the frame. Thus, in the horizontal position, the local coordinate system of the frame coincides with the global coordinate system. In the vertical position, the x-axis of the frame is in the global z-direction. The position of the local coordinate system of the frame is not fixed. It is translated in the plane of the frame where convenient. The local coordinate system is illustrated in Figure 32 and Figure 33.

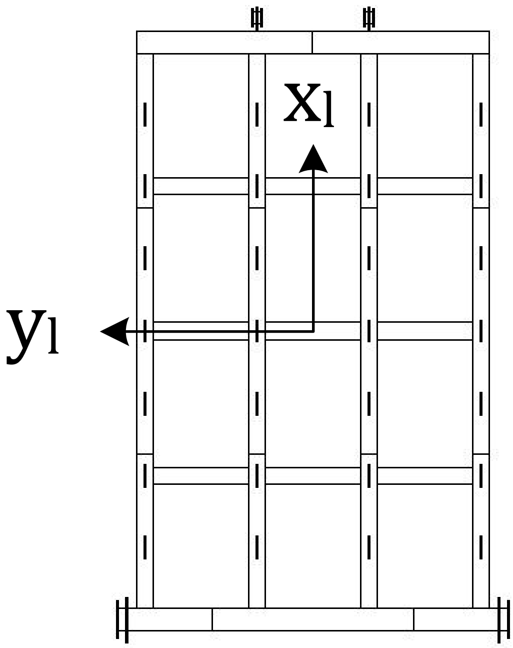

FIGURE 32: LOCAL COORDINATE SYSTEM

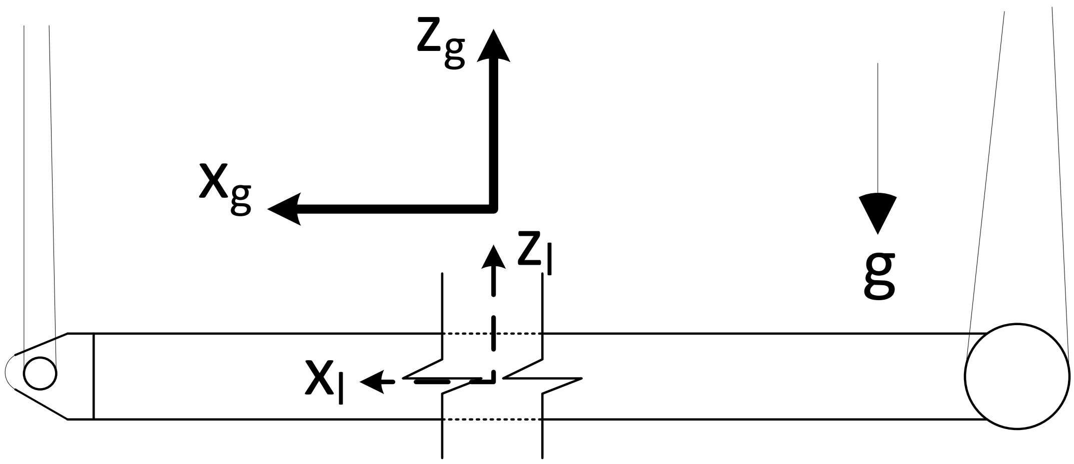

FIGURE 33: LOCAL AND GLOBAL COORDINATE SYSTEMS. FRAME IS IN HORIZONTAL POSITION

5.5. METHOD

The calculations are based on linear static calculations of the frame in Excel, accompanied by finite element calculations. The Excel calculations calculate forces in all members of the frame for a given load case. The results from Excel calculations are cross checked with results from identical finite element calculations to ensure correctness. Structural details are calculated using hand calculations and finite element software. Welds are checked according to standard Eurocode 3 Part 1-8.

5.6. COMPUTER SOFTWARE

For the simplified calculations, MS Excel was employed. MS Excel is a general purpose and visual calculation program, in which the user can write formulae and worksheets.

For finite element analysis, both Focus 3D and Abaqus/CAE have been employed. Focus 3D is a 1D-element program capable of calculation of 3D structures. Abaqus/CAE is a general purpose finite element program capable of elements of both 1D (bar), 2D (shell) and 3D (solid) elements, as well as both linear and nonlinear analysis. Both programs are used for the overall load situation, while Abaqus/CAE is used for simulations of structural details.

5.7. NONLINEARITIES

Nonlinearities can be due to material nonlinearities and geometric nonlinearities among other sources. The possible sources of nonlinearities in this project are explained in the following.

- Material nonlinearity

The elastic design conditions state that the maximum von Mises stress shall not exceed the design yield stress of the material. The stress-strain behavior of steel is roughly linear up to yield stress.

- Geometric nonlinearities

As the frame is rotated 180°, there is a geometric nonlinearity in the sense that the direction of forces relative to the orientation of the structure changes throughout. Theoretically, the frame could be analyzed with a complete dynamic analysis of the 180° rotation. However, it is difficult to build a trustworthy and efficient dynamic model of this situation. In stead, the rotation is analyzed statically by isolating the critical stages in the rotation, which are assumed to be at 0° and 90°.

Deformation of the structure causes nonlinear behavior of the system. However, as long as the stress does not exceed yield stress, it is assumed that deformations are small, such that linear theory is applicable. Nonetheless, both column buckling and plate buckling is considered in separate calculations.

- Load and support nonlinearities

As the frame is in motion during the rotation, inertia forces are present. The magnitude of the inertia forces depend on the weight of the structure and acceleration. Inertia forces are taken into account by including a dynamic amplification factor. Thus, the structural analysis remains linear.

Given the assumptions made, the structural analysis of the frame is a linear static analysis.

6. GEOMETRY AND MATERIAL DATA

6.1. FRAME GEOMETRY

The frame features a grid pattern in which all cells have equal dimensions. The geometry with dimensions is illustrated in Figure 34. The dimensions are given as distance between centerlines, which are indicated by dashed lines. The structural members of the frame are referred to with names throughout the document, also shown in Figure 34.

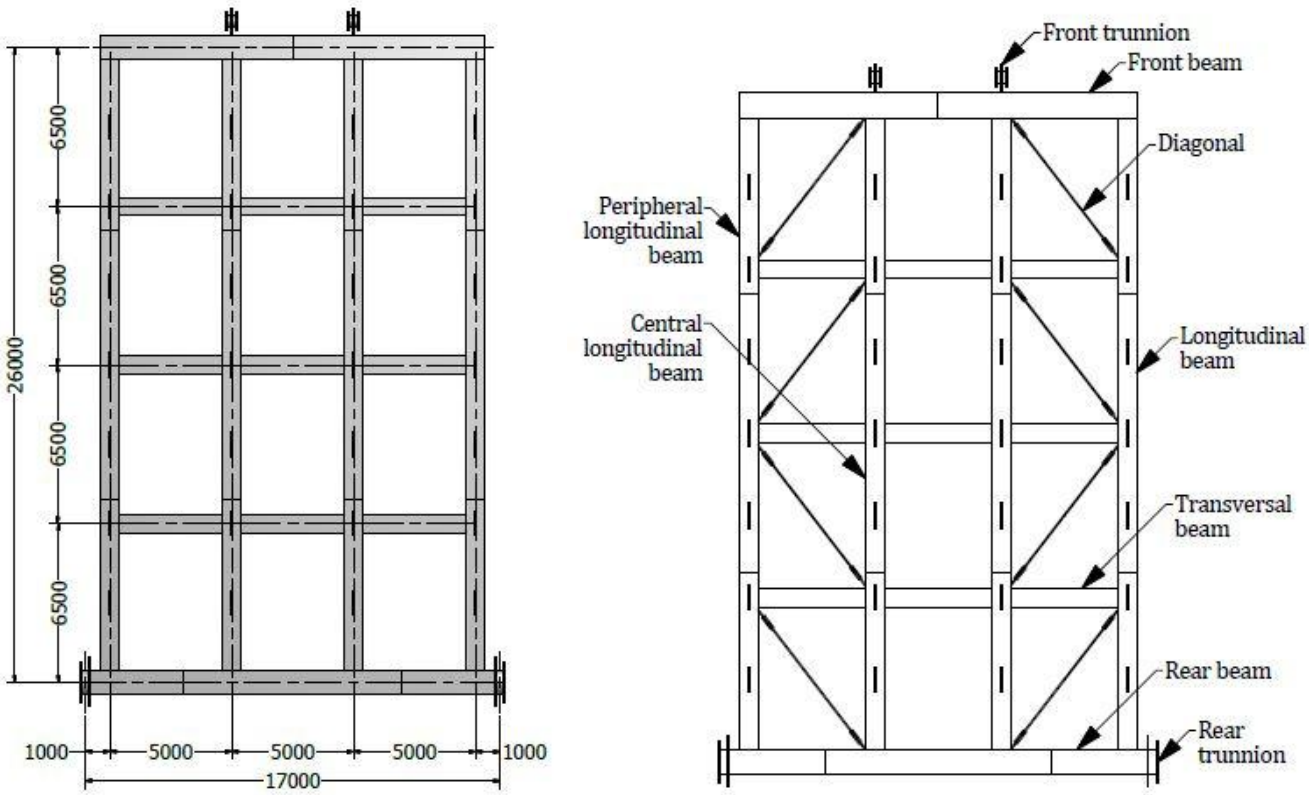

FIGURE 34: GEOMETRY DIMENSIONS AND MEMBER ANNOTATION

6.2. CROSS SECTION PROFILES

Information about the cross section profiles applied in the design is given in the following. The section dimensions given in Table 7: Dimensions of member cross sections are found based on simplified Excel calculations. The critical moment for each section are estimated from simple moment calculations and section properties. The critical moments are calculated by adding forces from the section to the frame. By changing the sizes of the flanges and web, the necessary section dimensions which fulfill the yielding criteria are found.

The thicknesses of the cross sections are chosen based on the wish to have as few sections dimensions as possible. This makes the whole process from ordering to assembly easier. For the welding of sections it’s better to have approximately the same section sizes, to avoid different heat development in the sections and problems with HAZ (heat affected zone). The stiffness also decreases when having connections with profiles of different thicknesses. The height of the section is the most important. The moment capacity seems to be the critical factor from the initial calculations and determines the section size. This needs to be verified in later calculations and the capacity check. This makes the section height and the flange thickness the most important cross section properties.

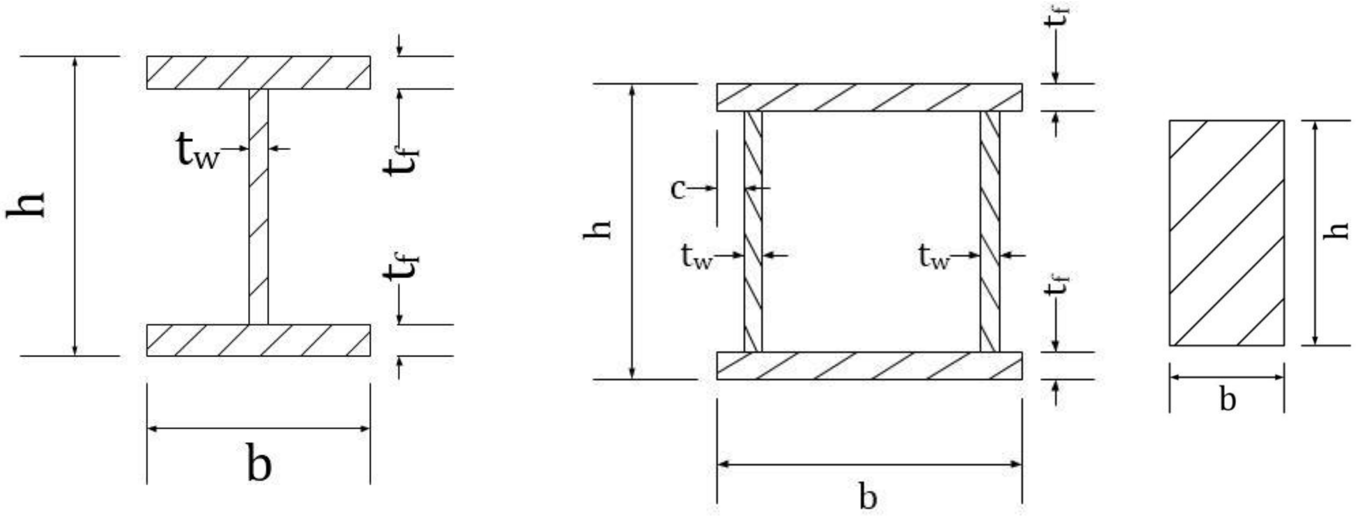

I/H-profile Box profile Rectangular profile

FIGURE 35: ANNOTATION OF CROSS SECTIONS

TABLE 7: DIMENSIONS OF MEMBER CROSS SECTIONS

Member	Longitudinal/Traverse	Front/Rear	Diagonal
Cross section profile	I/H	Box	Rectangular
b [mm]	750	1000	50
h [mm]	1500	1500	200
t_f [mm]	50	50	-
t_w [mm]	50	50	-
c [mm]	-	0	-

6.3. MATERIAL DATA

The steel alloy is standard 420G structural steel. This steel is characterized by a nominal yield stress of no less than 420MPa (MatWeb, 2013). The steel has a weight density of 78.5 kN/m^3(NS-EN 1991-1-1, 2008).

The design elastic modulus, or Youngs modulus, of structural steel is 210.000 MPa (NS-EN 1993-1-1, 2005).

The yield stress of the steel is treated with a material factor according to NS 5514 of 1.5. The maximum allowed von Mises stress is thus 280 MPa, following Table 8.

TABLE 8: CALCULATION OF MAXIMUM ALLOWED VON MISES STRESS

Maximum allowed stress according to NS 5514 and EC3 1-1	
Safety factor according to NS 5514, ν_E:	1.5
Steel nominal yield stress, σ_E [MPa]:	420
Allowed stress, σ_a [MPa]:	280

7. Loads and Boundary Conditions

The frame will carry live load as well as self weight. The live load is due to the weight of the topside module joined to the frame. As the frame is rotated 180°, the load situation changes accordingly. The loads are described in the following.

7.1. Live load

The frame shall be designed to carry a topside module, hereinafter module, of 500 tonnes of mass. Most modules will be of significantly less weight. The frame is assumed to be in operation 2 times per annum. The module is assumed to resemble a cubic shape of dimensions (L x W x H): 25m x 15m x 10m. The module is placed onto the frame with the length direction parallel to the x-axis of the frame. It is assumed in this project that the size of the module is proportional to the weight of the module. Thus, the module assumed previously is critical with regards to the capacity of the frame.

The module is connected to the frame through shear plates. The shear plates are welded to the upper surface of the beam flanges. The shear plates are of dimensions (L x W x H): 1000mm x 50mm x 250mm. They are strong at carrying normal loads in the z direction and shear force in the direction of the x-axis. The main live loads are directed in these axes. The design of the shear plates, as well as their distribution, is illustrated in Figure 36. The blue points indicate the position of shear plates. They are placed equidistantly across the grid. A high number of shear plates provides versatility for the connection of the module.

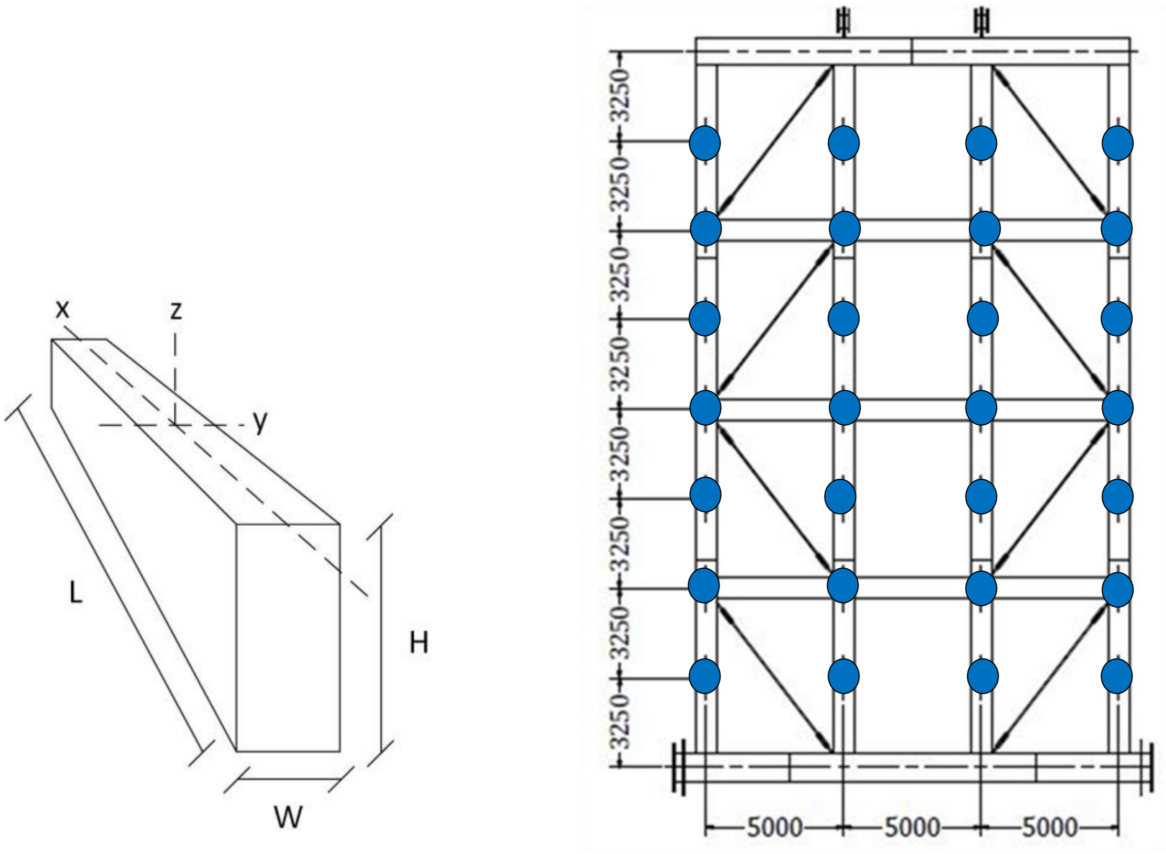

FIGURE 36: DESIGN AND DISTRIBUTION OF SHEAR PLATES

In the calculations, it is assumed that all load points are employed. For a 25 m long module, it is important to employ as many load points as possible to limit internal bending moments in the module. Modules that are shorter than 25 m may be positioned close to the rear of the frame, so as to reduce the bending moment in the longitudinals by moving the center of gravity away from the midspan of the frame.

The predicted deflection pattern of the frame is illustrated in Figure 37. The beam is likely to deflect into a sinusoidal or parabolic shape.

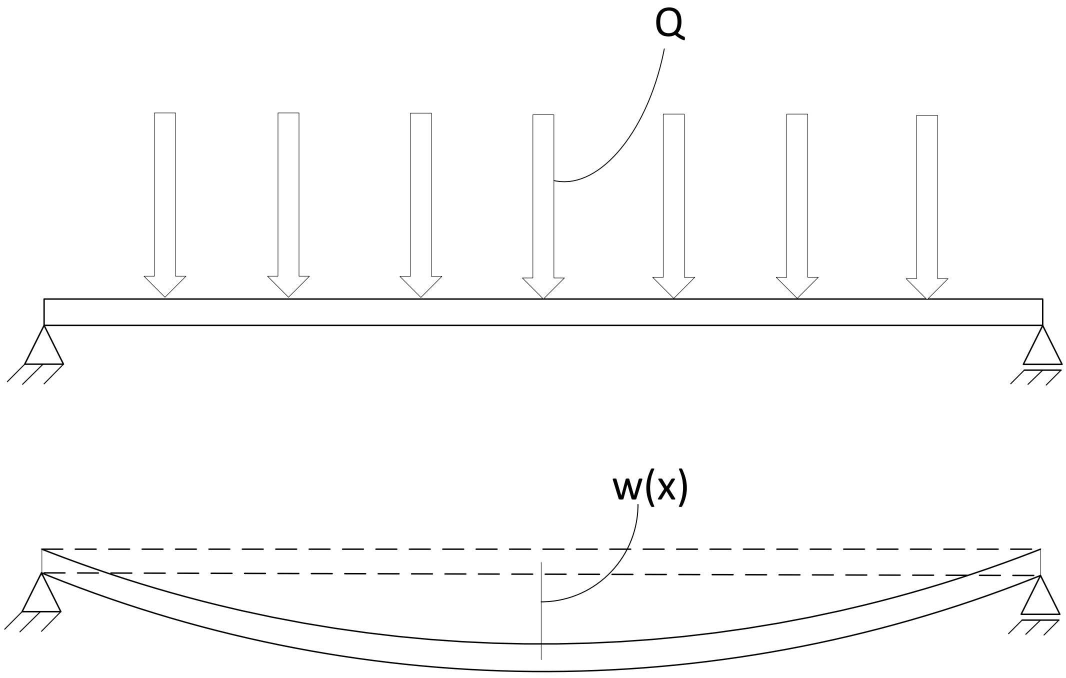

FIGURE 37: DEFLECTION OF FRAME

Q=LOAD. W(X)=DISPLACEMENT.

The shear plates are identical and, thus, have equal capacity. But, as the frame deflects, load could distribute unevenly throughout the length of the frame. As the beam deflects due to bending moment, the topside module will deflect as well. Depending on the bending stiffness of the topside module, the weight of the module would be distributed differently in the direction of the x-axis of the frame.

One can consider the topside module as a beam as well. Thus, the frame and the module will work together to carry the weight. As seen in Figure 38, the support provided by the frame to the topside module can be considered as spring supports. The spring effect is largely due to the bending stiffness, or rather flexibility, of the frame. Had the frame been completely rigid, then the springs could be considered as fixed supports. The spring stiffnesses are denoted with letter k in Figure 38.

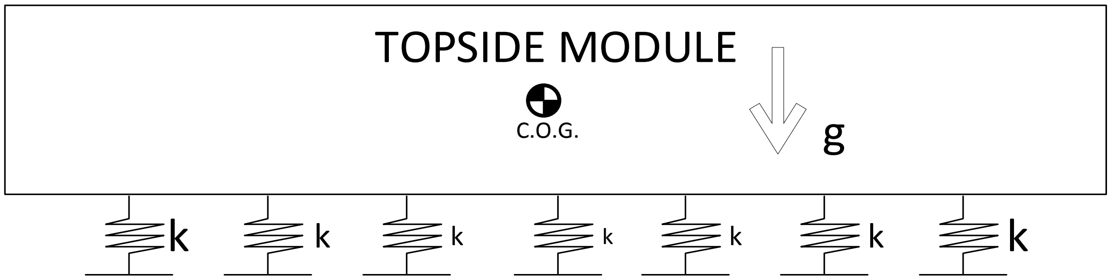

FIGURE 38: SPRING-LIKE SUPPORT OF THE TOPSIDE MODULE

Note the variation in size of the spring stiffnesses in Figure 38, indicated by the size of the letter k. The bending flexibility of the beam decreases the closer one gets to the supports of the beam, where the bending flexibility is zero. Stiffness is the inverse of flexibility, so the stiffness toward deflection is thus infinite if it is measured at a support. The definition of structural stiffness:

$$k = \frac{F}{\delta} \qquad \mathrm{k = stiffness, F = load, \delta = deflection}$$

Given a load distribution where all loads are equal in magnitude, it is straight forward to establish that the stiffness is lower at the midspan than elsewhere, since the deflection is largest at the midspan.

If the topside module is stiffer toward bending than the frame, one would suspect a load distribution as indicated in Figure 39. If the topside module is regarded infinitely stiff toward bending, then the module will not want to deflect at all. Since the bending of the module is coupled with the bending of the frame, the frame is not allowed to bend either. The topside module will exert moment on the frame which counters bending. Given that the topside module is infinitely stiff such that bending deflection is zero, the weight transferred to the midspan of the frame would actually be negative, i.e. the module would lift the midspan of the frame upwards. This is obviously a highly hypothetical scenario. As every topside module is unique, one should be careful making assumptions about the bending stiffness of the modules. However, it is highly unlikely that the topside module is ever stiffer than the frame. Also, it is generally beneficial for the frame if the module is in fact stiffer. It is therefore conservative to assume that the modules are not stiffer than the frame. Hence, it is assumed that the frame is stiffer or at least equally stiff.

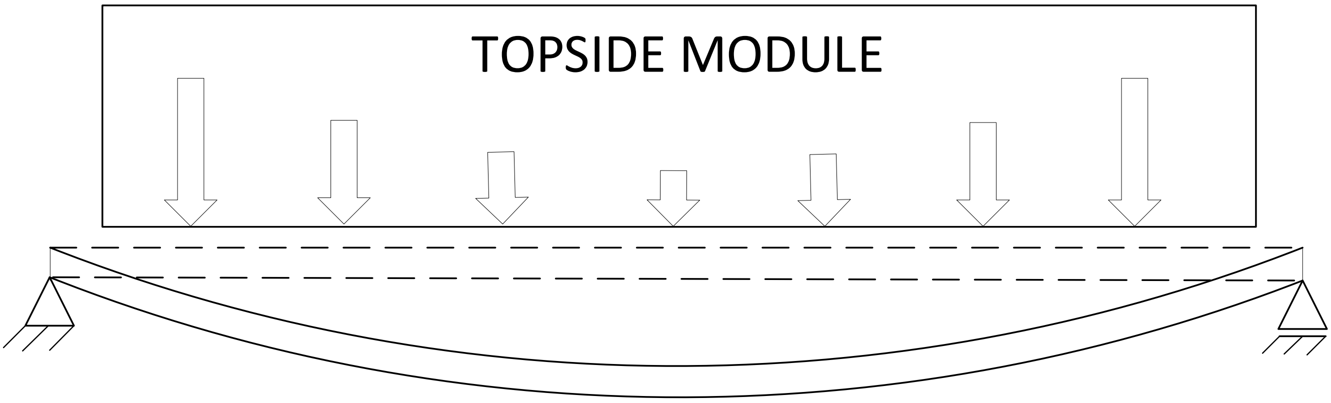

FIGURE 39: LOAD TRANSFER BETWEEN MODULE AND FRAME GIVEN THAT THE MODULE IS STIFFER

If the bending stiffness of the frame and the module are roughly equal, then the bending deflections will also be roughly equal. Figure 40 shows bending of the module on the spring support. One would assume that the forces in the springs would be roughly equal to each other, as the difference in deflection counter the difference in spring stiffness.

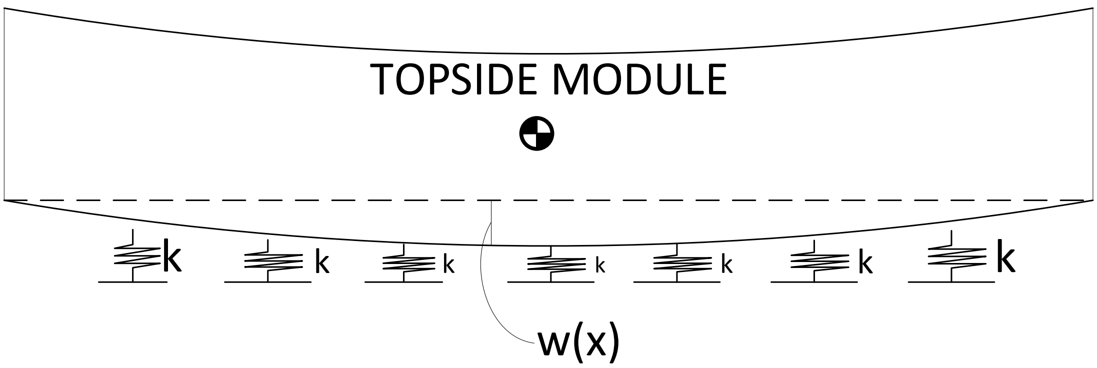

FIGURE 40: DEFLECTION OF MODULE

The most likely scenario is that the frame is significantly stiffer toward bending than the topside module. In this scenario, one can regard the frame as infinitely stiff. Thus, the module will feel like the supports are completely fixed. The scenario is illustrated in Figure 41.

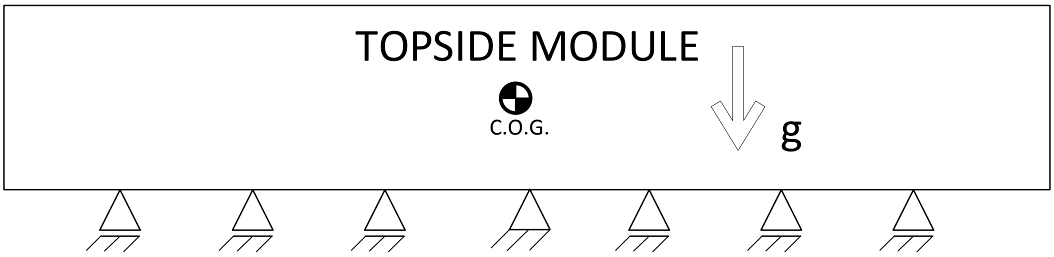

FIGURE 41: RIGID SUPPORTS OF MODULE

The shear force and bending moment diagrams are given in Figure 42. Each support will by and large carry the same amount of weight. Thus, the support loads are approximately equal throughout the length.

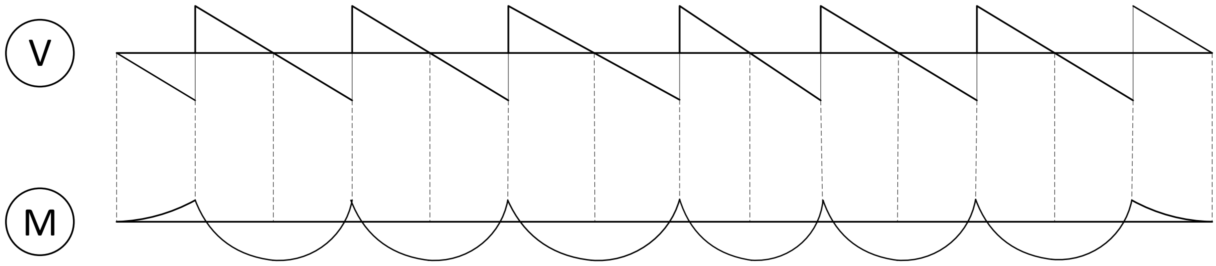

FIGURE 42: SHEAR FORCE AND BENDING MOMENT DIAGRAMS

The conclusion of the consideration of weight distribution is that it is most likely that the loads onto the frame due to the weight of the module are uniform. That is, their magnitude is equal. The same logic applies to the weight distribution across the width of the frame. This assumption is conservative; as the other possibility is that the loads are concentrated into load points closer to the periphery of the frame, where bending deflection is lower, which yields lower bending moments.

7.2. Boundary Conditions

Figure 31 shows the position of the upper and lower trolley. The upper trolley is connected to the rear and the lower trolley to the front. The frame is rotated 180° about the y-axis in Figure 32, in the positive direction. Thus, the front of the frame is lifted upwards relative to the rear. The ropes connected to the rear are placed wider apart, so that the rest of the frame can rotate around between them. This is illustrated in Figure 43. The ropes in the front, hereby denoted the front ropes, must be connected to a spreader beam, as there is only one rope extending from the lower trolley.

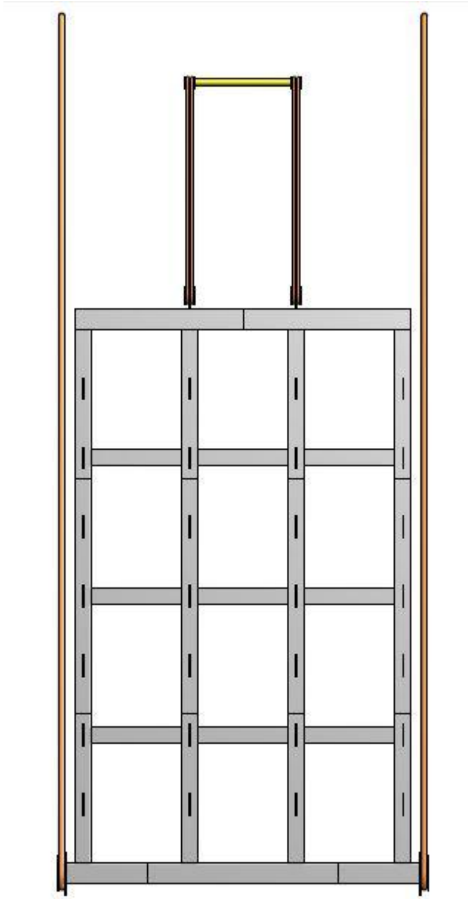

FIGURE 43: FRAME WITH ROPES IN VERTICAL POSITION

The crane operator determines how much load is carried by either the front or rear ropes. The crane has an electronic system which monitors the rope forces at all times, and the crane operator monitors the rope forces from a screen. The crane has restrictions on how much force one can apply to the trolleys. The lower trolley has a capacity of 450 tons while the upper has a capacity of 700 tons (2x350 tons). This limits the operator's possibility to position all the loads on one trolley, because the module weights maximum 500 tons and the frame has a self weight of approximate 250 tons. One trolley can not take this load alone, so the weight distribution becomes a boundary condition during the lifting operation.

The working load limit of the crane is 800 tonnes. To utilize the full working load limit, the trolleys are required to be no less than 15m apart. However, at some point in the rotation, the trolleys have to pass one another. Thus, total weight of the system cannot be 800 tonnes. For a situation where the full load is concentrated to the midspan of the gantry crane, the capacity is 700 tonnes. This is overlooked in this project, as a capacity of 800 tonnes was a premise set from the start.

Ropes do not have any bending stiffness. Neither do ropes have the ability to resist compression. Ropes can only support tension. The support forces on the trunnions are thus decided solely by:

- The position of the upper and lower trolley
- The stiffness and length of the ropes

The position of the upper and lower trolley and the length of the ropes decide which position the frame is in. That is, to which angle the frame is rotated. Both of the parameters are continuously adjusted by the crane operator. As the frame is rotated from 0° to 180°, the boundary conditions of the frame change continuously. The rotation is illustrated in Figure 44.

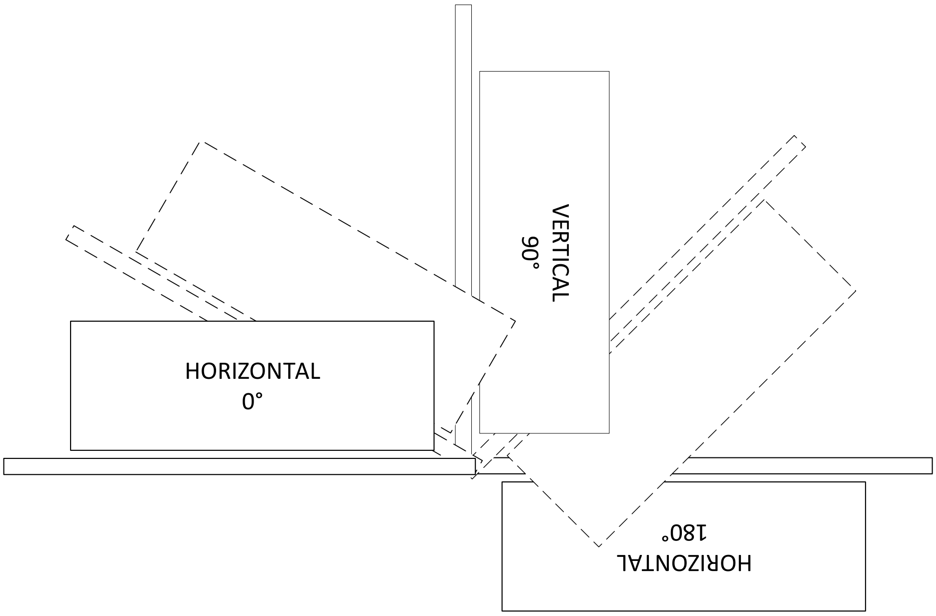

FIGURE 44: COMPLETE ROTATION OF THE FRAME

Figure 45 illustrates the horizontal position with vertical ropes. F_{front} and F_{rear} are the forces in the ropes, illustrated by the arrows. This situation resembles a simply supported beam, which is statically determinate. Thus, the support forces exactly are found by moment equilibrium in the supports. This means that if one changes the stiffness of the ropes, it should not affect the force distribution, as long as the deformations don't get too large.

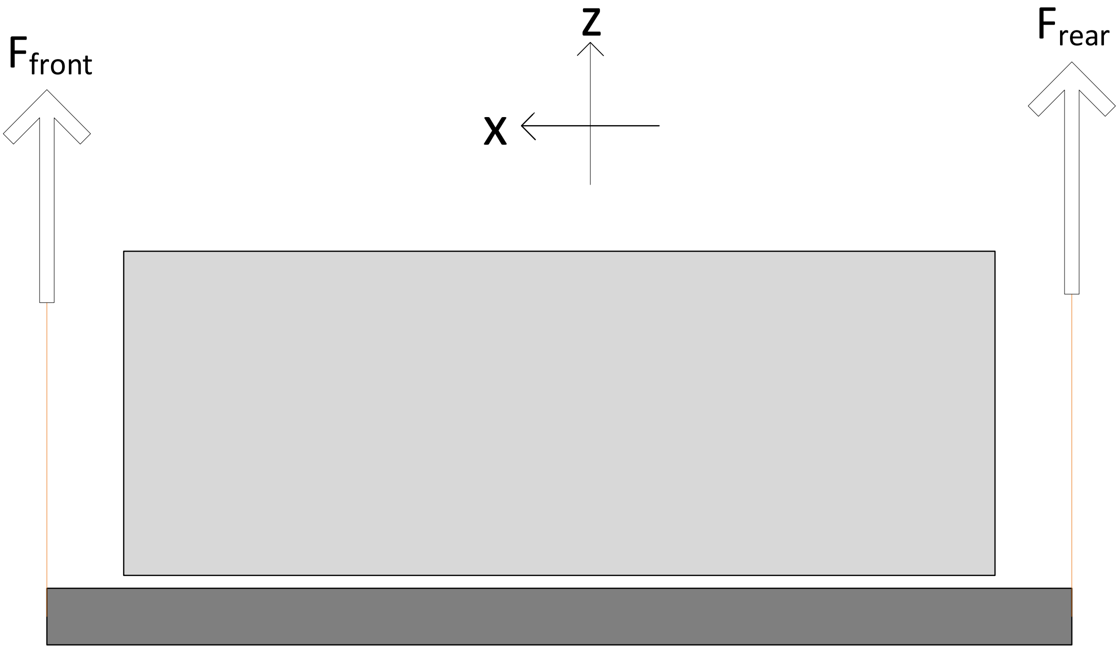

FIGURE 45: HORIZONTAL POSITION WITH VERTICAL ROPES

The ropes in Figure 45 are orthogonal to the plane of the frame, which is the xy-plane in the figure. It is beneficial that the ropes are always vertical. Then, the total load in the ropes is as low as possible. However, as the frame rotates, the ropes will not remain orthogonal to the xy-plane of the frame. Then, the support forces can be decomposed as illustrated in Figure 46.

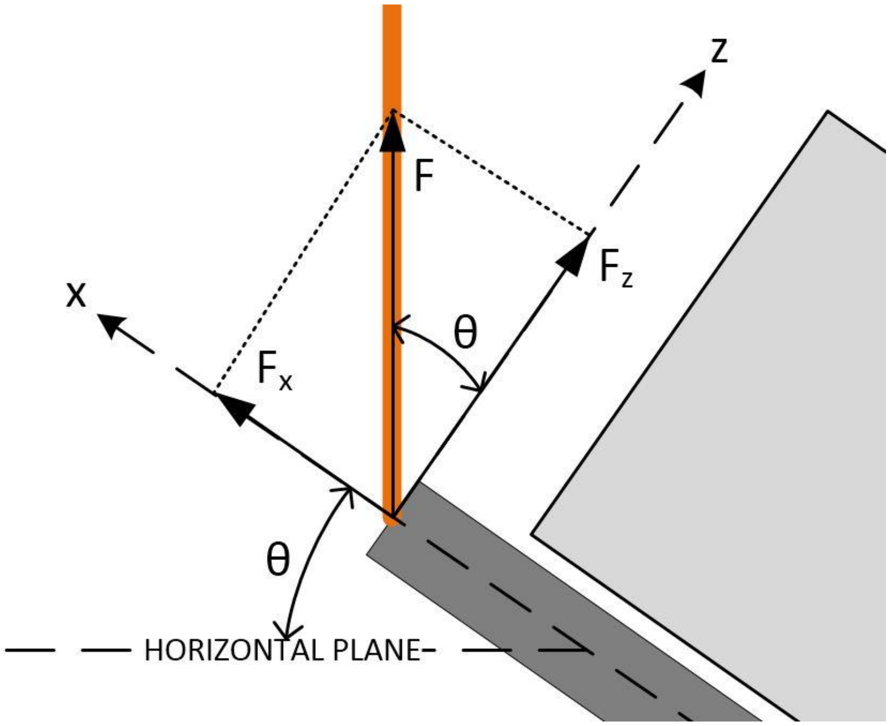

FIGURE 46: DECOMPOSITION OF SUPPORT FORCE IN FRONT

The decomposed force F_z remains statically determinate throughout the course of the rotation. Given an angle θ and F_z the rope force F can be found, as well as the component F_x. Thus, all support forces are known. Had the supports been fixed against translation, the component F_x would have been statically indeterminate. However, the condition that only axial load is allowed in the ropes yields an extra equation which makes the problem statically determinate.

In the vertical position the internal forces of the frame are statically indeterminate. The diagonals are contributing to the force distribution. This gives a complex system which is hard to calculate by hand.

Generally, for a given configuration of rope lengths, there is always one state of equilibrium. If the frame is not in a state of equilibrium, then it will translate and rotate toward an equilibrium state. Such motion can induce heavy loads on the system due to mass inertia. It is necessary to avoid accelerations of the body as far as possible. However, some motion is inevitable as motion is what makes the frame rotate in the first place.

When the frame is in equilibrium, there is no immediate resistance to motion in a plane orthogonal to the ropes. Thus, a gust of wind may induce motion of the body. As the body moves away from the equilibrium state, however, resistance toward the position increases and brings the body back to equilibrium, as illustrated with the ball in Figure 47.

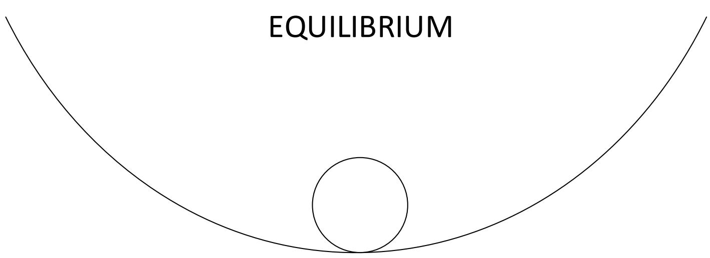

FIGURE 47: STATE OF EQUILIBRIUM OF THE BODY

For the frame to rotate, the trolleys of the crane must pass each other. Also, either one or both of the trolleys must release or retract rope. The controlling of the position of the trolleys as well as the length of the ropes governs the configuration of the equilibrium state. It is important that the frame follows a smooth equilibrium state at all times. Every action should be slow and smooth. Retraction and release of rope must be controlled carefully.

7.3. Equilibrium Equations and Static Indeterminacy

In a statically indeterminate system, internal forces and support forces are not uniquely defined by equilibrium equations alone. The structural stiffness of the elements is what determines the internal forces. In a statically indeterminate lifting operation, small deviations and imperfections may elicit severe loading conditions. To account for possibly unfortunate load situations, the loads are treated with a skew load factor for statically indeterminate lifting operations. Given a perfectly accurate system in which stiffness and geometry is known with an unrealistic degree of accuracy, an optimal load transmission is attainable. However, it is impossible to prescribe the alignment of the ropes with a sufficient level of accuracy such that unfortunate situations are avoided completely. Variations in stiffness of the ropes, as well as in the frame may elicit variations as well.

In statically determinate lifting operations, small imperfections do not elicit unfortunate consequences for the load transmission. The skew load factor for statically determinate systems is thus 1.

In the 3D space a rope force has 3 components, as seen in Figure 48.

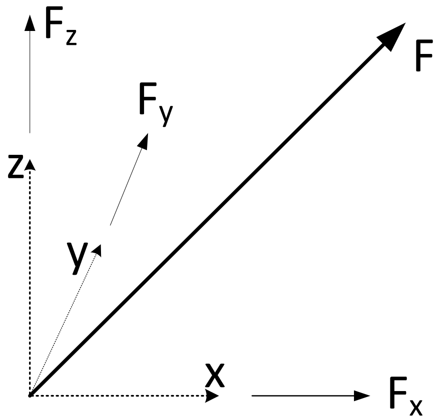

FIGURE 48: FORCE DECOMPOSITION

The components of the rope force constitute the rope force vector.

$$\{\boldsymbol{F}\} = \{F_x, F_y, F_z\}$$

The rope force is given by the Pythagorean Theorem.

$$F^2 = F_x^2 + F_y^2 + F_z^2$$

Ropes can only resist tensile force. Thus, the rope force vector must be parallel with the rope. The alignment of the rope may be given by a unit vector $\{\boldsymbol{l}\}$, whose absolute length is 1. The rope force vector is related to $\{\boldsymbol{l}\}$ by a constant, c. Thus, c and $\{\boldsymbol{l}\}$ uniquely defines the rope force.

$$\{\boldsymbol{F}\} = c\{\boldsymbol{l}\}$$

However, small deviations from the ideal arrangement may originate vast variations in load distribution in a statically indeterminate system

A unit vector constitutes 2 unknowns. There are 3 components of the unit vector, but there is also a condition that the absolute value of the unit vector must be equal to 1. Following this, there are 3 unknowns for each rope: 1 for constant c and 2 unit vector $\{\boldsymbol{l}\}$. There are four lifting points on the frame, so a situation with four unknown rope forces is considered. Thus, the total number of unknowns is 3x4=12. The rope forces are illustrated in Figure 49.

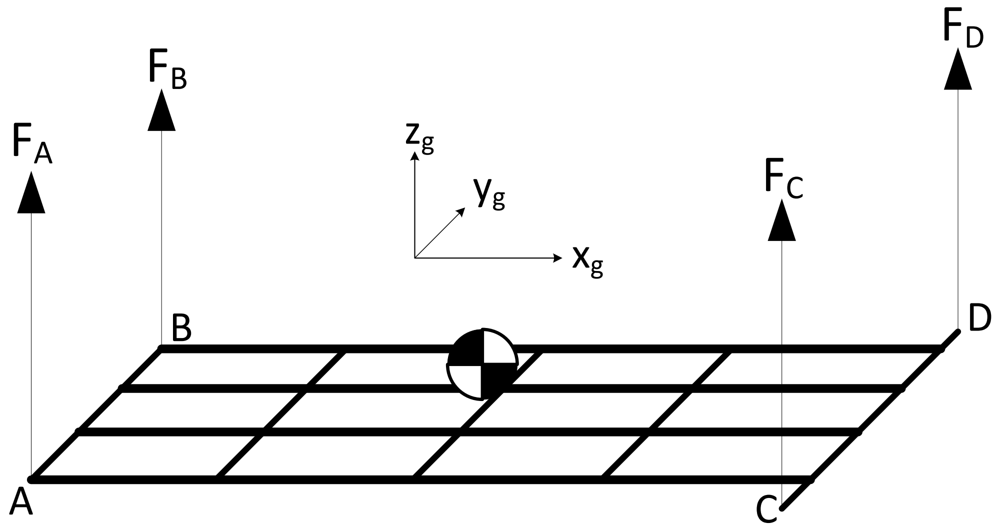

FIGURE 49: ROPE SUPPORTS OF FRAME

In the 3D space, there are 3 force equilibrium equations and 3 moment equilibrium equations.

$$\sum \begin{matrix} F_x = 0 \\ F_y = 0 \\ F_z = 0 \end{matrix} \qquad \sum \begin{matrix} M_x = 0 \\ M_y = 0 \\ M_z = 0 \end{matrix}$$

Together with the rope force condition, which constitutes 1 equilibrium equation for each rope, there are thus 10 equilibrium equations in total. The level of static indeterminacy is thus 12-10=2. If symmetry about the XZ-plane had been assumed, the rope forces would be uniquely defined, but symmetry conditions are not valid. For the statically indeterminate lifting operation of the frame, the rope forces will be concentrated about one of the diagonals illustrated in Figure 50. The forces F_i balance each other out and comply with all the equilibrium equations stated earlier. It is obviously an unfortunate situation. It is this effect that the skew load factor takes into account.

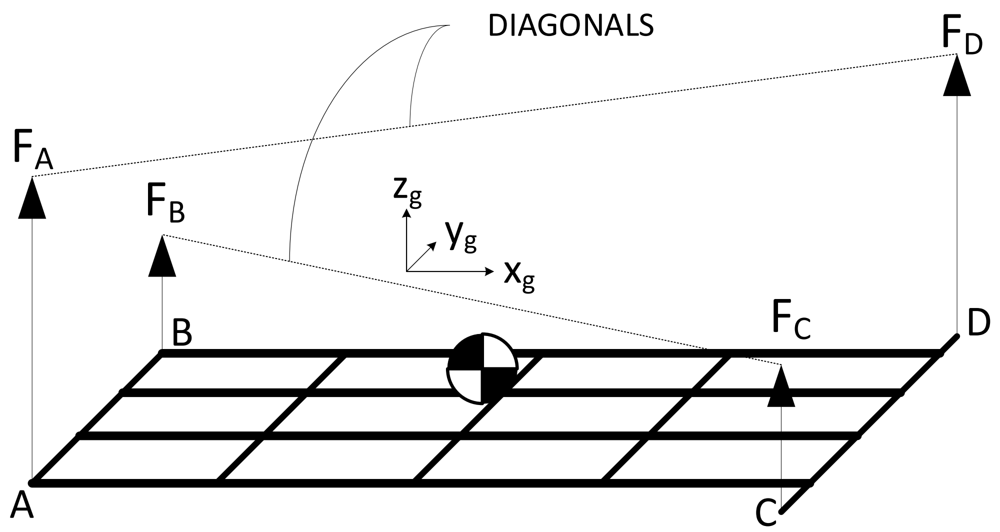

FIGURE 50: SKEW LOAD FACTOR DUE TO STATIC INDETERMINACY

Obtaining a statically determinate system

The gantry crane intended to use the turning frame has three ropes extending from it. The upper trolley has two ropes, and the lower trolley has one. The rope from the lower trolley is connected to the front of the frame, which is where points A and B are located in Figure 49. In the following, the suggestion of lifting arrangement (a) is assumed, as illustrated in Figure 30. With regards to static determinacy, arrangements (a) and (b) have the same properties. In arrangement (a), the single rope extending from the lower trolley is split into two ropes through a ring, as illustrated in Figure 51. Assuming that there is a coordinate system aligned with the single rope such that the z-axis of the coordinate system is parallel to the single rope, the force in the single rope has only one component. Thus, there is just one unknown value. There are three applicable equilibrium equations, which are force equilibrium in the 3 dimensions. Compared to the statically indeterminate system with four individual and independent ropes considered previously, the total number of unknowns has risen by 1 to 13. The total number of equilibrium equations has risen by 3 to 13 as well. Thus, the system is now statically determinate.

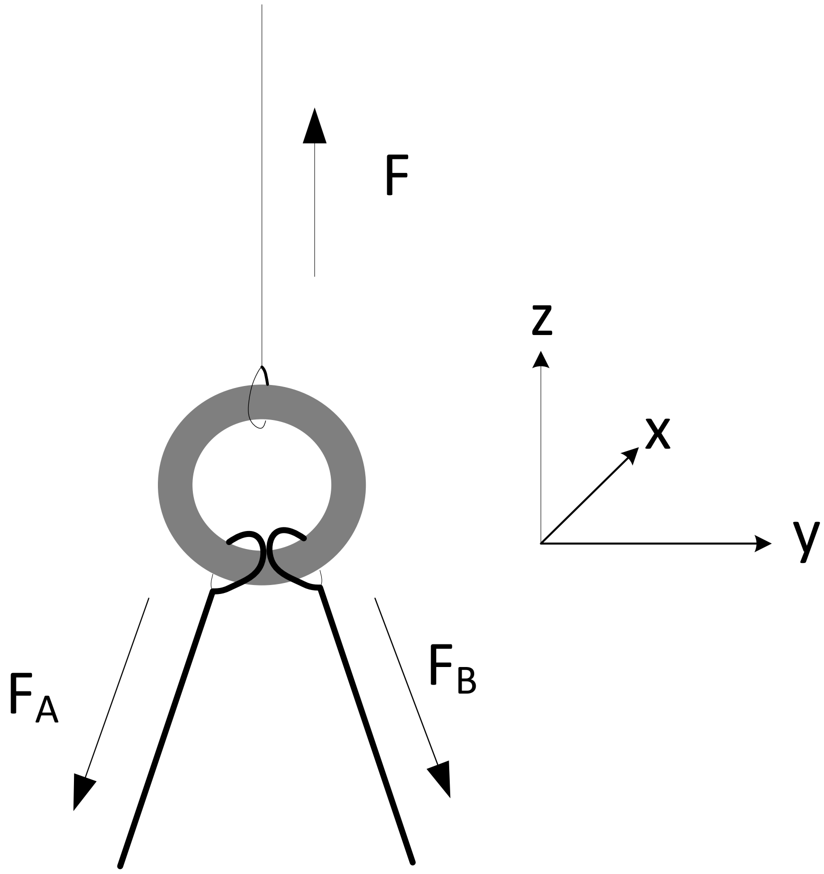

FIGURE 51: RING JOINT CONNECTING ROPES

In the statically determinate system, one has much more control over the distribution of loads. Small deviations from the intended alignment of the ropes do not elicit significant variations in the load situation. Thus, the skew load factor is set equal to 1.

In the vertical position, the length of the ropes, controlled by the crane operator, decide where the loads go. The rope forces are still statically determinate, but stability of the frame is a challenge, as is investigated in the following chapter.

7.4. Instability in Vertical Position

As the frame approaches the vertical position, approximately when the center of gravity of the system is vertically above the rear trunnion, the frame will potentially tip over if it is not restrained. Up to this point in the rotation, gravity has worked against the rotation. At the tipping point, the gravity suddenly becomes a driving force of further rotation. It is important that at this instant, there is resistance in place which restrains rotation. The situation is illustrated in Figure 54.

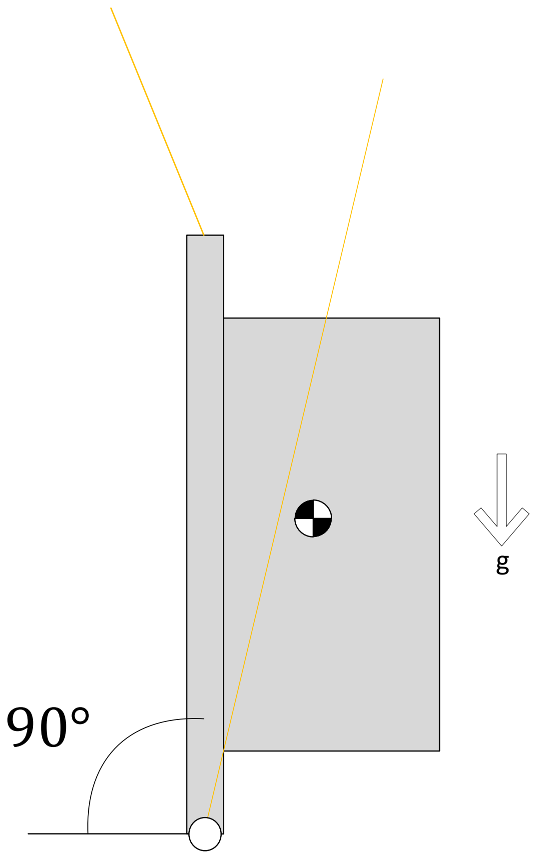

FIGURE 52: INSTABILITY IN VERTICAL POSITION

To keep rope forces to a minimum, they should be kept vertical, thus parallel to the direction of gravity forces, throughout the rotation. However, at the point where the lower trolley passes beneath the upper trolley, if the ropes are perfectly vertical, they can resist no moment. This is illustrated in Figure 53. Given the premise that ropes are kept perfectly vertical throughout the rotation, it is possible to calculate what the rope forces must be in order to maintain equilibrium. The rope forces go to infinity near 90° rotation. The force necessary in the front rope is zero around 70°. At this point, the frame wants to tip over.

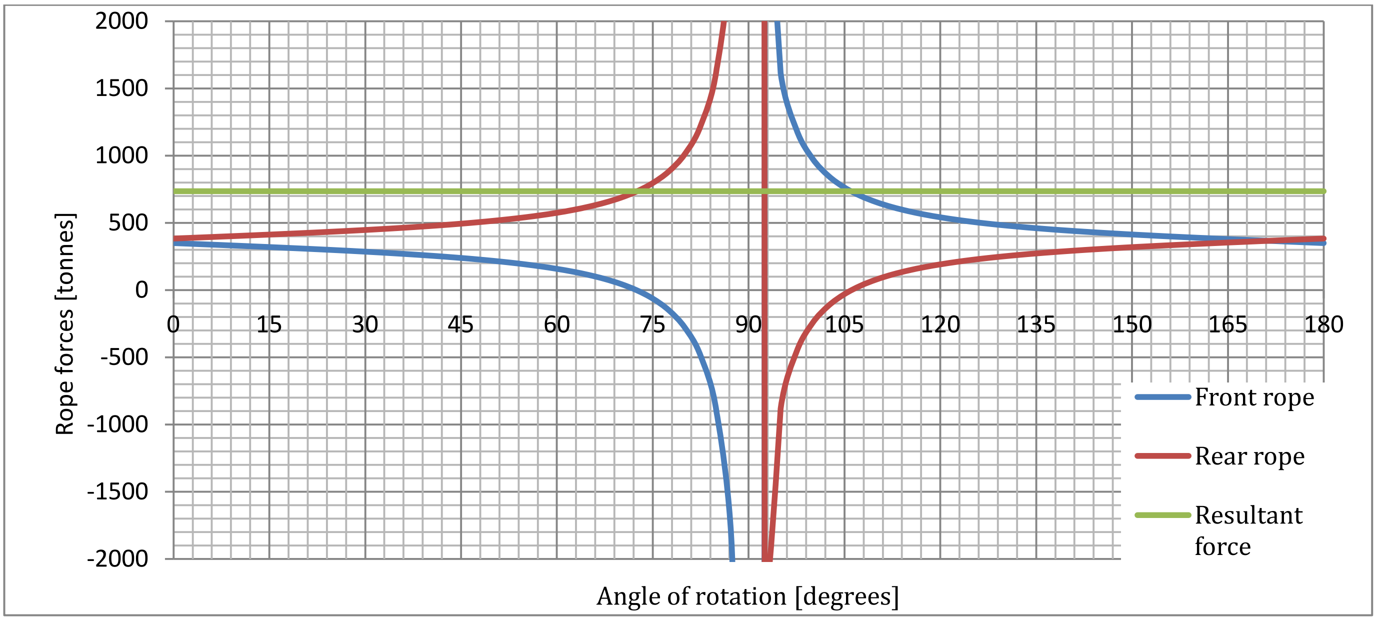

FIGURE 53: ROPE FORCES NECESSARY TO MAINTAIN EQUILIBRIUM WITH VERTICAL ROPES

From Figure 53 it is evident that the rope forces necessary to maintain equilibrium are unacceptable in the range from 60° to 120°. From 70° onwards the rope force is even negative, i.e. there is compression in the rope, which is impossible. To maintain equilibrium, there is no other way than to have an angle in the ropes. There must be a horizontal force component which balances the moment. The horizontal force component must be carried by the crane. The sum of horizontal forces must be zero, so the foundation of the crane will not notice any horizontal force. However, the trolleys must be able to resist the force. The trolleys have brakes which are used to constrain horizontal motion. It is this far unclear whether it is possible to utilize the brakes to be able to maintain equilibrium of the system. The brakes have limited capacity, and are not designed for this use.

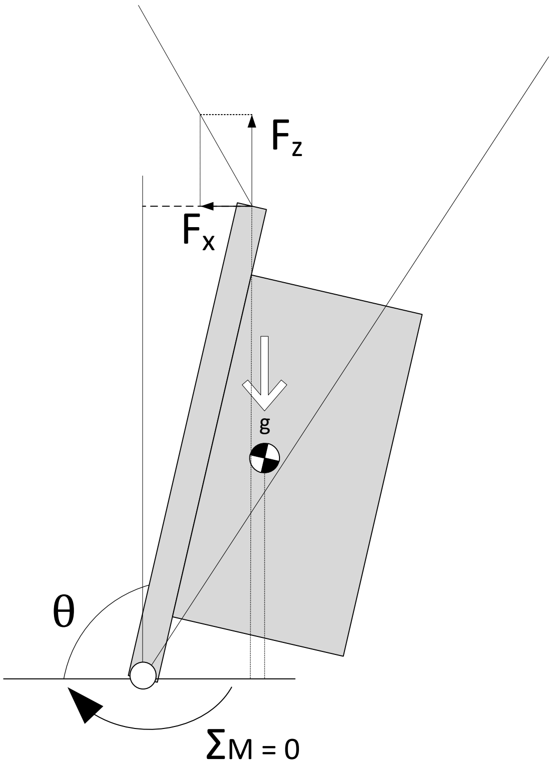

FIGURE 54: MOMENT EQUILIBRIUM ABOUT REAR TRUNNIONS

Figure 54 illustrates moment equilibrium about the rear trunnions at a given angle of rotation, θ. The forces exerting moment about the rear trunnions are the weight of the topside module and frame, and the components of the rope force in the front trunnion. The combined center of gravity for the module and the frame are indicated by the center of gravity sign. At a given angle θ, the positions of the center of gravity and the front trunnions relative to the rear trunnions are known. If one prescribes the vertical component of the rope force, F_z, the horizontal component, F_x, is the only unknown quantity in the equation.

As the trolleys capacity to horizontal load is unknown, it is desirable to limit the horizontal force as much as possible. Up to 90° rotation, the smaller the vertical force component of the front rope is, the smaller the horizontal component. However, if the vertical component is set to zero, the front rope needs to be perfectly horizontal, which is not possible. There is thus a trade-off between the maximum acceptable angle of the front rope and the magnitude of the horizontal force component. Figure 53 shows that it is acceptable to have purely vertical ropes up to approximately 60°, but after this point it is necessary to aid equilibrium with horizontal forces.

After 90° rotation, it is desirable to have as large vertical force component in the front rope as possible. This reduces the horizontal force component. However, the frame must rotate to roughly 120° before the horizontal force component of the ropes can be eliminated. From 150° through to 180°, horizontal forces are not necessary, as can be seen in Figure 53. Testing of various loading histories resulted in an optimal loading history as rendered in Figure 55.

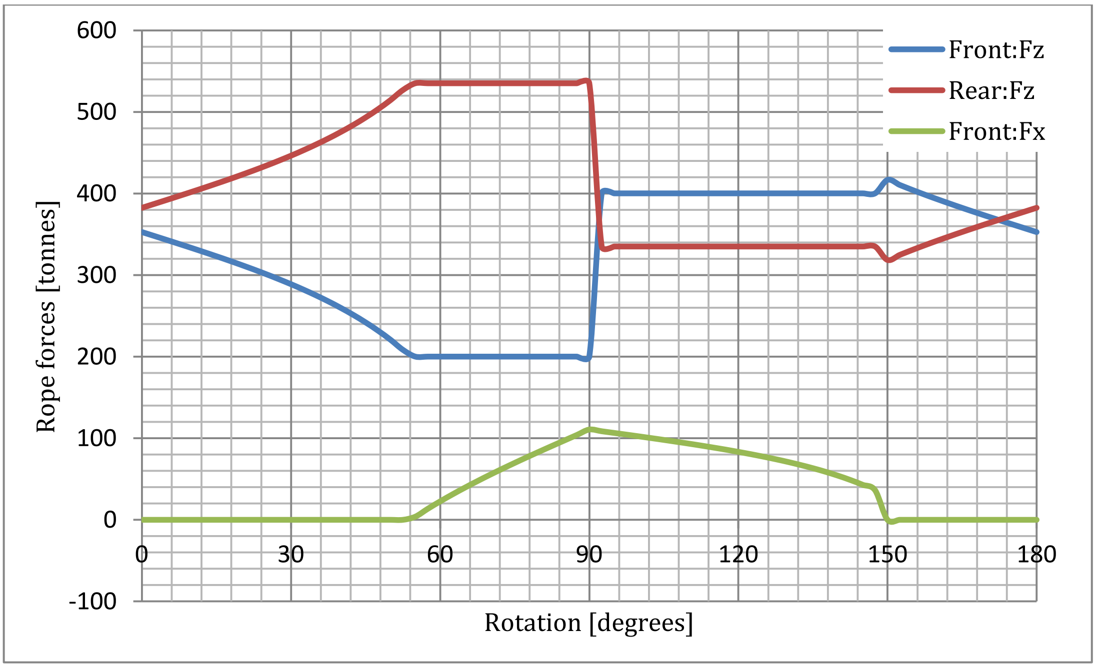

FIGURE 55: OPTIMAL FORCE HISTORY

Up to 50°, the ropes are kept vertical. The force in the front rope decreases gradually. At 50°, the load in the front rope is roughly 200 tonnes. From 50° on to 90°, the load in the front rope is kept at 200 tonnes. To maintain equilibrium, a horizontal component in the rope is necessary. The horizontal component grows gradually up to a maximum of 111 tonnes at 90° rotation. At this point, the angle of the front rope from the vertical direction is 29°. From 90° on to 150°, the vertical force component of the front rope is kept at 400 tonnes. The horizontal force component decreases gradually. At 150° on the ropes are kept vertical again, so there is no horizontal component of the rope forces.

Even in this optimized scheme, the horizontal component of the rope force climbs to 111 tonnes, not including any load factors. It is unlikely that the trolleys are able to carry this load. This is a major obstacle and a problem regarding the feasibility of the turning frame. The side wall frame design, which is discussed in the preliminary design stage, may avoid the problem of this moment. However, as stated in the discussion, the side wall frame is not compatible with the topside modules, as the modules can not withstand being lifted in this way.

8. Load combinations and checks

8.1. General

As the frame is rotated 180°, there is in theory a large number of load combinations. The most obvious ones are the horizontal position at 0° rotation and the vertical position at 90° rotation. It is shown in the following that not all positions are necessary to check, as they are not critical in terms of load. This is proved by a dynamic analysis of the complete rotation.

8.2. Load Combinations

The following load combinations are treated with linear static analysis.

1) Horizontal position
2) Vertical position
   a) Hand calculation
   b) Optimal force history

The vertical position is treated with two load combinations. The difference between 2)a) and 2)b) lies in the support forces. In the vertical position, the support forces on the frame are determined by the rope configuration at any given time, as explained in 7.2. In 7.4, an optimal support force history is proposed, which is the 2)b) load combination. However, in the MS Excel calculations, it is difficult to prescribe the support forces. In stead, the support forces are mere results of the simplifications made with respect to distribution of weight within the structure in the vertical position. Thus, load combination 2)a) refers to the resulting support forces of the hand calculations of the vertical position.

8.3. Load Factors

The following load factors are applied to the load combinations.

Live load variable action factor

The magnitude of live load is treated with a load factor according to NS-EN 1990. The load factor for leading variable action is due to insecurities in estimation of the magnitude of the live load. The true weight of the topside modules can be difficult to estimate. Considering the fact that the modules are in construction and unfinished structures, it can be difficult to establish the exact weight of the module at a specific point in the construction phase. Also, it may happen that the center of gravity is not located at the middle of the module. Although this incident should generally be beneficial for the severity of the loads on the frame, it can elicit unwanted effects upon local areas of the frame.

TABLE 9: LIVE LOAD FACTOR

Live load factor according to NS-EN 1990, Table A1.2(A):	
Leading variable action, γ_Q:	1.50

Self weight permanent action load factor

The self weight is treated with a load factor due to insecurity in the magnitude of the self weight. For large complex structures, like high-rise buildings, it may be a tedious task to calculate the self weight accurately. Also, as the structure is in construction, modifications may prove necessary due to unforeseen circumstances, resulting in higher self weight. The load factor takes these incidences into account. It is rather simple to establish the nominal self weight of the turning frame. However, unforeseen circumstances in construction may still arise. Thus, the self weight is treated with a load factor according to NS-EN 1990.

TABLE 10: SELF WEIGHT FACTOR

Self weight factor according to NS-EN 1990 Table A1.2(A):	
Permanent actions, unfavourable, γ_G:	1.20

DYNAMIC AMPLIFICATION FACTOR

Lifting operations involving cranes are treated with dynamic amplification factors, which take into account dynamic effects to the magnitude of load due to accelerations of mass inertia. The dynamic amplification factor is given in NS 5514.

TABLE 11: DYNAMIC AMPLIFICATION FACTOR

Dynamic factor according to NS 5514 1.2211:			
Formula: $\psi = 1+\xi V_L$	$1.15 \leq \psi \leq 1.6$	$V_L \leq 1$ m/s	
Hoisting velocity V_L [m/s]:			1
ξ for gantry cranes:			0.6
Dynamic factor, ψ:			1.6

The load factors have been applied to all of the load combinations.

8.4. LOAD CHARTS

The following loads are referred to the local coordinate system, as described in Figure 32.

The live loads in load combination 1) are given in Table 12. There are no loads in x- or y-direction in this load combination.

TABLE 12: F_Z (kN) IN HORIZONTAL POSITION

Load combination: 1 Horizontal position

x\y [mm]	-7500	-2500	2500	7500
0	0	0	0	0
3250	420	420	420	420
6500	420	420	420	420
9750	420	420	420	420
13000	420	420	420	420
16250	420	420	420	420
19500	420	420	420	420
22750	420	420	420	420
26000	0	0	0	0

The live loads in the vertical position are given in Table 13 and Table 14. The live loads are the same for both load combinations 2)a) and 2)b). Note that the loads F_x in the vertical position are equal to the loads F_z in the horizontal position. The loads F_z of the vertical position carry the moment due to the eccentricity of the center of gravity of the topside module from the mid plane of the frame.

TABLE 13: F_Z (kN) IN VERTICAL POSITION

Load combination: 2 Vertical position

x\y [mm]	-7500	-2500	2500	7500
0	0	0	0	0
3250	582	582	582	582
6500	388	388	388	388
9750	194	194	194	194
13000	0	0	0	0
16250	-194	-194	-194	-194
19500	-388	-388	-388	-388
22750	-582	-582	-582	-582
26000	0	0	0	0

TABLE 14: F_X (kN) IN VERTICAL POSITION

Load combination: 2 Vertical position

x\y [mm]	-7500	-2500	2500	7500
0	0	0	0	0
3250	420	420	420	420
6500	420	420	420	420
9750	420	420	420	420
13000	420	420	420	420
16250	420	420	420	420
19500	420	420	420	420
22750	420	420	420	420
26000	0	0	0	0

9. CALCULATIONS

9.1. GENERAL

The scope of the calculations is the following.

- Calculation of support forces and internal forces in the frame
- Cross section capacity check of frame members
- Buckling check of critical member
- Design of welds

The results of the calculation of support forces and internal forces are compared with FEA in order to verify the FE model. This calculation is done for the Case A design only, as explained in Figure 56. The Case B design was created at a late stage in the process, and has not been calculated due to lack of time. Nonetheless, it is assumed that, given that the FE model of Case A is verified by calculations, the FE model of Case B is verified as well, as the model of Case B is very similar to Case A.

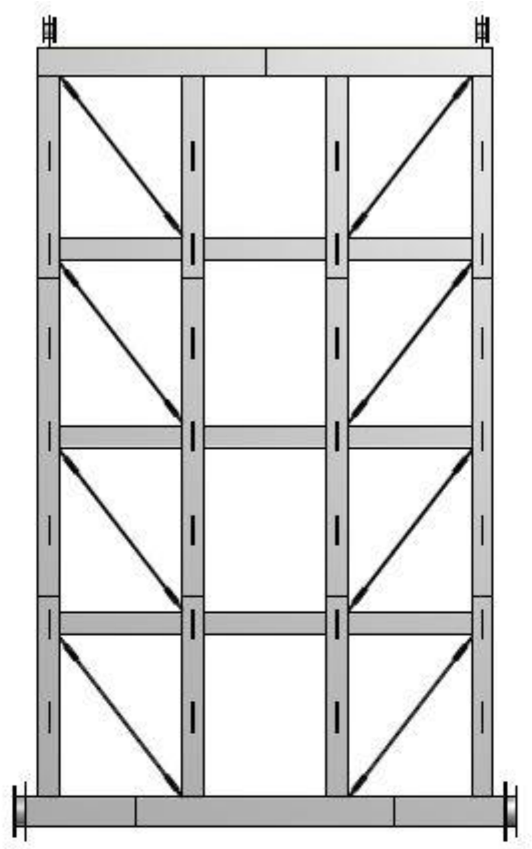

Case A

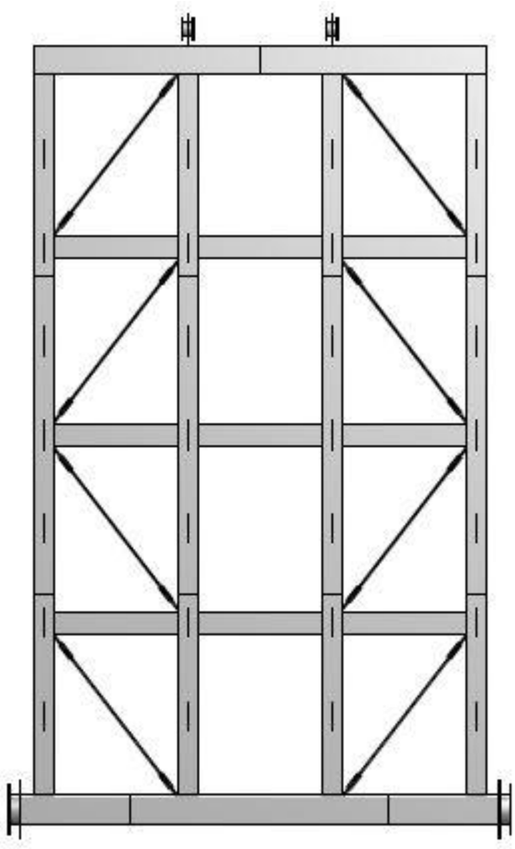

Case B

FIGURE 56: GEOMETRIES ASSESSED IN CALCULATIONS

The cross section capacity check is done only for Case A. Again, Case B was not checked due to lack of time. A column buckling check is performed of the critical member of the frame, applying results from the 1D FEA analyses. The column buckling check is performed according to NS-EN 1993-1-1.

9.2. SUPPORTS AND INTERNAL FORCES

GENERAL ASSUMPTIONS

All load points, i.e. all shear plates, of the frame is assumed to be employed. The topside module is assumed to have less bending stiffness than the frame. Thus, there are 28 load points on the frame, as indicated by the blue dots in Figure 57.

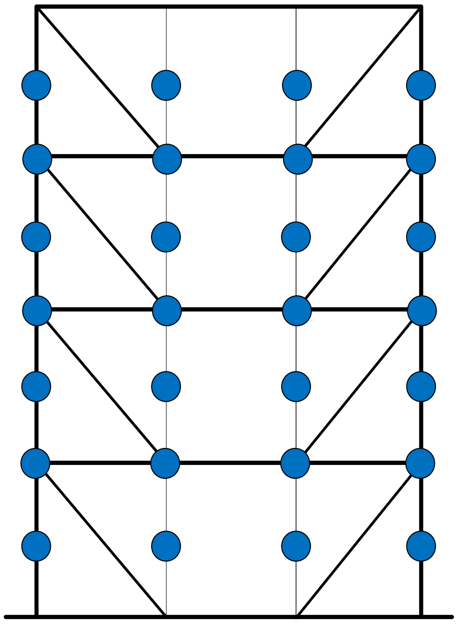

FIGURE 57: LOAD POINTS ON FRAME

The live load, i.e. the mass of the topside module, is assumed to be 500 tonnes. Coupled with a gravitational acceleration, g, of 9.81m/s^2, the nominal weight of the topside module is 4.905kN.

The topside module is assumed to resemble a cubic shape of dimensions (LxWxH): 25m x 15m x 10m. The center of gravity of the module is assumed to be located in the volumetric center of the cube.

The shear plates are of height 250mm. Thus, the eccentricity of the center of gravity of the topside module from the plane of the turning frame is the sum of half the height of the turning frame (750mm), the height of the shear plates (250mm) and half the height of the topside module (5000mm). The eccentricity is thus 6000mm.

MS EXCEL CALCULATIONS OF HORIZONTAL POSITION

The calculations of load combination 1) are carried out in MS Excel and are presented in tabular form in the following. The full spreadsheets are printed in the appendices. The calculation of the horizontal position is treated first. Table 15 shows the distribution of live loads as well as calculation of support loads in a unit load format for clarity. Note that the loads on the load points are all equal, as explained in 7.1. The calculation does not currently take into account the eccentricity of the front trunnion from the front beam, which is 1100mm. Table 16 shows the load distribution with real magnitudes with unit kN. Observe that a unit load corresponds to a real load of 420kN, which is the design weight of the topside module divided by the number of load points.

TABLE 15: DISTRIBUTION OF LIVE LOAD (UNIT LOADS) ON LONGITUDINALS

x/y [mm]	-7 500	-2 500	2 500	7 500	
0	3.50	3.50	3.50	3.50	Front support
3 250	1.00	1.00	1.00	1.00	
6 500	1.00	1.00	1.00	1.00	
9 750	1.00	1.00	1.00	1.00	
13 000	1.00	1.00	1.00	1.00	Load points
16 250	1.00	1.00	1.00	1.00	
19 500	1.00	1.00	1.00	1.00	
22 750	1.00	1.00	1.00	1.00	
26 000	3.50	3.50	3.50	3.50	Rear support

TABLE 16: DISTRIBUTION OF LIVE LOADS (kN) ON LONGITUDINALS

x/y [mm]	-7 500	-2 500	2 500	7 500	
0	1472	1472	1472	1472	Front support
3250	420	420	420	420	
6500	420	420	420	420	
9750	420	420	420	420	
13000	420	420	420	420	Load points
16250	420	420	420	420	
19500	420	420	420	420	
22750	420	420	420	420	
26000	1472	1472	1472	1472	Rear support

Table 15 and Table 16 look at the longitudinal beams (hereby longitudinals) in isolation. The front and rear supports are not the trunnions, but the front and rear beams. Thus, the support forces in the tables are the loads that the longitudinals transmit to the front and rear beams.

From Table 15 and Table 16 it is straight forward to calculate corresponding shear force and bending moment in the longitudinals. This is done in Table 17 and Table 18. The shear force, due to live load, is constant between load points, and is discontinuous in the load points. Thus, it is not perfectly sound to claim that the shear force in e.g. (x,y)=(3250,-7500)is simply 1051 kN. The shear force is in fact 1472kN on the segment $0<x<3250$ and 1051kN on the segment $3250<x<6500$. The tables should thus be understood such that the shear force in a cell describes the shear force from the x-coordinate of that cell to the x-coordinate of the next cell.

TABLE 17: SHEAR FORCES (UNIT LOADS) IN LONGITUDINALS

x/y [mm]	-7 500	-2 500	2 500	7 500
0	3.50	3.50	3.50	3.50
3250	2.50	2.50	2.50	2.50
6500	1.50	1.50	1.50	1.50
9750	0.50	0.50	0.50	0.50
13000	-0.50	-0.50	-0.50	-0.50
16250	-1.50	-1.50	-1.50	-1.50
19500	-2.50	-2.50	-2.50	-2.50
22750	-3.50	-3.50	-3.50	-3.50
26000	3.50	3.50	3.50	3.50

TABLE 18: SHEAR FORCES (kN) IN LONGITUDINALS

x/y [mm]	-7 500	-2 500	2 500	7 500
0	1472	1472	1472	1472
3250	1051	1051	1051	1051
6500	631	631	631	631
9750	210	210	210	210
13000	-210	-210	-210	-210
16250	-631	-631	-631	-631
19500	-1051	-1051	-1051	-1051
22750	-1472	-1472	-1472	-1472
26000	-1472	-1472	-1472	-1472

The resulting moment is given in Table 19. The longitudinals are for the time being assumed to be simply supported, such that moment is zero in the supports.

TABLE 19: BENDING MOMENT (kNm) OF LONGITUDINALS DUE TO LIVE LOAD

x/y [mm]	-7 500	-2 500	2 500	7 500
0	0	0	0	0
3250	4 782	4 782	4 782	4 782
6500	8 198	8 198	8 198	8 198
9750	10 248	10 248	10 248	10 248
13000	10 931	10 931	10 931	10 931
16250	10 248	10 248	10 248	10 248
19500	8 198	8 198	8 198	8 198
22750	4 782	4 782	4 782	4 782
26000	0	0	0	0

The shear forces of the longitudinals are transmitted to the front and rear beam. The resulting shear force and bending moment of the front and rear beam are calculated in Table 20 and Table 21.

TABLE 20: BENDING MOMENT (kNm) OF FRONT BEAM DUE TO LIVE LOAD

	y [mm]	Load	Shear	Moment
Trunnion	0	2943	2943	0
A	0	1472	1472	0
B	5000	1472	0	7 358
C	10000	1472	-1472	7 358
D	15000	1472	-2943	0
Trunnion	15000	2943	2943	0

TABLE 21: BENDING MOMENT OF REAR BEAM (kNm) DUE TO LIVE LOAD

	y [mm]	Load	Shear	Moment
Trunnion	0	2943	2943	0
A	1000	1472	1472	2 943
B	6000	1472	0	10 301
C	11000	1472	-1472	10 301
D	16000	1472	-2943	2 943
Trunnion	17000	2943	-2943	0

Loads due to self weight of the frame are treated much in the same way as live loads. The weight of the diagonals and the interior traverse beams is calculated and the weights of these members are then distributed evenly to the longitudinals. It is assumed that the weight of a single span is distributed 50% to each support.

TABLE 22: POINT LOADS (KN) ON LONGITUDINALS DUE TO WEIGHT OF DIAGONALS AND TRAVERSE BEAMS

x/y [mm]	-7500	-2500	2500	7500
0	104.6	209.3	209.3	104.6
0	6.1	12.1	12.1	6.1
3 250				
6 500	65.7	131.4	131.4	65.7
9 750				
13 000	65.7	131.4	131.4	65.7
16 250				
19 500	65.7	131.4	131.4	65.7
22 750				
26 000	6.1	12.1	12.1	6.1
26 000	104.6	209.3	209.3	104.6

The shear force and bending moment resulting from Table 22 are calculated similarly as for the live load. The weight of the longitudinals themselves elicits a bending moment given by the following formula.

$$M(x) = \frac{qL}{2}x - qx^2$$

The contributions to bending moment are added to find the total bending moment in the longitudinals due to self weight.

TABLE 23: BENDING MOMENT (KNM) OF LONGITUDINALS DUE TO SELF WEIGHT

x/y [mm]	-7500	-2500	2500	7500
0	0	0	0	0
0	0	0	0	0
3 250	1113	1433	1433	1113
6 500	2000	2640	2640	2000
9 750	2446	3194	3194	2446
13 000	2666	3520	3520	2666
16 250	2446	3194	3194	2446
19 500	2000	2640	2640	2000
22 750	1113	1433	1433	1113
26 000	0	0	0	0

The longitudinals are supported onto the front and rear beams. The loads transmitted from the longitudinals elicit bending moment in the front and rear beams. This contribution is added with the moment contribution from the front and rear beams' own self weight. The results are shown in Table 24 and Table 25.

TABLE 24: BENDING MOMENT [KNM] OF FRONT BEAM DUE TO SELF WEIGHT

y [mm]	Moment [kNm]
0	0
0	0
2 500	1 477
5 000	2 732
7 500	2 843
10 000	2 732
12 500	1 477
15 000	0
15 000	0

TABLE 25: BENDING MOMENT [KNM] OF REAR BEAM DUE TO SELF WEIGHT

y [mm]	Moment [kNm]
0	0
1 000	1 191
3 500	2 561
6 000	3 709
8 500	3 820
11 000	3 709
13 500	2 561
16 000	1 191
17 000	0

At this point, the bending moments of the longitudinals and the front and rear beam are established. The support loads in the trunnions are readily found from the shear force distribution of the front and rear beams. However, the preceding calculations are rather simplified, so it is not expected that the results are very accurate. The simplifications are necessary in order to obtain a statically determinate structure. The support forces are in any case statically determinate, but the internal forces are not originally statically determinate in the frame. The flaws of the calculations at this point are presented in the following.

ECCENTRICITY OF FRONT TRUNNIONS

The eccentricity of the front trunnions is not taken into account. The eccentricity is 1100mm from the centerline of the front beam. This eccentricity increases the total span of the beam, hence making bending moments more severe in the longitudinals.

BENDING OF TRAVERSE BEAMS

As the front and rear beams bend, as illustrated in Figure 58, the joints of the longitudinals, indicated by crosses, translate with the deflection. From Figure 58 it is visible that the joints of the central beams translate more than the joints of the peripheral beams.

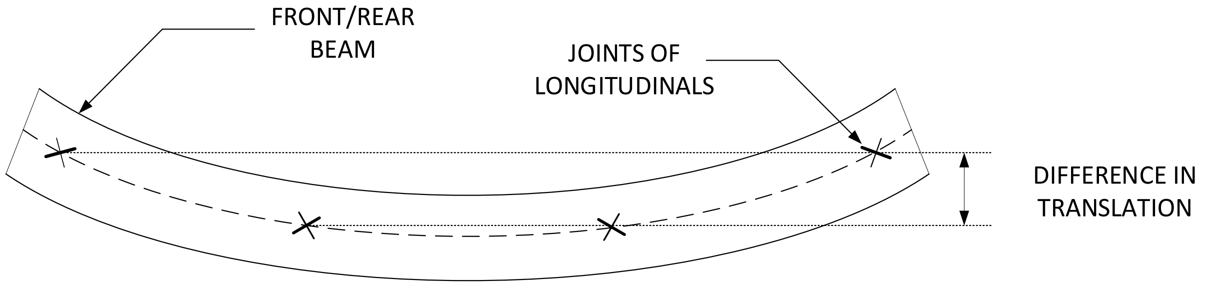

FIGURE 58: TRANSLATION OF SUPPORTS OF LONGITUDINAL BEAMS DUE TO BENDING OF FRONT AND REAR BEAMS

The traverse beams have to bend similarly to the illustration in Figure 59. The traverse beams have the same cross section as the longitudinals, so they are stiff toward bending. They will prevent the height difference of the peripheral and longitudinal beams by transmitting weight to the peripheral beams from the central beams. Hence, the traverse beams contribute to increase the load on the peripheral beams, and decrease the load on the central beams. As the traverse beams bend, they drag with them the longitudinals in the rotation, thus inflicting torsional moment in the longitudinals.

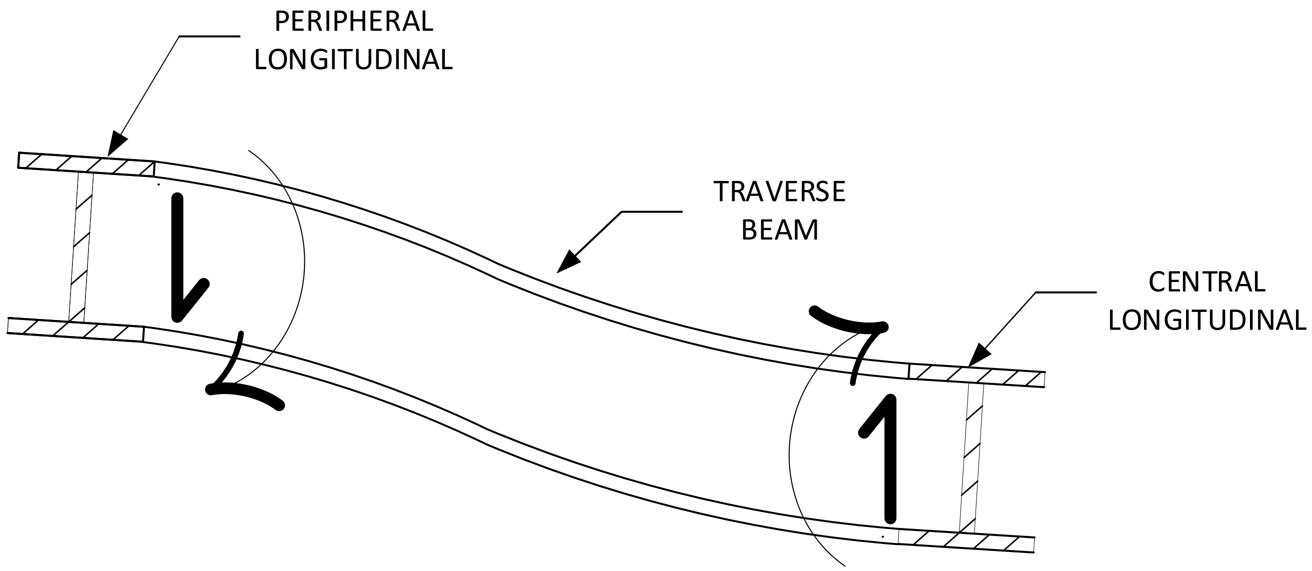

FIGURE 59: BENDING OF TRAVERSE BEAMS COUNTERING HEIGHT DIFFERENCE OF CENTRAL AND PERIPHERAL LONGITUDINALS

TORSION OF FRONT AND REAR BEAMS

The longitudinals are assumed simply supported in the connections with the front and rear beams. This is not true, as the beams are welded to make a fully fixed joint. Because of the traverse beams, the peripheral longitudinals receive more load than the central longitudinals. Thus, the peripheral beams will deflect more than the central beams. Consequently, the rotation in the supports will be larger for the peripheral longitudinals than for the central longitudinals. This is illustrated by the angle $\delta\theta$ in Figure 60. As the front and rear beams are large box profile beams with large torsional stiffness, they will resist this angle. The result is torsional moment which counters the rotation in the peripheral longitudinals and increase the rotation in the central longitudinals. Thus, the severity of the load reduces for the peripheral longitudinals, while the load increases for the central longitudinals. The effect of torsion in the front and rear beams thus counter the effect of bending of the traverse beams.

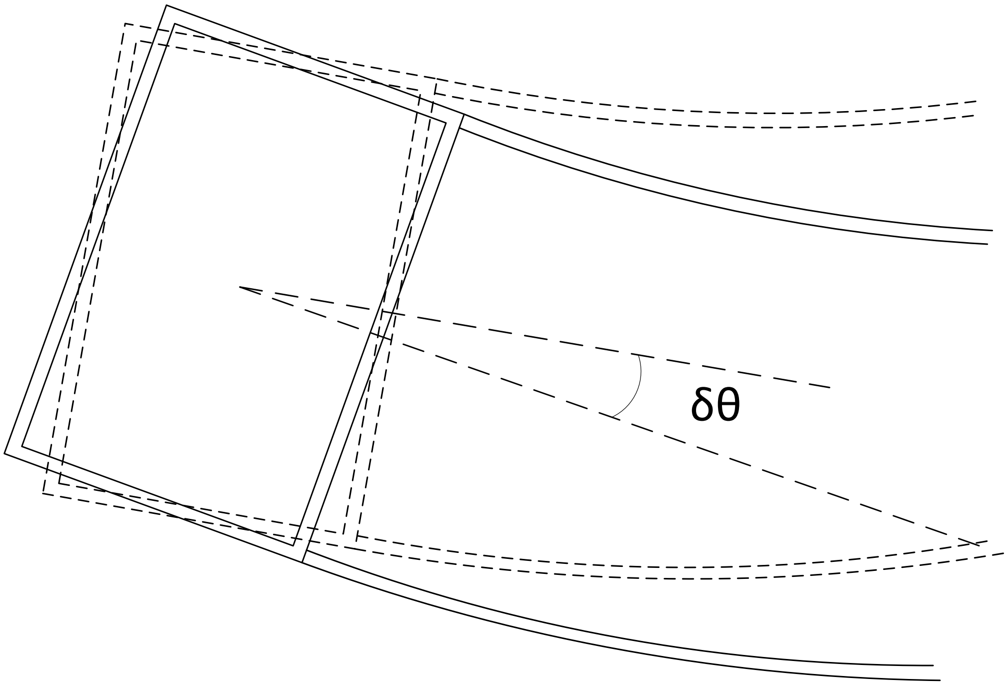

FIGURE 60: DIFFERENCE IN ROTATION IN JOINTS BETWEEN LONGITUDINALS AND FRONT/REAR BEAMS

IMPROVEMENTS

The structure was simplified in order to make calculations statically determinate. However, the errors due to the simplifications are likely to be very significant. In order to account for the true behavior of the statically indeterminate structure in MS Excel, an iterative scheme was attempted. The strategy of the scheme was to calculate displacements and rotations of all joints in the simplified structure as shown in the preceding. After the displacements and rotations were established, the resulting forces and moments that were let out of the simplified calculation were found and then applied to the simplified calculation. Then the resulting displacements and rotations were calculated again, applied to the simplified calculation, etc. The scheme managed to improve the results somewhat. However, there were problems obtaining convergence of the solutions. Comparison with the results from finite element analysis proved that the results did not match satisfactorily.

Another strategy provided much better accuracy of the MS Excel calculations. As the iterative scheme presented in the preceding paragraph failed to produce adequate accuracy, it was attempted to simply read the missing forces and moments from the output of the corresponding finite element analysis. For the calculation of the horizontal position, this meant to extract the torsional moments of the front and rear beams and the shear force in the traverse beams. It may be dubious to extract data from a finite element analysis to improve the correlation between MS Excel and the finite element analysis itself. However, the designers knew beforehand exactly which data was necessary to extract, and satisfactory accuracy was obtained. It is highly unlikely that the high level of accuracy was arbitrary. This was therefore considered an acceptable approach.

The eccentricity of 1100mm of the lifting points in the front trunnion is necessary to take into account. The span of the beam is thus 27 100mm, not 26 000mm, as the tables show. The frame still remains 26 000mm in the calculation, but an external moment and support force is applied to the frame to simulate the presence of the front trunnions. It is expected that, due to the eccentricity of the front trunnion, the support force in the front beam decreases, and the support force in the rear trunnion increases. Based on the support loads from the simplified calculation, an equivalent support moment and support force is calculated, illustrated in Figure 61.

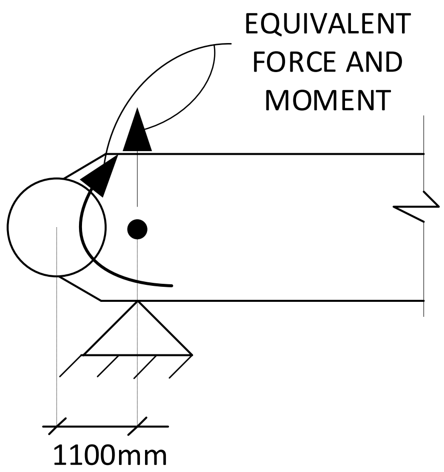

FIGURE 61: EQUIVALENT FORCE AND MOMENT DUE TO ECCENTRICITY OF FRONT TRUNNIONS

The equivalent support force is calculated from moment equilibrium with the equivalent support moment. A corresponding equivalent support force is applied to the rear trunnion to equilibrate the equivalent support force of the front trunnion. Thus, the expected effect upon the support loads due to the eccentricity of the front trunnion is obtained. The shear force and moment diagrams due to the equivalent forces are given in Figure 62.

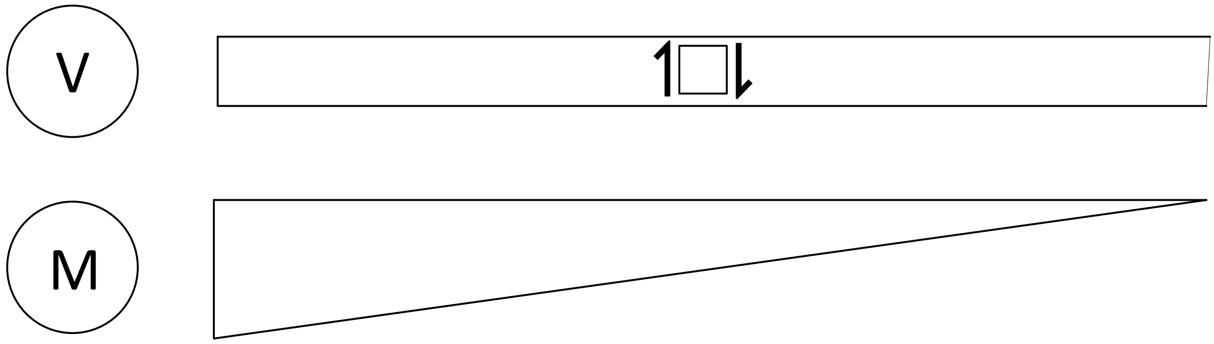

FIGURE 62: SHEAR AND MOMENT DIAGRAM

MS EXCEL CALCULATION OF VERTICAL POSITION

The MS Excel calculation of the vertical position refers to load combination 2)a). The calculation of the vertical position is more complicated because of static indeterminacy. The forces that were orthogonal to the plane of the frame in the horizontal position are now parallel to the local x-axis of the frame. There are four supports in the same plane carrying the weight. Thus, the stiffness of each support determines the distribution of load. Also, in the vertical position, the diagonals play an important role in transmitting weight to the support. Thus, the diagonals now have to be included in the calculation, which adds to the number of unknowns.

The strategy is similar to the calculation of the horizontal position. The structure must be simplified such that it is statically determinate. Then, the missing forces and moments are extracted from finite element analyses to obtain good accuracy.

The eccentricity of the center of gravity of the module from the plane of the frame, results in a moment in the vertical position. It is this moment that makes the system want to tip over if not restrained, as explained in 7.4.The frame carries this moment by forces in the horizontal direction. It is assumed that there is a linear relationship between the magnitude of the horizontal forces carrying the moment, and the distance from the midsection of the frame, as illustrated in Figure 63. The linear relationship corresponds to the linear relationship between displacement and distance from center of rotation. The magnitude of the forces is thus linked by a common coefficient, which is the only unknown. The common coefficient is calculated from moment equilibrium.

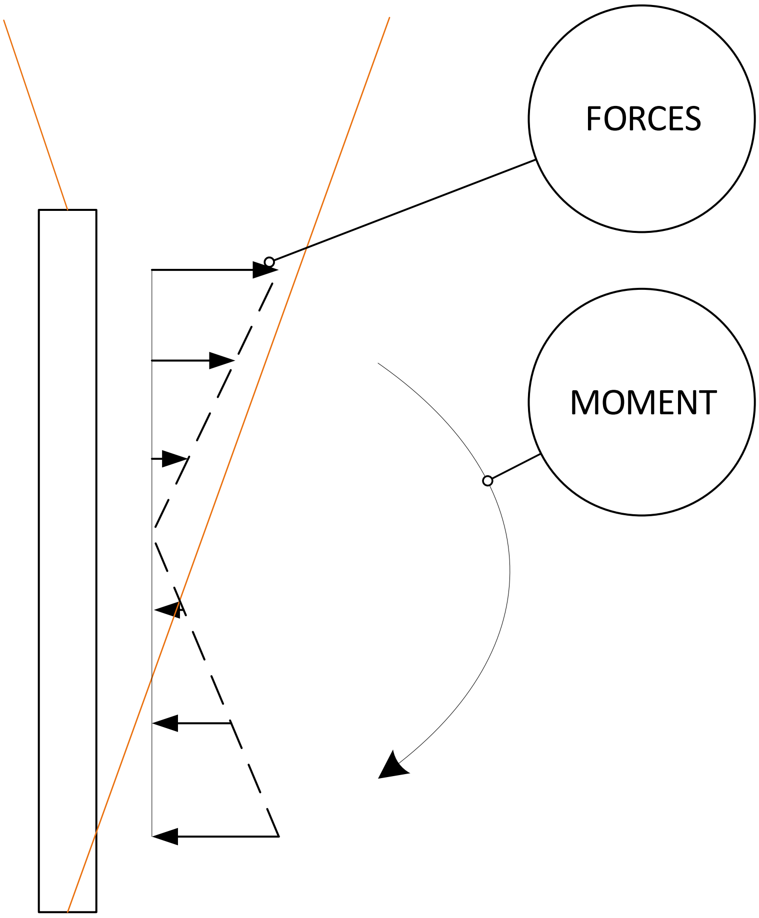

FIGURE 63: MOMENT AND RESULTING HORIZONTAL FORCES

Gravity loads elicit in-plane forces in the frame. This results in axial forces in the longitudinals. The weight of the module is assumed to distribute evenly to the load points of the frame. The front and rear beams, as well as the traverse beams, experience bending moments around the weak axis in this situation. This explains the choice of box profiles in the front and rear beams, as they need to carry heavy moment about both axes in the cross section. The traverse beams contribute with bending stiffness. The shear stiffness of the frame makes the frame carry the load much like a truss structure, or a 26m tall beam. These effects make the bending moments of the front and rear beams less severe.

The calculation of the in-plane forces of the frame needs to be simplified to be statically determinate. To start with, the traverse beams and the diagonals are disregarded. The vertical loads due to self weight and weight of the module result in axial forces in the longitudinals. The axial forces are transmitted to the front and rear beams, eliciting shear forces and bending moment. Since there are 4 supports carrying the vertical load, the system is still statically determinate. To find the vertical support forces, an assumption must be made. Thus, it was assumed that the axial stiffness of the frame itself was constant throughout the length of the frame, such that it resembles a linear bar. Hence, there is a linear relation between the support force of a given load and the distance from the support to the load point. The concept is illustrated in Figure 64.

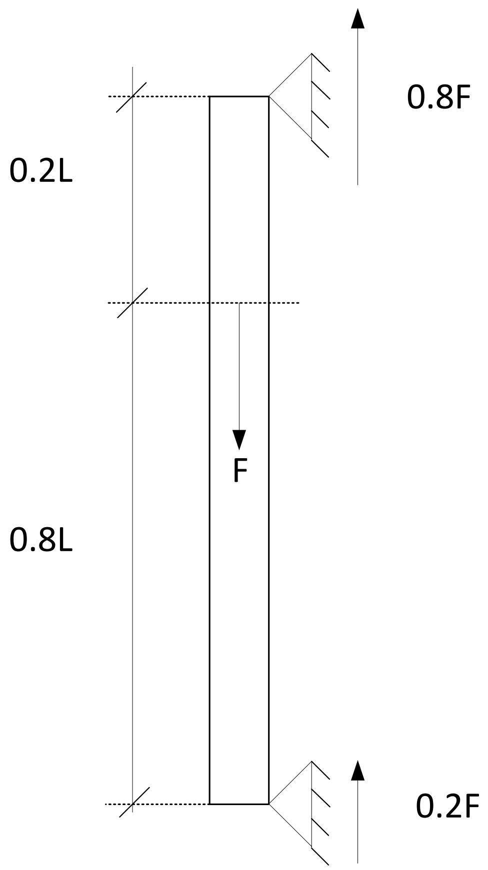

FIGURE 64: CONSTANT AXIAL STIFFNESS ASSUMPTION OF FRAME

The simplification made in the calculations must be made up for. As well as in the horizontal calculation, an iterative scheme based on stiffness and deformations was attempted for the vertical position. However, there were many effects that needed to be taken into account, so a lot of work was necessary for each iteration. Also, there were problems with divergence of the solutions. Ultimately, the iterative scheme in MS Excel was abandoned. In stead, a strategy similar to the one employed in the horizontal calculation was adopted. In the vertical calculation, it was necessary to extract the following data from the finite element analysis output.

- Shear forces about both axes of the traverse beams
- Torsional moment of front and rear beam
- Axial forces in diagonals
- Axial forces in longitudinals due to axial deformation of longitudinals

The diagonals did not contribute with any resistance in the horizontal position, but in the vertical position, the diagonals play an important part in transmitting weight to the supports. In short, the resistance to axial deformation of the diagonals transmits axial force between the longitudinals. The result is that the front and rear beams experience less shear force and thus less bending moment. The diagonals also make the frame much stiffer, which is important for the structural integrity of the topside module. Figure 65 illustrates how weight is transmitted through the diagonals. It is assumed that diagonals only carry weight through tensile forces, as Euler buckling severely limits the axial compression capacity of the diagonals. The forces extracted from the finite element analysis are applied to the corresponding joints of the frame.

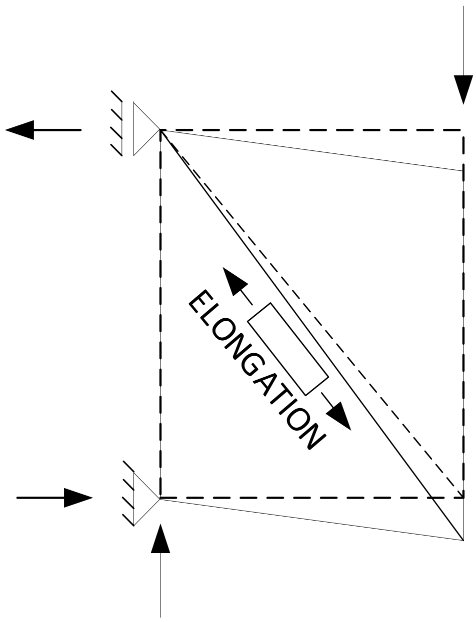

FIGURE 65: WEIGHT TRANSMISSION THROUGH DIAGONALS

9.3. CROSS SECTION CAPACITY CHECK

The cross section capacity check is performed for load combination 1) in the horizontal position and 2)a) in the vertical position.

The capacity check for the steel frame is conducted according to NS 5514 and NS-EN 1993-1-1. It is designed after the elastic cross section capacity and the von Mises criteria.

In a 3-dimesional state of stress the von Mises criteria says that yielding will occur when the stress components $\sigma_x, \sigma_y, \sigma_z, \tau_{xy}, \tau_{yz}, \tau_{zx}$, in the most critical point, meet the criteria:

$$\sqrt{(\sigma_x^2 + \sigma_y^2 + \sigma_z^2 - (\sigma_x\sigma_y + \sigma_y\sigma_z + \sigma_z\sigma_x) + 3(\tau_x^2 + \tau_y^2 + \tau_z^2)} = \sigma_a$$

The maximum allowed stress, σ_a, is given in NS 5514 as the yield stress f_y divided by the safety factor v_E which depends on the load case. There are three load cases given in NS 5514, point 1.3. The load cases are work with crane with or without wind, or with extraordinary load effects. In this project it is assumed no wind effects during the lifting operation. This gives the safety factor of 1.5 after NS 5514, 1.411. The maximum allowed stress then becomes:

$$\sigma_a = \frac{f_y}{v_E} = \frac{420}{1.5} = 280MPa$$

The frame is checked for axial (N), bending (M), shear (V) and torsion capacity (T). The frame is controlled in the most critical sections concerning the different effects, but also a maximum combination.

In the calculations the summation of stresses are direct - the stress given by the maximum shear force is added to the stress given from the moment independent of where their maximum occurs. This is a conservative approach. If the capacity utilization gets too high, a more thoroughly check has to be done. Normally the shear force is low compared to the maximum moment, such that it does not give a significant contribution.

9.4. WELDS

For the frame to work as a unit, the sections need to have connections with sufficient capacity. The frame is assembled by welding. The welds need to transfer all the loads acting and be designed as equally strong or stronger than the adjacent cross sections.

The capacity of the welds is calculated according to NS-EN 1993-1-8 and the design is done according to chapter 4.5.3. The design values for the welds and material are:

TABLE 26: CALCULATION VALUES

Steel grade	S420	
f_u	520 N/mm^2	
γ_{M2}	1.25	NS-EN 1993-1-8, NA.2.2(2)
βw	1.0	NS-EN 1993-1-8, Table 4.1

f_u is the nominal tensile strength of the weakest adjacent material, γ_{M2} is the material factor for welds and βw is a correlation factor.

Given these values the requirements for the capacity of the welds becomes:

TABLE 27: WELD CAPACITY REQUIREMENTS

$\sigma_{\perp,\max}$	374	N/mm^2
$\delta_{,\max}$	416	N/mm^2

$$\sigma_{\perp,\max} = \frac{0.9 \cdot f_u}{\gamma_{M2}} \text{ and } \delta_{,\max} = \frac{f_u}{\beta_w \cdot \gamma_{M2}}$$

Here δ is given as $\delta = \sqrt{\sigma_{\perp}^{2} + 3(\tau_{\parallel}^{2} + \tau_{\perp}^{2})}$

$\sigma_{\perp}$ is the stress normal to the weld-cross section, $\tau_{\parallel}$ is the shear force in the longitudinal direction and $\tau_{\perp}$ is the shear force normal to the longitudinal direction of the weld.

BUTT WELDS

When joining the plates together in the longitudinal direction, butt welds are used. If the ends are grinded so it is possible to achieve full penetration with butt welding, the capacity of the section lies in the weakest plate because the weld has higher strength than the base material. If not fully penetration is achieved the welds are treated as fillet welds with full penetration.

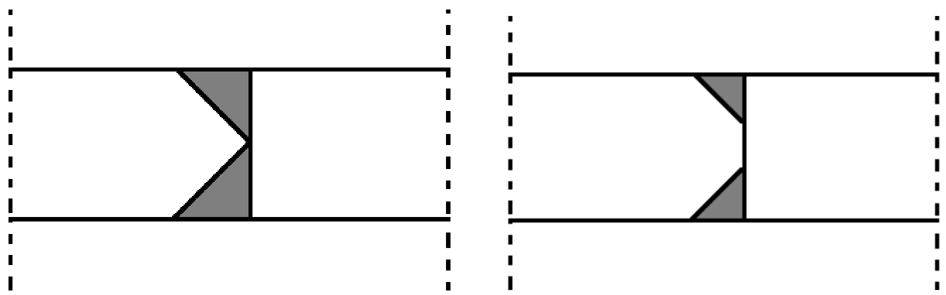

FIGURE 66: BUTT WELD WITH/WITHOUT FULL PENETRATION

For the sections in the frame, butt welds are assumed used when joining them in the longitudinal direction. The capacity is then dependent on the plate capacities.

FILLET WELDS

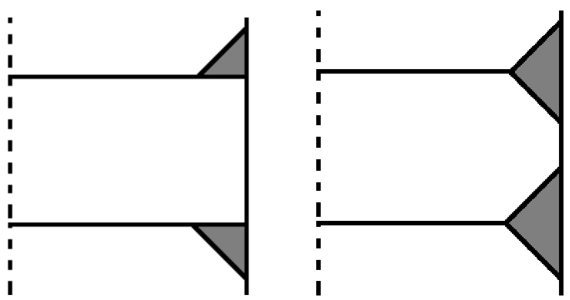

FIGURE 67: FILLET WELDS DESIGN

The minimum value of a fillet weld is 3mm according to NS-EN 1993-1-8, 4.5.2(2)

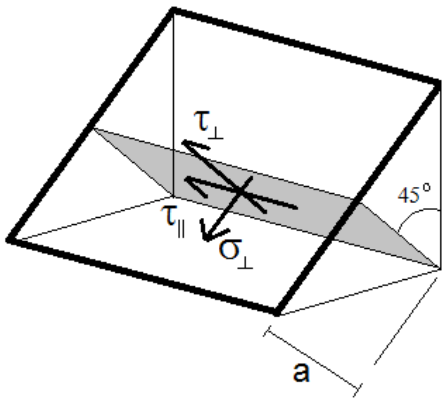

FIGURE 68: CROSS SECTION OF WELD WITH INTERNAL FORCES

In this assignment all joints are not calculated, but chosen joints with critical values.

1. Weld connecting flange and web in the longitudinal beams in the x-direction
2. Weld connecting the longitudinal and rear beam

1. The q(x) is a shear force given in N/mm which changes with the moment diagram. The moment can simply be given as a flange force with an arm h_f. This gives the relation $N(x) = M(x)/h_f$. N(x) can also be divided into a distributed force, q, over the length of the beam, x. $N(x) = q*x$. This distributed force, q, is the shear force in the longitudinal direction which the weld need to transfer.

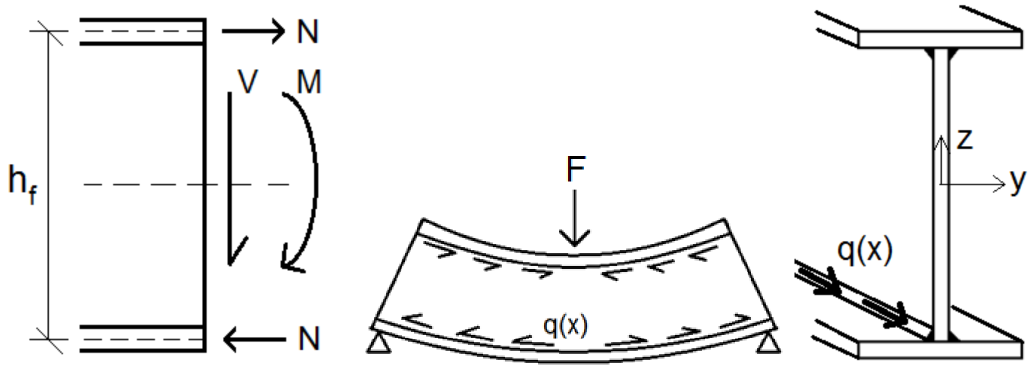

FIGURE 69: FORCES IN CROSS SECTION AND SHEAR FORCE IN WELDS

In this load situation there are many point loads along the length of the longitudinals. This gives moment diagram and shear force diagram approximate like the ones given in the figure.

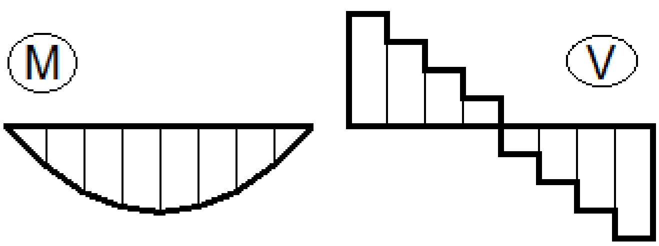

FIGURE 70: APPROXIMATE MOMENT AND SHEAR FORCE DIAGRAM FOR THE LOADED FRAME

The formula for calculating the shear force in the longitudinal weld is:

$$q = \frac{V_z \cdot S_y}{I_y \cdot t_w}$$

V_z – shear force in the cross section from the external loading
S_y – 1. Moment of area of the flange (the part outside the section in question. Here the section is across the welds between the web and the flange)
I_y – 2. moment of area of the whole cross section
t_w – the thickness of the weld

The highest shear force for the longitudinal beam is in the end by the rear beam. Here the shear force is 2444kN. Using the formula for shear force in welds and the requirement, the a-value becomes 1.5mm. This is below the minimum for fillet welds, and the requirement to the a-value becomes 3mm.

2. At the connection between the longitudinal and the rear beam the welds need to transfer moment, shear and axial forces from the longitudinals and over to the rear beam. Here the capacity of the welds is calculated with the welds folded down and the a-value as the width.

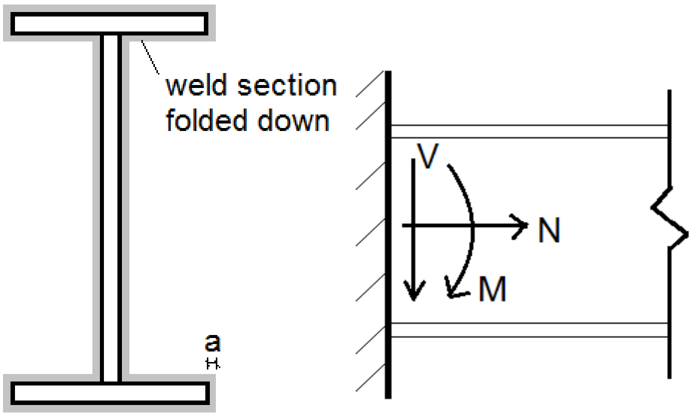

FIGURE 71: FORCES IN LONGITUDINAL - REAR BEAM JOINT

The design forces are retrieved from Abaqus/CAE in both the horizontal and vertical direction. The forces for the longitudinal-rear beam connection are given below.

TABLE 28: FORCES TRANSFER LONGITUDINAL-REAR BEAM, HORIZONTAL POSITION

Moment, strong axis, My	1666	kNm
Axial, N	0	kN
Shear, Vz	2425	kN

TABLE 29: FORCES TRANSFER LONGITUDINAL-REAR BEAM, VERTICAL POSITION

Moment, strong axis, My	452	kNm
Moment, weak axis, Mz	841	kNm
Axial, N	3528	kN
Shear, Vy	203	kN
Shear, Vz	788	kN

9.5. SHEAR RESISTANCE

Due to the loading from the section the beam shear force might cause the web to buckle. This is a global control of the web in the ultimate limit state. If the limit value is exceeded further calculations is necessary to verify the capacity.

9.6. LOCAL PLATE BUCKLING CHECK

Local buckling of the web might occur even though the general shear capacity against shear is sufficient. Each shear plate transfers a load from the module down to the frame. This load is spread through a thin connector (the shear plate) onto a wide and high plate. In this situation, local buckling of the plate in the top section can occur.

The picture shows two possibilities for buckling of the load carrying plate. The one to the left shows local failure of the web due to the point load applied on a concentrated area on top of the profile. This is called crippling and is seen as a folding mechanism in the web just below the area where the load is applied. It occurs due to high slenderness, i.e. tall web with small wall thickness. The one to the right shows a global failure. This can happen with medium slender beam. The folding mechanism comprises most of the web area.

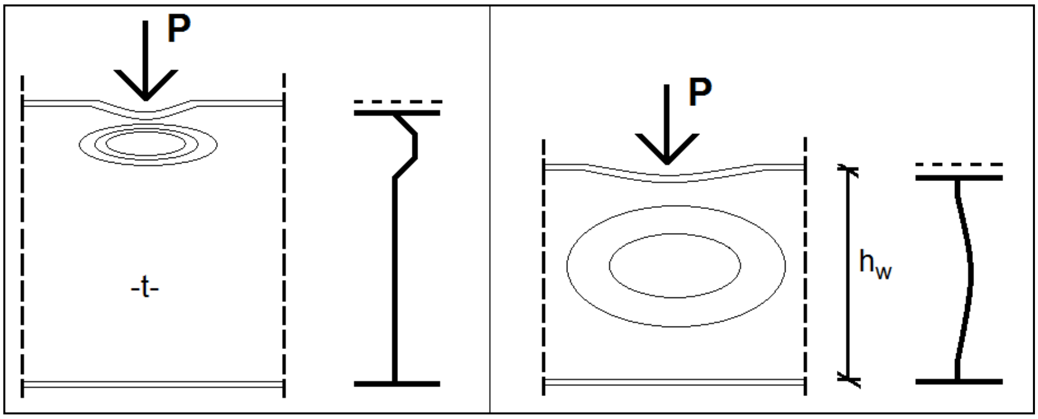

FIGURE 72: BUCKLING OF PLATE DUE TO TRAVERSE FORCE

The capacity check of the web for buckling is done according to NS-EN 1993-1-5. The section 6.2 in this standard gives formulas for calculating the design resistance to local buckling under traverse forces for unstiffened webs. The length s is the length of the shear plate, and *a* is the length between vertical stiffeners of the load carrying plate (in this case, this are the traverse beams).

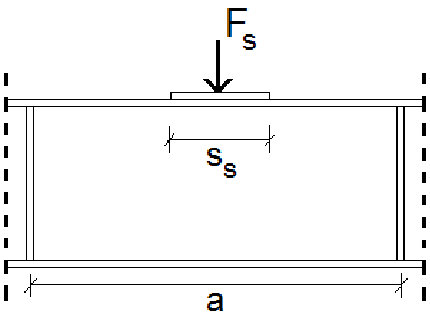

FIGURE 73: CALCULATION MODEL FOR PLATE RESISTANCE TO TRAVERSE FORCE

For the section profile that we have chosen the a-value becomes 6500mm, equal to the length between the traverse beams.

9.7. COLUMN BUCKLING CHECK

The most critical beam region of the frame is checked for column buckling according to NS-EN 1993-1-1. Only load combination 2)b) is checked, as this is the configuration which gives maximum axial compression in the longitudinals. The buckling length is considered to be 6500mm, i.e. the distance between two rows of traverse beams.

10. FINITE ELEMENT ANALYSIS

10.1. 1D ELEMENT ANALYSIS OF FRAME

The frame is modeled in Abaqus and Focus with 1 dimensional beam elements. 1 dimensional elements enable finite element analysis of the whole structure with reasonable computational costs. Both cases A and B are modeled for all load combinations. The results of the simulation of Case A are compared with the MS Excel results for load combinations 1) and 2)a).

The frame is modeled as a wire structure. The geometry of the frame is drawn as lines, and the lines are assigned sections with specific profiles and materials. The frame is subdivided into 1D elements of 50 mm length. The element type chosen is a standard 2-node linear beam element. This results in a total of 4969 elements, which yields a short calculation time for the static analysis. The wire models are rendered in Figure 74.

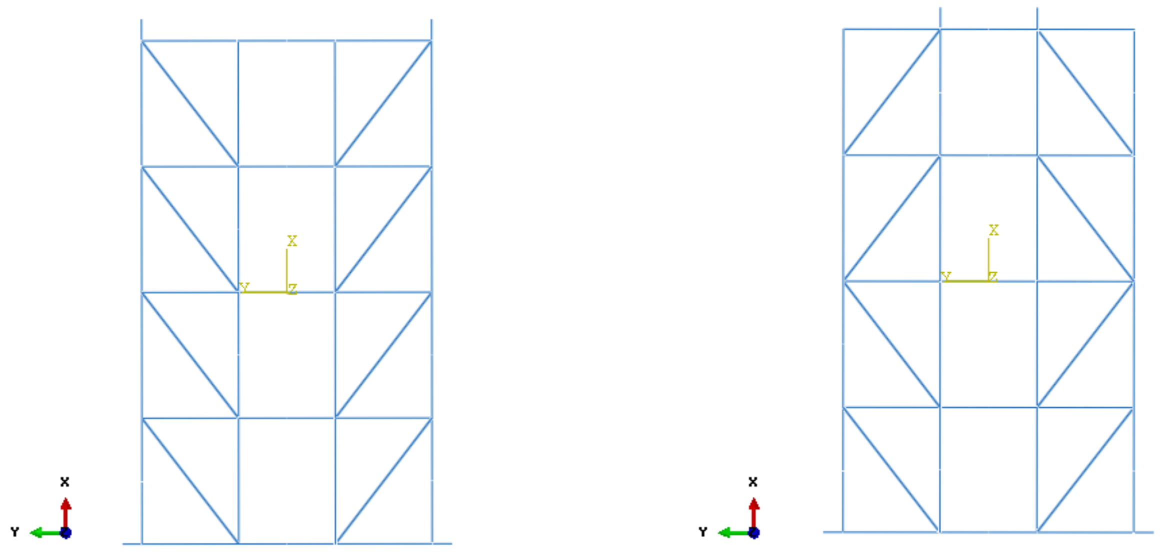

Case A Case B

FIGURE 74: WIRE MODELS OF CASE A AND B

The load is applied at specific points where the shear plates are positioned, as illustrated previously in Figure 57. The direction of the load changes with the rotation of the frame. Whereas gravitational loads due to the self weight of the frame is applied as point loads to the joints in the Excel calculations, Abaqus uses lumped mass distribution for lower order elements (Dassault Systèmes Simulia Corp., 2013) and distributes the lumped masses to the nodes of the mesh. Focus applies the same lumped mass distribution.

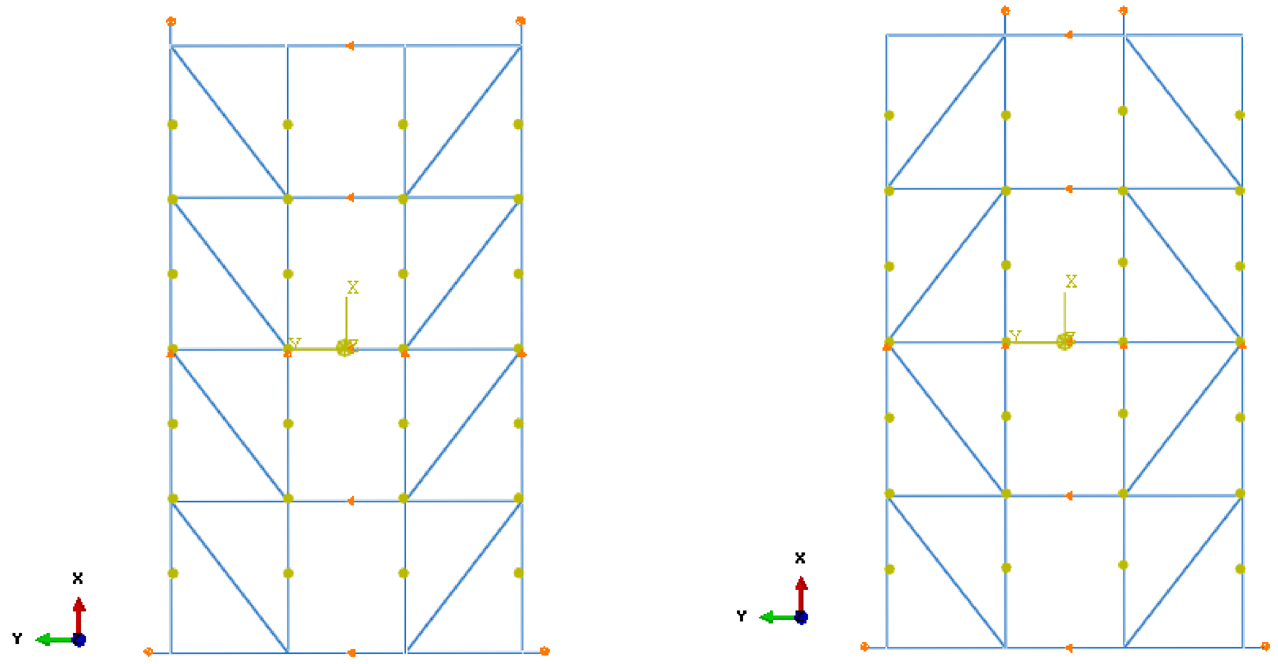

Case A Case B
Yellow dots: Loads
Orange dots: Boundary conditions

FIGURE 75: LOADS AND BOUNDARY CONDITIONS IN HORIZONTAL POSITION

The boundary conditions vary depending on the position of the frame. For the horizontal position, the supports are fixed toward translation in z-direction. The xz-plane of the frame is constrained in y-direction. The yz-plane is constrained in x-direction. This proves to not elicit deformation induced forces due to overconstraining, as the support loads in these directions are low, so is deemed acceptable boundary conditions for the horizontal position. Since the frame is statically determinate in the horizontal position, the force distribution to the supports is independent of the stiffness of each support.

In the vertical position, the choice of boundary conditions is more important. One must obtain the correct support forces as prescribed in load combinations 2)a) and 2)b). The supports may remain completely fixed toward translation as for the horizontal position, but this does not result in the correct support forces. Alternatively, the ropes can be modeled exactly or they can be approximated by linear springs. In the 1D element model, the ropes are modeled by linear springs with prescribed stiffnesses. The stiffnesses of the springs are thus chosen such that the prescribed support forces from load combinations 2)a) and 2)b) are obtained. The applied loads in the vertical position are illustrated in Figure 76.

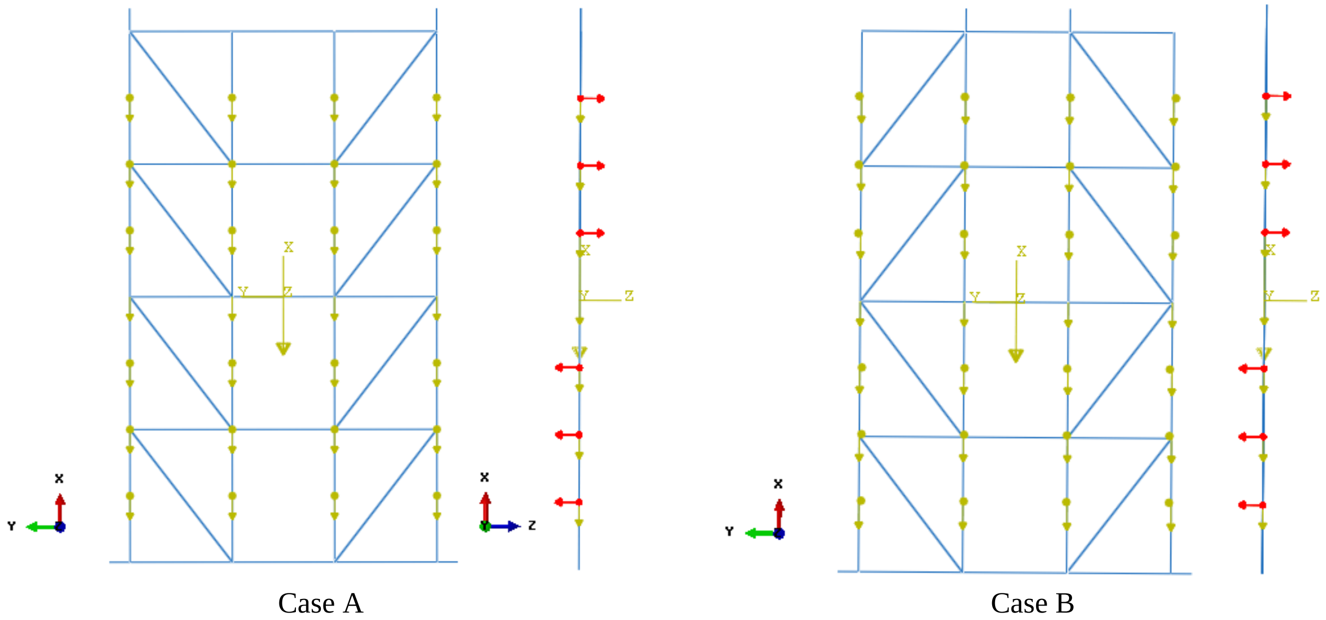

FIGURE 76: LOADS IN VERTICAL POSITION

Yellow dots and arrows indicate loads. The loads marked in red in the figures to the right indicate the forces due to the moment caused by the eccentricity of the center of gravity of the module. The boundary conditions in the vertical position are linear springs attached to the lifting points in the front and rear. There is one spring for each direction in the 3D space. The springs are given appropriate stiffnesses so as to obtain similar support forces as in the Excel calculations. The linear springs are illustrated in Figure 77.

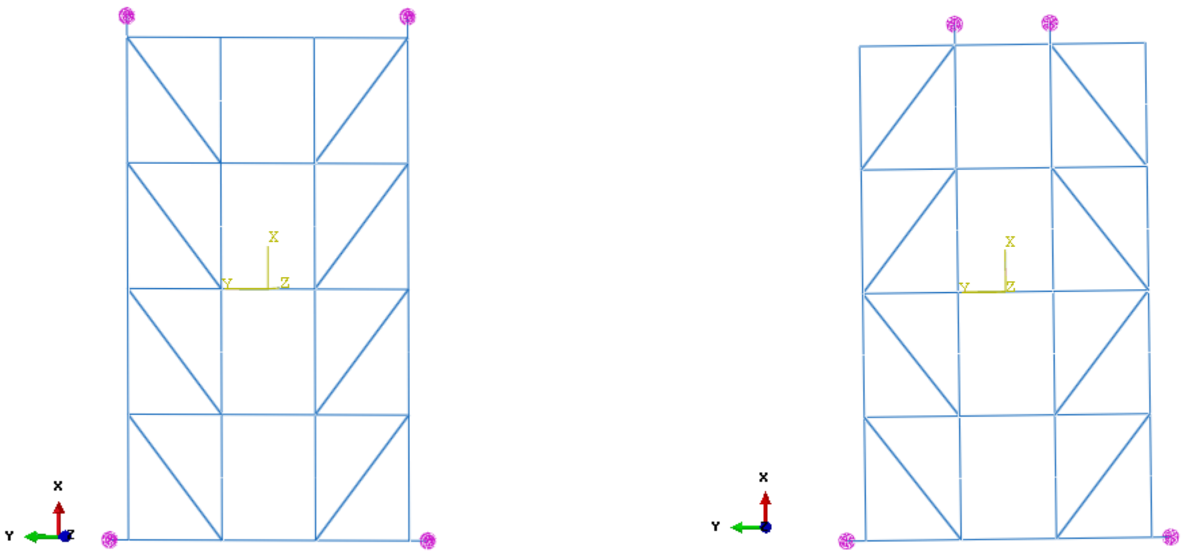

Purple dots: Linear spring supports

FIGURE 77: LINEAR SPRING SUPPORTS OF VERTICAL POSITION

The choice of spring stiffnesses are equal for Case A and Case B. The spring stiffnesses are summarized in Table 30.

TABLE 30: SPRING STIFFNESSES OF MODEL OF CASE A IN LOAD COMBINATION 2)a)

	Direction	Stiffness [N/mm]
Front	x	2.015E+06
	y	1.000E+07
	z	1.000E+07
Rear	x	1.000E+20
	y	1.000E+07
	z	1.000E+07

In order to obtain the prescribed support forces from load combination 2)b), the spring stiffnesses are modified. The spring stiffnesses are chosen according to Table 31.

TABLE 31: SPRING STIFFNESSES OF MODELS IN LOAD COMBINATION 2)b)

		Case A	Case B
	Direction	Stiffness [N/mm]	Stiffness [N/mm]
Front	x	4.250E+05	3.100E+05
	y	1.000E+07	1.000E+07
	z	1.000E+07	1.000E+07
Rear	x	1.000E+20	1.000E+09
	y	1.000E+07	1.000E+07
	z	1.000E+07	1.000E+07

10.2. 2D AND 3D ELEMENT ANALYSES

2D elements are widely referred to as “shell” elements. Shell elements are well suited to discretize bodies in which the thickness is significantly smaller than other dimensions. Shell elements are accurate at in-plane deformation, but behave too stiffly in out-of-plane bending deformation. Triangular elements may behave too stiffly also in in-plane deformation and have low convergence rate, so rectangular elements are preferred where geometry allows it. The rectangular elements may have linear stress (4 nodes, R4) or quadratic stress (8 nodes, R8). Quadratic elements, such as the R8 element, are better at describing high stress gradients.

The meshing tool in Abaqus allows a quad-dominated mesh, in which rectangular elements are preferred over triangular elements. However, if the shape of the body makes a pure quadrilateral mesh difficult, triangular elements are applied where necessary. This option is chosen in the following analyses in regions which are not rectangular.

In shell element models and solid element models, a phenomenon referred to as stress concentrations, or stress singularity arises. Stress concentrations usually appear in regions where there is an abrupt discontinuity in geometry, such as a 90° corner. Stress concentrations are to some extent realistic, as discontinuous geometry causes a “bottleneck” in the stress flow. However, in FEA analysis, stress concentrations are highly erratic in terms of stress. Mesh convergence is not attainable, as the stresses increase the more the mesh is refined. To verify mesh convergence, one must measure stresses outside stress concentrations. It is nonetheless important to avoid stress concentrations as far as possible, as they are realistic. Stress concentrations are effectively avoided by rounding off corners by chamfers or fillets. These details usually increase the complexity of the FEA model, as they need rather fine mesh to be described.

SHELL MODEL OF FRAME

As explained in the results, the Case B design is considered superior to Case A. Case A is therefore not considered in the 2D and 3D element analyses.

A shell model of the frame is made to visualize and verify the capacity of the frame further. A complete solid model of the frame using 3D elements is unfeasible due to computational cost. Most of the relevant behavior of the frame is adequately described by shell elements. The geometry of the trunnions is simplified to make meshing easier. The trunnions are investigated in isolation in other analyses. Another simplification is to take advantage of the symmetry of the frame. The frame is symmetric about the XZ-plane. Thus, only half of the frame needs to be modeled. Further, the diagonals are completely omitted from the model. They introduce severe complexity in the model, and it is a conservative choice to omit them. Otherwise, the frame is modeled exactly.

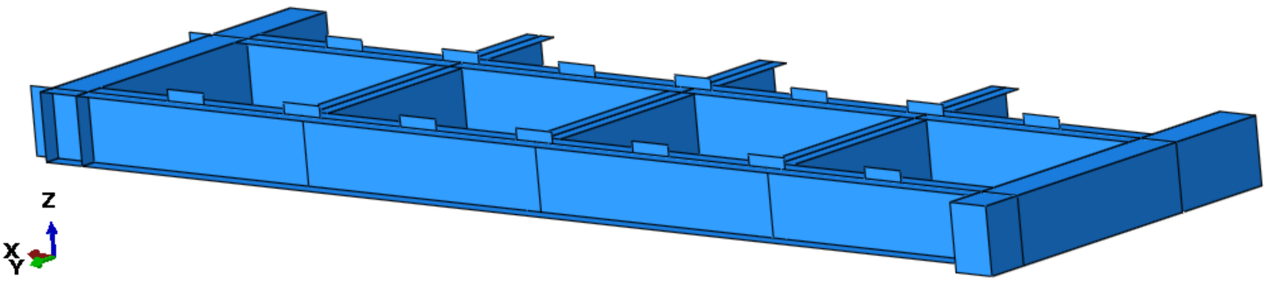

FIGURE 78: SHELL MODEL OF THE FRAME

The loads are applied at the shear plates as shell edge loads. Y-symmetry is applied to the midsection of the frame. The trunnions are made into rigid bodies related to reference points. Effectively, the translation and rotation of the reference point determines the translation and rotation of the rigid body. The reference points are constrained toward translation in X- and Z-directions. In the horizontal position, the reference points are constrained by fixed constraints in X- and Z-directions. In the vertical positions, the X-direction is constrained by linear springs with similar stiffness as in the 1D FE model of the Case B frame. The spring stiffnesses are chosen to obtain the prescribed support forces. The shell model of the frame is only analyzed for load combinations 1) and 2)b).

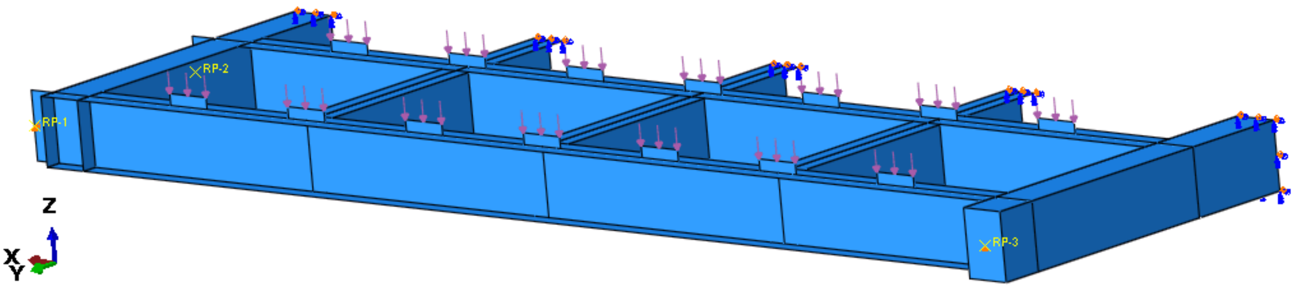

FIGURE 79: SHELL MODEL WITH LOADS AND BOUNDARY CONDITIONS

Due to the geometrical simplifications, the geometry of the model is easily meshed with rectangular elements.

SHELL MODEL OF FRONT TRUNNION

The front trunnion is appropriately modeled with shell elements. The shell model of the trunnion is rendered in Figure 80. The load is applied at the tube. The magnitudes of the loads are taken from the consideration about stability in 7.4. Thus, the loads applied to the trunnion correspond to acceptable rope forces considering the capacity of the lower trolley. The applied forces to the front trunnion are given in Table 32. The loads are applied as shell edge loads, referred to as q_x and q_z. The radius of the tube is 250 mm. The plate, which is a rendition of the front beam, is constrained to emulate the true conditions. The partition line is a tool to obtain better element mesh. Quadratic elements were employed, as the stress gradient near the tube was found to be large.

TABLE 32: APPLIED FORCES TO THE FRONT TRUNNION

Load combination		F_z [kN]	F_x [kN]	q_z [N/mm]	q_x [N/mm]
1)	Horizontal	3889	0	1238	0
2)b)	Vertical	2354	1307	749	416

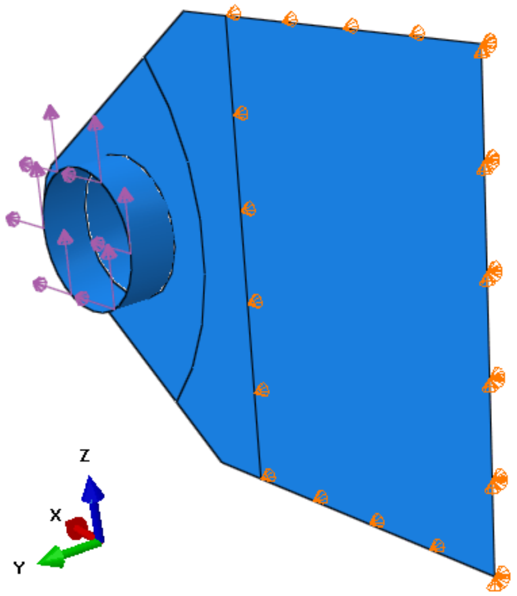

FIGURE 80: FRONT TRUNNION MODEL

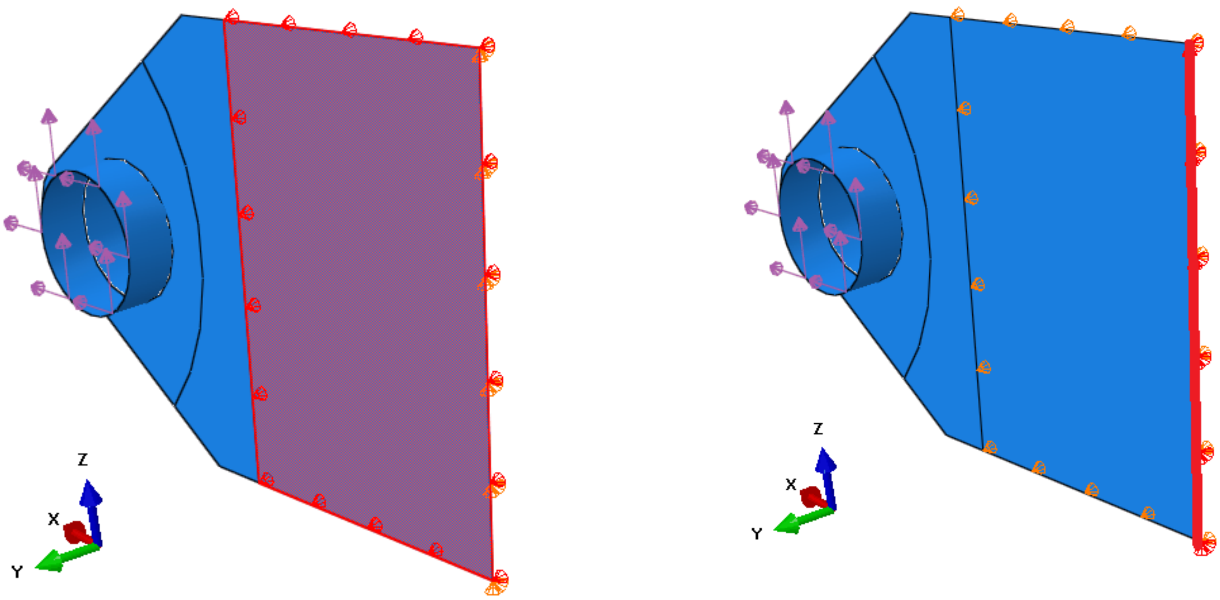

Red area restrained toward translation in y-direction (out-of-plane deformation)

Red line restrained toward translation in x- and z-directions.

FIGURE 81: BOUNDARY CONDITIONS OF SHELL MODEL OF FRONT TRUNNION

As the frame is loaded, it will bend slightly and the trunnions will rotate. The alignment of the ropes remains the same. The FEA model of the front trunnion does not take this rotation into account. However, the rotation is small, and is thus deemed negligible.

SOLID MODEL OF REAR TRUNNION

The rear trunnion features a plate which is subject to normal forces. As shell elements behave too stiffly for bending deformation, solid elements are regarded as the reliable option in this model. Figure 82 shows the 3D model of the rear trunnion.

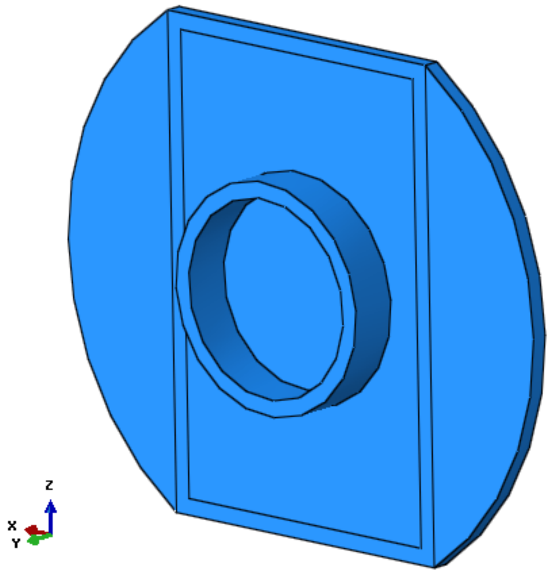

FIGURE 82: 3D MODEL OF REAR TRUNNION

As solid elements are rather expensive in terms of computation cost, reducing the number of elements by omitting regions which are not of interest, allows increased mesh refinement. The omitted regions must not affect the relevant stresses. Regions can be omitted if they can be replaced by equivalent boundary conditions. In the model of the rear trunnion, the rear beam is omitted and replaced by boundary conditions which fix the common cross section area, as shown in Figure 83. There are regions of the plate which are seen to have rather low stresses, but omitting them does influence peak stress significantly.

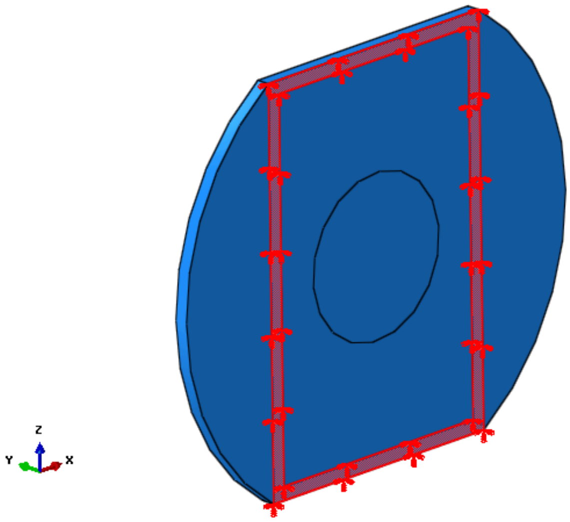

FIGURE 83: FIXED AREA OF REAR TRUNNION

The load is applied to the area of the tube as shown in Figure 84. The load is thus applied as a traction shear force, with unit MPa. The magnitude of the applied loads is taken from the consideration in 7.4, which gives acceptable rope forces. The traction area is a circular area with outer radius 350mm and inner radius 300mm. The applied forces are referred to the global coordinate system.

TABLE 33: APPLIED LOADS AT REAR TRUNNION

Load combination		F_z [kN]	F_x [kN]	q_z [N/mm]	q_x [N/mm]
1)	Horizontal	4231	0	20.720	0.000
2)b)	Vertical	6298	1307	30.842	6.400

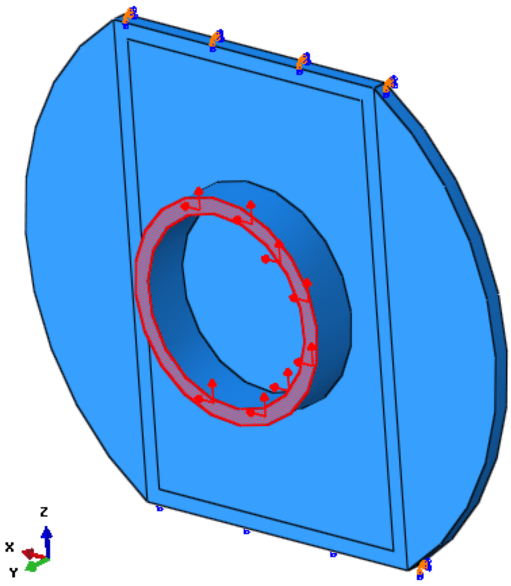

FIGURE 84: LOAD AT REAR TRUNNION

11. RESULTS

11.1. SUMMARY OF RESULTS

A short summary of the maximum von Mises stresses of the finite element models are given in Table 34.

TABLE 34: SUMMARY OF CRITICAL VON MISES STRESSES

Analysis	Case	Load comb.	Critical value [MPa]	Utilization
1D FEA	Case A	1)	228	81 %
		2)b)	180	64 %
	Case B	1)	222	79 %
		2)b)	145	52 %
2D Frame shell	Case B	1)	291	104 %
		2)b)	588	210 %
2D Front trunnion	Case B	1)	307	110 %
		2)b)	194	69 %
3D Rear trunnion	Case B	1)	283	101 %
		2)b)	376	134 %

Some of the peak stresses exceed the design requirement of 280 MPa. It is seen that the peak stresses are due to stress concentrations. Outside stress concentrations, peak stresses are generally within the requirement.

11.2. VERIFICATION OF FE MODEL

The results of the MS Excel are compared with the results of the 1D FE model in the following. The results of the support forces in the horizontal position are given in Table 35.

TABLE 35: SUPPORT FORCES IN HORIZONTAL POSITION [kN]

Load combination: 1) Horizontal position

	Excel		Abaqus		Focus	
	Left	Right	Left	Right	Left	Right
Front	3891	3891	3880	3880	3881	3881
Rear	4221	4221	4231	4231	4231	4231
Sum	8112	8112	8112	8112	8112	8112
Error			0.00 %	0.00 %	0.00 %	0.00 %

Also the internal moments of the longitudinal beams and the front and rear beams are compared. The moments are the most crucial load effects, and are important to get right. The bending moment is about the strong axis of the I/H-profiles, as illustrated in Figure 85. The bending moment is given in Table 36 and Table 37.

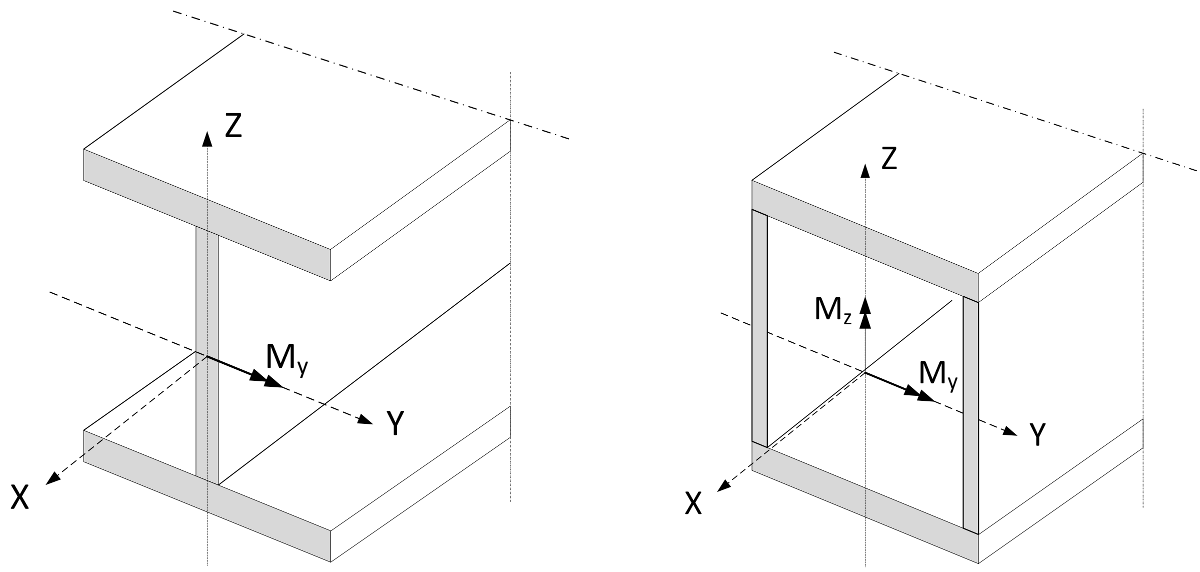

FIGURE 85: LOCAL AXIS SYSTEM OF BEAMS

TABLE 36: BENDING MOMENTS IN LONGITUDINAL BEAMS [kNm]

Load combination: 1) Horizontal position

	Peripheral beams			Central beams		
	Excel	Abaqus	Focus	Excel	Abaqus	Focus
Moment	15809	15976	15932	13917	13886	13932
Error		1.0 %	0.7 %		-0.2 %	0.2 %

TABLE 37: BENDING MOMENTS IN FRONT AND REAR BEAMS [kNm]

Load combination: 1) Horizontal position

	Front beam			Rear beam		
	Excel	Abaqus	Focus	Excel	Abaqus	Focus
Moment	9166	9071	9097	12611	12721	12619
Error		-0.9 %	-0.6 %		0.7 %	-0.1 %

The support forces in the vertical position have 2 components; both in the global x- and z-direction. The forces F_x, referred to the global coordinate system, carry the moment due to the eccentricity of the module. The support forces are given in Table 38 and Table 39.

TABLE 38: SUPPORT FORCES F_x IN VERTICAL POSITION [kN]

Load combination: 2)a) Vertical position

	Excel		Abaqus		Focus	
	Left	Right	Left	Right	Left	Right
Front	1303	1303	1303	1303	1303	1303
Rear	1303	1303	1303	1303	1303	1303
Sum	2606	2606	2606	2606	2606	2606
Error			0.00 %	0.00 %	0.00 %	0.00 %

TABLE 39: SUPPORT FORCES F_z IN VERTICAL POSITION [kN]

Load combination: 2)a) Vertical position

	Excel		Abaqus		Focus	
	Left	Right	Left	Right	Left	Right
Front	4612	4612	4615	4615	4622	4622
Rear	3500	3500	3497	3497	3489	3490
Sum	8112	8112	8112	8112	8111	8112
Error			0.00 %	0.00 %	0.00 %	0.00 %

The bending moments are given in Table 40, Table 41 and Table 42.

TABLE 40: BENDING MOMENTS M_y IN VERTICAL POSITION [kNm]

Load combination: 2)a) Vertical position

	Peripheral beams			Central beams		
	Excel	Abaqus	Focus	Excel	Abaqus	Focus
Moment	3394	3376	3394	2726	2735	2725
Error		-0.5 %	0.0 %		0.3 %	0.0 %

TABLE 41: BENDING MOMENTS M_y IN VERTICAL POSITION [kNm]

Load combination: 2)a) Vertical position

	Front beam			Rear beam		
	Excel	Abaqus	Focus	Excel	Abaqus	Focus
Moment	3030	3028	3029	3834	3877	3832
Error		-0.1 %	-0.1 %		1.1 %	-0.1 %

TABLE 42: BENDING MOMENTS M_s IN VERTICAL POSITION [kNm]

Load combination: 2)a) Vertical position

	Front beam			Rear beam		
	Excel	Abaqus	Focus	Excel	Abaqus	Focus
Moment	1701	1614	1723	2528	2495	2552
Error	0	-5.1 %	1.3 %	0	-1.3 %	0.9 %

DISCUSSION

The Excel calculations are aided by extracting values from the 1D FEA results. It is not always obvious where the values shall be picked from, and this adds to the uncertainty of the results. There may also be a degree of coincidence or luck that makes the results correlate better than they should have. Nonetheless, it is unlikely that the results correlate to such a degree by chance. The results are considered to show that decent understanding about the behavior of the frame is obtained. Also, the 1D FEA model is deemed to be verified by the results.

11.3. INVESTIGATION AND COMPARISON OF CASE A AND CASE B DESIGNS

The explanation to the expressions used in Abaqus is summarized in Table 43. Note also that the units of the expressions in Abaqus are given as well.

TABLE 43: EXPLANATIONS TO REFERENCES AND UNITS IN ABAQUS

Common reference	Abaqus reference
x-axis	1
y-axis	2
z-axis	3
Moment about y-axis, M_y	SM1
Moment about z-axis, M_z	SM2
Torsional moment, about x-axis, M_x	SM3
Axial force	SF1
Shear force in y-direction, V_y	SF2
Shear force in z-direction, V_z	SF3
Units in Abaqus	
Force	N
Distance	mm
Moment	Nmm
Stress	N/mm^2

The results of the simulations of the horizontal position for Case A and Case B are summarized in Table 44.

TABLE 44: BENDING MOMENT AND VON MISES STRESS OF CASE A AND B IN 1) HORIZONTAL POSITION

CASE A

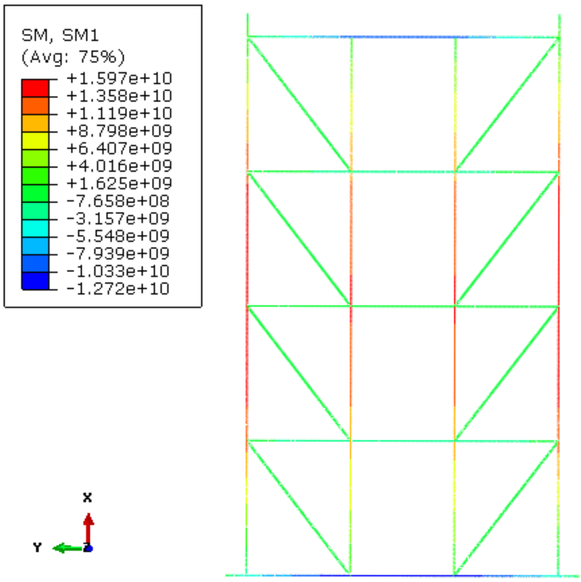

CASE B

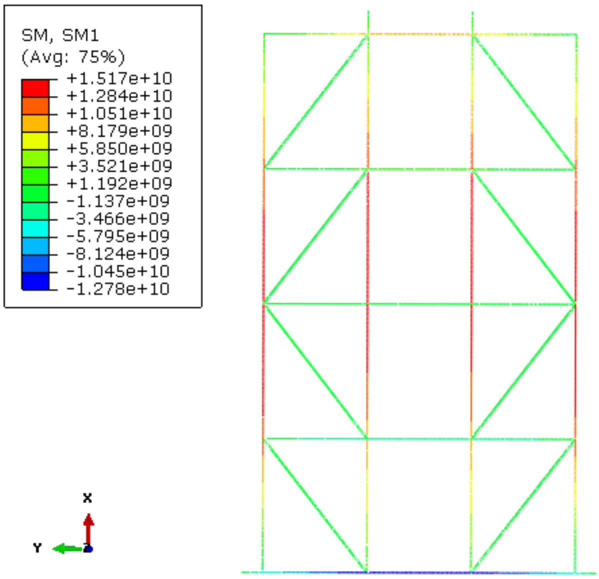

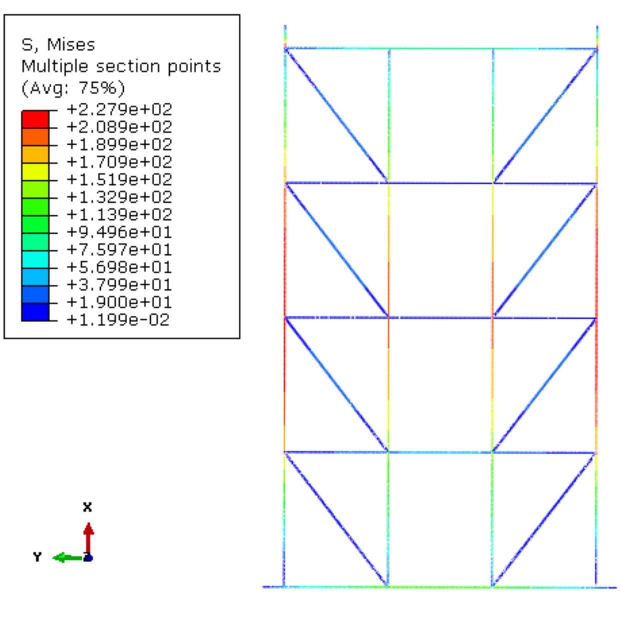	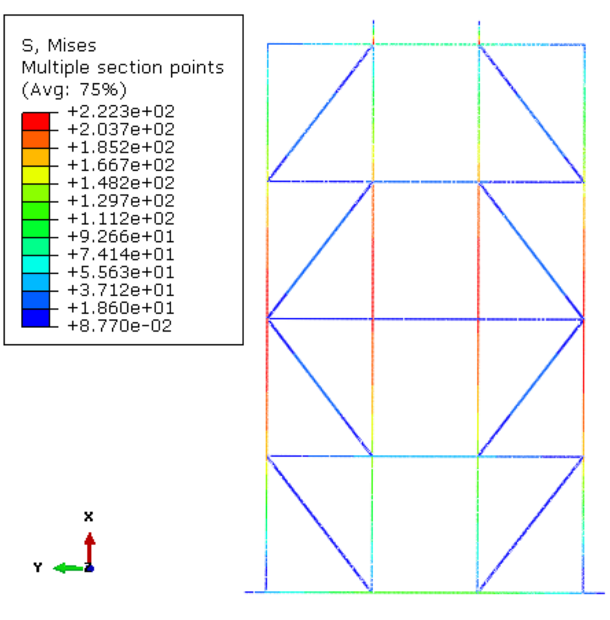

The results of the simulations of the vertical position for Case A and Case B are summarized in Table 45.

TABLE 45: COMPARISON OF ELEMENT ANALYSES OF CASE A AND CASE B IN 2)b) VERTICAL POSITION

CASE A	CASE B
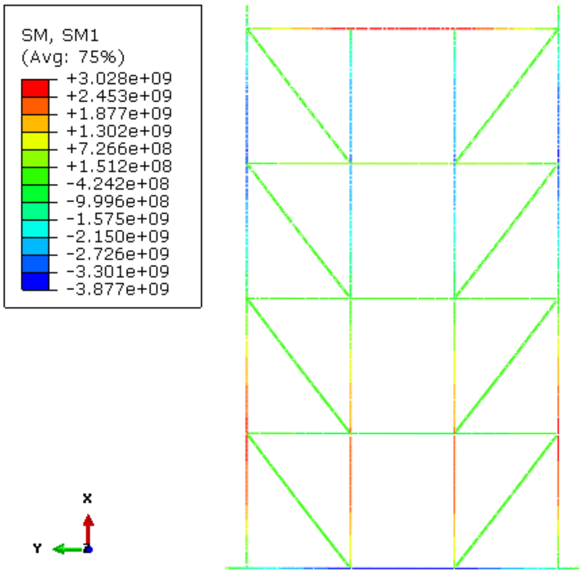	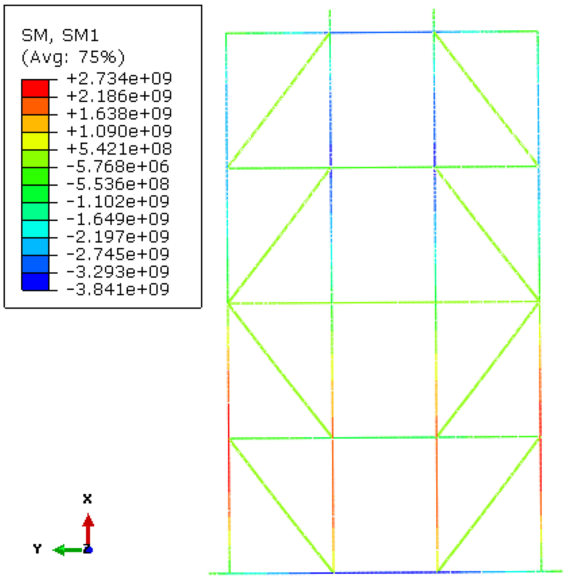

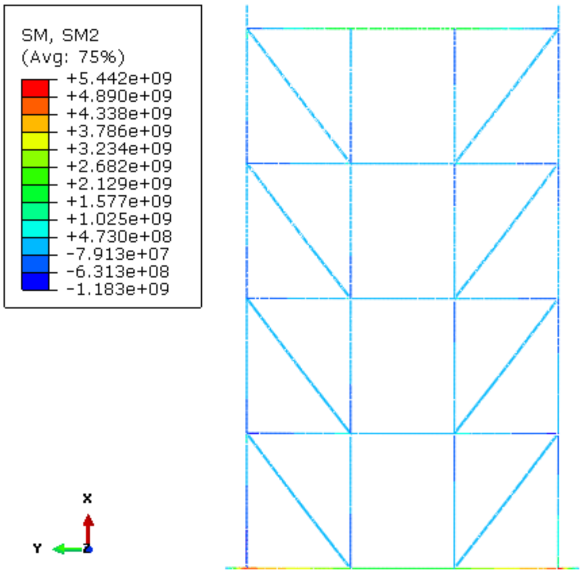
SM, SM2
(Avg: 75%)
+5.442e+09
+4.890e+09
+4.338e+09
+3.786e+09
+3.234e+09
+2.682e+09
+2.129e+09
+1.577e+09
+1.025e+09
+4.730e+08
-7.913e+07
-6.313e+08
-1.183e+09
X
Y

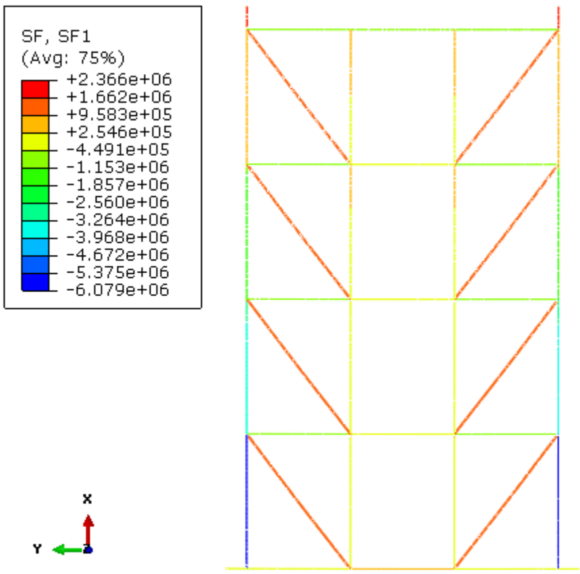
SF, SF1
(Avg: 75%)
+2.366e+06
+1.662e+06
+9.583e+05
+2.546e+05
-4.491e+05
-1.153e+06
-1.857e+06
-2.560e+06
-3.264e+06
-3.968e+06
-4.672e+06
-5.375e+06
-6.079e+06
X
Y

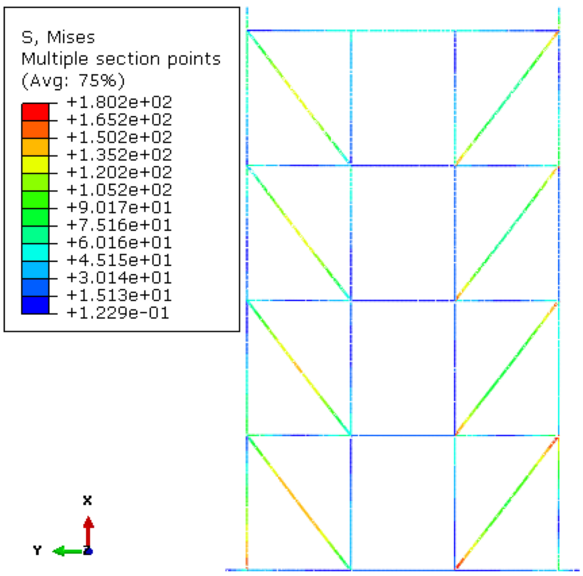
S, Mises
Multiple section points
(Avg: 75%)
+1.802e+02
+1.652e+02
+1.502e+02
+1.352e+02
+1.202e+02
+1.052e+02
+9.017e+01
+7.516e+01
+6.016e+01
+4.515e+01
+3.014e+01
+1.513e+01
+1.229e-01
X
Y

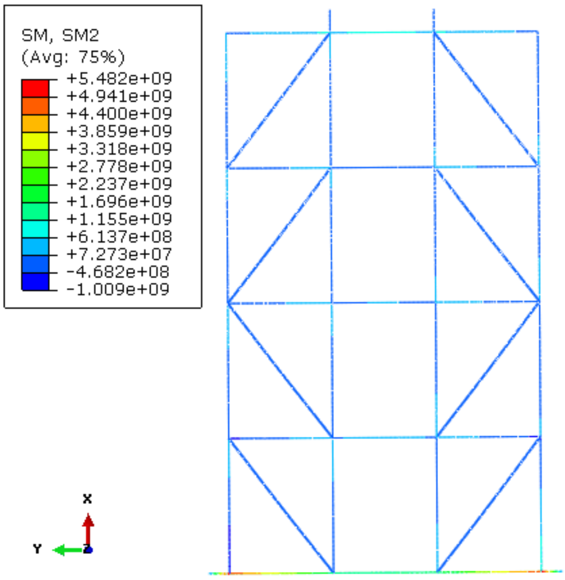
SM, SM2
(Avg: 75%)
+5.482e+09
+4.941e+09
+4.400e+09
+3.859e+09
+3.318e+09
+2.778e+09
+2.237e+09
+1.696e+09
+1.155e+09
+6.137e+08
+7.273e+07
-4.682e+08
-1.009e+09
X
Y

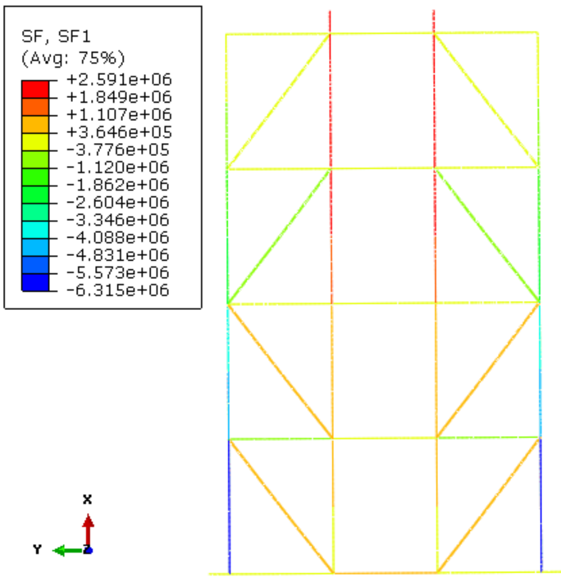
SF, SF1
(Avg: 75%)
+2.591e+06
+1.849e+06
+1.107e+06
+3.646e+05
-3.776e+05
-1.120e+06
-1.862e+06
-2.604e+06
-3.346e+06
-4.088e+06
-4.831e+06
-5.573e+06
-6.315e+06
X
Y

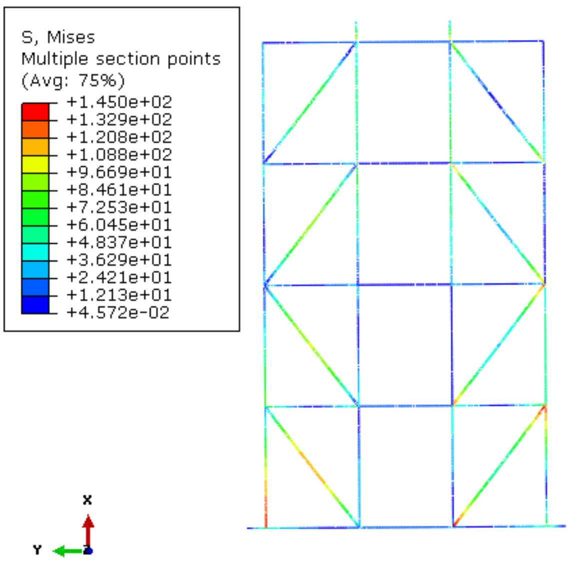
S, Mises
Multiple section points
(Avg: 75%)
+1.450e+02
+1.329e+02
+1.208e+02
+1.088e+02
+9.669e+01
+8.461e+01
+7.253e+01
+6.045e+01
+4.837e+01
+3.629e+01
+2.421e+01
+1.213e+01
+4.572e-02
X
Y

DISCUSSION

In the horizontal position, there is not much difference in the results of Case A and Case B. The bending moment and the maximum von Mises stress are fairly equal. In the vertical position, the results vary more. The bending moment SM1 is significantly different. The rear beam receives the maximum SM1 of roughly 3800 kNm (note: with negative sign), in both cases, but the maximum moment in the longitudinals is lower. The central longitudinals contribute more to carry the moment in Case B than Case A. The effect of the diagonals seems much lower in Case B than Case A, as the diagonals have much lower SF1, i.e. axial force, in Case B. The diagonals can perhaps be omitted completely from the design in Case B. This makes the manufacturing of the frame simpler and cheaper. Finally, the von Mises stress is significantly lower in Case B. This can be exploited by downsizing cross sections to obtain better utilization of material.

Case B is considered the superior design, and is thus the only design considered in 2D and 3D element analyses.

11.4. 2D AND 3D FEA MODELS

The frame is investigated in detail to explore peak stresses in the design. The stress is evaluated as von Mises stress, given in N/mm^2.

SHELL MODELS

The shell model of the frame features geometric discontinuities which create stress concentrations, e.g. in the shear plates, as seen in Figure 87. Mesh convergence is proved by measuring von Mises stress in regions outside stress concentrations. The stress distribution and deformation in both horizontal and vertical position are shown in Figure 86 and Figure 88. Note that the deformation is scaled up to be visible. The corresponding support forces are given in the appendices.

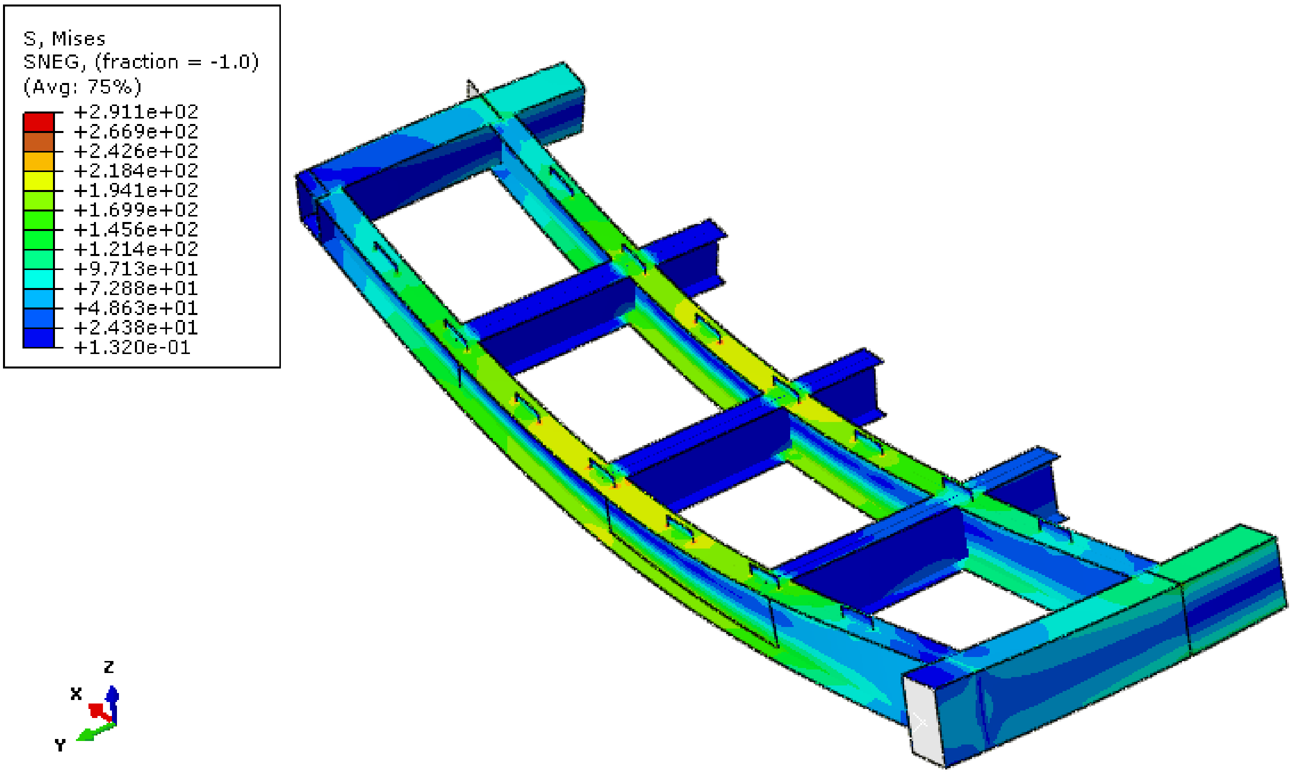

FIGURE 86: STRESS DISTRIBUTION AND DEFOMATION IN HORIZONTAL POSITION

The peak stress in the horizontal position is 291 MPa. This stress occurs in the transition from shear plate to flange of the peripheral longitudinal. The peak stress in the stress concentrations is likely to grow beyond the maximum measure of 291 MPa, depending on element size. However, the shear plates are to be welded to the flange. The stress concentration is negated by the fillet weld connecting the shear plate to the flange. Thus, the stress concentration in the shear plates is deemed acceptable. There are also stress concentrations in the joints of the traverse beams and the longitudinals, however, these are of minor severity. The joints can be improved by welding in a triangular plate to the sharp corner to round the corners off. The stress concentrations of the horizontal position are thus regarded as acceptable.

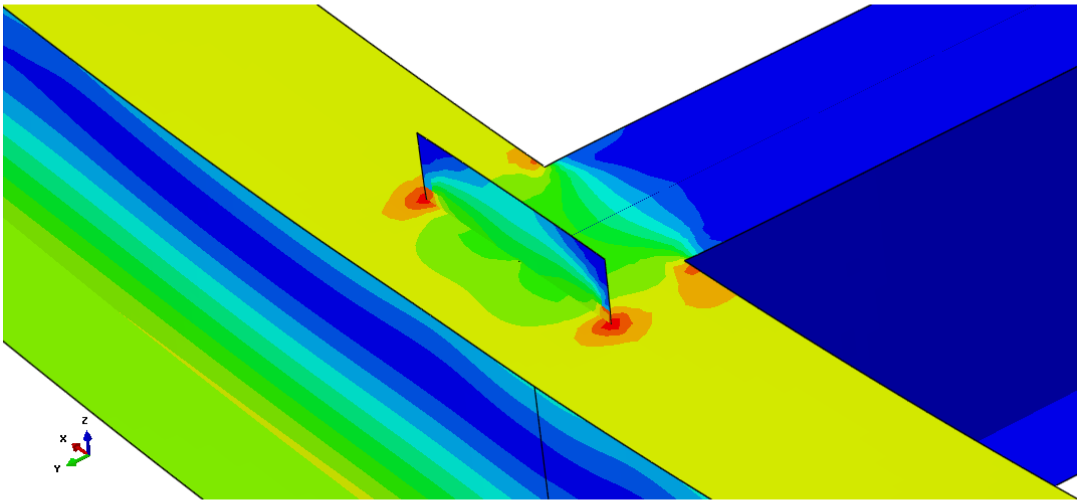

FIGURE 87: STRESS SINGULARITIES OF SHEAR PLATES

Figure 88 shows the results of the analysis of the vertical position. The image is taken from the tipping point scheme. The frame is largely blue in color, as there is a severe stress concentration shown in Figure 89. The peak stress is up to 588 MPa, which is not acceptable. Even considering that stress concentrations may exaggerate the stress somewhat, a stress concentration of this severity can not be neglected. The corner must be rounded off using a plate to stiffen up the joint.

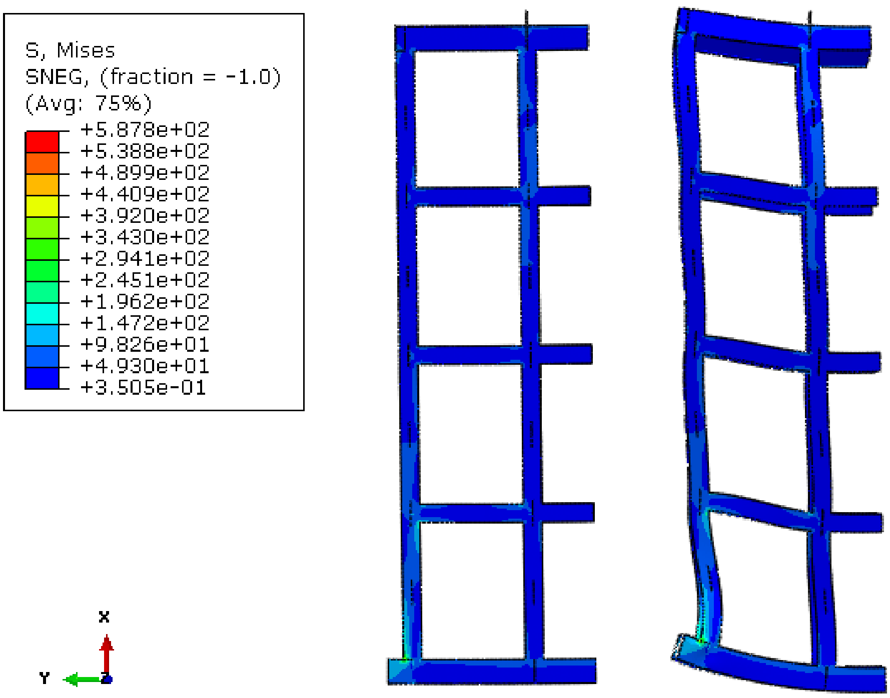

FIGURE 88: STRESS DISTRIBUTION AND DEFORMATION IN VERTICAL POSITION

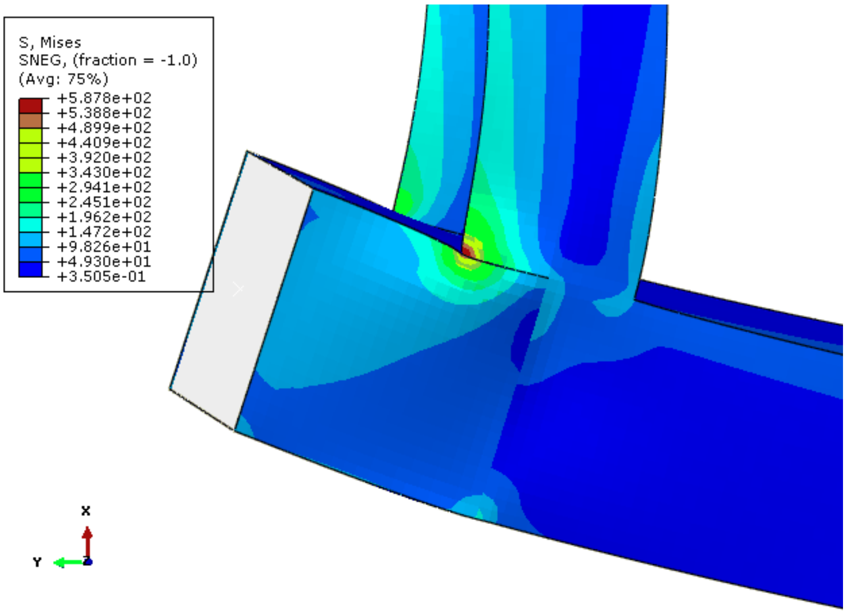

FIGURE 89: STRESS CONCENTRATION IN VERTICAL POSITION

Looking beyond the stress concentrations, it is seen that the highest stresses do occur in the rear beam, but the stresses are at a reasonable level of maximum 243 MPa, as seen in Figure 90.

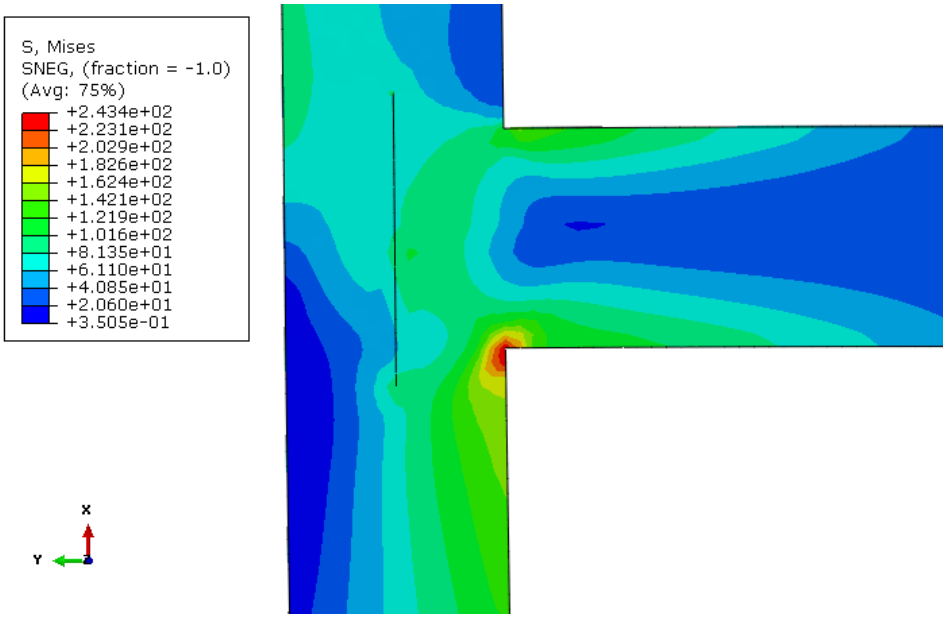

FIGURE 90: MAX STRESS IN LONGITUDINAL

FRONT TRUNNION

Figure 91 and Figure 92 show the stress distribution of the front trunnion in both horizontal and vertical position. The part of the model which represents the front beam is omitted from the visualization. There is a stress concentration at the transition between the tube and the plate. The stress does not converge in this area, but outside the area, the stresses have converged.

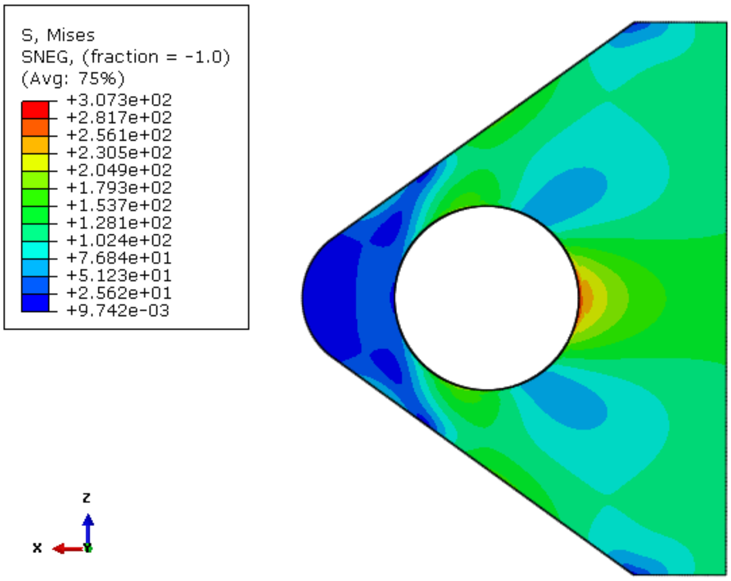

FIGURE 91: STRESS AND DEFORMATION OF FRONT TRUNNION IN 1) HORIZONTAL POSITION

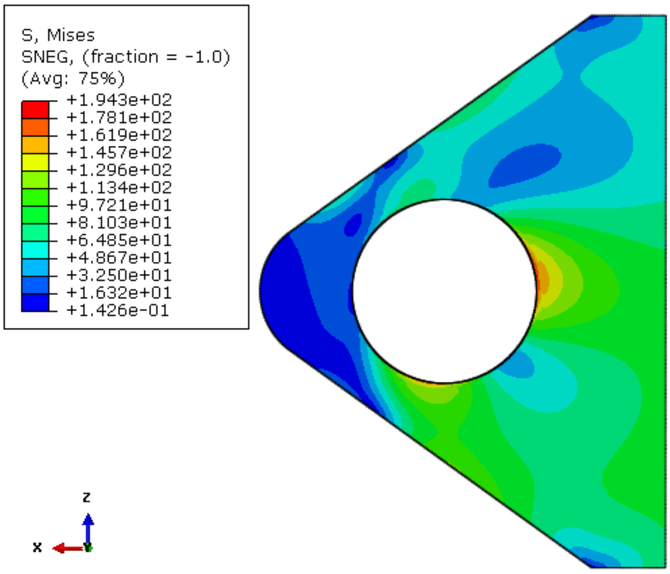

FIGURE 92: STRESS AND DEFORMATION OF FRONT TRUNNION IN 2)b) VERTICAL POSITION

Zooming in on the stress concentration, it is seen that it is indeed very shallow. The stress decreases to acceptable levels rapidly. Also, in practice, the peak stress will be relieved significantly by the fillet weld joining the plate and the tube. The maximum stress is thus deemed acceptable.

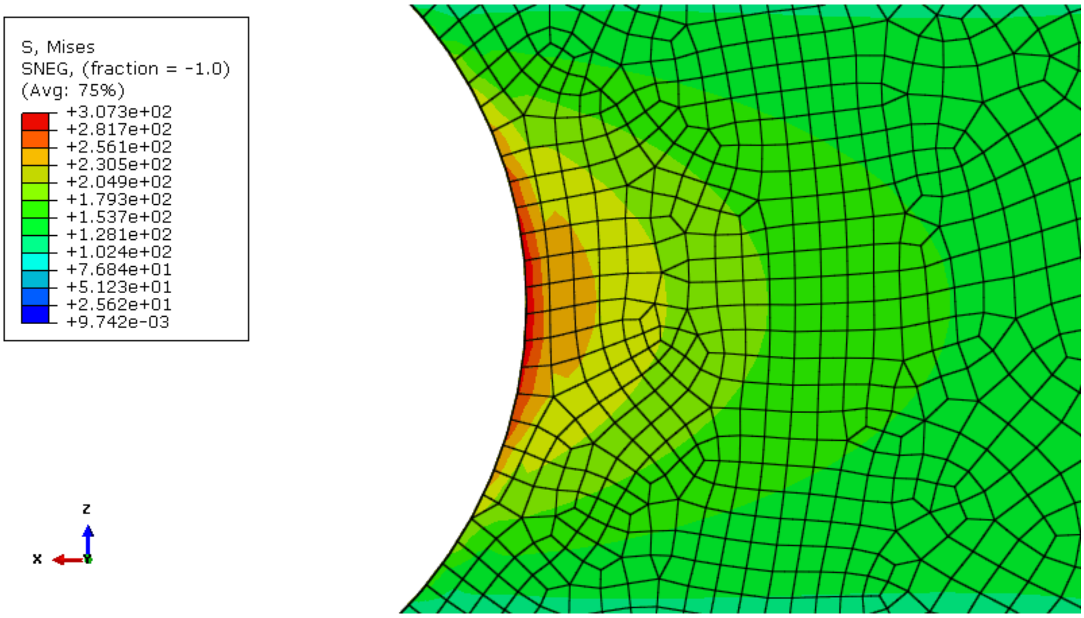

FIGURE 93: STRESS CONCENTRATION OF FRONT TRUNNION

REAR TRUNNION

Figure 94 shows the stress distribution of the rear trunnion in the horizontal and vertical position. There are stress concentrations in the transition between the tube and the plate, in which high peak stresses form, as in the front trunnion. The stress gradient is high, so quadratic elements are employed.

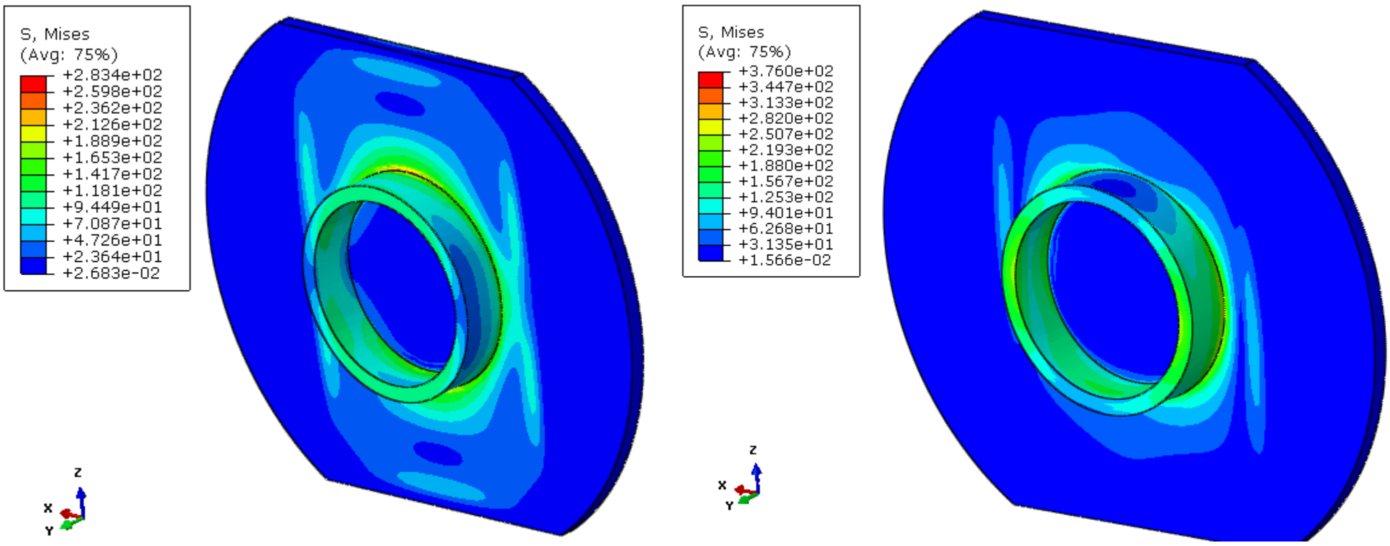

1) HORIZONTAL POSITION 2)b) VERTICAL POSITION

FIGURE 94: STRESS DISTRIBUTION IN REAR TRUNNION

Investigation of the critical areas shows that they are limited to a very small area, as seen in Figure 95. The depth of the high stress region is very shallow, as seen in Figure 96.

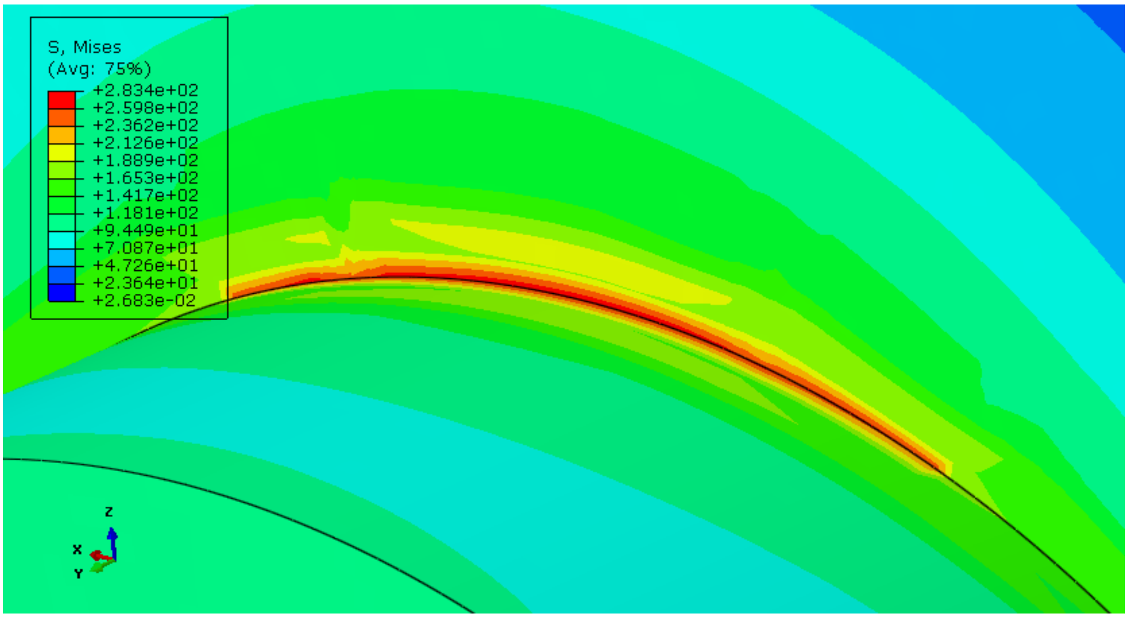

FIGURE 95: ILLUSTRATION OF THE EXPANSE OF THE CRITICAL AREA

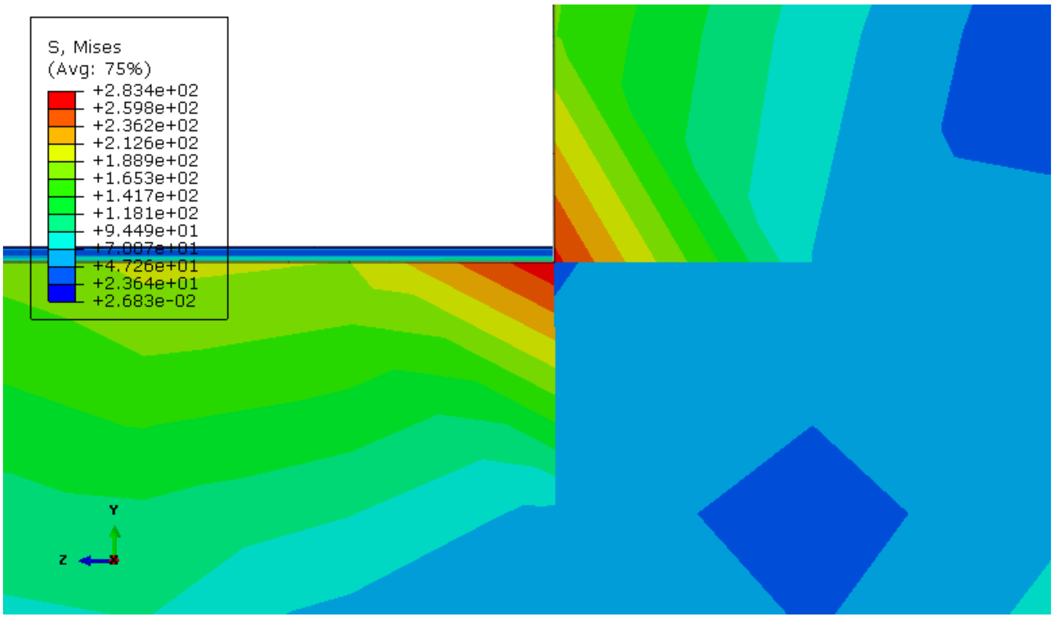

FIGURE 96: ILLUSTRATION OF THE DEPTH OF THE CRITICAL STRESS AREA IN HORIZONTAL POSITION

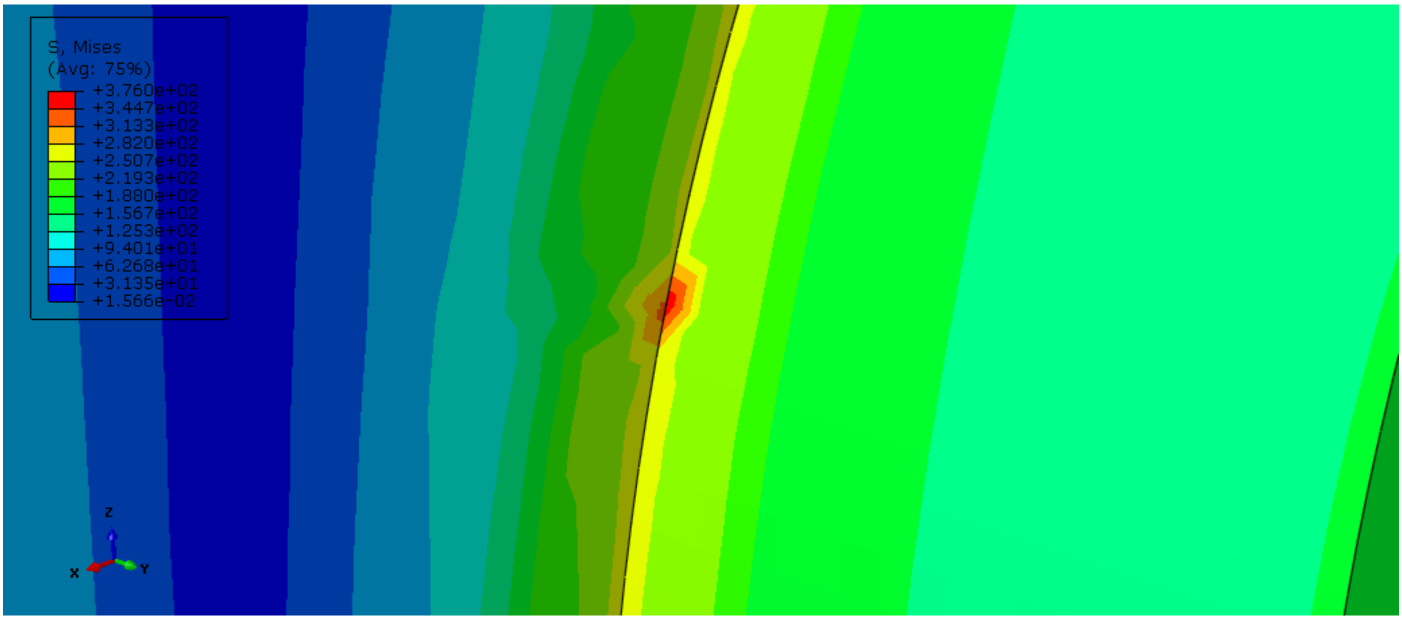

FIGURE 97: PEAK STRESS IN REAR TRUNNION IN VERTICAL POSITION

The sharp corner between the tube and the plate elicit a stress singularity. The stress singularity is not only a theoretical phenomenon. It represents the true behavior of geometrical discontinuities, albeit slightly exaggerated in some cases. It is therefore an important consideration in structural design to avoid severe geometrical discontinuities. A good strategy to avoid stress concentrations, or at least reduce the severity of them, is to round edges off with chamfers or fillets. The tube has to be welded to the plate of the rear trunnion, thus creating a fillet weld which rounds off the corner. The stress peak in the vertical position seems to be due to a flaw in the element mesh. There is no particular reason why the stress should peak as in Figure 97. Outside the small region of the peak the stresses are at an acceptable level.

The design of the rear trunnion is deemed to be acceptable. More work can be put into investigation of the stress concentrations and the effect of a fillet weld on the peak stress.

11.5. CROSS SECTION CAPACITY CHECKS

The result of the cross section capacity check is presented in the following. Case A is the design considered in this calculation, as there was not time to analyze Case B. However, the critical load effects are fairly similar for the two cases, so the results of the check of Case A is considered to be relevant also for Case B. The cross section capacity check is done for load combinations 1) and 2)a).

HORIZONTAL POSITION

In the horizontal position there are no axial forces in a linear analysis. Only a nonlinear calculation will give axial forces, but these help to reduce the moment. The linear calculation gives a more conservative answer and this will be used in this assignment.

The design forces: Values are taken from the FEA analysis in Focus

- Box-profiles (front and rear beam)

TABLE 46: DESIGN FORCES, BOX-PROFILE, 1) HORIZONTAL POSITION

Section forces		Max moment	Max shear	Max torsion	Max combination
Tension	$N_{Ed,t}$ [kN]	0	0	0	0
Compression	$N_{Ed,c}$ [kN]	0	0	0	0
Moment, about strong axis	$M_{Ed,y}$ [kNm]	12619	0	8971	12495
Moment, about weak axis	$M_{Ed,z}$ [kNm]	0	0	0	0
Shear, y-direction	$V_{Ed,y}$ [kN]	0	0	0	0
Shear, z-direction	$V_{Ed,z}$ [kN]	0	4231	1714	1576
Torsion	T_{Ed} [kNm]	0	0	2173	1794
Utilization	[%]	20	12	12	22

Maximum moment occurs at the mid span of the rear beam. Maximum shear occurs in the cross section close up to the rear support. Maximum torsion occurs in the front beam – using the value close to the two middle beams. The maximum combination occurs in the rear beam by the two middle nodes where we have shear, moment and torsion working.

- I-profiles (longitudinal and traverse beams)

TABLE 47: DESIGN FORCES, I-PROFILE, 1) HORIZONTAL POSITION

Section forces		Max moment	Max shear	Max torsion	Max combination
Tension	$N_{Ed,t}$ [kN]	0	0	0	0
Compression	$N_{Ed,c}$ [kN]	0	0	0	0
Moment, about strong axis	$M_{Ed,y}$ [kNm]	15933	1777	1777	13090
Moment, about weak axis	$M_{Ed,z}$ [kNm]	0	0	0	0
Shear, y-direction	$V_{Ed,y}$ [kN]	0	0	0	0
Shear, z-direction	$V_{Ed,z}$ [kN]	283	2445	2445	1417
Torsion	T_{Ed} [kNm]	2	5	5	4
Utilization	[%]	70	7	7	50

Maximum moment occurs at the mid span of the longitudinal beam, maximum shear in the outer longitudinal beam at the support towards the rear beam (maximum torsion the same place). Maximum combination occurs in the longitudinal by the outer traverse beams.

- Diagonals

No forces in the horizontal position

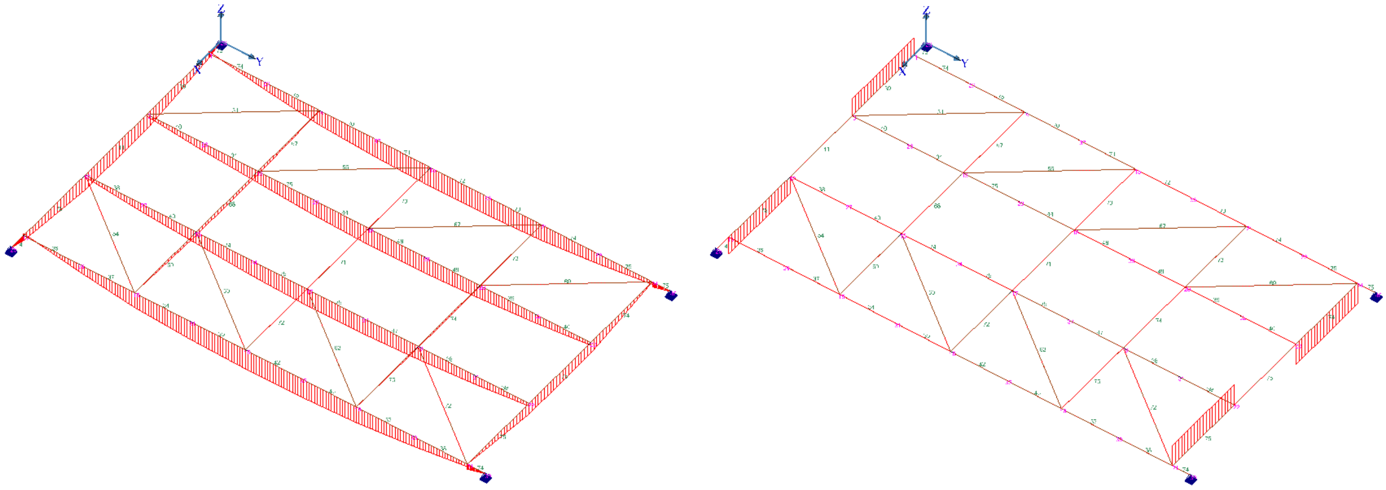

FIGURE 98: MOMENT AND TORSION DIAGRAM, HORIZONTAL POSITION

Vertical position

In the vertical position we have the diagonals contributing to the force distribution. These help to reduce the peak moment in the front and rear beam.

The supports in Abaqus and Focus are modeled by springs. The spring stiffness determines how much force is transmitted into each support. In Focus one have to enter the cross section properties manually when not using a standard profile. This can cause smaller deviations in the results if incorrect value or too few decimals are entered.

As mentioned earlier the force distribution is determined by the crane conductor and how much force he applies by pull/release of the ropes. Here we have chosen to use a calculation where the force distributes with 57/43 front/back. This deviates a bit from the horizontal position where the force distributes with approximate 48/52 front/back.

- Box-profiles (front and rear beam)

TABLE 48: DESIGN FORCES, BOX-PROFILE, 2)a) VERTICAL POSITION

Section forces		Max moment	Max shear	Max torsion	Max combination
Tension	$N_{Ed,t}$ [kN]	873	0	0	0
Compression	$N_{Ed,c}$ [kN]	0	0	796	0
Moment, about strong axis	$M_{Ed,y}$ [kNm]	1612	0	2386	3491
Moment, about weak axis	$M_{Ed,z}$ [kNm]	3727	0	2890	1311
Shear, y-direction	$V_{Ed,y}$ [kN]	0	1303	578	1303
Shear, z-direction	$V_{Ed,z}$ [kN]	9	3488	520	3455
Torsion	T_{ed} [kNm]	0	0	909	0
Utilization	[%]	6	12	6	15

The maximum moment occurs at the middle of the rear beam, maximum shear at the rear beam support, maximum torsion in the front beam by the middle longitudinal beam. And the maximum combination in the rear beam by the outer longitudinal beam.

- I-profiles (longitudinal and traverse beams)

TABLE 49: DESIGN FORCES, I-PROFILE, 2)a) VERTICAL POSITION

Section forces		Max moment	Max shear	Max torsion	Max combination
Tension	$N_{Ed,t}$ [kN]	2518	0	0	0
Compression	$N_{Ed,c}$ [kN]	0	3525	3525	3525
Moment, about strong axis	$M_{Ed,y}$ [kNm]	3345	697	697	697
Moment, about weak axis	$M_{Ed,z}$ [kNm]	397	857	857	857
Shear, y-direction	$V_{Ed,y}$ [kN]	154	207	207	207
Shear, z-direction	$V_{Ed,z}$ [kN]	143	818	818	818
Torsion	T_{ed} [kNm]	1	1	1	1
Utilization	[%]	15	22	22	22

Maximum moment occurs in the outer longitudinal beam by the upper traverse beam. Maximum shear occurs at outer longitudinal support to the rear beam.

- Diagonals

TABLE 50: DESIGN FORCES, DIAGONALS, 2)a) VERTICAL POSITION

Section forces		Max axial
Tension	$N_{Ed,t}$ [kN]	1063
Utilization	[%]	38

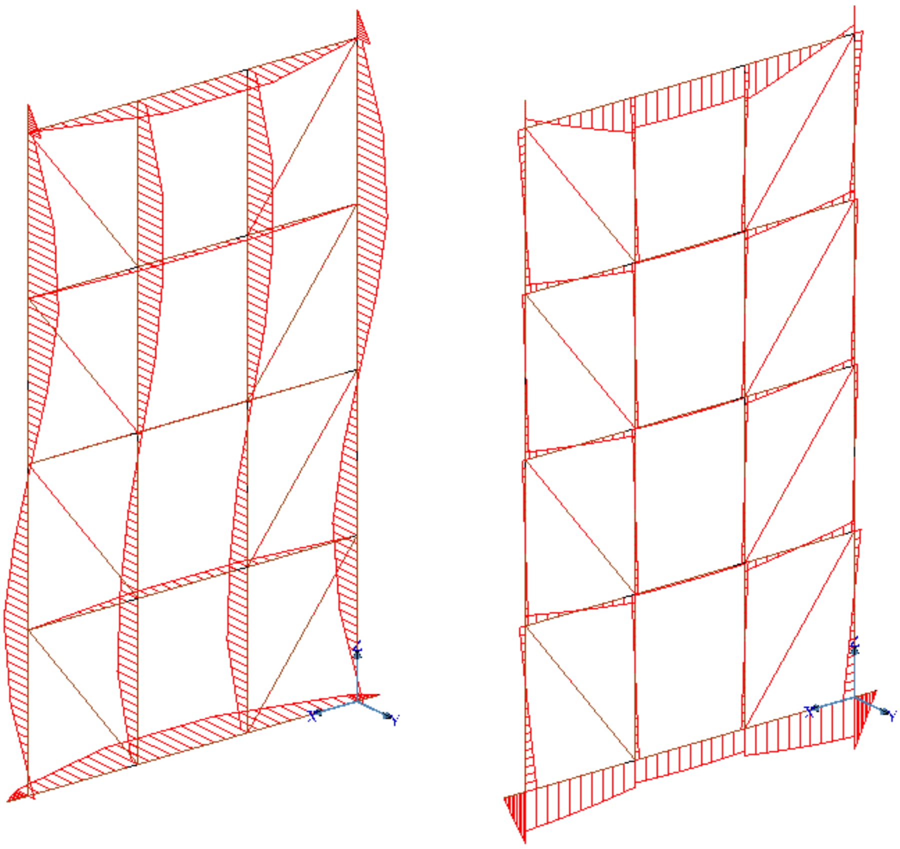

FIGURE 99: FORCES IN VERTICAL POSITION: LEFT - AXIAL FORCE, RIGHT - MOMENT ABOUT STRONG AXIS

DISCUSSION

The results of the cross section capacity check shows that utilization of the cross sections is generally low. The maximum utilization of bending moment capacity in the longitudinals is at 70% of elastic capacity. The low utilization gives low risk of structural failure, but in an economical perspective the low utilization means that unnecessarily much material is used. This is at the expense of not only material purchase costs, but the total weight of the structure and the strain put on the gantry crane which shall use it. It is therefore recommended in further work to optimize the cross sections to increase material efficiency.

11.6. WELDS

In the horizontal position the needed a-level becomes 4 mm for the flange and 5 mm for the web. In the vertical position the needed a-level becomes 7 mm for the flange and 6 mm for the web. The vertical position is the design requirement for the welds.

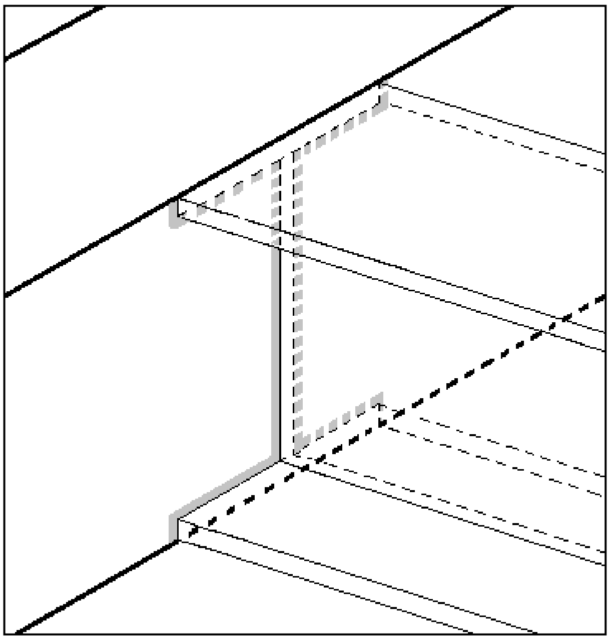

FIGURE 100: LONGITUDINAL - REAR BEAM JOINT

TABLE 51: SUMMARY OF THE WELDING CALCULATIONS

Welded joint	Required a-level	
Longitudinal beam (joining of plates)	3 mm	
	Flange	*Web*
Longitudinal beam – rear beam	7 mm	6 mm

11.7. SHEAR RESISTANCE

According to NS-EN 1993-1-5, 5.1(2) an unstiffened plate with greater $\frac{h_w}{t}$ than $\frac{72}{\eta}\varepsilon$ should be checked for resistance to shear buckling. For the I-profile the web height is 1400 mm and the thickness of the web is 50 mm. The distance between the load points are 6500 mm, and is assumed so long that the web can be characterized as unstiffened.

η is a constant which is 1.2 according to NS-EN 1993-1-5, NA.5.1(2). ε is defined as $\sqrt{\frac{235}{f_y}}$ where f_y is the steel yield stress.

$$\frac{h_w}{t} = \frac{1400}{50} = 28 \quad \leq \quad \frac{72}{\eta}\varepsilon = \frac{72}{1.2}\cdot\sqrt{\frac{235}{420}} = 45$$

Shear buckling of the I-beam will not occur, due to the thickness of the web.

11.8. LOCAL PLATE BUCKLING CHECK

The result of the calculation of capacity toward local plate buckling is given in Table 52. The critical load is found in the vertical position. As a result of the eccentricity of the center of gravity of the module, the design load in terms of local plate buckling is 582 kN. The magnitude of this load is equal for both load combinations 2)a) and 2)b) in the vertical position.

TABLE 52: RESULTS OF LOCAL PLATE BUCKLING CHECK

Design load	582	kN
Design capacity	28382	kN
Utilization	2 %	

The result shows that the web of the I-profiles has more than sufficient capacity.

11.9. COLUMN BUCKLING CHECK

A summary of the results is given in Table 53. Explanations to the symbols in Table 53 are given in Table 54.

TABLE 53: RESULTS OF COLUMN BUCKLING CHECK FOR LOAD COMBINATION 2)b) VERTICAL POSITION

Load comb:	2		Load comb:	2	
Buckling about strong axis			Buckling about weak axis		
N_{Ed}	3929	kN	N_{Ed}	3929	kN
$M_{y1,Ed}$	2730	kNm	$M_{z1,Ed}$	490	kNm
$M_{y2,Ed}$	-497	kNm	$M_{z2,Ed}$	-223	kNm
L_k	6500	mm	L_k	6500	mm
I_1	50 871	10^6 mm^4	I_2	3 530	10^6mm^4
Utilization	15 %		Utilization	25 %	

TABLE 54: EXPLANATIONS TO SYMBOLS

N_{Ed}	Design normal force
$M_{y1,Ed}$	Design moment about strong axis
$M_{y2,Ed}$	Design moment about weak axis
L_k	Buckling length
I_1	2nd moment of area about strong axis
I_2	2nd moment of are about weak axis

PART 3: CONCLUSION AND FURTHER WORK

CONCLUSIONS

The conclusions are summarized in the following list.

- From the concepts evaluated in the report, the superior solution is deemed to be a plane frame on top of which the topside modules are mounted by welds.
- Structural analysis of the frame results in largely acceptable stresses. The frame has sufficient cross sectional capacity toward in both the horizontal and the vertical position. The trunnions which constitute the lifting points have acceptable capacity. The exceptions are local stress concentrations which should be mitigated by rounding off sharp corners, e.g. by attaching welded plates to the corners.
- The resulting horizontal rope force components due to the eccentricity of the center of gravity of the system in the vertical position are deemed unacceptable. There are no suggested solutions to this problem. Consequently, the concept of the turning frame is deemed unfeasible unless this problem is solved.

FURTHER WORK

It is advised that in any further work, the following issues should be addressed.

- A solution to the issue concerning the unacceptable horizontal rope force components in the vertical position must be found.
- The capacity of the topside modules toward the 180° rotation should be verified, as the modules are not originally designed for this situation and there should be very low risk of damage to the modules.
- The structural analysis of the frame is yet incomplete, and should be revised and extended by a fatigue assessment and additional analyses.
- There is significant excess capacity in the design of the frame in many regions. In order to reduce weight and costs, the design should be optimized to utilize material more efficiently.
- A comprehensive economic assessment should be conducted in order to determine whether the turning frame is economically feasible.
- Friction between the ropes and the trunnions should be investigated and clarified, and the current solution should be evaluated.
- A detailed user’s manual should be prepared for the staff and crane operator to follow, as the lifting operation is rather complex. Substantial training and education of staff should be undertaken.
- An inspection routine and maintenance program should be prepared for the frame.

BIBLIOGRAPHY

Cross, N., 2000. *Engineering Design Methods.* 1st ed. s.l.:John Wiley & Sons Ltd.

Dassault Systèmes Simulia Corp., 2013. *Abaqus Analysis User's Manual*, s.l.: s.n.

Dawson Group Ltd, 2013. *Heavy Lift Polyester Round Slings.* [Online]
Available at: http://www.dawson-group.com/dawsongroup/Round-Lifting-Slings/heavy-lift-polyester-round-slings.htm
[Accessed 28 May 2013].

KoneCranes, 2013. *Goliath Gantry Cranes.* [Online]
Available at: http://www.konecranes.com/equipment/shipyard-cranes/goliath-gantry-crane
[Accessed 02 June 2013].

MatWeb, 2013. *ThyssenKrupp PAS 420 Structural Steel for Cold Forming.* [Online]
Available at: http://www.matweb.com/search/DataSheet.aspx?MatGUID=0bb90e2770864e33891b60a26b4f5118
[Accessed 14 May 2013].

NS-EN 1991-1-1, 2008. *NS-EN 1991-1-1.* s.l.:Standard Norge.

NS-EN 1993-1-1, 2005. *NS-EN 1993-1-1.* s.l.:Standard Norge.

NS-EN 1993-1-5, 2006. *NS-EN 1993-1-5.* s.l.:Standard Norge.

NS-EN 1993-1-8, 2005. *NS-EN 1993-1-8.* s.l.:Standard Norge.

Rautaruukki Corporation, 2013. *Ruukki.* [Online]
Available at: www.ruukki.com
[Accessed 18 April 2013].

APPENDICES

The contents of the appendices are not numbered with page numbers.

CONTENTS OF APPENDICES

Appendix A: Verification of FE model

Visualization plots with values from the analysis of Case A to be verified are given in the following.

Results from horizontal position

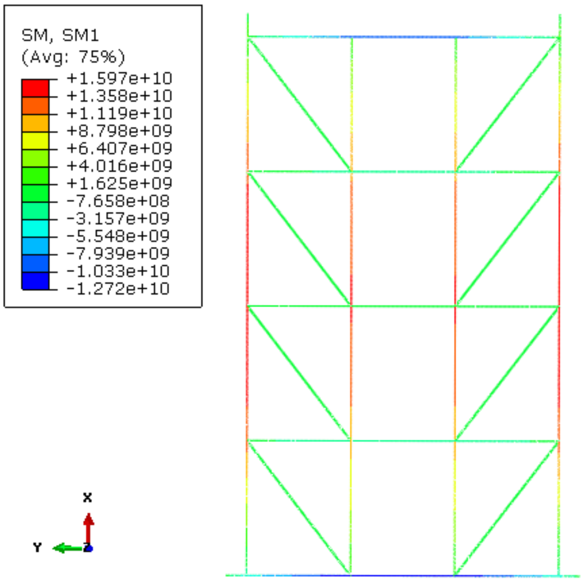

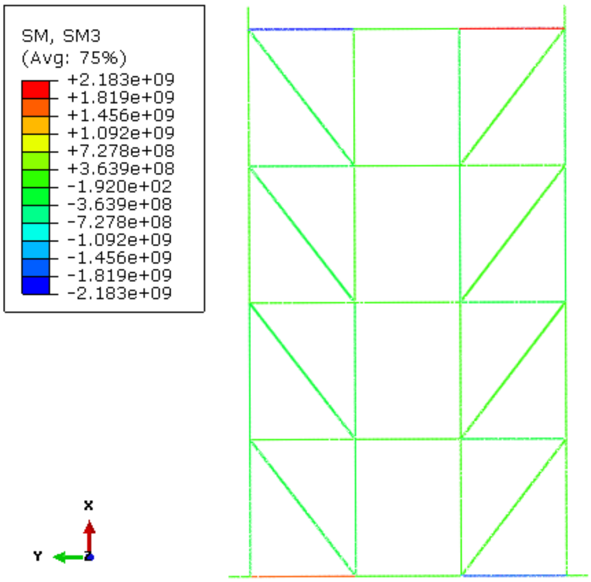

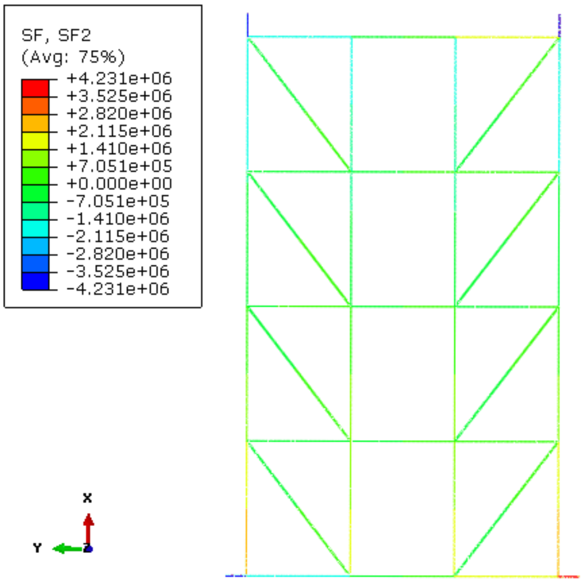

RESULTS FROM VERTICAL POSITION

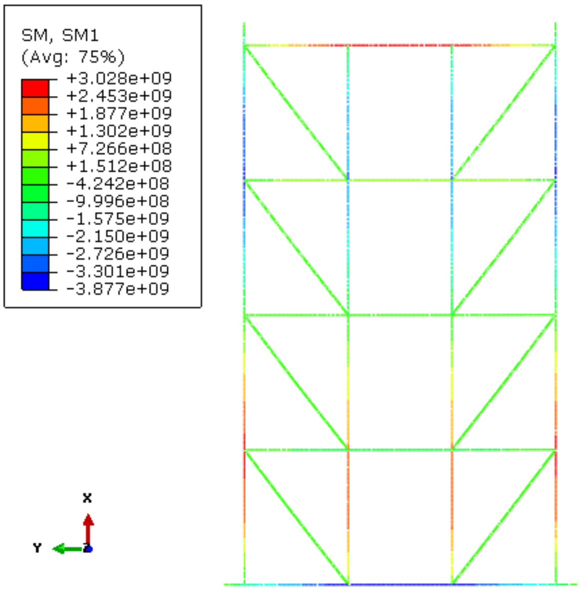

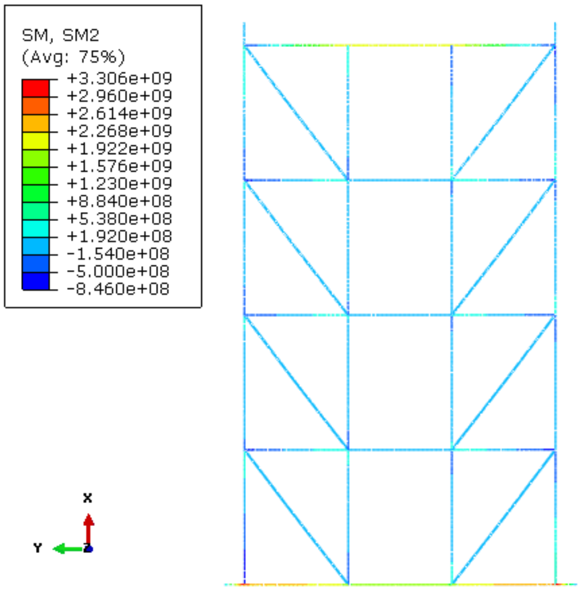

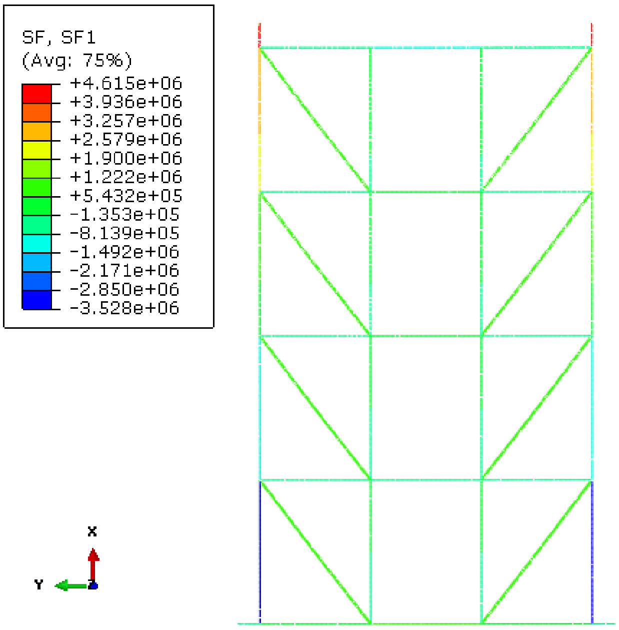

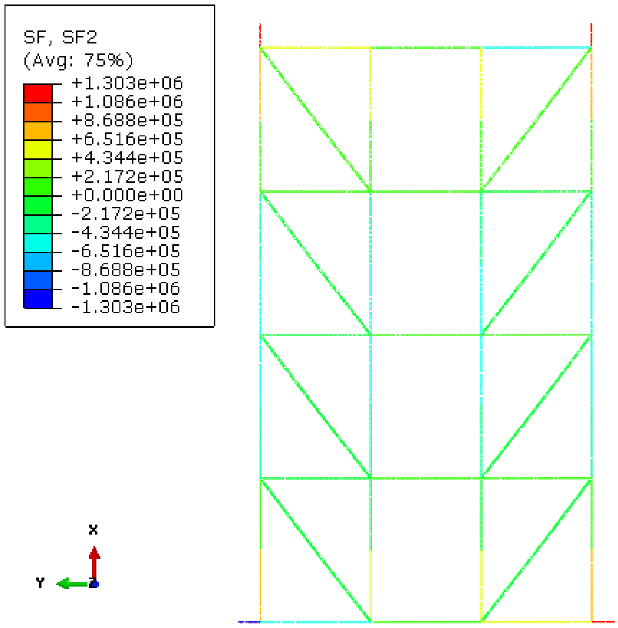

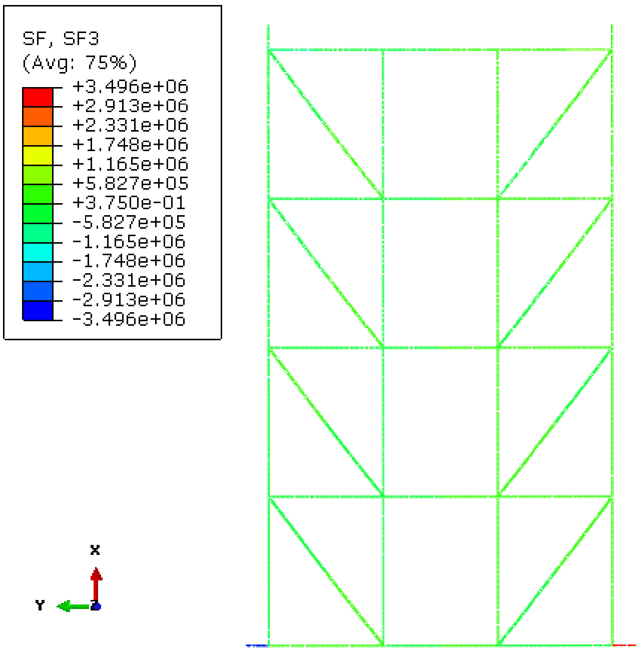

APPENDIX B: 1D FEA RESULTS OF CASE A AND CASE B

These analysis are for load combinations 1) and 2)b).

HORIZONTAL POSITION

CASE A

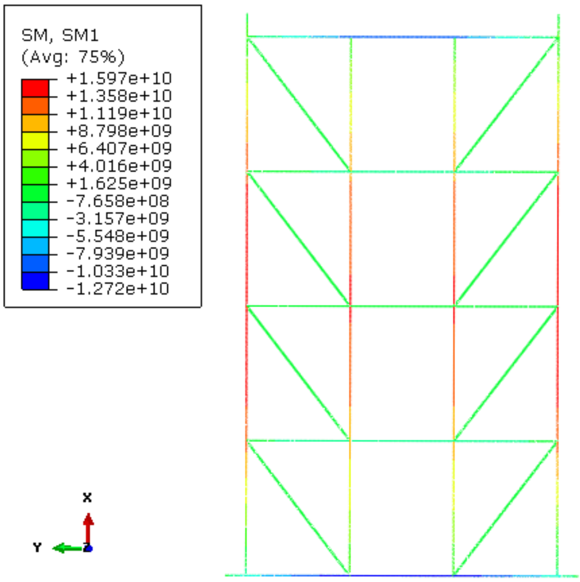

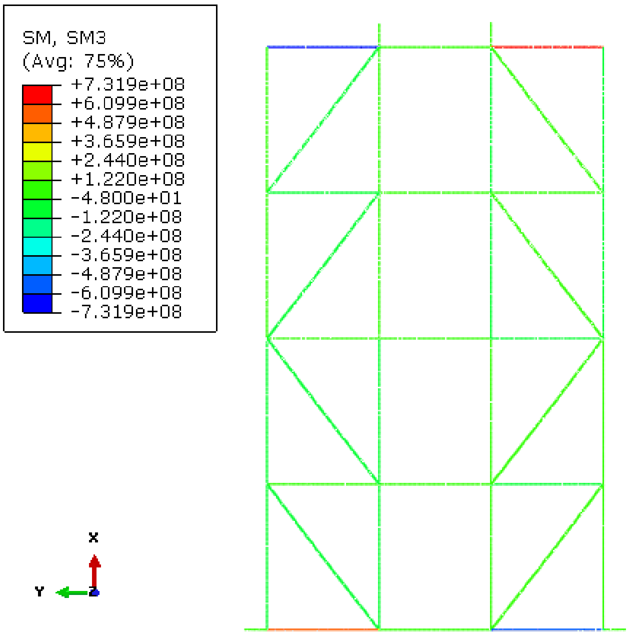

CASE B

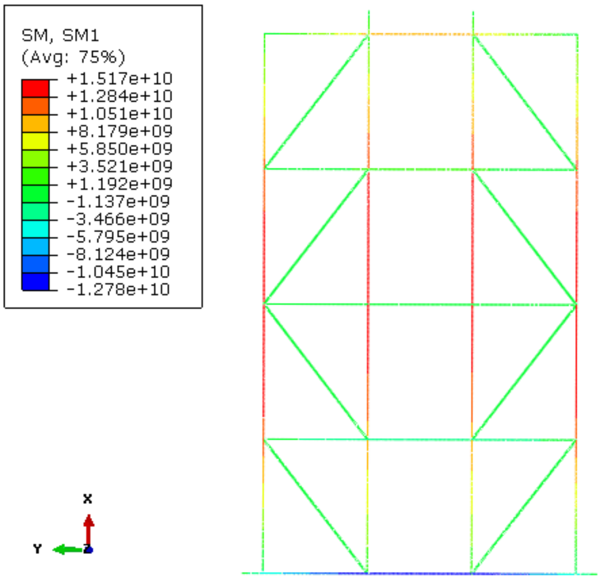

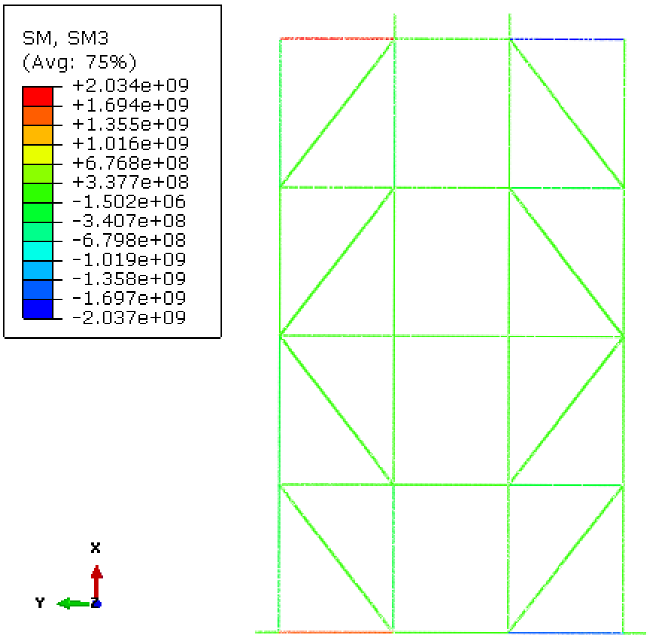

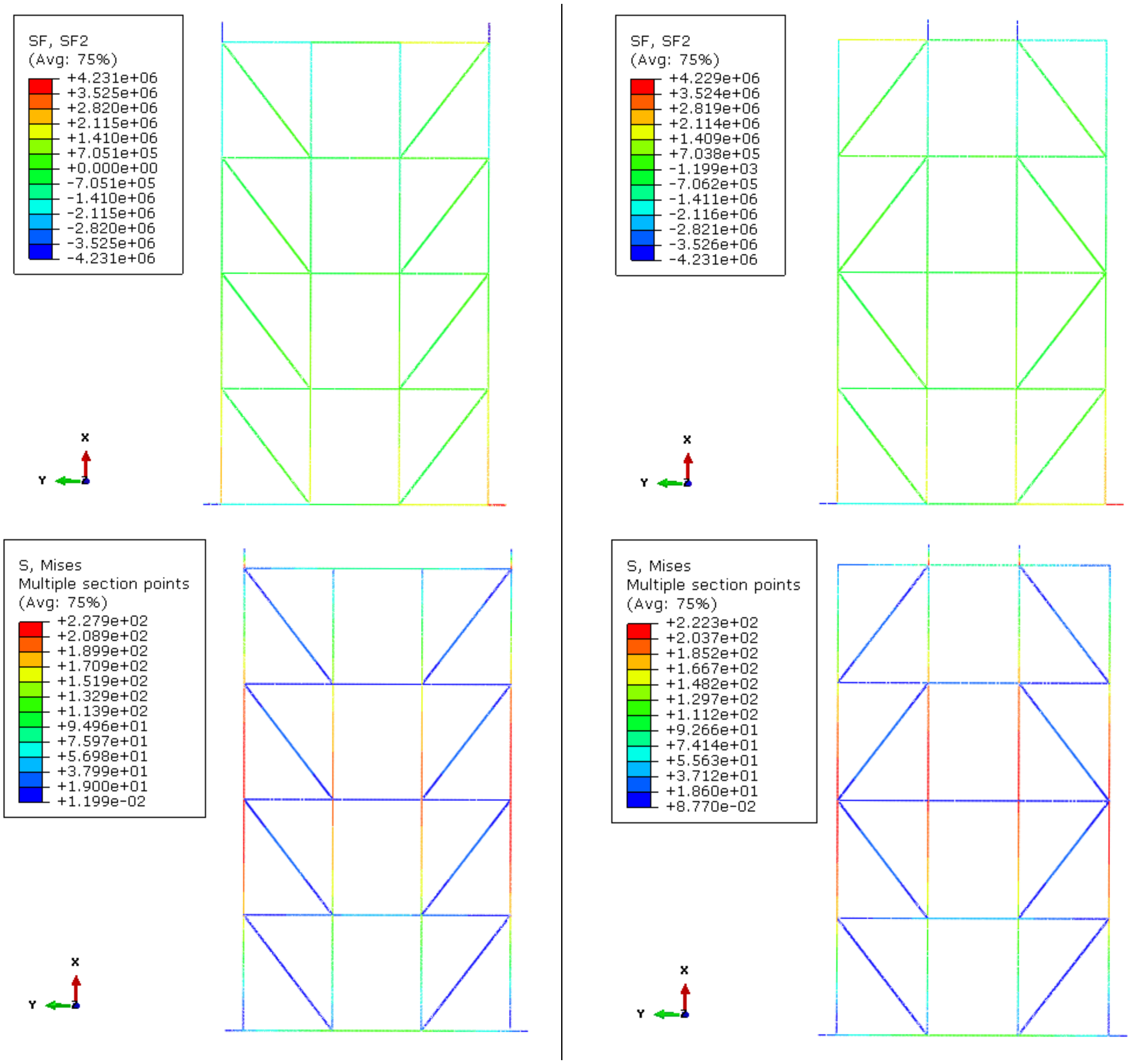
SF, SF2
(Avg: 75%)
+4.231e+06
+3.525e+06
+2.820e+06
+2.115e+06
+1.410e+06
+7.051e+05
+0.000e+00
-7.051e+05
-1.410e+06
-2.115e+06
-2.820e+06
-3.525e+06
-4.231e+06
X
Y
SF, SF2
(Avg: 75%)
+4.229e+06
+3.524e+06
+2.819e+06
+2.114e+06
+1.409e+06
+7.038e+05
-1.199e+03
-7.062e+05
-1.411e+06
-2.116e+06
-2.821e+06
-3.526e+06
-4.231e+06
X
Y
S, Mises
Multiple section points
(Avg: 75%)
+2.279e+02
+2.089e+02
+1.899e+02
+1.709e+02
+1.519e+02
+1.329e+02
+1.139e+02
+9.496e+01
+7.597e+01
+5.698e+01
+3.799e+01
+1.900e+01
+1.199e-02
X
Y
S, Mises
Multiple section points
(Avg: 75%)
+2.223e+02
+2.037e+02
+1.852e+02
+1.667e+02
+1.482e+02
+1.297e+02
+1.112e+02
+9.266e+01
+7.414e+01
+5.563e+01
+3.712e+01
+1.860e+01
+8.770e-02
X
Y

VERTICAL POSITION

CASE A

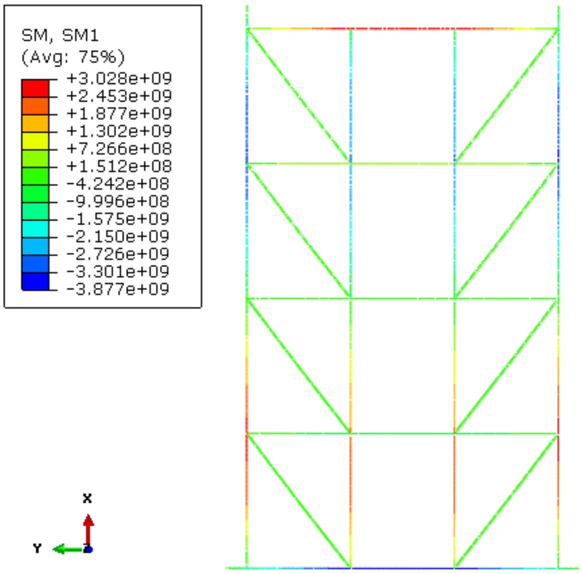

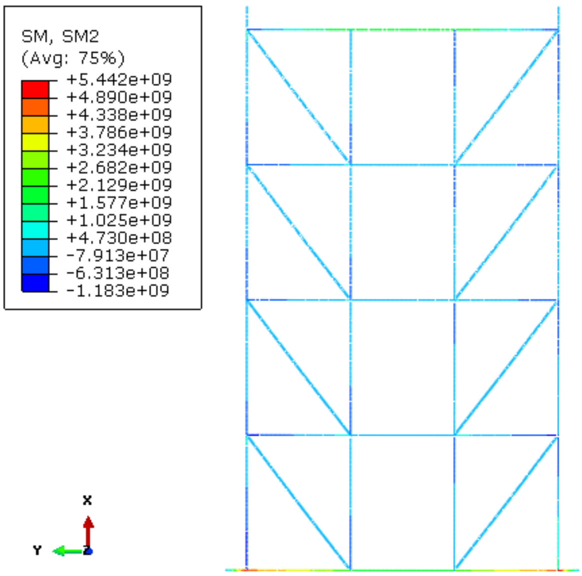

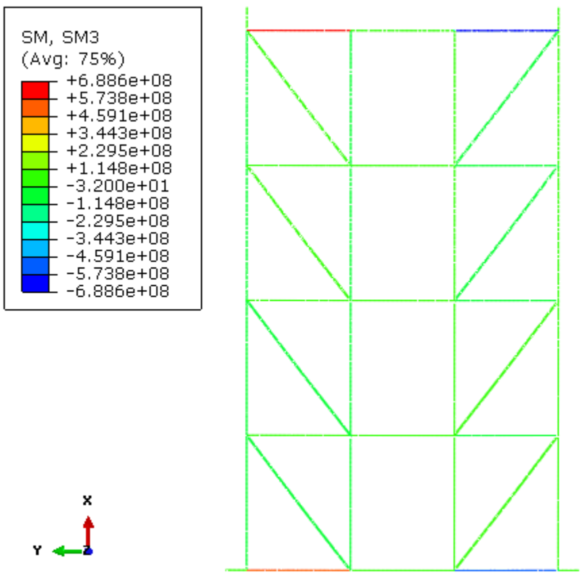

CASE B

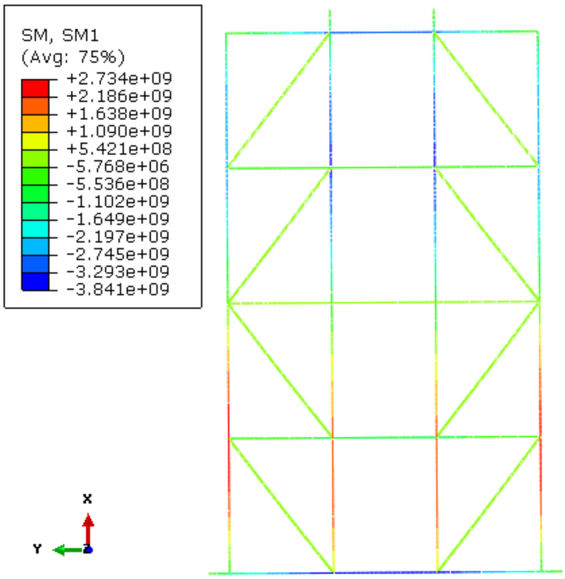

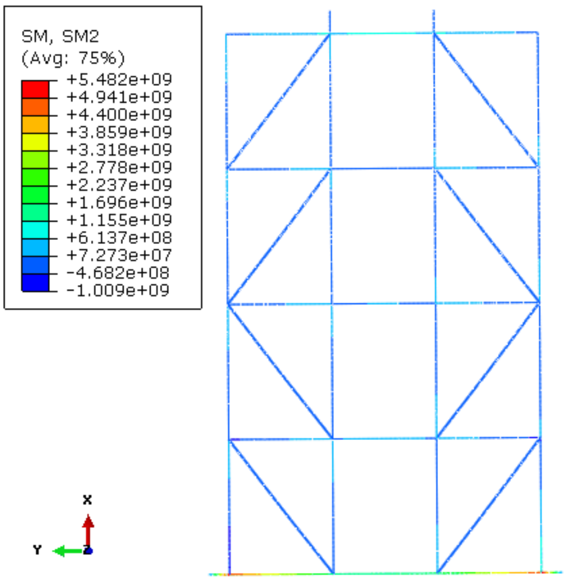

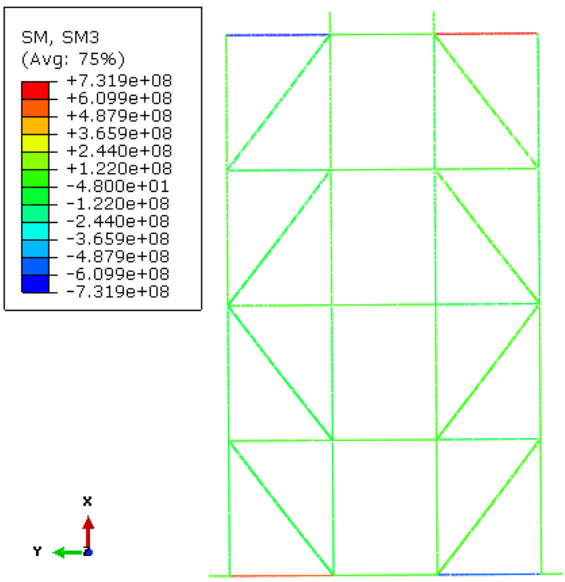

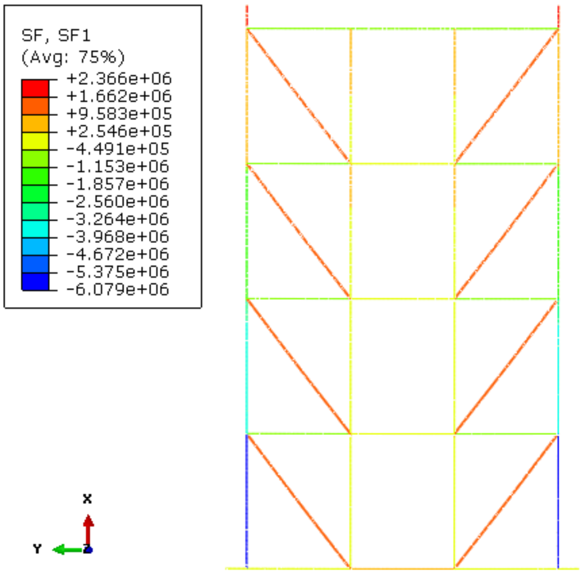
SF, SF1
(Avg: 75%)
+2.366e+06
+1.662e+06
+9.583e+05
+2.546e+05
-4.491e+05
-1.153e+06
-1.857e+06
-2.560e+06
-3.264e+06
-3.968e+06
-4.672e+06
-5.375e+06
-6.079e+06
X
Y

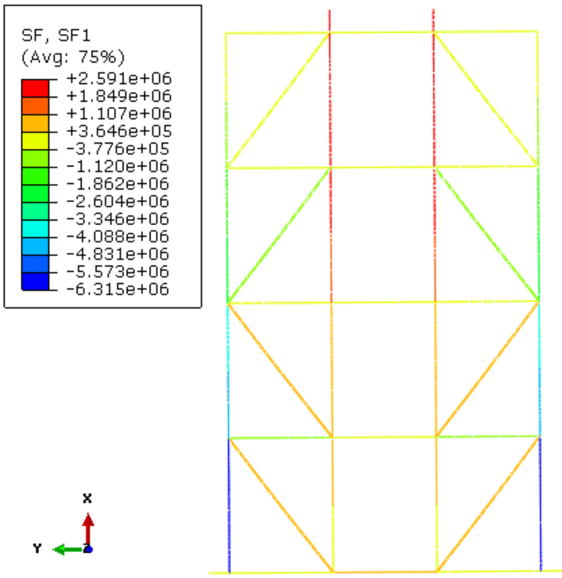
SF, SF1
(Avg: 75%)
+2.591e+06
+1.849e+06
+1.107e+06
+3.646e+05
-3.776e+05
-1.120e+06
-1.862e+06
-2.604e+06
-3.346e+06
-4.088e+06
-4.831e+06
-5.573e+06
-6.315e+06
X
Y

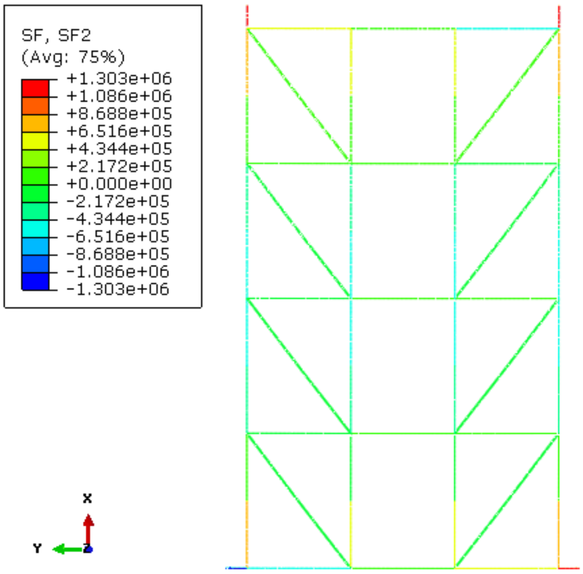
SF, SF2
(Avg: 75%)
+1.303e+06
+1.086e+06
+8.688e+05
+6.516e+05
+4.344e+05
+2.172e+05
+0.000e+00
-2.172e+05
-4.344e+05
-6.516e+05
-8.688e+05
-1.086e+06
-1.303e+06
X
Y

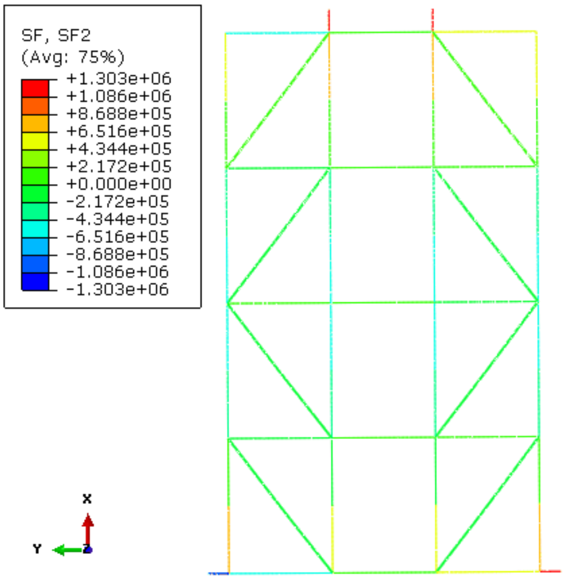
SF, SF2
(Avg: 75%)
+1.303e+06
+1.086e+06
+8.688e+05
+6.516e+05
+4.344e+05
+2.172e+05
+0.000e+00
-2.172e+05
-4.344e+05
-6.516e+05
-8.688e+05
-1.086e+06
-1.303e+06
X
Y

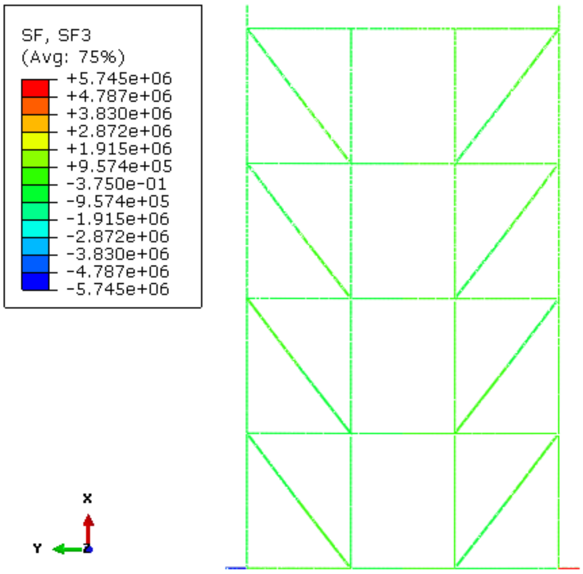
SF, SF3
(Avg: 75%)
+5.745e+06
+4.787e+06
+3.830e+06
+2.872e+06
+1.915e+06
+9.574e+05
-3.750e-01
-9.574e+05
-1.915e+06
-2.872e+06
-3.830e+06
-4.787e+06
-5.745e+06
X
Y

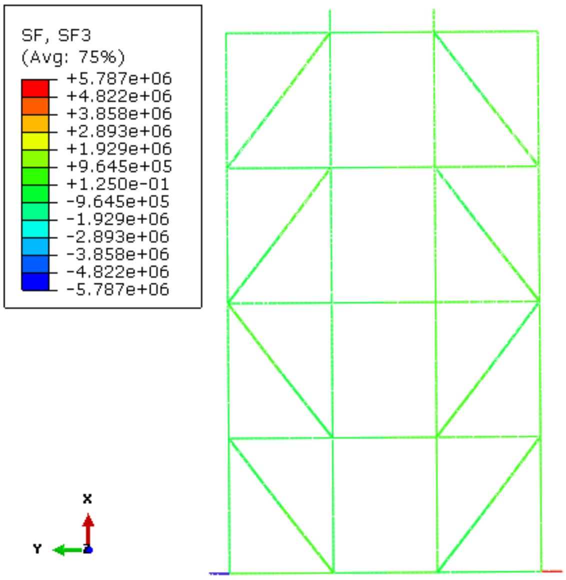
SF, SF3
(Avg: 75%)
+5.787e+06
+4.822e+06
+3.858e+06
+2.893e+06
+1.929e+06
+9.645e+05
+1.250e-01
-9.645e+05
-1.929e+06
-2.893e+06
-3.858e+06
-4.822e+06
-5.787e+06
X
Y

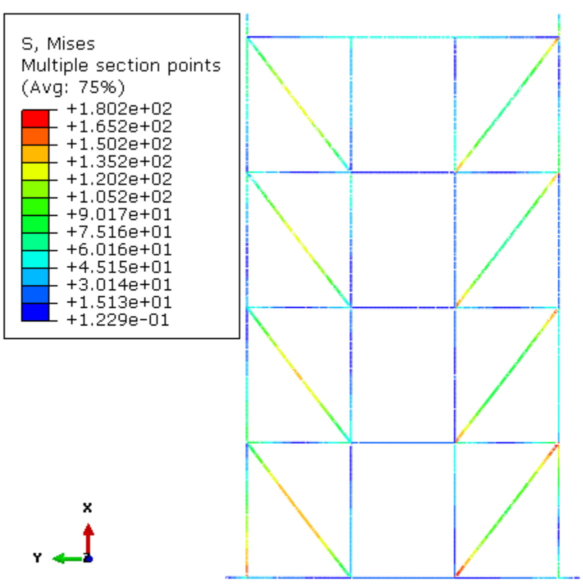
S, Mises
Multiple section points
(Avg: 75%)
+1.802e+02
+1.652e+02
+1.502e+02
+1.352e+02
+1.202e+02
+1.052e+02
+9.017e+01
+7.516e+01
+6.016e+01
+4.515e+01
+3.014e+01
+1.513e+01
+1.229e-01
X
Y

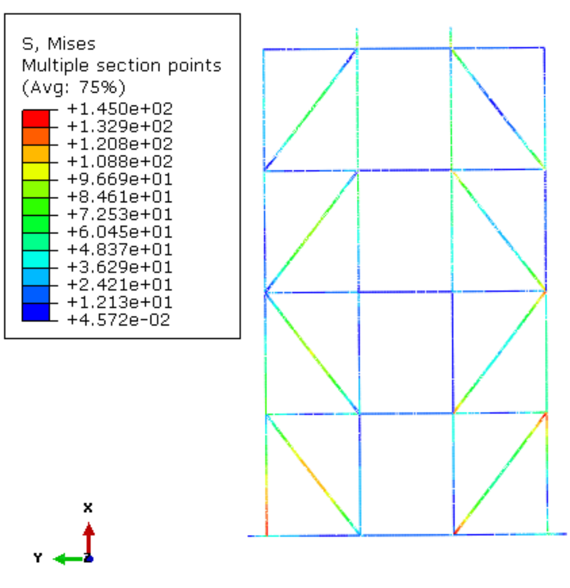
S, Mises
Multiple section points
(Avg: 75%)
+1.450e+02
+1.329e+02
+1.208e+02
+1.088e+02
+9.669e+01
+8.461e+01
+7.253e+01
+6.045e+01
+4.837e+01
+3.629e+01
+2.421e+01
+1.213e+01
+4.572e-02
X
Y

APPENDIX C: PEAK STRESS IN SHELL MODEL OF FRAME

The support forces for the shell model are given in Table 1, Table 2 and Table 3. The sum of the support forces is different in the shell model from the 1D FE model. The reasons for this are summarized in the following list.

- The diagonals are omitted from the shell model
- The stiffener plates in the front and rear beam are not included in the 1D FE model and the Excel calculations
- The weight of the shear plates are not included in the 1D FE model or the Excel calculations

The support forces are referred to the global coordinate system. Note that in the vertical position, the global z-direction is equivalent to the x-direction in the local coordinate system of the frame. Conversely, the global x-axis is in the direction of the frame local z-axis. The Abaqus model is not rotated as the vertical analysis is conducted. Only the direction of loads and boundary conditions are modified. Thus, the coordinate system present in the following illustrations is the local coordinate system of the frame, in which the x-axis is in the length direction of the frame.

TABLE 1: SUPPORT FORCES F_z IN HORIZONTAL POSITION [kN]

Load combination: 1) Horizontal position

	1D model		Shell model	
	Left	Right	Left	Right
Front	3880	3880	3897	3897
Rear	4231	4231	4253	4253
Sum	8112	8112	8150	8150
Error			0.47 %	0.47 %

TABLE 2: SUPPORT FORCES F_x IN VERTICAL POSITION [kN]

Load combination: 2)b) Vertical position

	1D model		Shell model	
	Left	Right	Left	Right
Front	1303	1303	1308	1308
Rear	-1303	-1303	-1308	-1308
Sum	0	0	0	0
Error			0.38 %	0.38 %

TABLE 3: SUPPORT FORCES F_z IN VERTICAL POSITION [kN]

Load combination: 2)b) Vertical position

	1D model		Shell model	
	Left	Right	Left	Right
Front	2324	2324	2564	2564
Rear	5788	5788	5585	5585
Sum	8112	8112	8149	8149
Error			0.46 %	0.46 %

In the following, stress plots of the frame are presented. The expressions from the Abaqus plots are explained in Table 4.

TABLE 4: EXPRESSIONS AND UNITS IN ABAQUS

Common reference	Abaqus reference
Principal stress in x-direction	S11
Principal stress in y-direction	S22
Principal stress in z-direction	S33

Horizontal position

S11 is interesting because it reflects the axial stresses in the longitudinal beams due to the bending moment. S11 does not show the same stress concentrations as von Mises stress does in the horizontal position.

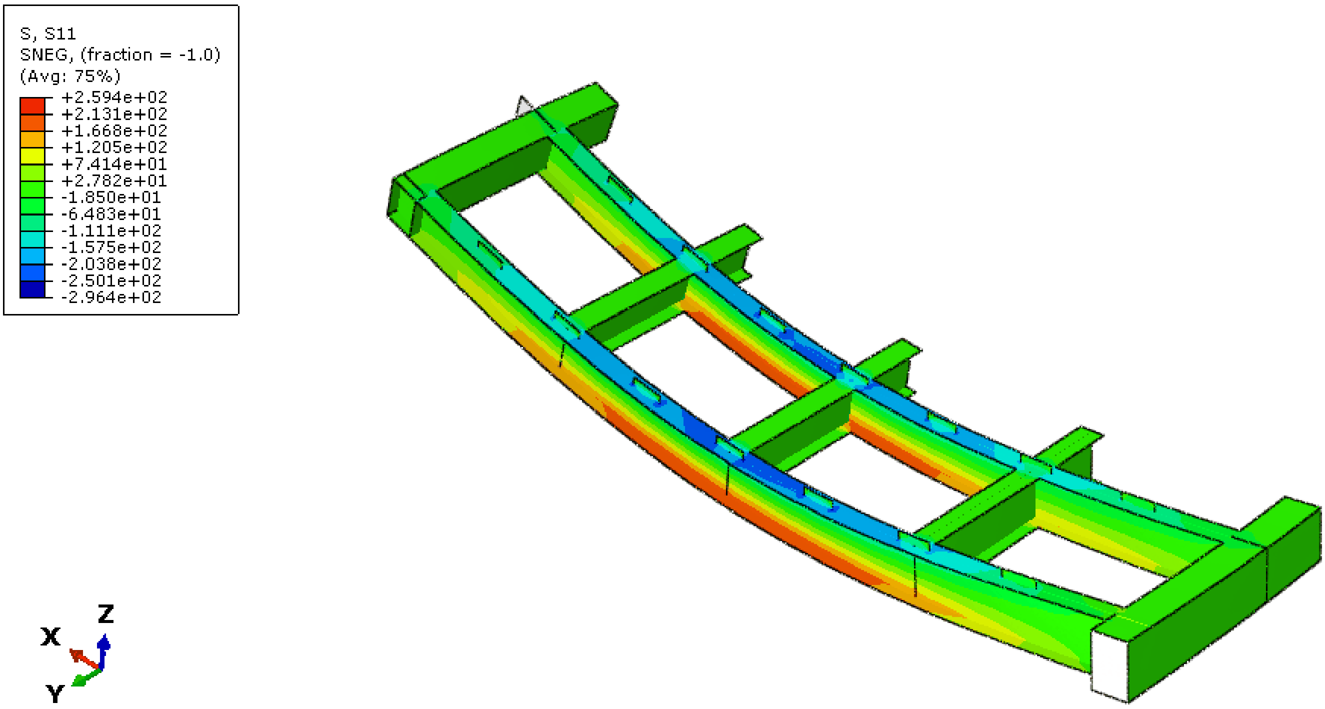

VERTICAL POSITION

In the vertical position, there is a severe stress concentration in the corner between the longitudinal beam and the rear beam. This stress concentration should be mitigated by attaching a triangular plate of same thickness as the flanges of the beams. The plate relieves the stress concentration by rounding off the corner and improving stress flow.

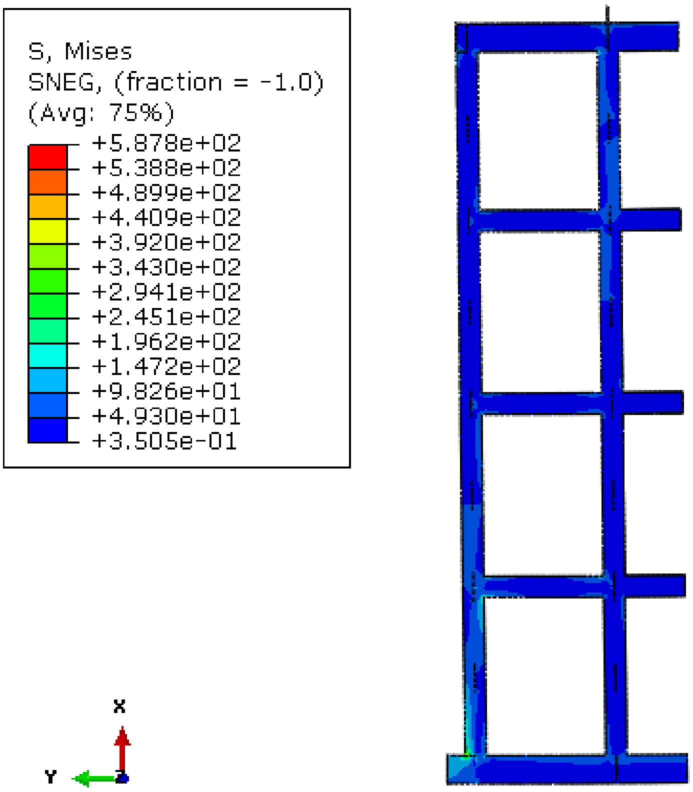

The stress concentration above is reflected in the plot of S11, i.e. axial stress.As is seen from the below figure, the maximum compressive stress (i.e. negative sign) at -565.7 MPa, appears in the same region.It is seen that maximum tensile stress at 389.8 MPa also appears in the stress concentration.

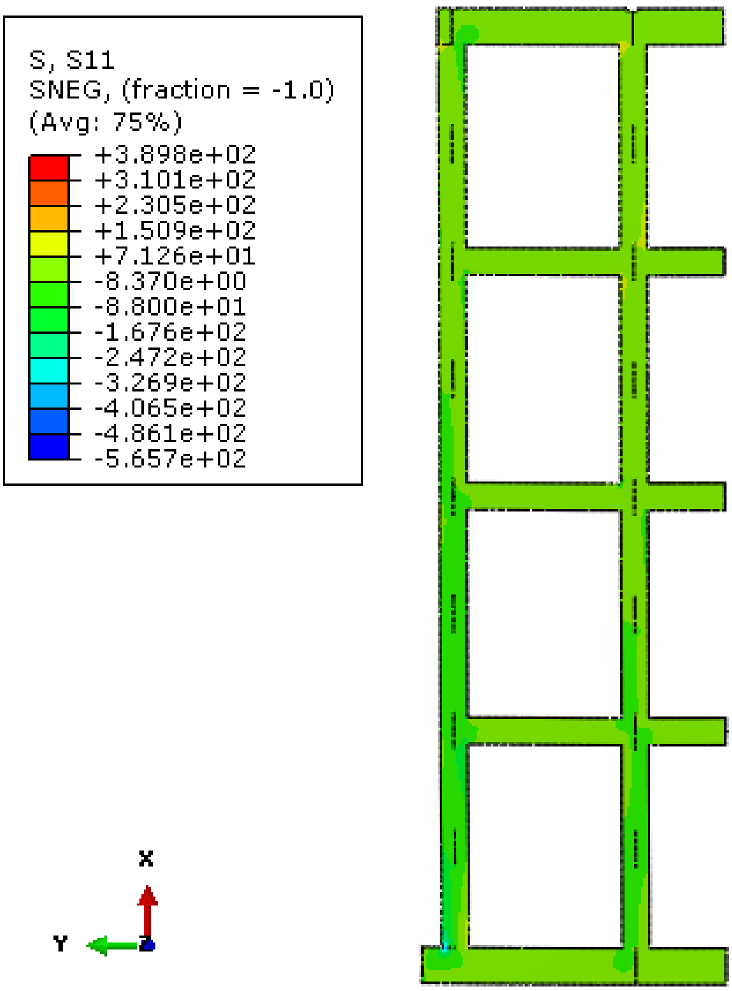
S, S11
SNEG, (fraction = -1.0)
(Avg: 75%)
+3.898e+02
+3.101e+02
+2.305e+02
+1.509e+02
+7.126e+01
-8.370e+00
-8.800e+01
-1.676e+02
-2.472e+02
-3.269e+02
-4.065e+02
-4.861e+02
-5.657e+02
X
Y
Z

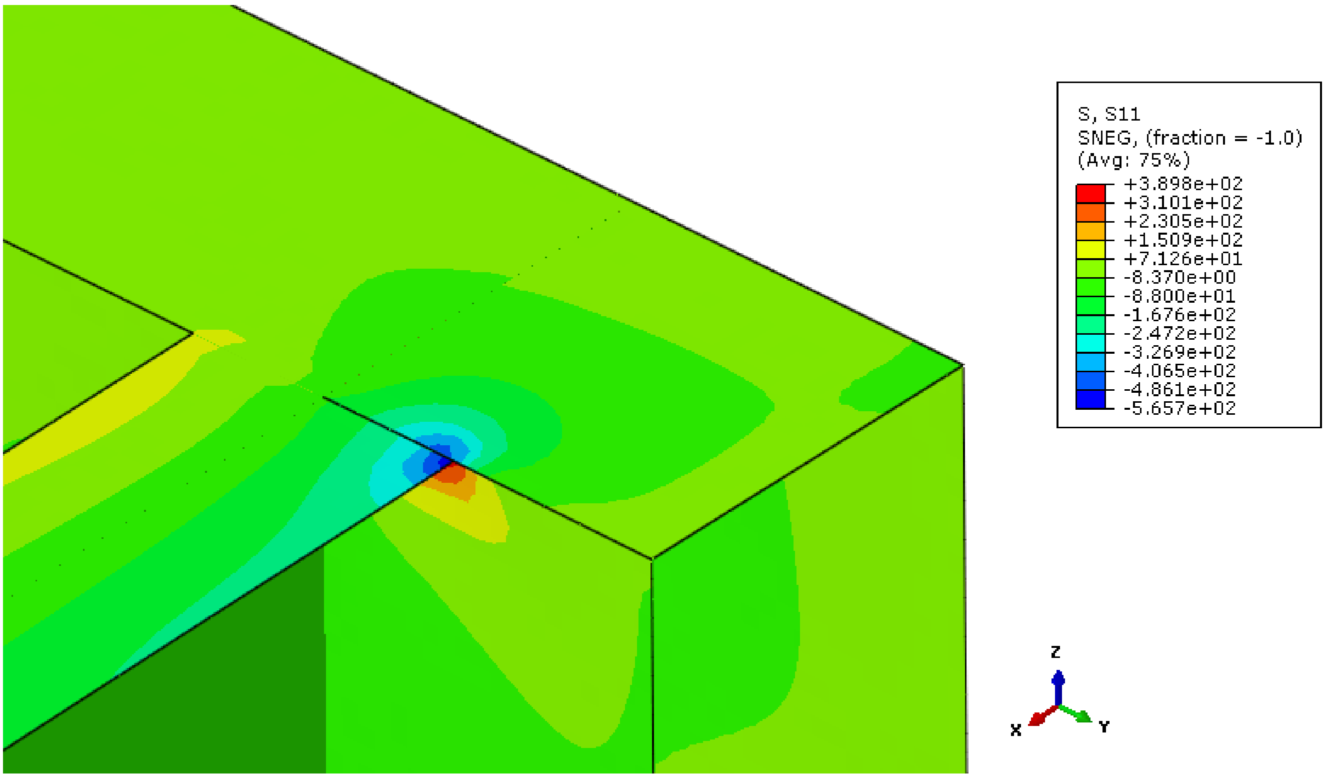
S, S11
SNEG, (fraction = -1.0)
(Avg: 75%)
+3.898e+02
+3.101e+02
+2.305e+02
+1.509e+02
+7.126e+01
-8.370e+00
-8.800e+01
-1.676e+02
-2.472e+02
-3.269e+02
-4.065e+02
-4.861e+02
-5.657e+02
Z
X
Y

APPENDIX D: TECHNICAL DRAWINGS

Technical drawings of the Case B frame is given in the following. The diagonals are not included in the drawings.

Overview of structure

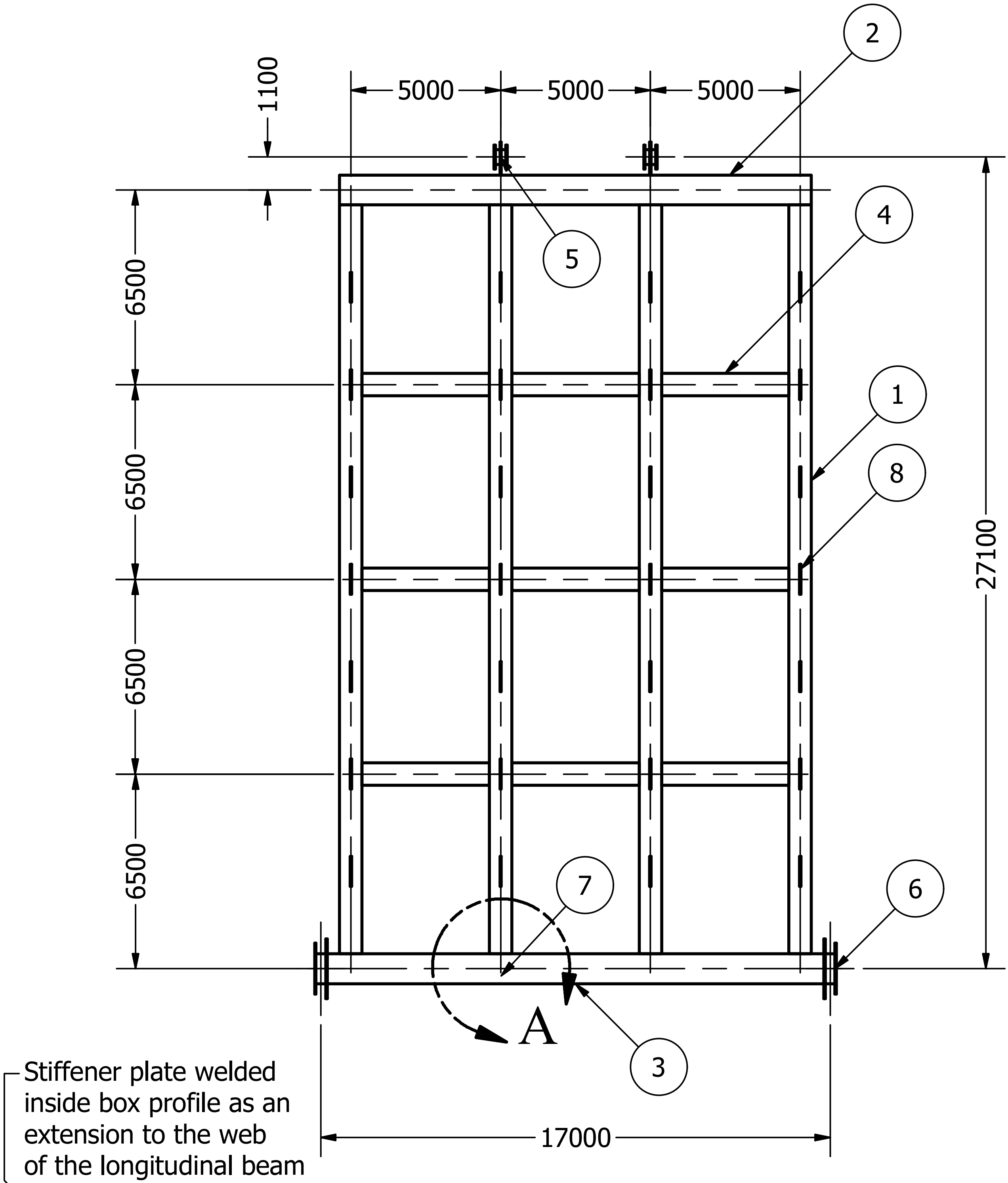

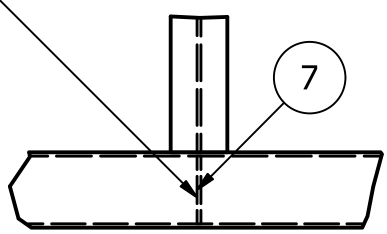

DETAIL A
STIFFENER PLATE

PARTS LIST		
ITEM	QTY	DESCRIPTION
1	4	Longitudinal
2	1	Front
3	1	Rear
4	9	Transversal
5	2	Front trunnion
6	2	Rear trunnion
7	8	Stiffener plate
8	28	Shear plate

PRODUCED BY AN AUTODESK EDUCATIONAL PRODUCT
PRODUCED BY AN AUTODESK EDUCATIONAL PRODUCT
PRODUCED BY AN AUTODESK EDUCATIONAL PRODUCT

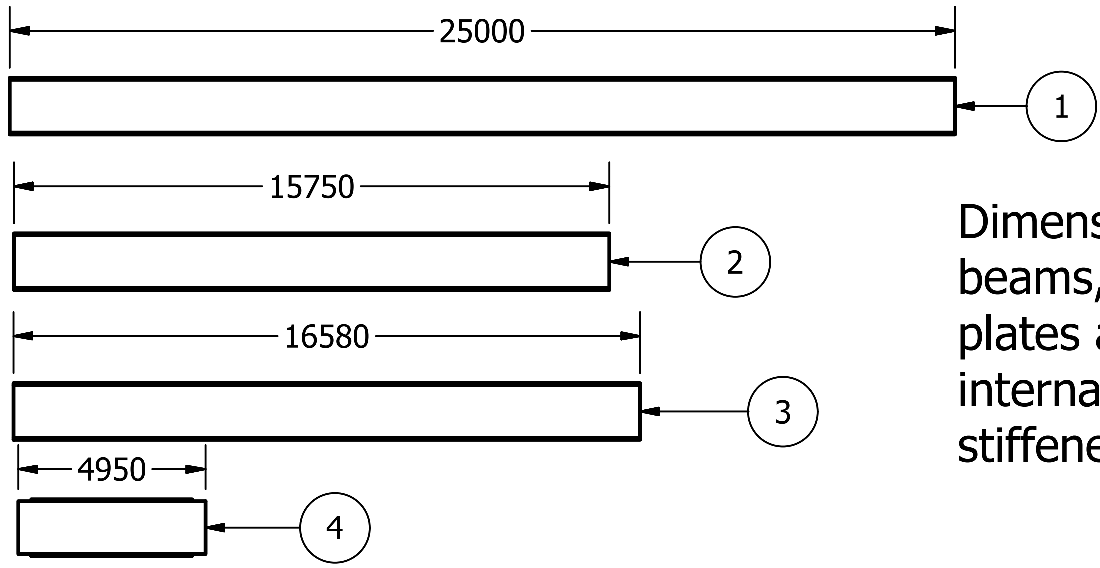

Dimensions of beams, shear plates and internal stiffener plates

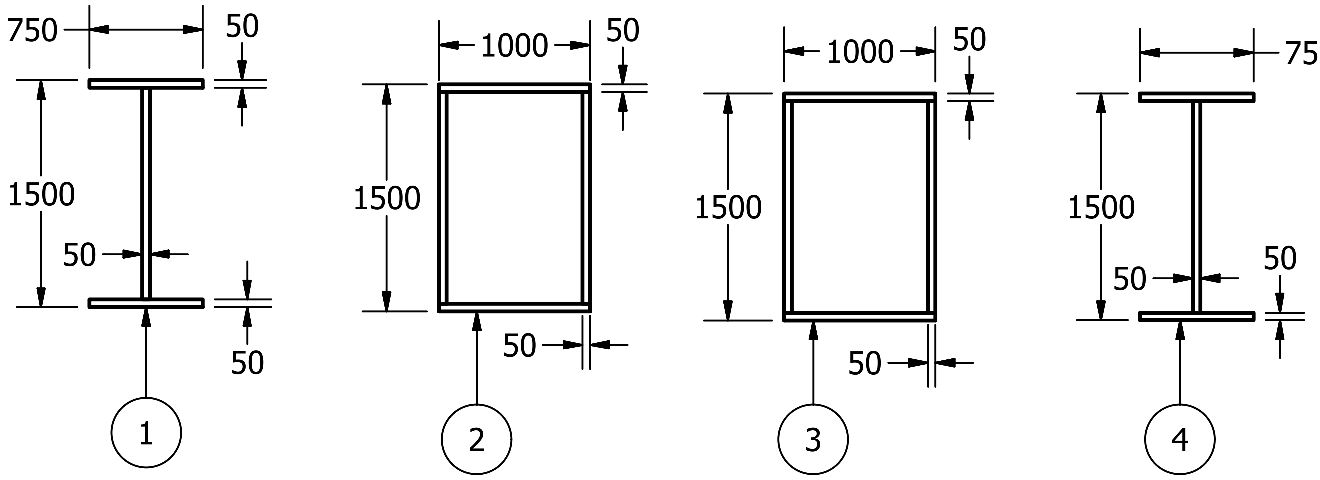

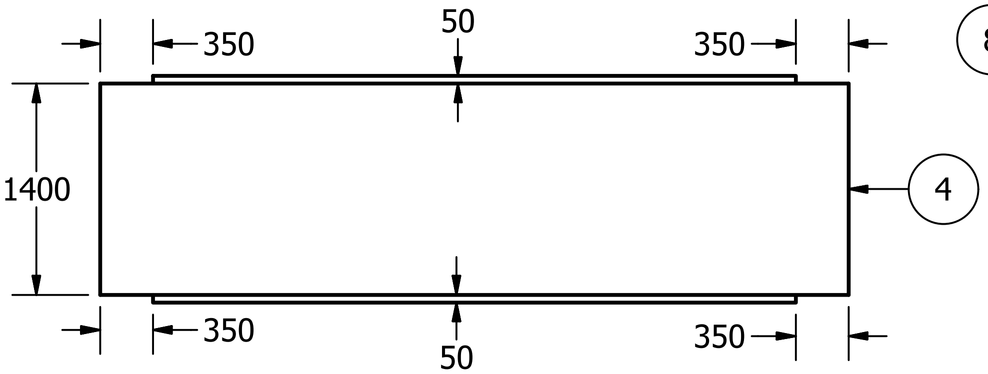

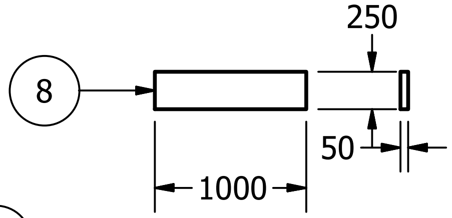

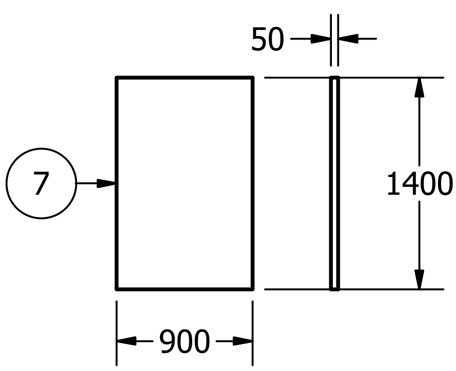

PARTS LIST		
ITEM	QTY	DESCRIPTION
1	4	Longitudinal
2	1	Front
3	1	Rear
4	9	Transversal
5	2	Front trunnion
6	2	Rear trunnion
7	8	Stiffener plate
8	28	Shear plate

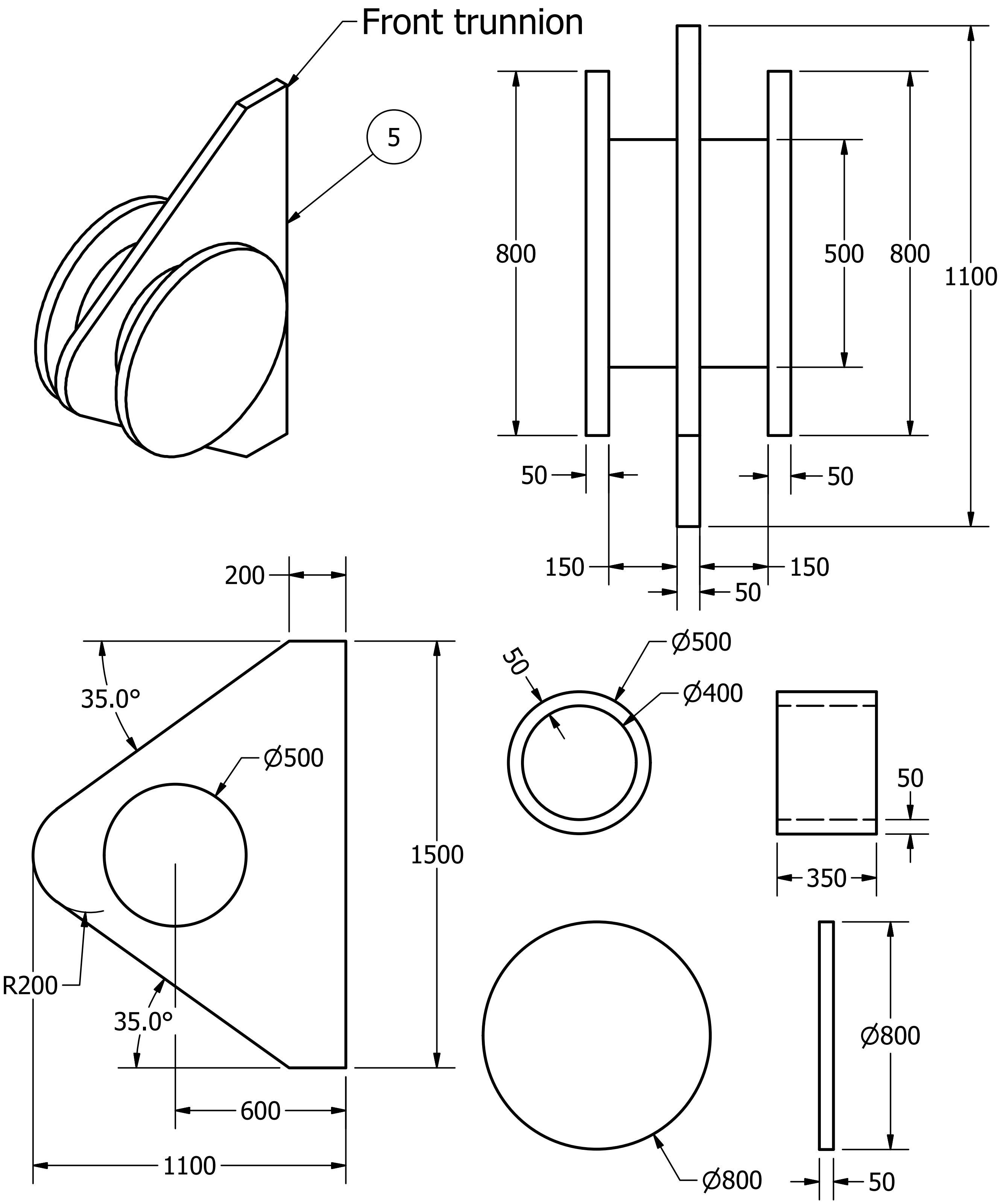

PARTS LIST		
ITEM	QTY	DESCRIPTION
1	4	Longitudinal
2	1	Front
3	1	Rear
4	9	Transversal
5	2	Front trunnion
6	2	Rear trunnion
7	8	Stiffener plate
8	28	Shear plate

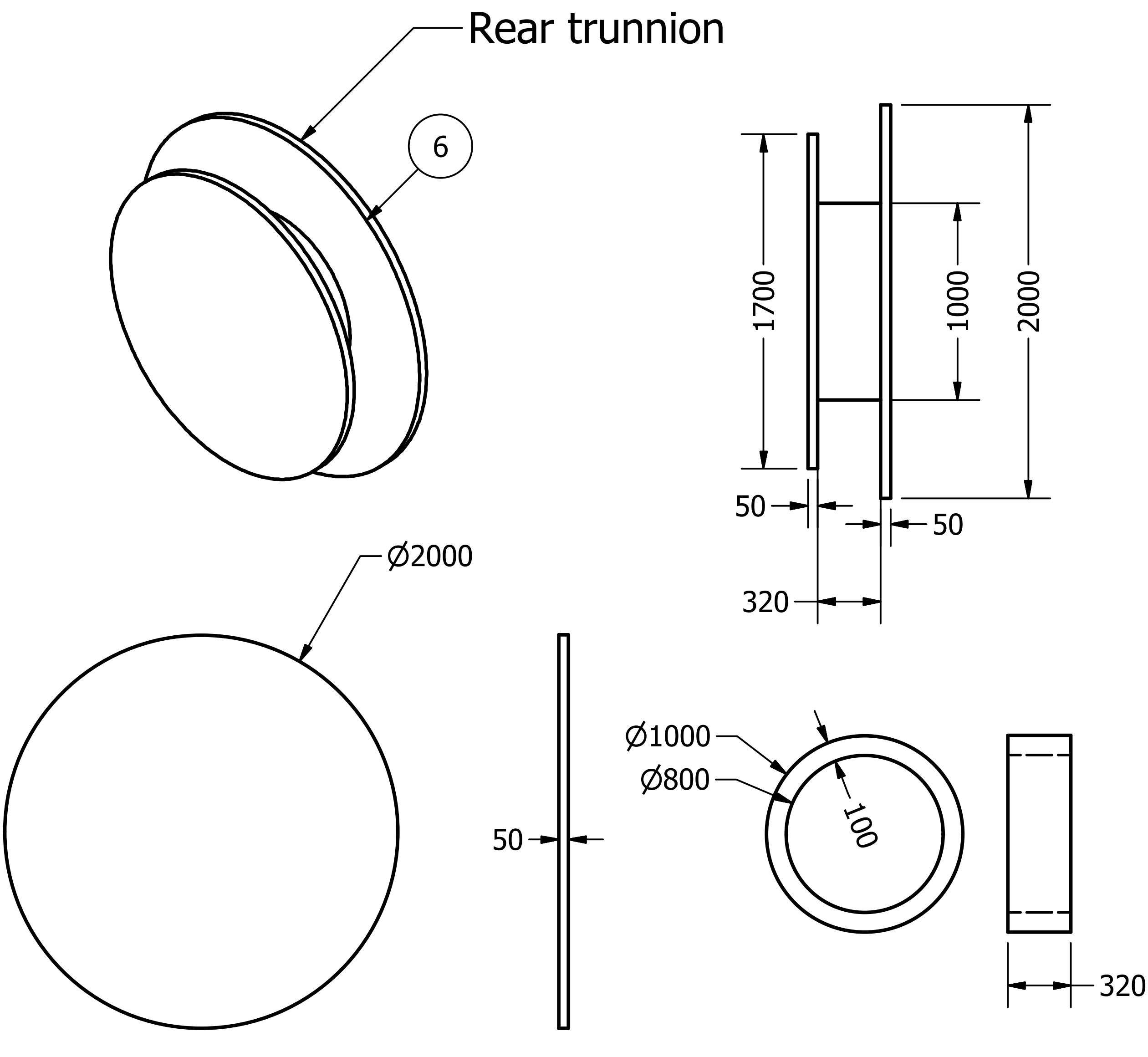

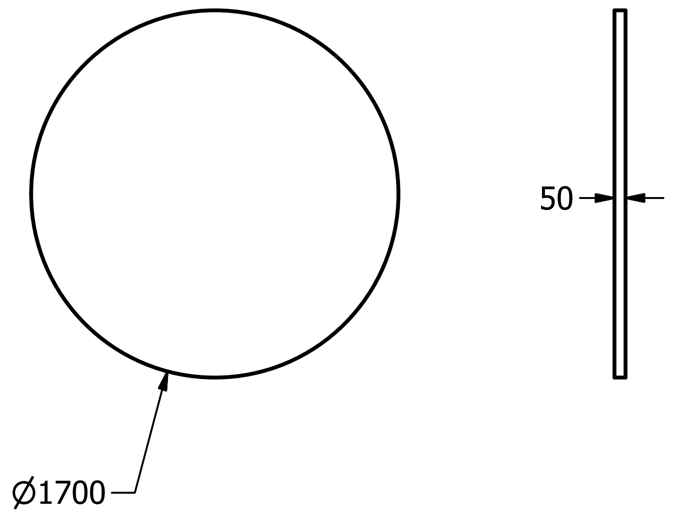

PARTS LIST

ITEM	QTY	DESCRIPTION
1	4	Longitudinal
2	1	Front
3	1	Rear
4	9	Transversal
5	2	Front trunnion
6	2	Rear trunnion
7	8	Stiffener plate
8	28	Shear plate

APPENDIX E: EXCEL CALCULATIONS

The complete spreadsheets of the MS Excel calculations are given in the following.

	A	B	C	D	E	F	G	H	I	J	K	L	M	N	O	P	Q	R	S	T
1	Excel calculation of horizontal position- Results & Comparison																			
2																				
3																				
4																				
5	Support load comparison																			
6																				
7		Excel			Abaqus			Focus			Excel			Abaqus			Focus			
8		Support loads			Support loads			Support loads			Live load			Live load			Live load			
9																				
10		A	G		A	G		A	G		A	G		A	G		A	G		
11	1	3891	3891		3880	3880		3881	3881		2824	2824		2824	2824		2824	2824		
12	9	4221	4221		4231	4231		4231	4231		3062	3062		3062	3062		3062	3062		
13	SUM	8112	8112		8112	8112		8112	8112		5886	5886		5886	5886		5886	5886		
14	Error				0.00 %	0.00 %		0.00 %	0.00 %					0.00 %	0.00 %		0.00 %	0.00 %		
15		Sum	16223								Sum	11772								
16																				
17																				
18		Excel			Abaqus			Focus												
19		Self weight			Self weight			Self weight												
20																				
21		A	G		A	G		A	G											
22		1067	1067		1057	1057		1057	1057											
23		1158	1158		1169	1169		1169	1169											
24		2226	2226		2226	2226		2226	2226											
25					0.00 %	0.00 %		0.00 %	0.00 %											
26		Sum	4451																	
27																				
28		Live load																		
29		Beam	A			C			E			G			Front			Rear		
30			Excel	Abaqus	Focus	Excel	Abaqus	Focus	Excel	Abaqus	Focus	Excel	Abaqus	Focus	Excel	Abaqus	Focus	Excel	Abaqus	Focus
31			13896	12464	12435	9519	10940	10980	9519	10940	10980	13896	12464	12435	6456	6384	6411	8968	9031	8952
32		Error		-10 %	-11 %		15 %	15 %		15 %	15 %		-10 %	-11 %		-1 %	-1 %		1 %	0 %
33					0.2 %			-0.4 %			-0.4 %			0.2 %			-0.4 %			0.9 %
34																				
35		Self weight																		
36		Beam	A			C			E			G			Front			Rear		
37			Excel	Abaqus	Focus	Excel	Abaqus	Focus	Excel	Abaqus	Focus	Excel	Abaqus	Focus	Excel	Abaqus	Focus	Excel	Abaqus	Focus
38			3897	3513	3497	2415	2945	2952	2415	2945	2952	3897	3513	3497	2710	2687	2687	3643	3690	3666
39		Error		-10 %	-10 %		22 %	22 %		22 %	22 %		-10 %	-10 %		-1 %	-1 %		1 %	1 %
40					0.4 %			-0.2 %			-0.2 %			0.4 %			0.0 %			0.6 %
41																				
42		Combined loads																		
43		Beam	A			C			E			G			Front			Rear		
44			Excel	Abaqus	Focus	Excel	Abaqus	Focus	Excel	Abaqus	Focus	Excel	Abaqus	Focus	Excel	Abaqus	Focus	Excel	Abaqus	Focus
45			17793	15976	15932.5	11934	13886	13932	11934	13886	13932	17793	15976	15932	9166	9071	9097	12611	12721	12619
46		Error		-10 %	-10 %		16 %	17 %		16 %	17 %		-10 %	-10 %		-1 %	-1 %		1 %	0 %
47					0.3 %			-0.3 %			-0.3 %			0.3 %			-0.3 %			0.8 %

	A	B	C	D	E	F	G	H	I	J	K	L	M	N	O	P	Q	R	S	T
48																				
49				**Insert the values to the solver you wish to compare with (do the same also for shear force in live load and selfweight)**																
50			Torsional moments [kNm]							Abaqus		Focus								
51			Live load			Self weight				Live load	Self weight	Live load	Self weight							
52			Front beam		1583	Front beam		589.84		1590	593	1583	590							
53			Rear beam		1304	Rear beam		490.26		1257	470	1304	490							
54																				
55																				
56		Live load																		
57		Beam	A			C			E			G			Front			Rear		
58			Excel	Abaqus	Focus	Excel	Abaqus	Focus	Excel	Abaqus	Focus	Excel	Abaqus	Focus	Excel	Abaqus	Focus	Excel	Abaqus	Focus
59			12453	12464	12435	10962	10940	10980	10962	10940	10980	12453	12464	12435	6456	6384	6411	8968	9031	8952
60		Error		0.1 %	-0.1 %		-0.2 %	0.2 %		-0.2 %	0.2 %		0.1 %	-0.1 %		-1.1 %	-0.7 %		0.7 %	-0.2 %
61																				
62																				
63		Self weight																		
64		Beam	A			C			E			G			Front			Rear		
65			Excel	Abaqus	Focus	Excel	Abaqus	Focus	Excel	Abaqus	Focus	Excel	Abaqus	Focus	Excel	Abaqus	Focus	Excel	Abaqus	Focus
66			3357	3513	3497	2955	2945	2952	2955	2945	2952	3357	3513	3497	2710	2687	2687	3643	3690	3666
67		Error		4.6 %	4.2 %		-0.3 %	-0.1 %		-0.3 %	-0.1 %		4.6 %	4.2 %		-0.8 %	-0.8 %		1.3 %	0.6 %
68																				
69																				
70		Combined loads																		
71		Beam	A			C			E			G			Front			Rear		
72			Excel	Abaqus	Focus	Excel	Abaqus	Focus	Excel	Abaqus	Focus	Excel	Abaqus	Focus	Excel	Abaqus	Focus	Excel	Abaqus	Focus
73			15809	15976	15932	13917	13886	13932	13917	13886	13932	15809	15976	15932	9166	9071	9097	12611	12721	12619
74		Error		1.1 %	0.8 %		-0.2 %	0.1 %		-0.2 %	0.1 %		1.1 %	0.8 %		-1.0 %	-0.7 %		0.9 %	0.1 %

Live load calculation

Row		[mm]	[m]	
3	Number of load points:		28	
4	Number of vertical load points:		28	
5	Distance between load points in vertical direction:	3250	3.25	
6	Distance between load points in horizontal direction:	5000	5	
7	Length of longitudinal beams:	26000	26	
8	Length of front and interior traverse beams:	15000	15	
9	Length of rear beam:	17000	17	
15	Live load (mass of section) [kg]:	500 000		
16	Ground acceleration, g [m/s^2]	9.81		
20	Nominal load per load point in horizontal position [kN]:	175		
21	Nominal load per load point in vertical position [kN]:	175		
23	Dynamic factor according to NS 5514 1.2211:			
24	Formula: $\psi = 1+\xi V_L$ $1.15 \leq \psi \leq 1.6$			
25	Hoisting velocity V_L [m/s]:	1		$V_L \leq 1$ m/s
26	ξ for gantry cranes:	0.6		
27	Dynamic factor, ψ:	1.6		
29	Live load factor according to NS-EN 1990, Table A1.2(A):			
30	Leading variable action, γ_Q:	1.50		
32	Dynamic design load per load point [kN]:	420		

Loads in action

Grey areas are unavailable

	A	B	C	D
1				
2	1.00	1.00	1.00	1.00
3	1.00	1.00	1.00	1.00
4	1.00	1.00	1.00	1.00
5	1.00	1.00	1.00	1.00
6	1.00	1.00	1.00	1.00
7	1.00	1.00	1.00	1.00
8	1.00	1.00	1.00	1.00
9				

From Abaqus:

Load distribution due to bending of traverses [kN]

		A	B	C	D
	0				
1	0				
2	3.25				
3	6.5	143.31	-143.31	-143.31	143.31
4	9.75				
5	13	-36.20	36.20	36.20	-36.20
6	16.25				
7	19.5	363.56	-363.56	-363.56	363.56
8	22.75				
9	26				

Abaqus	Focus
143.306	190.34
-36.202	-12.76
363.555	432.72

	A	B	C	D	E	F	G	H	I	J
34										
35	Unit loads									
36										
37										
38	Horizontal position									
39										
40	Longitudinal beams									
41										
42		Load distribution								
43		x	A	B	C	D				
44	Support	0	3.50	3.50	3.50	3.50	Support loads			
45	1	0	0.00	0.00	0.00	0.00	Front beam			
46	2	3.25	1.00	1.00	1.00	1.00				
47	3	6.5	1.00	1.00	1.00	1.00				
48	4	9.75	1.00	1.00	1.00	1.00				
49	5	13	1.00	1.00	1.00	1.00				
50	6	16.25	1.00	1.00	1.00	1.00				
51	7	19.5	1.00	1.00	1.00	1.00				
52	8	22.75	1.00	1.00	1.00	1.00				
53	9	26	3.50	3.50	3.50	3.50	Support loads			
54										
55										
56	Support forces due to support moment due to eccentricity of lifting lug [kN]									
57		x								
58	Front	0	-0.29615	0	0	-0.29615				
59	Rear	26	0.296154	0	0	0.296154				

	K	L	M	N	O	P	Q	R	S	T
34										
35	Real loads									
36										
37										
38	Horizontal position									
39										
40	Longitudinal beams									
41										
42		Load distribution [kN]								
43		x	A	B	C	D				
44		0	1652	1291	1291	1652	Support loads			
45	1	0	0	0	0	0				
46	2	3.25	420	420	420	420				
47	3	6.5	564	277	277	564				
48	4	9.75	420	420	420	420				
49	5	13	384	457	457	384				
50	6	16.25	420	420	420	420				
51	7	19.5	784	57	57	784				
52	8	22.75	420	420	420	420				
53	9	26	1762	1181	1181	1762	Support loads			
54										
55										
56	Support forces due to support moment due to eccentricity of lifting lug [kN]									
57		x								
58	Front	0	-119.467	0	0	-119.467				
59	Rear	26	119.4666	0	0	119.4666				

			A	B	C	D
60						
61						
62			Shear force			
63		x	A	B	C	D
64		0	3.20	3.50	3.50	3.20
65	1	0	3.20	3.50	3.50	3.20
66	2	3.25	2.20	2.50	2.50	2.20
67	3	6.5	1.20	1.50	1.50	1.20
68	4	9.75	0.20	0.50	0.50	0.20
69	5	13	-0.80	-0.50	-0.50	-0.80
70	6	16.25	-1.80	-1.50	-1.50	-1.80
71	7	19.5	-2.80	-2.50	-2.50	-2.80
72	8	22.75	-3.80	-3.50	-3.50	-3.80
73	9	26	3.80	3.50	3.50	3.80
74						
75						
76			Moment			
77		x	A	B	C	D
78		0	-0.3	0.0	0.0	0.0
79	1	0	-0.3	0.0	0.0	0.0
80	2	3.25	10.1	11.4	11.4	10.4
81	3	6.5	17.3	19.5	19.5	17.6
82	4	9.75	21.2	24.4	24.4	21.5
83	5	13	21.9	26.0	26.0	22.2
84	6	16.25	19.3	24.4	24.4	19.6
85	7	19.5	13.4	19.5	19.5	13.7
86	8	22.75	4.3	11.4	11.4	4.6
87	9	26	-8.0	0.0	0.0	-7.7
88						

			A	B	C	D
62		Shear force [kN]				
63		x	A	B	C	D
64		0	1532	1291	1291	1532
65	1	0	1532	1291	1291	1532
66	2	3.25	1112	871	871	1112
67	3	6.5	548	594	594	548
68	4	9.75	128	173	173	128
69	5	13	-257	-283	-283	-257
70	6	16.25	-677	-704	-704	-677
71	7	19.5	-1461	-761	-761	-1461
72	8	22.75	-1881	-1181	-1181	-1881
73	9	26	-1881	-1181	-1181	-1881
76		Moment [kNm]				
77		x	A	B	C	D
78		0	3 106	0	0	3 106
79	1	0	3105.9	0.0	0.0	3105.9
80	2	3.25	8085.9	4 197	4 197	8 086
81	3	6.5	11 699	7 027	7 027	11 699
82	4	9.75	13 481	8 956	8 956	13 481
83	5	13	13 896	9 519	9 519	13 896
84	6	16.25	13 062	8 598	8 598	13 062
85	7	19.5	10 862	6 311	6 311	10 862
86	8	22.75	6 114	3 839	3 839	6 114
87	9	26	0	0	0	0
88	MAX		13 896	9 519	9 519	13 896

	A	B	C	D	E	F	G	H	I	J
89										
90										
91	Traverse beams									
92										
93	Rear beam									
94	Eccentricity of supports [m]:			1						
95										
96		y	Load	Shear	Moment					
97	Support	0.000	7.00	7.00	0.00					
98	A	1.000	3.50	3.50	7.00					
99	B	6.000	3.50	0.00	24.50					
100	C	11.000	3.50	-3.50	24.50					
101	D	16.000	3.50	-7.00	7.00					
102	Support	17.000	7.00	-7.00	0.00					
103										
104										
105	Front beam									
106	Eccentricity of supports [m]:			0						
107		y	Load	Shear	Moment					
108	Support	0.000	7.00	7.00	0.00					
109	A	0.000	3.50	3.50	0.00					
110	B	5.000	3.50	0.00	17.50					
111	C	10.000	3.50	-3.50	17.50					
112	D	15.000	3.50	-7.00	0.00					
113	Support	15.000	7.00	7.00	0.00					
114										
115										
116	Support moment on beam A and D due to eccentricity of lifting lug [kNm]									
117	Eccentricity of lifting lug [mm]:			1100						
118										
119			A	B	C	D				
120			7.7	0	0	7.7				
121										
122	Support forces due to support moment due to eccentricity of lifting lug [kN]									
123		x								
124	Front	0	-0.29615	0	0	-0.29615				
125	Rear	26	0.296154	0	0	0.296154				
126										
127										

	K	L	M	N	O	P	Q	R	S	T
91	Traverse beams									
93	Rear beam									
94	Eccentricity of supports [m]:			1						
96		y	Load	Shear	Moment					
97	Support	0.000	3062	3062.47	0					
98	A	1.000	1881	1181.11	3 062					
99	B	6.000	1181	0.00	8 968					
100	C	11.000	1181	-1181.11	8 968					
101	D	16.000	1881	-3062.47	3 062					
102	Support	17.000	3062	-2943	0					
103	MAX				8 968					
105	Front beam									
106	No eccentricity									
107		y	Load	Shear	Moment					
108	Support	0.000	2824	2824	0					
109	A	0.000	1532	1291	0					
110	B	5.000	1291	0	6 456					
111	C	10.000	1291	-1291	6 456					
112	D	15.000	1532	-2824	0					
113	Support	15.000	2824	2824	0					
114	MAX				6 456					
116	Support moment on beam A and D due to eccentricity of lifting lug [kNm]									
117	Eccentricity of lifting lug [mm]:			1100						
119			A	B	C	D				
120			3105.887	0	0	3105.887				
122	Support forces due to support moment due to eccentricity of lifting lug [kN]									
123		x								
124	Front	0	-119.457	0	0	-119.457				
125	Rear	26	119.4572	0	0	119.4572				

	A	G	H
1	Self weight calculation		
2			
3			
4		[mm]	[m]
5	Distance between load points in vertical direction:	3250	3.250
6	Distance between load points in horizontal direction:	5000	5.000
7	Distance between centerlines of front and rear beam:	26000	26.000
8	Length of front and interior traverse beams:	15000	15.000
9	Length of rear beam:	17000	17.000
10	Length of lifting lugs:	1100	1.100
11	Length of diagonals:	8201	8
12			
13	Number of diagonals:	8	
14			
15			
16	Mass density of steel, ρ [kg/m^3]:	7850.00	
17	Ground acceleration, g [m/s^2]	9.81	
18			
19	Maximum allowed stress according to NS 5514 and EC3 1-1		
20	Safety factor according to NS 5514, ν_E:	1.5	
21	Material factor according to EC3 1-1, γ_M:	1.05	
22	Steel nominal yield stress, σ_E [MPa]:	420	
23	Allowed stress, σ_a [MPa]:	267	

	A	B	C	D	E	F	G	H	I	J	K
24											
25	Cross-section data:			Longitudinal beams				Traverse beams		Diagonals	Lugs
26	Beam		A-A	C-C	E-E	G-G	Rear	Front	Interior	All	
27	$W_{strong,req} \cdot 10^{-6}$ [mm^3]		59.29	52.19	52.19	59.29	47.29				
28	$W_{weak,req} \cdot 10^{-6}$ [mm^3]						0.00	46.63			
29	$A \cdot 10^{-3}$ [mm^2]		145.00	145.00	145.00	145.00	240.00	240.00	145.00	10	75
30	$W_{strong} \cdot 10^{-6}$ [mm^3]		67.83	67.83	67.83	67.83	100.60	100.60	67.83		
31											
32	$W_{weak} \cdot 10^{-6}$ [mm^3]		9.41	9.41	9.41	9.41	79.90	79.90	9.41		
33											
34	Weight, q [kN/m]		11.17	11.17	11.17	11.17	18.48	18.48	11.17	0.77	5.78
35	Total weight [kN]:		290.32	290.32	290.32	290.32	314.19	277.23	167.49	6.32	6.35
36	Percentage of total:		12.56 %	12.56 %	12.56 %	12.56 %	13.59 %	11.99 %	7.24 %	0.27 %	0.27 %
37											
38	Total self weight in tonnes:				235.68						
39											
40	The self weight must also be treated with a dynamic factor according to NS 5514.										
41	Dynamic factor according to NS 5514 1.2211:										
42	Formula: $\psi = 1+\xi V_L$			$1.15 \leq \psi \leq 1.6$							
43	Hoisting velocity V_L [m/s]:						1				
44	ξ for gantry cranes:						0.6				
45	Dynamic factor, ψ:						1.6				

	A	B	C	D	E	F	G	H	I	J	K
46											
47	Self weight factor according to NS-EN 1990 Table A1.2(A):										
48	Permanent actions, unfavourable, γ_G:						1.20				
49											
50			A-A	C-C	E-E	G-G	Rear	Front	Interior	Diagonals	Lugs
51	q_{dyn} [kN/m]:		21.4	21.4	21.4	21.4	35.5	35.49	21.4	1.5	11.1
52	$q_{dyn} \cdot L$ [kN]:		557.4	557.4	557.4	557.4	603.3	532.3	321.6	12.1	12.2
53											
54	Self weight loads										
55	The self weight of the beams is treated as evenly distributed loads.										
56	The traverse beams other than the rear beam have dimensions equal to the front beam.										
57											
58	Longitudinal beams										
59	From Abaqus:										
60	Point loads from bending of interior traverse beams [kN]:										
61		x	A	B	C	D					
62	Support	0	106.29	-106.29	-106.29	106.29					
63	1	0.000									
64	2	3.250						Abaqus	Focus		
65	3	6.500	78.89	-78.89	-78.89	78.89		78.89	78.89		
66	4	9.750									
67	5	13.000	7.28	-7.28	-7.28	7.28		7.28	7.28		
68	6	16.250									
69	7	19.500	173.94	-173.94	-173.94	173.94		173.94	173.94		
70	8	22.750									
71	9	26.000									
72	Support	26.000	153.82	-153.82	-153.82	153.82					

	A	B	C	D	E	F
73						
74	Point loads from weight of interior traverse beams [kN]:					
75		x	A	B	C	D
76	Support	0	80.40	160.79	160.79	80.40
77	1	0.000	0	0	0	0
78	2	3.250				
79	3	6.500	53.60	107.20	107.20	53.60
80	4	9.750				
81	5	13.000	53.60	107.20	107.20	53.60
82	6	16.250				
83	7	19.500	53.60	107.20	107.20	53.60
84	8	22.750				
85	9	26.000	0	0	0	0
86	Support	26.000	80.40	160.79	160.79	80.40
87						
88	Point loads from weight of lifting lugs [kN]:					
89		x	A	B	C	D
90	Support	0	12.20	0.00	0.00	12.20
91	1	0.000	12.2			12.2
92	2	3.250				
93	3	6.500				
94	4	9.750				
95	5	13.000				
96	6	16.250				
97	7	19.500				
98	8	22.750				
99	9	26.000				
100	Support	26.000	0.00	0.00	0.00	0.00

	A	B	C	D	E	F	G	H	I	J	K
101											
102	Point loads from weight of diagonal beams [kN]										
103	Unit loads										
104		x	A	B	C	D					
105	Support	0	1.25	0.75	0.75	1.25					
106	1	0.000	0.50	0.00	0.00	0.50					
107	2	3.250									
108	3	6.500	0.50	0.50	0.50	0.50					
109	4	9.750									
110	5	13.000	0.50	0.50	0.50	0.50					
111	6	16.250									
112	7	19.500	0.50	0.50	0.50	0.50					
113	8	22.750									
114	9	26.000	0.00	0.50	0.50	0.00					
115	Support	26.000	0.75	1.25	1.25	0.75					
116											
117	Real loads										
118		x	A	B	C	D					
119	Support	0	15.16	9.09	9.09	15.16					
120	1	0.000	6.06	0.00	0.00	6.06					
121	2	3.250									
122	3	6.500	6.06	6.06	6.06	6.06					
123	4	9.750									
124	5	13.000	6.06	6.06	6.06	6.06					
125	6	16.250									
126	7	19.500	6.06	6.06	6.06	6.06					
127	8	22.750									
128	9	26.000	0.00	6.06	6.06	0.00					
129	Support	26.000	9.09	15.16	15.16	9.09					

	A	B	C	D	E	F
130						
131	Total loads on longitudinals [kN]:					
132		x	A	B	C	D
133	Support	0	214.04	63.60	63.60	214.04
134	1	0.000	18.26	0.00	0.00	18.26
135	2	3.250	0.00	0.00	0.00	0.00
136	3	6.500	138.55	34.37	34.37	138.55
137	4	9.750	0.00	0.00	0.00	0.00
138	5	13.000	66.94	105.98	105.98	66.94
139	6	16.250	0.00	0.00	0.00	0.00
140	7	19.500	233.60	-60.68	-60.68	233.60
141	8	22.750	0.00	0.00	0.00	0.00
142	9	26.000	0.00	6.06	6.06	0.00
143	Support	26.000	243.31	22.13	22.13	243.31
144						
145	Shear force [kN]:					
146		x	A	B	C	D
147	Support	0.000	214.04	63.60	63.60	214.04
148	1	0.000	195.78	63.60	63.60	195.78
149	2	3.250	195.78	63.60	63.60	195.78
150	3	6.500	57.23	29.23	29.23	57.23
151	4	9.750	57.23	29.23	29.23	57.23
152	5	13.000	-9.71	-76.75	-76.75	-9.71
153	6	16.250	-9.71	-76.75	-76.75	-9.71
154	7	19.500	-243.31	-16.07	-16.07	-243.31
155	8	22.750	-243.31	-16.07	-16.07	-243.31
156	9	26.000	-243.31	-22.13	-22.13	-243.31

	A	B	C	D	E	F
157						
158	Moment [kNm]:					
159		x	A	B	C	D
160	Support	0.000	0	0	0	0
161	1	0.000	0	0	0	0
162	2	3.250	636	207	207	636
163	3	6.500	1 273	413	413	1 273
164	4	9.750	1 459	508	508	1 459
165	5	13.000	1 645	603	603	1 645
166	6	16.250	1 613	354	354	1 613
167	7	19.500	1 582	104	104	1 582
168	8	22.750	791	52	52	791
169	9	26.000	0	0	0	0
170						
171	Moment in front of longitudinals due to eccentricity of lifting lugs:					
172	Eccentricity [m]		1.100			
173						
174			A	B	C	D
175	Moment [kNm]		881			881
176						
177	Support forces [kN]		A	B	C	D
178			33.8953			33.8953
179			Copy numbers above to cells below to iterate (avoid circular reference)			
180			33.8953			33.8953

	A	B	C	D	E	F	G	H	I	J	K
181											
182											
183	Shear force [kN]:										
184		x	A	B	C	D					
185	Support	0.000	33.90	0.00	0.00	33.90					
186	1	0.000	33.90	0.00	0.00	33.90					
187	2	3.250	33.90	0.00	0.00	33.90					
188	3	6.500	33.90	0.00	0.00	33.90					
189	4	9.750	33.90	0.00	0.00	33.90					
190	5	13.000	33.90	0.00	0.00	33.90					
191	6	16.250	33.90	0.00	0.00	33.90					
192	7	19.500	33.90	0.00	0.00	33.90					
193	8	22.750	33.90	0.00	0.00	33.90					
194	9	26.000	33.90	0.00	0.00	33.90					
195											
196											
197	Moment [kNm]:										
198		x	A	B	C	D					
199	Support	0.000	881	0	0	881					
200	1	0.000	881	0	0	881					
201	2	3.250	771	0	0	771					
202	3	6.500	661	0	0	661					
203	4	9.750	551	0	0	551					
204	5	13.000	441	0	0	441					
205	6	16.250	330	0	0	330					
206	7	19.500	220	0	0	220					
207	8	22.750	110	0	0	110					
208	9	26.000	0	0	0	0					

Moment from self weight of longitudinal beams [kNm]:

M(x) = qL/2*x - q*x*x/2

	x	A	B	C	D
Support	0	0	0	0	0
1	0.000	0	0	0	0
2	3.250	793	793	793	793
3	6.500	1 359	1 359	1 359	1 359
4	9.750	1 698	1 698	1 698	1 698
5	13.000	1 812	1 812	1 812	1 812
6	16.250	1 698	1 698	1 698	1 698
7	19.500	1 359	1 359	1 359	1 359
8	22.750	793	793	793	793
9	26.000	0	0	0	0

Total moment on longitudinal beams due to self weight [kNm]:

	x	A	B	C	D
	0	881	0	0	881
1	0	881	0	0	881
2	3.250	2200	999	999	2200
3	6.500	3292	1772	1772	3292
4	9.750	3708	2207	2207	3708
5	13.000	3897	2415	2415	3897
6	16.250	3642	2052	2052	3642
7	19.500	3161	1463	1463	3161
8	22.750	1693	845	845	1693
9	26.000	0	0	0	0

	A	B	C	D	E	F	G	H	I	J	K
237											
238											
239											
240											
241	Rear beam										
242	Eccentricity of rear beam [m]:			1							
243	Length of rear beam [m]:			17							
244											
245	Loads on rear beam due to self weight of longitudinal and interior transverse beams [kN]:										
246		y	Loads on longitudinals		Lug eccentricity		Longitudinal		Total	Shear	Moment
247	Support	0.000		265.44		33.90		557.42	856.75	856.75	0.00
248	A	1.000		243.31		33.90		278.71	555.91	300.84	856.75
249		3.500								300.84	1608.86
250	B	6.000		22.13				278.71	300.84	0.00	2360.96
251		8.500								0.00	2360.96
252	C	11.000		22.13				278.71	300.84	-300.84	2360.96
253		13.500								-300.84	1608.86
254	D	16.000		243.31		33.90		278.71	555.91	-856.75	856.75
255	Support	17.000		265.44		33.90		557.42	856.75	-856.75	0.00
256											
257	Moment on rear beam due to self weight of rear beam [kNm]:										
258	Distributed weight of rear beam, q [kN/m]:				35.4855168						
259		x	Moment								
260	Support	0		0.00							
261	A	1.000		283.88							
262		3.500		838.35							
263	B	6.000		1171.02							
264		8.500		1281.91							
265	C	11.000		1171.02							
266		13.500		838.35							
267	D	16.000		283.88							
268	Support	17.000		0.00							

	A	B	C	D	E	F	G	H	I	J	K
269											
270	Total moment on rear beam [kNm]:										
271		x	Total moment								
272	Support	0		0.00							
273	A	1.000		1 140.64							
274		3.500		2 447.20							
275	B	6.000		3 531.99							
276		8.500		3 642.88							
277	C	11.000		3 531.99							
278		13.500		2 447.20							
279	D	16.000		1 140.64							
280	Support	17.000		0.00							
281											
282											
283	Front beam										
284	Eccentricity of supports in front [m]:				0						
285	Length of front beam [m]:				15						
286											
287	Loads on front beam due to self weight of longitudinal and interior transverse beams [kN]:										
288		y	Loads on longitudinals		Lug eccentricity		Longitudinal		Total	Shear	Moment
289	Support	0.000		277.64		-33.90		557.42	801.16	801.16	0
290	A	0.000		214.04		-33.90		278.71	458.86	342.30	0
291		2.500								342.30	856
292	B	5.000		63.60				278.71	342.30	0.00	1712
293		7.500								0.00	1712
294	C	10.000		63.60				278.71	342.30	-342.30	1712
295		12.500								-342.30	856
296	D	15.000		214.04		-33.90		278.71	458.86	-801.16	0
297	Support	15.000		277.64		-33.90		557.42	801.16	-801.16	0

	A	B	C	D	E
298					
299	Moment on front beam due to self weight of front beam [kNm]:				
300	Distributed weight of front beam, q [kN/m]:				35.4855168
301		x	Moment		
302	Support	0		0	
303	A	0.000		0	
304		2.500		554	
305	B	5.000		887	
306		7.500		998	
307	C	10.000		887	
308		12.500		554	
309	D	15.000		0	
310	Support	15.000		0	
311					
312					
313	Total moment on front beam [kNm]:				
314		x	Total moment		
315	Support	0		0	
316	A	0.000		0	
317		2.500		1 410	
318	B	5.000		2 599	
319		7.500		2 710	
320	C	10.000		2 599	
321		12.500		1 410	
322	D	15.000		0	
323	Support	15.000		0	

	L	M	N	O	P	Q	R	S	T	U	V
1											
2											
3											
4											
5											
6											
7											
8	Diagonal beams										
9		A			B			C			D
10	1										
11	2		1.00							1.00	
12	3										
13	4		1.00							1.00	
14	5										
15	6		1.00							1.00	
16	7										
17	8		1.00							1.00	
18	9										
19											
20											
21											
22											
23											

Cross section geometry

H beam

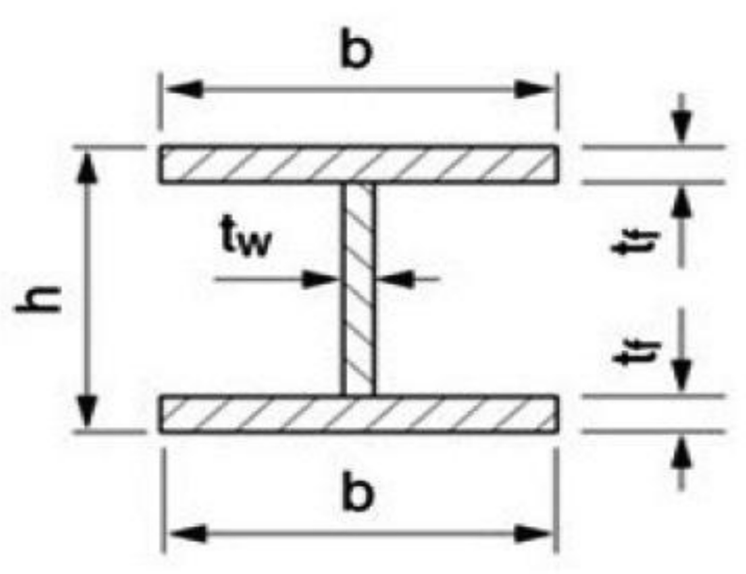

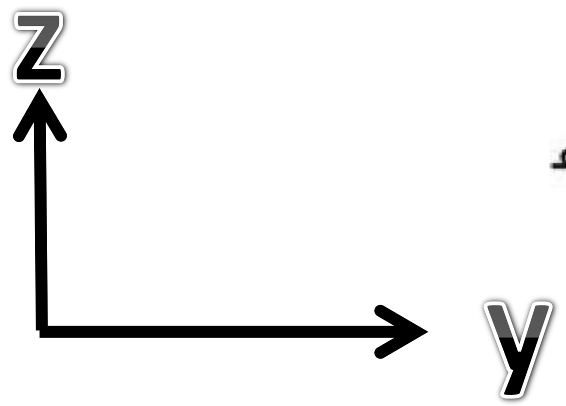

Box beam

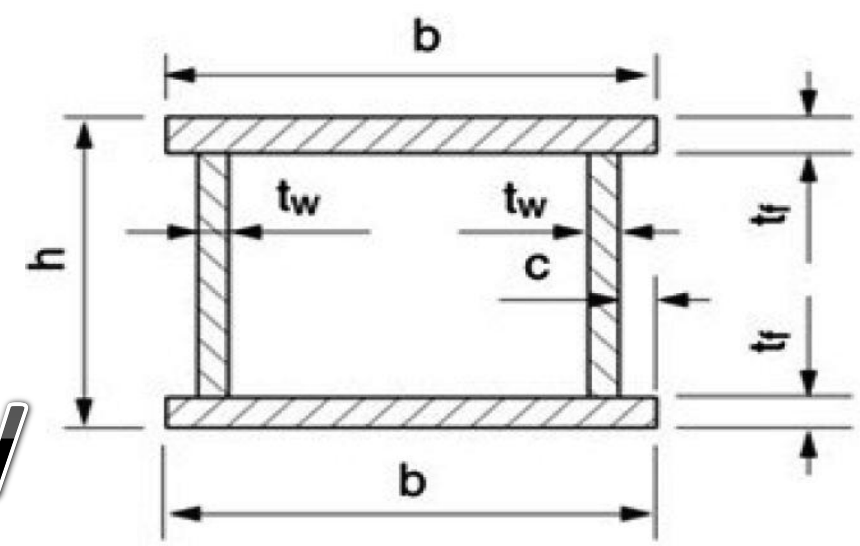

Flat bar

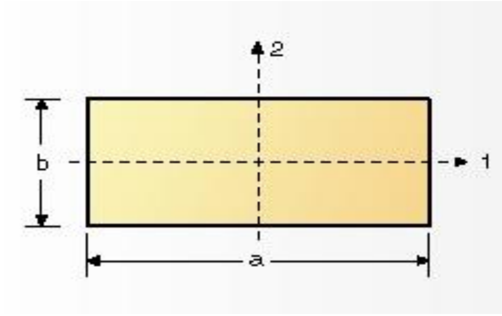

Longitudinal beams	
b [mm]	750
h [mm]	1500
t_f [mm]	50
t_w [mm]	50
H or Box [H:1, Box:2]	1
c [mm]	
$A \cdot 10^{-3}$ [mm^2]	145.00000
z_{max} [mm]	750.00000
$I_y \cdot 10^{-6}$ [mm^4]	50 870.83333
$W_y \cdot 10^{-6}$ [mm^3]	67.82778
y_{max} [mm]	375.00000
a_w [mm]	0.00000
$I_z \cdot 10^{-6}$ [mm^4]	3 530.20833
$W_z \cdot 10^{-6}$ [mm^3]	9.41389
$I_T \cdot 10^{-6}$ [mm^4]	120.83
$S_y \cdot 10^{-6}$ [mm^3]	41.25
$S_z \cdot 10^{-6}$ [mm^3]	7.47
$A_y \cdot 10^{-3}$ [mm^2]	75.00
$A_z \cdot 10^{-3}$ [mm^2]	70.00

Traverse beams	
b [mm]	750
h [mm]	1500
t_f [mm]	50
t_w [mm]	50
H or Box [H:1, Box:2]	1
c [mm]	
$A \cdot 10^{-3}$ [mm^2]	145.00
z_{max} [mm]	750
$I_y \cdot 10^{-6}$ [mm^4]	50 871
$W_y \cdot 10^{-6}$ [mm^3]	67.83
y_{max} [mm]	375
a_w [mm]	0
$I_z \cdot 10^{-6}$ [mm^4]	3 530.21
$W_z \cdot 10^{-6}$ [mm^3]	9.41
$I_T \cdot 10^{-6}$ [mm^4]	120.83
$S_y \cdot 10^{-6}$ [mm^3]	41.25
$S_z \cdot 10^{-6}$ [mm^3]	7.47
$A_y \cdot 10^{-3}$ [mm^2]	75.00
$A_z \cdot 10^{-3}$ [mm^2]	70.00

Rear Beam	
b [mm]	1000
h [mm]	1500
t_f [mm]	50
t_w [mm]	50
H or Box	2
c [mm]	0
$A \cdot 10^{-3}$ [mm^2]	240.00
z_{max} [mm]	750
$I_y \cdot 10^{-6}$ [mm^4]	75 450
$W_y \cdot 10^{-6}$ [mm^3]	100.60
y_{max} [mm]	500
a_w [mm]	475
$I_z \cdot 10^{-6}$ [mm^4]	39 950.00
$W_z \cdot 10^{-6}$ [mm^3]	79.90000
$I_T \cdot 10^{-6}$ [mm^4]	79062.76
$S_y \cdot 10^{-6}$ [mm^3]	50.3125000
$S_z \cdot 10^{-6}$ [mm^3]	12.937500
$A_y \cdot 10^{-3}$ [mm^2]	100.00
$A_z \cdot 10^{-3}$ [mm^2]	140.00

Front beam	
b [mm]	1000
h [mm]	1500
t_f [mm]	50
t_w [mm]	50
H or Box	2
c [mm]	0
$A \cdot 10^{-3}$ [mm^2]	240.00
z_{max} [mm]	750
$I_y \cdot 10^{-6}$ [mm^4]	75 450
$W_y \cdot 10^{-6}$ [mm^3]	100.60
y_{max} [mm]	500
a_w [mm]	475
$I_z \cdot 10^{-6}$ [mm^4]	39 950.00
$W_z \cdot 10^{-6}$ [mm^3]	79.90
$I_T \cdot 10^{-6}$ [mm^4]	79062.76
$S_y \cdot 10^{-6}$ [mm^3]	50.31
$S_z \cdot 10^{-6}$ [mm^3]	12.94
$A_y \cdot 10^{-3}$ [mm^2]	100.00
$A_z \cdot 10^{-3}$ [mm^2]	75.00

Flat bar diagonals	
a [mm]	200
b [mm]	50
$A \cdot 10^{-3}$ [mm^2]	10.00
$I_T \cdot 10^{-6}$ [mm^4]	8.33

Lifting lug in front	
Rectangular plate	
Thickness [mm]:	50
Height [mm]:	1500
$A \cdot 10^{-3}$ [mm^2]	75

Excel calculations of vertical position - Results & Comparison

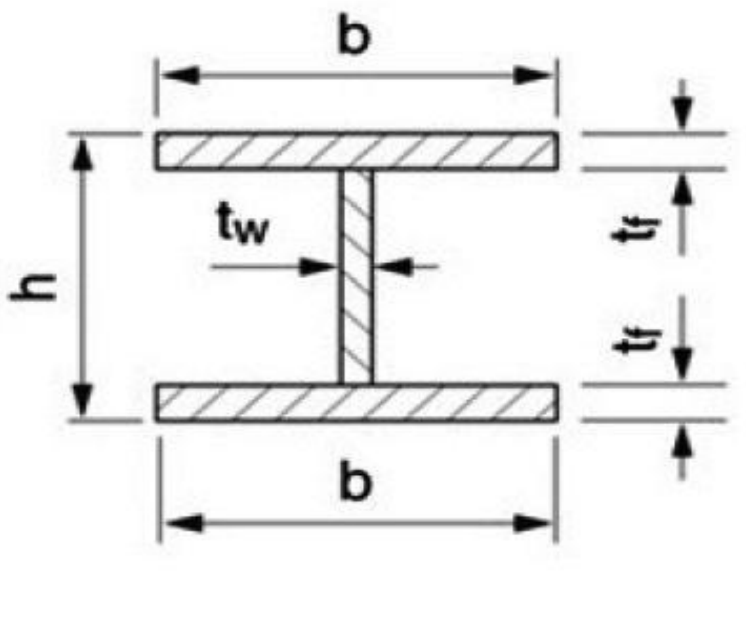

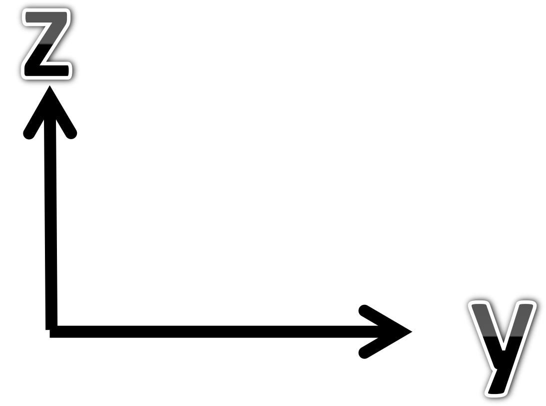

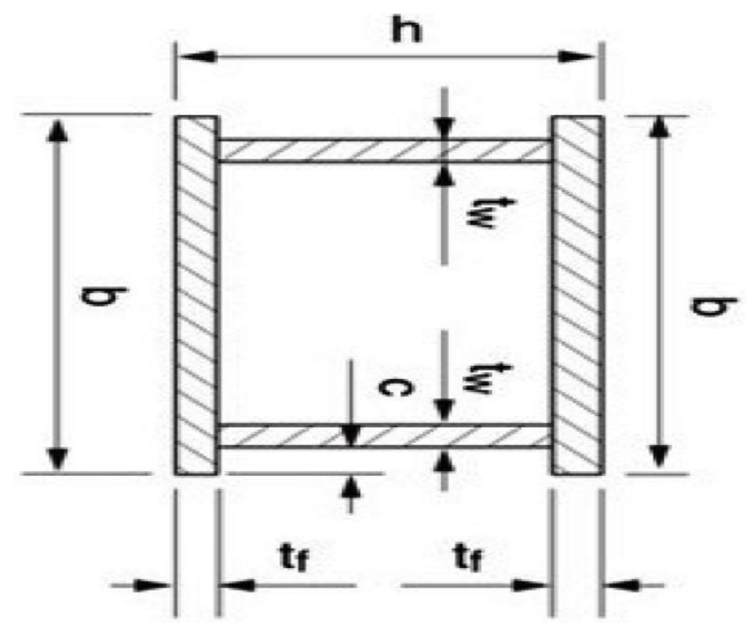

Reaction forces in vertical direction [kN]

Combined

		Excel A	Excel G		Abaqus A	Abaqus G		Focus A	Focus G
	1	4612	4612	1	4615	4615	1	4613	4612
	9	3500	3500	9	3497	3497	9	3499	3499
SUM		8112	8112		8112	8112		8112	8111
Error					0.0 %	0.0 %		0.0 %	0.0 %

Live load

		Excel A	Excel G		Abaqus A	Abaqus G		Focus A	Focus G
	1	3358	3358	1	3330	3330	1	3326	3326
	9	2528	2528	9	2556	2556	9	2560	2560
SUM		5886	5886		5886	5886		5886	5886
Error					0.0 %	0.0 %		0.0 %	0.0 %

Self weight

		Excel A	Excel G		Abaqus A	Abaqus G		Focus A	Focus G
	1	1253.9	1253.9	1	1283	1283	1	1286	1286
	9	972	972	9	942	942	9	940	939
SUM		2226	2226		2226	2226		2226	2225
Error					0.0 %	0.0 %		0.0 %	0.0 %

Reaction forces in vertical direction [kN]

Combined

Excel

	A	G
1	1303	1303
9	1303	1303
	2606	2606

Abaqus

	A	G
1	1303	1303
9	1303	1303
	2606	2606
	0.0 %	0.0 %

Focus

	A	G
1	1303	1303
9	1303	1303
	2606	2606
	0.0 %	0.0 %

	A	B	C	D	E	F	G	H	I	J	K	L	M	N	O	P	Q	R
45																		
46																		
47																		
48	Beam			A, G			C, E			Front			Rear					
49	Live loads			Excel	Abaqus	Focus	Excel	Abaqus	Focus	Excel	Abaqus	Focus	Excel	Abaqus	Focus			
50	Moment about y-axis [kNm]			3394	3376	3394	2726	2735	2725	3030	3028	3029	3834	3877	3832			
51	(max value)		Error		-0.5 %	0.0 %		0.3 %	0.0 %		-0.1 %	-0.1 %		1.1 %	-0.1 %			
52	Moment about z-axis [kNm]									1701	1614	1723	2528	2495	2552			
53	(max value)		Error								-5 %	1.3 %		-1.3 %	0.9 %			
54	Compressive forces [kN]			2624	2431	2783	431	647	384									
55	(max value, longitudinals)		Error		-7 %	6 %		50 %	-11 %									
56	Tensile forces [kN]			2369	2676	2246	396	686										
57	(max value, longitudinals)		Error		13 %	-5 %			-100 %									
58	Shear force, normal, front [kN]			606	697	578	606											
59	(max value, out of plane)		Error			-5 %			-100 %									
60	Shear force, normal, rear [kN]			506	788	485	506											
61	(max value, out of plane)		Error			-4 %			-100 %									
62	Self weight			Excel	Abaqus	Focus	Excel	Abaqus	Focus	Excel	Abaqus	Focus	Excel	Abaqus	Focus			
63	Moment about z-axis [kNm]									604	635	662	954	905	952			
64			Error								5 %	9.7 %		-5.1 %	-0.2 %			
65	Compressive forces [kN] (longitudinals, max)			862		919	98		131									
66	Tensile forces [kN] (longitudinals, max)			761		767	193		100									
67																		
68																		
69			A, G			C, E			Front			Rear						
70	Combined loads		Excel	Abaqus	Focus	Excel	Abaqus	Focus	Excel	Abaqus	Focus	Excel	Abaqus	Focus				
71	Moment about y-axis [kNm]		3394	3376	3394	2726	2735	2725	3030	3028	3029	3834	3877	3832				
72	Deviation			-0.5 %	0.0 %		0.3 %	0.0 %		-0.1 %	-0.1 %		1.1 %	-0.1 %				
73	Moment about z-axis [kNm]								2305	2249	2385	3482	3400	3504				
74	Deviation									-2.4 %	3.5 %		-2.3 %	0.6 %				

Live load calculation

3	Number of load points:	28
4	Number of vertical load points:	28
5	Distance between load points in vertical direction [m]:	3.25
6	Distance between load points in horizontal direction [m]:	5
7	Length of longitudinal beams [m]:	26
8	Length of front and interior traverse beams [m]:	15
9	Length of rear beam [m]:	17
10	Live load (mass of module) [kg]:	500 000
11	Ground acceleration, g [m/s^2]	9.81
12	Distance from centerline of support forces to centre of gravity of module	
13	Half of longitudinal beams [mm]	750
14	Shear plates [mm]	250
15	Distance to the gravity centre of the module [mm]	5000
16	Total eccentricity [mm]	6000
17	x-coordinate of COG of module structure [m]:	0
18		
19		
20	Nominal load per load point in horizontal position [kN]:	175.18
21	Nominal load per load point in vertical position [kN]:	175.18
22		
23	<u>Dynamic factor according to NS 5514 1.2211:</u>	
24	Formula: $\psi = 1+\xi V_L$ $1.15 \leq \psi \leq 1.6$	
25	Hoisting velocity V_L [m/s]:	1 $V_L \leq 1$ m/s
26	ξ for gantry cranes:	0.6
27	Dynamic factor, ψ:	1.6
28		
29	<u>Live load factor according to NS-EN 1990, Table A1.2(A):</u>	
30	Leading variable action, γ_Q:	1.50
31		
32	Dynamic load per load point in vertical position [kN]:	420.428571
33	Design moment due to eccentricity of module structure [kNm]:	70 632

<u>Loads in action</u>

Grey areas are unavailable. Copy from table in "Deflections" to iterate (copy with values only).

		A	B	C	D	E	F	G
13	1		0.00	0.00	0.00	0.00	0.00	
9.75	2	1.00		1.00		1.00		1.00
6.5	3	1.00	0.00	1.00	0.00	1.00	0.00	1.00
3.25	4	1.00		1.00		1.00		1.00
0	5	1.00	0.00	1.00	0.00	1.00	0.00	1.00
-3.25	6	1.00		1.00		1.00		1.00
-6.5	7	1.00	0.00	1.00	0.00	1.00	0.00	1.00
-9.75	8	1.00		1.00		1.00		1.00
-13	9		0.00	0.00	0.00	0.00	0.00	
		V	H	V	H	V	H	V

36 The calculation of the vertical position is in practice an extension of the calculation of the horizontal position.
37 The module will contribute with loads directed in the plane of the frame, and a moment due to the eccentricity from the plane of the frame.
38 The approach of this calculation will be to calculate the load effects of the moment and the loads separately, thus applying the principle of superposition, which is allowed as long as linear elastic material and small deformations is assumed.
39 The calculation will take into account the effect of diagonal stiffeners. The frame without diagonal stiffeners is not intended to be stiff toward shear.
40 Hence it is intended that the diagonal stiffeners will contribute with the main part of the shear stiffness of the frame.
41 However, carrying out a complete calculation including the diagonals is considered unfeasible due to complexity. The frame will be statically indeterminate and stiffnesses will decide the load effects.
42 To simplify the calculation, the following procedure is assumed:
43 The calculation will only consider the longitudinal and transverse beams, i.e. not the diagonals, in the first step.
44 The loads will be applied, and load effects and deformations calculated. From the deformations, it is straight forward to calculate the corresponding load in the diagonals.
45 Then these loads will be applied to the joints where the diagonals are welded to the frame.
46 Thus, the calculation is carried out again, and iterated until the deformation converges to a solution which is assumed to be close to correct.

	A	B	C	D	E	F	G	H	I	J	K	L	M	N	O
49	Loads from moment due to eccentricity of the frame.														
50															
51															
52	Calculation of moment contribution								Calculation of moment contribution						
53	1	13		0	0				1	13		0	0		
54	2	9.75	95	95	95	95			2	9.75	95	95	95	95	
55	3	6.5	42	42	42	42			3	6.5	42	42	42	42	
56	4	3.25	11	11	11	11			4	3.25	11	11	11	11	
57	5	0	0	0	0	0			5	0	0	0	0	0	
58	6	-3.25	11	11	11	11			6	-3.25	11	11	11	11	
59	7	-6.5	42	42	42	42			7	-6.5	42	42	42	42	
60	8	-9.75	95	95	95	95			8	-9.75	95	95	95	95	
61	9	-13		0	0				9	-13		0	0		
62															
63	Calculation of constant c (see explanation)														
64	c	59.7058326							Shear forces in traverse due to eccentricity of module - values from FEM (kN)						
65										x	A	C	E	G	
66	Point loads supporting moment due to eccentricity of module [kN]:										25.82	-25.82	-25.82	25.82	
67		x	A	C	E	G			0	0					
68		0							1	1.1					
69	1	1.1	0.0	0.0	0.0	0.0			2	4.35					
70	2	9.75	582.131868132	582.1	582.1	582.13			3	7.60	110.4	-110.4	-110.4	110.4	
71	3	6.5	388.087912088	388.1	388.1	388.09			4	10.85					
72	4	3.25	194.043956044	194.0	194.0	194.04			5	14.10	-13.3	13.3	13.3	-13.3	
73	5	0	0.0	0.0	0.0	0.00			6	17.35					
74	6	-3.25	-194.0	-194.0	-194.0	-194.04			7	20.60	-197.0	197.0	197.0	-197.0	
75	7	-6.5	-388.1	-388.1	-388.1	-388.09			8	23.85					
76	8	-9.75	-582.1	-582.1	-582.1	-582.13			9	27.10					
77	9	-13	0.0	0.0	0.0	0.00					-137.68	137.68	137.68	-137.68	
78															
79	Longitudinal beams														
80	Load distribution [kN]														
81		x		A	C	E	G								
82	Support	0	27.100	651.59			651.59								
83		1.1	26.000	0	679.15	679.15	0								
84	1	1.1	26.000	0	0	0	0								
85	2	4.350	22.750	582.13	582	582	582								
86	3	7.600	19.500	388.09	388	388	388								
87	4	10.850	16.250	194.04	194	194	194								
88	5	14.100	13.000	0.00	0	0	0								
89	6	17.350	9.750	-194.04	-194	-194	-194								
90	7	20.600	6.500	-388.09	-388	-388	-388								
91	8	23.850	3.250	-582.13	-582	-582	-582								
92	9	27.100	0.000	0	0	0	0								
93	Support			-651.59	-679.15	-679.15	-651.59								
94															
95															

	A	B	C	D	E	F	G	H	I	J	K	L	M	N	O
96															
97		Load distribution [kN]									Shear force [kN]		Red values: inserted from Focus		
98		x		A	C	E	G				x	A	C	E	G
99		Support		677.41			677.41			Support	0	1303			1303
100		1.1	26.000	0	652.24	652.24	0			0	1.1	1303	606	606	1303
101	1	1.1	26.000	0	0	0	0			1	1.1	697	606	606	697
102	2	4.35	22.750	582	582	582	582			2	4.35	115	24	24	115
103	3	7.600	19.500	499	278	278	499			3	7.6	-383	-254	-254	-383
104	4	10.85	16.250	194	194	194	194			4	10.85	-578	-448	-448	-578
105	5	14.1	13.000	-13	13	13	-13			5	14.1	-564	-461	-461	-564
106	6	17.35	9.750	-194	-194	-194	-194			6	17.35	-370	-267	-267	-370
107	7	20.6	6.500	-585	-191	-191	-585			7	20.6	215	-76	-76	215
108	8	23.85	3.250	-582	-582	-582	-582			8	23.85	797	506	506	797
109	9	27.1	0.000	0	0	0	0			9	27.1	797	506	506	797
110		Support		-777.29	-552.36	-552.36	-777.29				Support	1303			1303
111															
112															
113															
114	Torsjonsbidrag frå torsjon i front og rear beam														
115															
116			Moment [kNm]	Moment, top	Moment, bottom	Shear [kN]									
117	Torsion, front		678.71	27.5	651.2	25.0									
118	Torsion, rear [kNm]		521			19.2									
119						5.82									
120															
121		Moment due to torsion in front and rear beam [kNm]													
122		x			A	C	E	G							
123	Support	0	0	0	0	0	0	0							
124	0	1.1	1.00	0.04	-6.4	0	0	-6							
125	1	1.1	1.00	0.04	672	-672	-672	672							
126	2	4.35	0.88	0.16	653	-653	-653	653							
127	3	7.6	0.75	0.28	634	-634	-634	634							
128	4	10.85	0.63	0.40	616	-616	-616	616							
129	5	14.1	0.50	0.52	597	-597	-597	597							
130	6	17.35	0.38	0.64	578	-578	-578	578							
131	7	20.6	0.25	0.76	559	-559	-559	559							
132	8	23.85	0.13	0.88	540	-540	-540	540							
133	9	27.1	0	1	521	-521	-521	521							
134	Support	27.1	0	1	521	-521	-521	521							
135															
136		Moment [kNm]													
137		x			A	C	E	G							
138	Support	0			0			0							
139	0	1.1	1.00	0	1433			1433							
140	1	1.1	1.00	0	1433	0	0	1433							
141	2	4.35	0.86	0.14	3 699	1 970	1 970	3 699							
142	3	7.6	0.71	0.29	4 073	2 047	2 047	4 073							
143	4	10.85	0.57	0.43	2 827	1 223	1 223	2 827							
144	5	14.1	-0.67	0.57	950	-233	-233	950							
145	6	17.35	-0.81	0.71	-884	-1 731	-1 731	-884							
146	7	20.6	-0.95	0.86	-2 087	-2 599	-2 599	-2 087							
147	8	23.85	-1.10	1	-1 389	-2 846	-2 846	-1 389							
148	9	27.1			1 202	-1 201	-1 201	1 202							
149	Support	27.1													

	A	B	C	D	E	F	G	H	I	J	K	L	M	N	O
150															
151															
152		Total moment [kNm]													
153		x			A	C	E	G							
154	Support	0			0			0							
155	0	1.1	1	0	1 433	0	0	1 433							
156	1	1.1	1.00	0	761	672	672	761							
157	2	4.35	0.86	0.14	3 027	2 642	2 642	3027							
158	3	7.6	0.71	0.29	3 394	2 726	2 726	3394							
159	4	10.85	0.57	0.43	2 148	1 901	1 901	2148							
160	5	14.1	0.43	0.57	271	446	446	271							
161	6	17.35	-0.81	0.71	-1 563	-1 053	-1 053	-1563							
162	7	20.6	-0.95	0.86	-2 766	-1 921	-1 921	-2766							
163	8	23.85	-1.10	1.00	-2 068	-2 168	-2 168	-2068							
164	9	27.1	-1.24	1.14	523	-523	-523	523							
165	Support	27.1			2	-2	-2	2							
166															
167															
168															
169	**Moment due to eccenticity of module**														
170	Traverse beams														
171															
172	Rear beam														
173	Eccentricity of supports [m]:			1											
174															
175		y	Load	Shear	Moment										
176	Support	0.000	1303.18	1303.18	0										
177	A	1.000	797	506	1 303										
178	B	3.500	0	506	2 569										
179	C	6.000	506	0	3 834										
180	D	8.500	0	0	3 834										
181	E	11.000	506	-506	3 834										
182	F	13.500	0	-506	2 569										
183	G	16.000	797	-1303	1 303										
184	Support	17.000	1303.18	-1303.18	0										
185	MAX				3 834										
186															
187	Front beam														
188	Eccentricity of supports [m]:			0											
189		y	Load	Shear	Moment										
190	Support	1.000	1303.18	1303.18	0										
191	A	1.000	697	606.03	0										
192	B	3.500	0	606.03	1 515										
193	C	6.000	606	0	3 030										
194	D	8.500	0	0	3 030										
195	E	11.000	606	-606.03	3 030										
196	F	13.500	0	-606.03	1 515										
197	G	16.000	697	-1303.18	0										
198	Support	16.000	1303.18	1303.18	0										
199	MAX				3 030										
200															

	A	B	C	D	E	F	G	H	I	J	K	L	M	N	O
201															
202	**Axial loads due to weight of module**														
203															
204	Longitudinal beams														
205	Load distribution														
206		From weight of module structure [kN]:								From weight of module structure [kN]:					
207		x		A	C	E	G			x		A	C	E	G
208		Support		1411.77	1411.77	1411.77	1411.77			Support		1471.50	1471.50	1471.50	1471.50
209	0	0	27.100	0					0	0	27.100	0			
210	1	1.1	26.000	0	0	0	0		1	1.1	26.000	0	0	0	0
211	2	4.350	22.750	420	420	420	420		2	4.350	22.750	420	420	420	420
212	3	7.600	19.500	420	420	420	420		3	7.600	19.500	420	420	420	420
213	4	10.850	16.250	420	420	420	420		4	10.850	16.250	420	420	420	420
214	5	14.100	13.000	420	420	420	420		5	14.100	13.000	420	420	420	420
215	6	17.350	9.750	420	420	420	420		6	17.350	9.750	420	420	420	420
216	7	20.600	6.500	420	420	420	420		7	20.600	6.500	420	420	420	420
217	8	23.850	3.250	420	420	420	420		8	23.850	3.250	420	420	420	420
218	9	27.100	0.000	0	0	0	0		9	27.100	0.000	0	0	0	0
219		Support		1531.23	1531.23	1531.23	1531.23			Support		1471.50	1471.50	1471.50	1471.50
220															
221															
222													Shear force in traverse		
223		**Collect values from the solver you use**											Focus	Abaqus	
224		From forces in diagonals due to deformation [kN]:							Force in diagonals			0			
225									Focus	Abaqus		1.1			
226	Axial force in diagonals due to deformation [kN]								748	762		4.35			
227	Collect from solver								670	682		7.6	165	156	
228		B \	B /	D \	D /	F \	F /		644	655		10.85			
229	1	748	0	0	0	0	748		665	675		14.1	140	135	
230	2	670	0	0	0	0	670					17.35			
231	3	644	0	0	0	0	644					20.6	177	169	
232	4	665	0	0	0	0	665					23.85			
233												27.1			
234		Angle of diagonals													
235		diagonals angle		0.915100701											
236															
237		From forces in diagonals [kN]								From shear forces in traverses due to deformation [kN]:					
238		x	A	C	E	G				x	A	C	E	G	
239		Support	1668.04	-1056.97	-1056.97	1668.04	1222.15			Support	228.27	-228.27	-228.27	228.27	
240	0	0							0	0					
241	1	1.1	748	0	0	748			1	1.1					
242	2	4.350							2	4.350					
243	3	7.600	670	-748	-748	670			3	7.600	165	-165	-165	165	
244	4	10.850							4	10.850					
245	5	14.100	644	-670	-670	644			5	14.100	140	-140	-140	140	
246	6	17.350							6	17.350					
247	7	20.600	665	-644	-644	665			7	20.600	177	-177	-177	177	
248	8	23.850							8	23.850					
249	9	27.100	0	-665	-665	0			9	27.100					
250		Support	1058.55	-1669.63	-1669.63	1058.55	-1222.15			Support	253.42	-253.42	-253.42	253.42	

	A	B	C	D	E	F	G	H	I	J	K	L	M	N	O
251															
252															
253		Combined forces from weight of module and diagonals [kN]:													
254		x	A	C	E	G									
255		Support	2962.17	395.79	395.79	2962.17									
256	0	0	0	0	0	0									
257	1	1.100	593	0	0	593				0.000	26.000	0.000	0		
258	2	4.350	420	420	420	420				3.250	22.750	52.554	368		
259	3	7.600	1117	-337	-337	1117				6.500	19.500	-84.333	-253		
260	4	10.850	420	420	420	420				9.750	16.250	157.661	263		
261	5	14.100	1071	-251	-251	1071				13.000	13.000	-125.439	-125		
262	6	17.350	420	420	420	420				16.250	9.750	262.768	158		
263	7	20.600	1124	-266	-266	1124				19.500	6.500	-199.872	-67		
264	8	23.850	420	420	420	420				22.750	3.250	367.875	53		
265	9	27.100	0	-527	-527	0				26.000	0.000	-526.857	0		
266		Support	2623.68	-95.64	-95.64	2623.68						-95.645	396		
267															
268		Axial force													
269		x	A	C	E	G			Point loads rear						
270		Support	2962	396	396	2962			Abaqus				Focus		
271	1	0	2962	396	396	2962			y	Load [kN]	Moment [kNm]		y	Load [kN]	Moment [kN
272	2	1.100	2369	396	396	2369			0				0		
273	3	4.350	1949	-25	-25	1949			1	0			1	0	
274	4	7.600	832	313	313	832			1	2783	628.7		1	2783	628.7
275	5	10.850	412	-108	-108	412			3.5				3.5		
276	6	14.100	-659	143	143	-659			6	384.5	202		6	384.5	202
277	7	17.350	-1079	-277	-277	-1079			8.5				8.5		
278	8	20.600	-2203	-11	-11	-2203			11	384.5	-202		11	384.5	-202
279	9	23.850	-2624	-431	-431	-2624			13.5				13.5		
280		27.100	-2624	96	96	-2624			16	2783	-628.7		16	2783	-628.7
281		Support	-2624	96	96	-2624			17	2560			17	2560	
282															
283	**Moment due to weight of module**														
284	Traverse beams														
285															
286	Rear beam														
287	Eccentricity of supports [m]:			1					From Focus						
288									Point loads on rear beam						
289		y	Load	Shear	Moment					y	Load [kN]	Moment [kNm]	Shear from momer	Axial force in longitudinals d	
290	Support	0	-2528	-2528	0				Support	0					
291	Av	1		-2528	-2528				Av	1	0				
292	Ah	1	-2624	133	-1 899				Ah	1	2783	628.7	37.0		
293	B	3.5		133	-1 568				B	3.5					
294	Cv	6		133	-1 236				C	6	384.5	202	11.9	397.2	
295	Ch	6	-96	25	-1 034				D	8.5					
296	Dt	8.5		25	-972				E	11	384.5	-202	-11.9	397.2	
297	Db	8.5		25	-972				F	13.5					
298	Ev	11	-96	25	-1 034				G	16	2783	-628.7	-37.0		
299	Eh	11		133	-1 236				Support	17	2560				
300	F	13.5		133	-1 568										
301	Gv	16	-2624	133	-1 899								Front	384.5000	
302	Gh	16		-2528	-2 528								Rear	409.9	
303	Support	17	-2528	-2528	0										
304	MAX				2 528										

	A	B	C	D	E	F	G	H	I	J	K	L	M	N	O
305															
306	Front beam								From Focus						
307	Eccentricity of supports [m]:			0					Point loads on front beam						
308		y	Load	Shear	Moment					y	Load [kN]	Moment [kNm]	Shear from momer	Axial force in longitudinals d	
309	Support	0	3358	0	0				Support	0					
310	A	0	2962	424	417				A	0	2246	417	27.8		
311	B	2.5		424	-642				B	2.5					
312	Cv	5	396	11	-1 701				C	5	409.9	247	16.5	397.2	
313	Ch	5		11	-1 454				D	7.5					
314	Dt	7.5		11	-1 425				E	10	409.9	247	16.5	397.2	
315	Db	7.5		-11	-1 482				F	12.5					
316	Ev	10		-11	-1 454				G	15	2246	417	27.8		
317	Eh	10	396	-11	-1 701				Support	15					
318	F	12.5		-424	-642										
319	G	15	2962	-424	417								Front	384.5000	
320	Support	15	3358	0	0								Rear	409.9	
321	MAX				1 701										

Self weight calculation

	A	B	C	D	E	F	G	H	I	J	K
1	Self weight calculation										
2											
3											
4											
5	Distance between load points in vertical direction [m]:						3.250				
6	Distance between load points in horizontal direction [m]:						5.000				
7	Length of longitudinal beams [m]:						26				
8	Length of front and interior traverse beams [m]:						15				
9	Length of rear beam [m]:						17				
10	Length of diagonals [m]:						8.201				
11	Number of diagonals:						24				
12	Lenght of lifting lugs						1.1				
13	Sine angle of diagonals						0.9151				
14											
15	Mass density of steel, ρ [kg/m^3]:						7850.00				
16	Ground acceleration, g [m/s^2]						9.81				
17											
18											
19	Maximum allowed stress according to NS 5514 and EC3 1-1										
20	Safety factor according to NS 5514, ν_E:						1.5				
21	Material factor according to EC3 1-1, γ_M:						1.05	We don't include this value - don't mix values from different standards.			
22	Steel nominal yield stress, σ_E [MPa]:						420				
23	Allowed stress, σ_a [MPa]:						280				
24											
25											
26	Cross-section data:										
27	Profile description:			Longitudinal beams				Traverse beams		Diagonals	Lugs
28	Beam		A-A	C-C	E-E	G-G	Rear	Front	Interior		
29	$W_{strong,req} \cdot 10^{-6}$ [mm^3]										
30	$W_{weak,req} \cdot 10^{-6}$ [mm^3]										
31	$A \cdot 10^{-3}$ [mm^2]		145.00	145.00	145.00	145.00	240.00	240.00	145.00	10	75
32	$W_{strong} \cdot 10^{-6}$ [mm^3]		67.83	67.83	67.83	67.83	100.60	100.60	67.83		
33											
34	$W_{weak} \cdot 10^{-6}$ [mm^3]		-	-	-	-	79.90	79.90	9.41		
35											
36	Weight, q [kN/m]		11.17	11.17	11.17	11.17	18.48	18.48	11.17	0.77	5.78
37	Total weight [kN]:		290.32	290.32	290.32	290.32	314.19	277.23	167.49	6.32	6.35
38											
39	Total nominal self weight in tonnes:				245.98						
40											
41	The self weight must also be treated with a dynamic factor according to NS 5514.										
42	Dynamic factor according to NS 5514 1.2211:										
43	Formula: $\psi = 1+\xi V_L$			$1.15 \leq \psi \leq 1.6$							
44	Hoisting velocity V_L [m/s]:						1				
45	ξ for gantry cranes:						0.6				
46	Dynamic factor, ψ:						1.6				
47											
48	Self weight factor according to NS-EN 1990 Table A1.2(A):										
49	Permanent actions, unfavourable, γ_G:						1.2				

	A	B	C	D	E	F	G	H	I	J	K
50											
51			A-A	C-C	E-E	G-G	Rear	Front	Interior	Diagonals	Lugs
52	q_d [kN/m]:		21.44	21.44	21.44	21.44	35.49	35.49	21.44	1.48	11.09
53	Dynamic weight [kN]:		557.42	557.42	557.42	557.42	603.25	532.28	321.59	12.13	12.20
54											
55	Total load [kN]:		4451.37								
56											
57	Self weight loads										
58	The self weight of the beams is treated as evenly distributed loads.										
59	The traverse beams have same cross section as the longitudinals.										
60											
61	Vertical position										
62											
63											
64	Longitudinal beams										
65											
66	Point loads on longitudinals due to weight of diagonals [kN]:										
67		x		A	C	E	G				
68	Support	0	27.100	14.54			14.54		47.27		
69		1.1	26.000		9.09	9.09					
70	1	1.1	26.000	6.06	0.00	0.00	6.06				
71	2	4.350	22.750								
72	3	7.600	19.500	6.06	6.06	6.06	6.06		**Ok**	97.00	
73	4	10.850	16.250							97.00	
74	5	14.100	13.000	6.06	6.06	6.06	6.06				
75	6	17.350	9.750								
76	7	20.600	6.500	6.06	6.06	6.06	6.06				
77	8	23.850	3.250								
78	9	27.100	0.000	0.00	6.06	6.06	0.00		49.73		
79	Support			9.71	15.16	15.16	9.71				
80											
81	Axial force in diagonals due to deformation in (Self weight) [kN]										
82	Collect from solver										
83		B \	B /	D \	D /	F \	F /				
84	1	314	0	0	0	0	314				
85	2	288	0	0	0	0	288				
86	3	280	0	0	0	0	280				
87	4	290	0	0	0	0	290				
88											
89	Vertical component of force [kN]:										
90	Sine angle [radians]:		0.92								
91		B \	B /	D \	D /	F \	F /				
92	1	249	0	0	0	0	249				
93	2	228	0	0	0	0	228				
94	3	222	0	0	0	0	222				
95	4	230	0	0	0	0	230				

	A	B	C	D	E	F	G	H	I	J	K
96											
97											
98	Point loads from weight of lifting lugs [kN]:										
99		x	A	B	C	D					
100	Support	0	11.70			11.70					
101		0		0.00	0.00						
102	1	1.100	12.2			12.2			Ok		
103	2	4.350									
104	3	7.600									
105	4	10.850									
106	5	14.100									
107	6	17.350									
108	7	20.600									
109	8	23.850									
110	9	27.100									
111	Support	27.100	0.50	0.00	0.00	0.50					
112											
113											
114	Point loads on longitudinals due to axial force in diagonals [kN]:										
115		x	A	C	E	G					
116	Support	0	564.39			564.39			416.436		
117		1.1		-356.17	-356.17						
118	1	1.1	249			249		+ nedover			
119	2	4.350						- oppover			
120	3	7.600	228	-249	-249	228					
121	4	10.850							Ok		
122	5	14.100	222	-228	-228	222					
123	6	17.350									
124	7	20.600	230	-222	-222	230					
125	8	23.850									
126	9	27.100		-230	-230						
127	Support		363.99	-572.21	-572.21	363.99			-416.436		
128											
129											
130	Shear forces in traverses										
131											
132		Row	Shear force [kN]		Focus	Abaqus		Insert values corresponding to the solver you use			
133		3	67.6		67.6	63.95					
134		5	57.14		57.14	54.73					
135		7	70.86		70.86	67.54					
136											

	A	B	C	D	E	F	G	H	I	J	K
137											
138	Point loads on longitudinals due to shear force in traverses [kN]:										
139		x	A	C	E	G					
140	Support	0	93.05			93.05		-7.87			
141		1.1		-96.99	-96.99						
142	1	1.1	0.00	0.00	0.00	0.00					
143	2	4.350									
144	3	7.600	67.60	-67.60	-67.60	67.60					
145	4	10.850							Ok		
146	5	14.100	57.14	-57.14	-57.14	57.14					
147	6	17.350									
148	7	20.600	70.86	-70.86	-70.86	70.86					
149	8	23.850									
150	9	27.100	0.00	0.00	0.00	0.00					
151	Support		102.55	-98.62	-98.62	102.55		7.87			
152											
153											
154	Point loads from weight of interior traverse beams [kN]:										
155		x	A	C	E	G					
156	Support	0	77.13			77.13		964.7625	964.762488		
157		1.1		160.79	160.79						
158	1	1.1									
159	2	4.350							Ok		
160	3	7.600	53.60	107.20	107.20	53.60					
161	4	10.850									
162	5	14.100	53.60	107.20	107.20	53.60					
163	6	17.350									
164	7	20.600	53.60	107.20	107.20	53.60					
165	8	23.850									
166	9	27.100									
167	Support	27.100	83.66	160.79	160.79	83.66					
168											
169											
170	Axial force in longitudinal beams due to weight of diagonals and interior traverse beams [kN]:										
171		x	A	C	E	G					
172	Support	0	749.11			749.11		931.69			
173		1.1		-283.27	-283.27						
174	1	1.1	494.01	-283.27	-283.27	494.01	0.00				
175	2	4.350	494.01	-283.27	-283.27	494.01					
176	3	7.600	138.87	-79.89	-79.89	138.87					
177	4	10.850	138.87	-79.89	-79.89	138.87					
178	5	14.100	-199.74	91.87	91.87	-199.74					
179	6	17.350	-199.74	91.87	91.87	-199.74					
180	7	20.600	-559.91	271.28	271.28	-559.91				Ok!!	
181	8	23.850	-559.91	271.28	271.28	-559.91					
182	9	27.100	-559.91	494.88	494.88	-559.91					
183	Support	27.100	-559.91	494.88	494.88	-559.91		-130.08	1061.76	1061.763446	
184											

	A	B	C	D	E	F	G	H	I	J	K
185	Axial force in longitudinal beams due to self weight of longitudinal beams [kN]:										
186		x	A	C	E	G					
187	Support	0	255.13			255.13			2229.6733		1004.24
188		1.1		255.13	255.13				2229.673306		
189	1	1.1	255.13	255.13	255.13	255.13					
190	2	4.350	185.45	185.45	185.45	185.45					
191	3	7.600	115.77	115.77	115.77	115.77					
192	4	10.850	46.09	46.09	46.09	46.09					
193	5	14.100	-23.58	-23.58	-23.58	-23.58					
194	6	17.350	-93.26	-93.26	-93.26	-93.26					
195	7	20.600	-162.94	-162.94	-162.94	-162.94					
196	8	23.850	-232.61	-232.61	-232.61	-232.61					
197	9	27.100	-302.29	-302.29	-302.29	-302.29					
198	Support	27.100	-302.29	-302.29	-302.29	-302.29					
199											
200	Total axial force in longitudinal beams [kN]:										
201		x	A	C	E	G					
202	Support	0	1015.94			1015.94					
203		0		-28.14	-28.14						
204	1	1.1	761.33	-28.14	-28.14	761.33					
205	2	4.350	679.46	-97.82	-97.82	679.46					
206	3	7.600	254.64	35.88	35.88	254.64					
207	4	10.850	184.96	-33.79	-33.79	184.96					
208	5	14.100	-223.32	68.29	68.29	-223.32					
209	6	17.350	-293.00	-1.39	-1.39	-293.00					
210	7	20.600	-722.85	108.35	108.35	-722.85					
211	8	23.850	-792.53	38.67	38.67	-792.53					
212	9	27.100	-862.21	192.58	192.58	-862.21					
213	Support	27.100	-862.70	192.58	192.58	-862.70				**Support load**	
214										Front, one side	1253.94
215										Rear, one side	971.74
216	Rear beam									One side	2225.68
217	Eccentricity of supports [m]:			1						Sum	4451.370
218											
219	Moment due to self weight of rear beam				301.627						
220		y	Moment [kNm]	Shear							
221	Support	0.000	0		301.627						
222	A	1.000	284		266.1						
223	B	3.500	838		177.4						
224	C	6.000	1171		88.7						
225	D	8.500	1282		0.0		**Ok!**				
226	E	11.000	1171		-88.7						
227	F	13.500	838		-177.4						
228	G	16.000	284		-266.1						
229	Support	17.000	0		-301.6						

	A	B	C	D	E	F	G	H	I	J	K
230											
231											
232	Moment due to axial loads in longitudinal beams										
233		y	Load [kN]	Shear [kN]							
234	Support	0.000	-670	670							
235	A	1.000	-863	-193							
236	B	3.500		-193							
237	C	6.000	193	0							
238	D	8.500		0							
239	E	11.000	193	193							
240	F	13.500		193							
241	G	16.000	-863	-670							
242	Support	17.000	-670	-670							
243											
244											
245											
246											
247											
248											
249											
250	Front beam										
251	Eccentricity of supports [m]:			0							
252											
253	Moment due to self weight of front beam				532.3						
254		y	Moment [kNm]								
255	Support	0.000	0		0						
256	A	0.000	0		266.1						
257	B	2.500	554		177.4						
258	C	5.000	887		88.7						
259	D	7.500	998		0						
260	E	10.000	887		-88.7						
261	F	12.500	554		-177.4						
262	G	15.000	0		-266.1						
263	Support	15.000	0		0						
264											

	A	B	C	D	E	F	G	H	I	J	K
265											
266	Moment due to axial loads in longitudinal beams										
267		y	Load	Shear							
268	Support	0.000	987.8	1253.94							
269	A	0.000	1015.9	238.00							
270	B	2.500		238.00							
271	C	5.000	-28.1	266.14							
272	D	7.500		266.14							
273	E	10.000	-28.1	238.00							
274	F	12.500		238.00							
275	G	15.000	1015.9	-777.95							
276	Support	15.000	987.8	-1253.94							
277											
278											
279	Total moment in front beam										
280		y	Moment [kNm]								
281	Support	0.000	0								
282	A	0.000	0	0							
283	B	2.500	554	554.4612							
284	C	5.000	887	887.13792							
285	D	7.500	998	998.03016							
286	E	10.000	887	887.13792							
287	F	12.500	554	554.4612							
288	G	15.000	0	0							
289	Support	15.000	0								
290	MAX		998								
291											

Cross section geometry

H beam

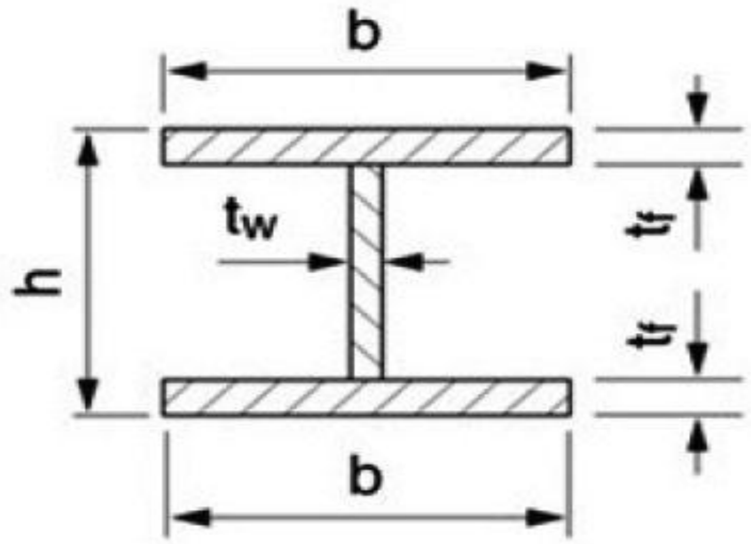

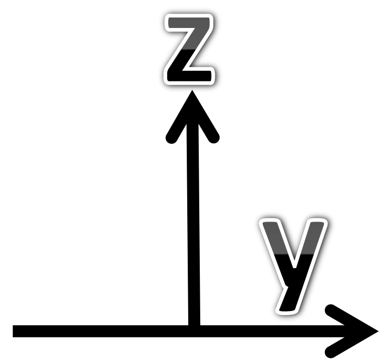

Box beam

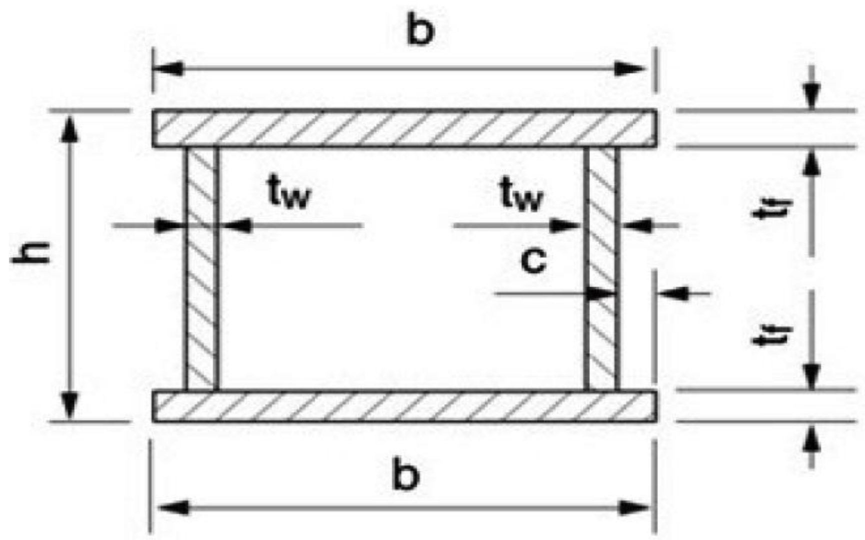

Flat bar diagonals

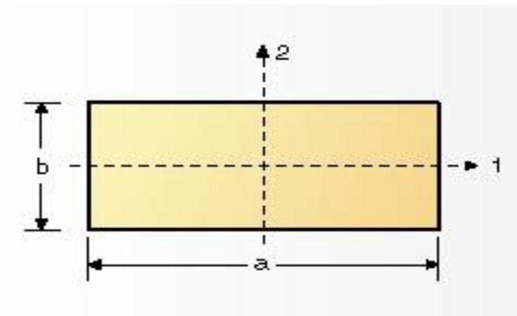

Longitudinal beams	
b [mm]	750
h [mm]	1500
t_f [mm]	50
t_w [mm]	50
H or Box	1
c [mm]	
$A \cdot 10^{-3}$ [mm^2]	145.00
z_{max} [mm]	750
$I_y \cdot 10^{-6}$ [mm^4]	50 871
$W_y \cdot 10^{-6}$ [mm^3]	67.83
y_{max} [mm]	375
a_w [mm]	0
$I_z \cdot 10^{-6}$ [mm^4]	3 530.21
$W_z \cdot 10^{-6}$ [mm^3]	9.41
Δ_{max} [mm] Horizontal	
Δ_{max} [mm] Vertical	
$I_T \cdot 10^{-6}$ [mm^4]	120.83
$S_y \cdot 10^{-6}$ [mm^3]	41.25
$S_z \cdot 10^{-6}$ [mm^3]	7.47
$A_y \cdot 10^{-3}$ [mm^2]	75.00
$A_z \cdot 10^{-3}$ [mm^2]	70.00

Traverses	
b [mm]	750
h [mm]	1500
t_f [mm]	50
t_w [mm]	50
H or Box	1
c [mm]	
$A \cdot 10^{-3}$ [mm^2]	145.00
z_{max} [mm]	750
$I_y \cdot 10^{-6}$ [mm^4]	50 871
$W_y \cdot 10^{-6}$ [mm^3]	67.83
y_{max} [mm]	375
a_w [mm]	0
$I_z \cdot 10^{-6}$ [mm^4]	3 530.21
$W_z \cdot 10^{-6}$ [mm^3]	9.41
Δ_{max} [mm] Horizontal	
Δ_{max} [mm] Vertical	
$I_T \cdot 10^{-6}$ [mm^4]	120.83
$S_y \cdot 10^{-6}$ [mm^3]	41.25
$S_z \cdot 10^{-6}$ [mm^3]	7.47
$A_y \cdot 10^{-3}$ [mm^2]	75.00
$A_z \cdot 10^{-3}$ [mm^2]	70.00

Rear Beam	
b [mm]	1000
h [mm]	1500
t_f [mm]	50
t_w [mm]	50
H or Box	2
c [mm]	0
$A \cdot 10^{-3}$ [mm^2]	240.000000
z_{max} [mm]	750
$I_y \cdot 10^{-6}$ [mm^4]	75 450.0000
$W_y \cdot 10^{-6}$ [mm^3]	100.60
y_{max} [mm]	500
a_w [mm]	475
$I_z \cdot 10^{-6}$ [mm^4]	39 950.000000
$W_z \cdot 10^{-6}$ [mm^3]	79.90
Δ_{max} [mm] Horizontal	
Δ_{max} [mm] Vertical	
$I_T \cdot 10^{-6}$ [mm^4]	79062.76
$S_y \cdot 10^{-6}$ [mm^3]	50.3125000
$S_z \cdot 10^{-6}$ [mm^3]	12.937500
$A_y \cdot 10^{-3}$ [mm^2]	100.00
$A_z \cdot 10^{-3}$ [mm^2]	140.00

Front beam	
b [mm]	1000
h [mm]	1500
t_f [mm]	50
t_w [mm]	50
H or Box	2
c [mm]	0
$A \cdot 10^{-3}$ [mm^2]	240.00
z_{max} [mm]	750
$I_y \cdot 10^{-6}$ [mm^4]	75 450
$W_y \cdot 10^{-6}$ [mm^3]	100.60
y_{max} [mm]	500
a_w [mm]	475
$I_z \cdot 10^{-6}$ [mm^4]	39 950.00
$W_z \cdot 10^{-6}$ [mm^3]	79.90
Δ_{max} [mm] Horizontal	
Δ_{max} [mm] Vertical	
$I_T \cdot 10^{-6}$ [mm^4]	79062.76
$S_y \cdot 10^{-6}$ [mm^3]	50.31
$S_z \cdot 10^{-6}$ [mm^3]	12.94
$A_y \cdot 10^{-3}$ [mm^2]	100.00
$A_z \cdot 10^{-3}$ [mm^2]	75.00

Diagonals	
a [mm]	200
b [mm]	50
$A \cdot 10^{-3}$ [mm^2]	10
$I_T \cdot 10^{-6}$ [mm^4]	8.33

Lifting lug in front	
Rectangular plate	
Thickness [mm]:	50
Height [mm]:	1500
$A \cdot 10^{3}$ [mm^2]	75

APPENDIX F: LOCAL PLATE BUCKLING

The web of the longitudinal beam is checked for buckling due to point loads from the module.

Capacity of plates with point load

Buckling of web, according to NS-EN 1993-1-5, chapter 6

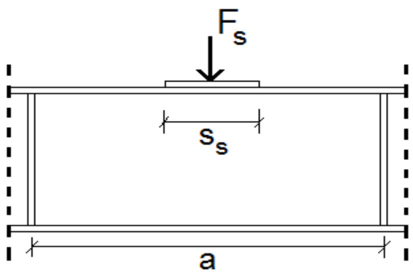

γ_{M1}	1.05	
$f_{y,w}$	420	N/mm^2
$f_{y,f}$	420	N/mm^2
E	210000	N/mm^2
h_w	1400	mm
t_w	50	mm
b_f	750	mm
t_f	50	mm
s_s	1000	mm — load distribution (load spread through the entire shear plate)
a	6500	mm — distance between vertical stiffeners

If l_f is smaler than 0,5 in the left calculation then we use the calculation on the right

k_F	6.09		k_F	6.09	
F_{cr}	102815680	N	F_{cr}	102815680	N
m_1	15.0		m_1	15.0	
m_2	15.7		m_2	0.0	
l_y	1653.9	mm	l_y	1487.3	mm
l_f	0.58	use left calculation	l_f	0.55	
c_{eff}	0.860		c_{eff}	0.91	
L_{eff}	1422.8	mm	L_{eff}	1349.2	mm
F_{Rd}	28456012	N	F_{Rd}	26984792	N
	28456	kN		26985	kN

Weight of section	500	tonnes
	4905	kN
# lifting points	28	
Dynamic factor	1.6	
Live load factor	1.5	
Live load	11772	kN
Force per lifting point	420	kN

Equations

$$k_F = 6 + 2\left(\frac{h_w}{a}\right)^2$$

$$F_{cr} = 0.9 \cdot k_F \cdot E \cdot \frac{t_w^{\;3}}{h_w}$$

$$\chi_F = \frac{0.5}{\lambda_f} \quad ; \chi_F \le 1.0$$

$$\lambda_F = \sqrt{\frac{f_{yw} \cdot t_w \cdot l_y}{F_{cr}}}$$

$$m_1 = \frac{f_{yf} \cdot b_f}{f_{yw} \cdot t_w}$$

$$m_2 = 0.02\left(\frac{h_w}{t_f}\right)^2 \quad \text{for } \lambda_F \succ 0.5$$

$$m_2 = 0 \quad \text{for } \lambda_F \le 0.5$$

$$l_y = s_s + 2 \cdot t_f \cdot (1 + \sqrt{m_1 + m_2}) \quad ; l_y \le a$$

ok

$$F_{Rd} = \frac{f_{yw} \cdot t_w \cdot \chi_F \cdot l_y}{\gamma_{M1}}$$

APPENDIX G: WELDS

The weld capacity is calculated according to NS-EN 1993-1-8, 4.5.3.

The welds calculated:

- Longitudinal beam – rear beam joint
  - The critical joint between the longitudinals and the beams in the traverse direction. The maximum forces occurs in the joint by the rear beam.
- Flange – web in the longitudinal beam
  - The weld has to transfer the shear forces acting between the flange and the web for the cross section to work as a unit.

	A	B	C	D	E	F	G	H	I	J	K	L
1	Welding: longitudinal - rear beam connection, horizontal position											
2	Beam joint with moment, shear and axial forces											
3												
4												
5	Steel grade	S420										
6	fu	520	N/mm^2									
7	γ_{M2}	1.25	NS-EN 1993-1-8, NA.2.2(2)									
8	βw	1.0	NS-EN 1993-1-8, Tabell 4.1									
9	***Requirements***											
10	From NS-EN 1993-1-8, 4.5.3.2(6)											
11	$s_{\wedge,\,max}$	374.4	N/mm^2									
12	d	416.0	N/mm^2									
13												
14	$\delta = \sqrt{(\sigma_{\perp}^{\ 2} + 3(\tau_{\perp}^{\ 2} + \tau_{\parallel}^{\ 2})}$											
15												
16	**Welded section**											
17	***Flange***			***Web***								
18	af	4	mm	aw	5	mm						
19	bf	750	mm	hw	1400	mm						
20	tf	50	mm	tw	50	mm						
21												
22	***Section parameters***		(for nedbretta tverrsnitt)									
23	I ǁ	8789556747	mm^4									
24	A	26320	mm^2									
25	A ( )	14000	mm^2									
26												
27	***Forces in the weld***											
28	Moment, M	1666	kNm									
29	Axial, N	0	kN									
30	Shear, V	2425	kN									
31												
32	***Flanges***						***Web***					
33	s (M)	142.5	N/mm^2				s (M)	132.7	N/mm^2			
34	s (N)	0.0	N/mm^2				s (N)	0.0	N/mm^2			
35												
36	s (^)	100.8	N/mm^2	**ok**	26.9 %		s (^)	93.8	N/mm^2	**ok**	25.1 %	
37	τ (^)	100.8	N/mm^2				τ (^)	93.8	N/mm^2			
38	τ ( )	0	N/mm^2				τ ( )	173.2	N/mm^2			
39	d	201.6	N/mm^2	**ok**	48.5 %		d	353.9	N/mm^2	**ok**	85.1 %	
40												
41		flange	web									
42	**Required a-value [mm]**	4	5									
43												

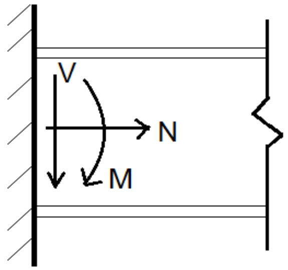

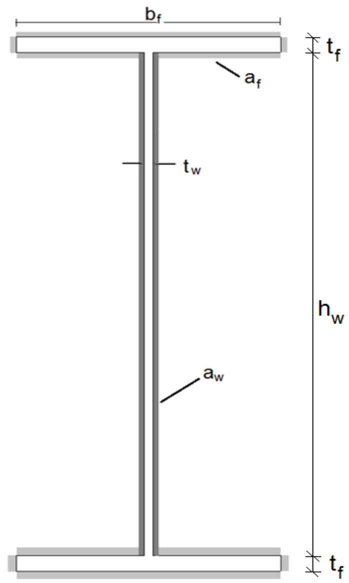

Welding: longitudinal - rear beam connection, vertical position

Beam joint with moment, shear and axial forces

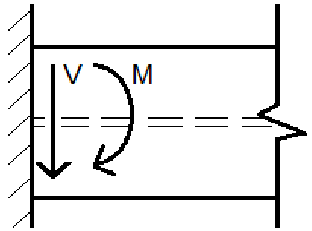

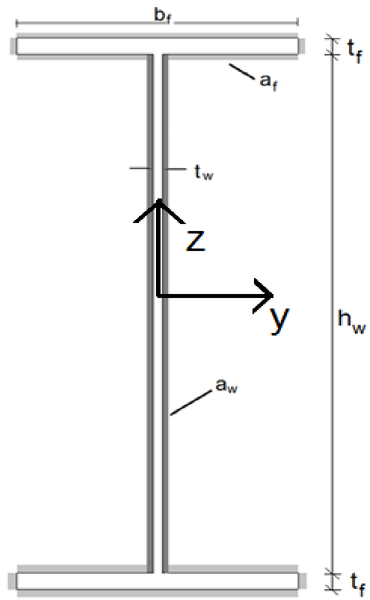

Steel grade	S420		
fu	520	N/mm²	
γ_{M2}	1.25	-	NS-EN 1993-1-8, NA.2.2(2)
βw	1.0	-	NS-EN 1993-1-8, Tabell 4.1

Requirements

From NS-EN 1993-1-8, 4.5.3.2(6)

$s_{^, max}$	374.4	N/mm²
d	416.0	N/mm²

$$\delta = \sqrt{(\sigma_\perp{}^2 + 3(\tau_\perp{}^2 + \tau_\parallel{}^2)}$$

Welded section

Flange			***Web***		
af	7	mm	aw	6	mm
bf	750	mm	hw	1400	mm
tf	50	mm	tw	50	mm

Section parameters (for folded down section)

Iy	14113979817	mm⁴
Iz	2196429765	mm⁴
A ‖	38332	N/mm²
A (‖) z	16800	N/mm²
A ( ) y	20132	N/mm²

Forces in the weld

Moment, strong axis, My	452	kNm
Moment, weak axis, Mz	841	kNm
Axial, N	3528	kN
Shear, Vy	203	kN
Shear, Vz	788	kN

Flanges

s (My)	24.1	N/mm²		
s (Mz)	144.9	N/mm²		
s (N)	92.0	N/mm²		
s (^)	184.6	N/mm²	**ok**	49 %
τ (‖)	184.6	N/mm²		
τ (‖) y	10.1	N/mm²		
τ ( ) z	46.9	N/mm²		
d	378.1	N/mm²	**ok**	91 %

Web

s (M) y	22.4	N/mm²		
s (N)	92.0	N/mm²		
s (^)	80.9	N/mm²	**ok**	22 %
τ (^)	80.9	N/mm²		
τ ( ) z	12.1	N/mm²		
d	163.2	N/mm²	**ok**	39 %

	A	B	C	D	E	F	G	H
1	Welding: weld between flange and web in longitudinal beam							
2								
3	Welded section							
4	*Flange-web*				Steel grade	S420		
5	a_{fw}	1.57	mm		fu	520	N/mm^2	
6	b_f	750	mm		γ_{M2}	1.25	-	NS-EN 1993-1-8, NA.2.2(2)
7	t_f	50	mm		βw	1.0	-	NS-EN 1993-1-8, Tabell 4.1
8	h_w	1400			***Requirements***			
9	t_w	50			From NS-EN 1993-1-8, 4.5.3.2(6)			
10					$s_{\wedge,\ max}$	374.4	N/mm^2	
11	V_y	2444	kN		d	416.0	N/mm^2	
12	I_z	50870833333	mm^4					
13	S	27187500	mm^3		$\delta = \sqrt{(\sigma_{\perp}^{2} + 3(\tau_{\perp}^{2} + \tau_{\parallel}^{2})}$			
14	$\boldsymbol{\tau_{,weld}}$	**416.0**	N/mm^2					
15		**ok**						
16								
17	Change the required a_{fw} until the capacity of the weld is sufficient.							
18								
19								
20	***Required a-value***	3	mm					
21